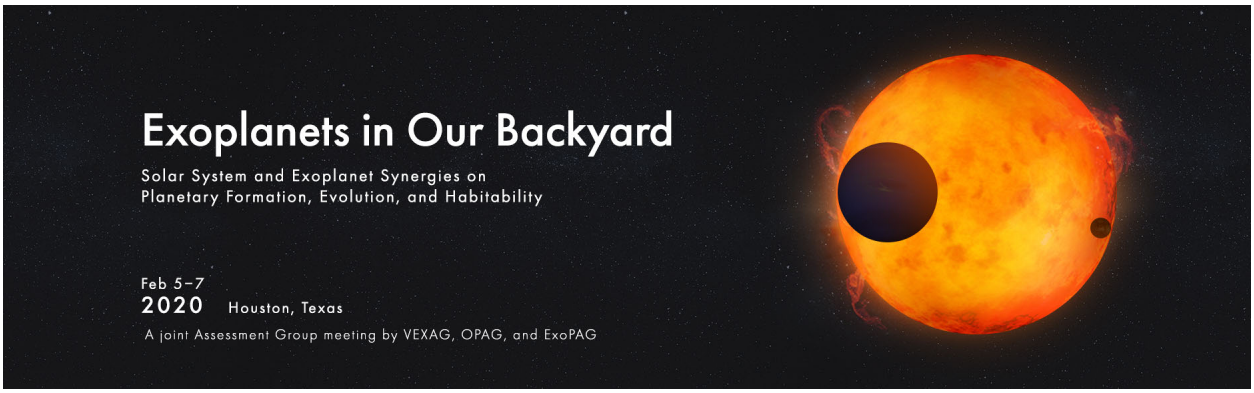

Program and Abstracts

LPI

USRA

Exoplanets in Our Backyard:

Solar System and Exoplanet Synergies on Planetary Formation

February 5–7, 2020
Houston, Texas

Institutional Support

Lunar and Planetary Institute
Universities Space Research Association

Conveners

Giada Arney
NASA Goddard Space Flight Center

Noam Izenberg
Johns Hopkins University Applied Physics Laboratory

Co-Conveners

Stephen Kane
University of California, Riverside

Victoria Meadows
University of Washington

Kathleen Mandt
Johns Hopkins University Applied Physics Laboratory

Lynnae Quick
NASA Goddard Space Flight Center

Abigail Rymer
Johns Hopkins University Applied Physics Laboratory

Lunar and Planetary Institute 3600 Bay Area Boulevard Houston TX 77058-1113

Abstracts for this conference are available via the conference website at
https://www.hou.usra.edu/meetings/exoplanets2020/
Abstracts can be cited as
Author A. B. and Author C. D. (2020) Title of abstract. In *Exoplanets in Our Backyard: Solar System and Exoplanet Synergies on Planetary Formation, Evolution, and Habitability,* Abstract #XXXX.
LPI Contribution No. 2195, Lunar and Planetary Institute, Houston.

Program

Exoplanets in Our Backyard:

Solar System and Exoplanet Synergies on Planetary Formation, Evolution, and Habitability

February 5–7, 2020

Wednesday, February 5, 2020
SESSION 1: OVERVIEW TALKS AND PANEL DISCUSSION
8:50 a.m. Lecture Hall
An overview of topics relevant to the workshop by experts in solar system and exoplanet research.
Moderator/Session Chair: Shawn Domagal-Goldman
Panel Members: Stephen Kane, Kathleen Mandt, Victoria Meadows

Times	Authors (*Denotes Presenter)	Abstract Title and Summary
8:50 a.m.		*Morning Announcements*
9:00 a.m.	Kane S.	*Inner Planets*
9:20 a.m.	Mandt K.	*Outer Planets*
9:40 a.m.	Meadows V.	*Exoplanets*
10:00 a.m.		*Panel Discussion*
10:30 a.m.	BREAK	

Wednesday, February 5, 2020
SESSION 2: NASA HEADQUARTERS TOWN HALL
11:00 a.m. Lecture Hall
Discuss with NASA leadership the challenges and opportunities of interdisciplinary solar system and exoplanet science.

Times	Authors (*Denotes Presenter)	Abstract Title and Summary
11:00 a.m.		*NASA Headquarters Town Hall*
12:30 p.m.	LUNCH	

Wednesday, February 5, 2020
SESSION 2B: SUCCESS STORIES INTEGRATING SOLAR SYSTEM AND EXOPLANET RESEARCH
1:15 p.m. Lecture Hall
Hear from members of the solar system and exoplanet communities who have achieved success in interdisciplinary, cross-divisional research.
Moderator/Session Chair: Adrienn Luspay Kuti
Panel Members: Shawn Domagal-Goldman, Michael Way, Julianne Moses

Wednesday, February 5, 2020

SESSION 3: FORMATION AND EVOLUTION OF PLANETS

2:00 p.m. Lecture Hall

This session will explore how planets form and evolve.

Moderators/Session Chairs: Noam Izenberg and Kristin Sotzen

Panel Members: Laura Schaefer, Steve Desch, Shannon Curry, Nader Haghighipour

Times	Authors (*Denotes Presenter)	Abstract Title and Summary
2:00 p.m.	Schaefer L.	*Planet Evolution Processes*
2:20 p.m.	Curry S. M. Luhmann J. G.	*Atmospheric Escape at Mars and Venus: Past, Present, and Future* **[#3067]** Earth, Venus, and Mars formed at similar times, yet their atmospheres have evolved drastically differently. We will present in-situ observations of atmospheric escape at Mars and Venus and how atmospheric evolution affects habitability.
2:35 p.m.	Desch S. J. Jackson A. P. Mai C. Noviello J. L.	*Pebble Accretion by Bodies on Eccentric Orbits and the Mass Ratios of Exoplanets* **[#3061]** We show pebble accretion is faster for embryos on eccentric orbits than the typically assumed circular orbit. Embryos gain similar masses before eccentricity damping, possibly explaining the observed similarity in exoplanet masses within systems.
2:50 p.m.	Haghighipour N.	*Formation of Rocky Planets and Super-Earths in Systems with Migrating Giant Planets* **[#3042]** We present results of an extensive study of the formation of rocky planets in systems with migrating giant planets. We present a detailed analysis of the results and make a comparison with the frequency of the currently known extrasolar planets.
3:05 p.m.		*Panel*
3:30 p.m.	BREAK	

Wednesday, February 5, 2020
SESSION 4: INTERIOR AND SURFACE PROCESSES
4:00 p.m. Lecture Hall
This session explores interior and surfaces processes on planets.
Moderators/Session Chairs: Helene Piet and Lynnae Quick
Panel Members: Alfred McEwen, Jani Radebaugh, Karalee Brugman, Rory Barnes

Times	Authors (*Denotes Presenter)	*Abstract Title and Summary*
4:00 p.m.	McEwen A. S. de Kleer K. Park R. S. Bierson C. J. Davies A. G. DellaGuistina D. Ermakov A. I. Fuller J. Hamilton C. Harris C. Hay H. Keane J. Kestay L. Khurana K. Kirby K. Lainey V. Matsuyama I. Mandt K. E. McCarthy C. Nimmo F. Panning M. Pommier A. Rathbun J. Steinbrügge G. Stevenson D. Tsai V. C. Turtle E.	*Tidal Heating: Lessons from Io and the Jovian System; Relevance to Exoplanets* **[#3005]** Tidal heating is a fundamental process in the evolution of many worlds across our solar system and beyond.
4:20 p.m.	Radebaugh J. Barnes R. Keith J.	*The Ol Doinyo Lengai Volcano, Tanzania, as an Analogue for Carbon Planets* **[#3070]** The Ol Doinyo Lengai (ODL) volcano of Tanzania is currently erupting carbon-rich lavas, unique on Earth. They may be analogous to those that would erupt on a carbon planet, making ODL to our knowledge the first field analogue of an exoplanet.
4:35 p.m.	Brugman K. K. Phillips M. G. Till C. B.	*Exoplanet Crust Compositions as Determined by Petrological Experiments* **[#3016]** We use established methods from experimental petrology to investigate compositions of exoplanet mantle melts. Our results can be used to predict differences in crust compositions of exoplanets with similar bulk compositions to those explored here.
4:50 p.m.	Barnes R. K. Green J. A. M. Blackledge B. W. Way M. J. Egbert G. D. Sharples J.	*Physical Oceanography in the Solar System and Beyond* **[#3049]** We present models of tidal effects on exoplanets, the application of a physical oceanography model to an ancient Venus ocean, and the application of that model to an ensemble of “alternative Earths” with a range of continental and seafloor properties.
5:05 p.m.		*Panel*
5:30 p.m.		*Adjourn*

Thursday, February 6, 2020

SESSION 5: PLANETARY ATMOSPHERES THIN AND THICK

8:50 a.m. Lecture Hall

This session will explore planetary atmospheres on worlds ranging from terrestrials to gas giants.

Moderators/Session Chairs: Daria Pidhorodetska and Joseph Serigano

Panel Members: Ravi Kopparapu, Julianne Moses, Sarah Moran, Paul Dalba

Times	Authors (*Denotes Presenter)	Abstract Title and Summary
8:50 a.m.		*Morning Announcements*
9:00 a.m.	Kopparapu R.	*Strange New Worlds* **[#3003]** I will discuss a classification scheme for exoplanets in planetary radius and stellar flux bins, based on chemical species' condensation sequences in planetary atmospheres, and provide updates to Venus zone limits for planets around M-dwarf stars.
9:20 a.m.	Moses J. I.	*Exoplanet Atmospheric Chemistry and Composition: Some Lessons Learned from Solar-System Giant Planets* **[#3037]** Lessons derived from studies of our solar system giant planets are described in the context of exoplanet atmospheres.
9:35 a.m.	Moran S. E. Hörst S. M. Vuitton V. He C. Lewis N. K. Bishop N. Flandinet L. Moses J. I. Orthous-Daunay F.-R. Sebree J. Wolters C.	*Chemistry of Laboratory Exoplanet Hazes* **[#3030]** I will present results of the composition of exoplanet haze particles determined from very high resolution mass spectrometry and elemental analysis. This work is part of ongoing exoplanet laboratory studies in the JHU PHAZER laboratory.
9:50 a.m.	Dalba P. A. Tamburo P.	*A Transiting Outer Giant Exoplanet Poised for Comparative Planetology with Jupiter and Saturn* **[#3007]** We present Spitzer observations of a transit of Kepler-167e, a Jupiter-analog exoplanet with a 2.9-yr orbital period. We refine the ephemeris of this rare outer transiting planet to enable future unprecedented comparative investigations with Jupiter.
10:05 a.m.		*Panel*
10:30 a.m.	BREAK	

Thursday, February 6, 2020
SESSION 6: STAR-PLANET INTERACTIONS
11:00 a.m. Lecture Hall
This session moves beyond the planet to explore stellar interactions.
Moderators/Session Chairs: Alison Farrish and Christopher Johns-Krull
Panel Members: David Brain, Melinda Soares-Furtado, Robin Ramstad, Anthony Sciola

Times	Authors (*Denotes Presenter)	*Abstract Title and Summary*
11:00 a.m.	Brain D. Chaffin M. Curry S. Egan H. Ramstad R. Jakosky B. Luhmann J. Dong C. Yelle R.	*Atmospheric Escape from Mars: Lessons for Studies of Exoplanets* **[#3039]** We review atmospheric escape processes from Mars as measured by the MAVEN mission, and consider how the martian atmosphere would fare if Mars orbited an active M Dwarf star.
11:20 a.m.	Soares-Furtado M. MacLeod M. Cantiello M.	*Using Engulfment Events to Probe Planetary Interiors* **[#3008]** I explore the statistically-significant engulfment signatures among cannibal stars that have engulfed a planetary companion. In particular, I review the strength and survival time of 7Li enrichment in the convective envelopes.
11:35 a.m.	Ramstad R. Barabash S.	*Do Intrinsic Magnetic Fields Protect Planetary Atmospheres from Stellar Winds? Lessons from Measurements in the Solar System* **[#3026]** We compare measured solar wind driven atmospheric escape rates from Venus, Earth, and Mars, including dependencies on upstream solar wind and solar EUV. The latest results challenge the current paradigm of the role of the magnetic field.
11:50 a.m.	Sciola A. M. Toffoletto F. R. Alexander D. Farrish A. O.	*Incorporating Saturation Behavior of Magnetosphere-Ionosphere Interaction in Radio Emission Estimates for Extrasolar Planets* **[#3044]** We present a method of estimating planetary radio emission which accounts for conditions where the transfer of energy from the solar wind to ionosphere becomes proportionally limited. Most exoplanets are expected to exist within this regime.
12:05 p.m.		*Panel*
12:30 p.m.	LUNCH	

Thursday, February 6, 2020
SESSION 7: UNCONFERENCE
2:00 p.m. Lecture Hall
The Unconference is a participant-led discussion of topics selected by meeting attendees.

Times	Authors (*Denotes Presenter)	Abstract Title and Summary
2:00 p.m.		*Unconference*
4:00 p.m.	BREAK	

Thursday, February 6, 2020
SESSION 8A: POSTERS LIGHTNING TALKS
4:30 p.m. Lecture Hall

Thursday, February 6, 2020
SESSION 8B: POSTERS
5:00–6:30 p.m. Great Hall

Friday, February 7, 2020

SESSION 9: HABITABILITY AND ASTROBIOLOGY NEAR AND FAR

8:50 a.m. Lecture Hall

We will explore habitability and astrobiology on worlds near and far.

Moderators/Session Chairs: Alex Bixel and Michael Wong

Panel Members: Steve Vance, Giada Arney, Laura Mayorga, Johnny Seales

Times	Authors (*Denotes Presenter)	Abstract Title and Summary
8:50 a.m.		*Morning Announcements*
9:00 a.m.	Vance S. D. Barnes R. K. Journaux B.	*Exo-Oceans in Our Backyard: Our Solar System's Ocean Worlds as Analogue Habitable Ice-Covered Exoplanets* **[#3069]** We will describe recent work modeling the extent of fluid-rock interactions in icy ocean worlds and recent progress enabling the detailed modeling of habitable ice-covered exoplanets (HICEPs).
9:20 a.m.	Arney G. N.	*Earth is More than One Planet: The Many Faces of Earth History as Analogs for Habitable Exoplanets* **[#3052]** To guide studies of the diversity of exoplanets we will someday encounter, we must consider the different environmental conditions and dominant biospheres that existed during Earth's history.
9:35 a.m.	Mayorga L. C. Charbonneau D. Thorngren D. P.	*Reflected Light Observations of the Galilean Satellites from Cassini: A Testbed for Cold Terrestrial Exoplanets* **[#3065]** For terrestrial exoplanets with thin atmospheres, the surface will contribute to the reflected light signal of the planet. We present the expected contrast ratios of icy terrestrial exoplanets and discuss the implications on direct-imaging missions.
9:50 a.m.	Seales J. Lenardic A.	*Planetary Models Contribute to Studies of Exoplanet Habitability in an Uncertain and Statistical Way* **[#3004]** We use an uncertainty assessment of coupled Earth system models along with constraints on Earth's surface temperature and internal evolution to assess the potential evolutionary paths Earth has taken and what this implies for habitability studies.
10:05 a.m.		*Panel*
10:30 a.m.	BREAK	

Friday, February 7, 2020
SESSION 10: MISSIONS
11:00 a.m. Lecture Hall
In this session, we will explore how missions can inform our understanding of solar system and exoplanet bodies.
Moderators/Session Chairs: Emily Martin and Colby Ostberg
Panel Members: Knicole Colón, Martha Gilmore, Abigail Rymer, James Head

Times	Authors (*Denotes Presenter)	*Abstract Title and Summary*
11:00 a.m.	Colón K. D.	*Exoplanet and Solar System Science with the James Webb Space Telescope* **[#3009]** This presentation serves to provide an overview of the status and capabilities of the upcoming James Webb Space Telescope for exoplanet and solar system science.
11:20 a.m.	Gilmore M. S. Beauchamp P. M. Kane S. R. Venus Flagship Study Science Tea m	*Venus Flagship Mission Planetary Decadal Study, a Mission to the Closest Exoplanet* **[#3045]** Venus is the most accessible Earth-sized planet in the galaxy. We seek input as to what measurements we can make at Venus that help us interpret data from exoplanets.
11:35 a.m.	Rymer A. M. Hofstadter M. Simon A. Mandt K. Sayanagi K. M. de Pater I.	*Solar System Ice Giants Versus Exoplanet Ice Giants* **[#3055]** Exoplanet detection and characterization have taught us that planets with the sizes of Neptune are common in our galaxy and, therefore, a better understanding of this planetary class is desirable — how useful are solar system ice giants in adding to that understanding?
11:50 a.m.	Head J. W.	*The Solar System as an Exoplanet Guide: Findings, Surprises, and Caveats from the First Phase of Human and Robotic Exploration* **[#3054]** Sixty years of human and robotic space exploration has provided unprecedented knowledge of the origin and evolution of our solar system. We outline themes and caveats that can be applied to the exploration of exoplanets and other planetary systems.
12:05 p.m.		*Panel*

Friday, February 7, 2020
REVIEW, DISCUSSION, FINDINGS, FUTURE PLANS — WORKING LUNCH
12:30 p.m. Lecture Hall
We will discuss workshop findings and next steps.

Times	Authors (*Denotes Presenter)	Abstract Title and Summary
12:30 p.m.		*Review, Discussion, Findings, Future Plans — Working Lunch*
2:00 p.m.		*Adjourn*

CONTENTS

Interaction Between Iron/Magnesium Oxides and Hydrogen H. Allen-Sutter[1], S. Speziale[2], V. Prakapenka[3], and S.-H. Shim[1] [1]Arizona State University (hallens@asu.edu, sshim5@asu.edu), [2]Helmholtz Centre Potsdam (sergio.speziale@gfz-potsdam.de) [3]GSECARS Argonne National Lab, University of Chicago (prakapenka@cars.uchicago.edu).

Introduction: Hydrogen is the most abundant element in the universe and is the main constituent of gas giants (Jupiter and Saturn) in our solar system. However, due to its small size and reactive nature, very few experimental studies have been conducted at the high pressure-temperature conditions of planetary interiors, particularly with other planetary building materials, such as silicates and metals.

Gas giants in our solar system and exoplanetary systems [1] would be formed by accretion of a hydrogen and helium envelope around a rocky core [2]. Hydrogen is very reactive and could interact with the rocky core of these planets at the rock-fluid interface, or with infalling rocky bodies.

Such reactions become particularly important as the Juno mission revealed that internal density distributions in Jupiter is much more complicated than expected and requires a significant amount of heavier elements in the H-rich layer [3]. Therefore, it is important to understand reactions between hydrogen and other planetary building materials. Theoretical studies have explore the solubility of rocky materials in hydrogen at high pressure and temperatures [4], but technical difficulties have limited experimental exploration of these systems.

Methods: We used Laser-Heated Diamond-Anvil Cells (LHDAC) to study the interaction between iron/magnesium oxides under high pressure and temperature. Working with hydrogen in diamond anvil cells is particularly challenging because molecular hydrogen is extremely mobile and migrates into the diamond anvils and rhenium gaskets causing them to fail. This effect is exacerbated at high temperature. To overcome these problems we utilize a pulsed laser heating system [5] at GSECARS beamline 13-IDD at the Advanced Photon Source in Argonne National Lab. The short heating duration mitigates thermal diffusion of hydrogen. We also coat the rhenium gaskets in gold to lessen the migration of hydrogen into the gasket and formation of rhenium hydrides. Starting materials of Fe_2O_3, $(Mg_{0.5}Fe_{0.5})O$, and $(Mg_{0.9}Fe_{0.1})O$ were loaded into LHDAC's with a particle of gold for pressure calibration. These were then loaded with pure H_2 gas as a pressure medium then compressed to pressures ranging from 20-40 GPa. XRD diffraction patterns were collected in-situ.

Results: At pressures of 28 and 38 GPa, Fe_2O_3 was heated to temperatures of 1200-2600 K. During heating, Iron was reduced from $Fe^{+3}{}_2O_3$, to $Fe^{+2}O$, to FeH [6].

At a pressure of 30 GPa, $(Mg_{0.5}Fe_{0.5})O$ was heated to temperatures of 2000-3500 K. Heating produced FeH, ε'-Fe, and unknown phases. This observation suggests that Fe can be reduced by H from oxides and precipitates as metal or metal hydride. Decompression to 7 GPa yielded pure ε'-Fe implying all other phases are only stable at higher pressures.

At a pressure of 30 GPa, $(Mg_{0.9}Fe_{0.1})O$ was heated to temperatures as high as 4000 K. In all cases we observed the formation of brucite ($Mg(OH)_2$), with more being formed at lower temperatures. This observation suggests that oxides can be hydrogenated in H-rich environments at high pressure and high temperature.

Implications: In all cases, we observed reactions between oxides and hydrogen. In iron rich samples it stripped off iron, while in the magnesium rich sample it stripped off magnesium. Reactions between these rocky materials and hydrogen with significant amounts of hydrogen stored in the products could mean that the interface between the fluid hydrogen/helium layer and the rocky core could be gradual rather than sharp. Experimental results like these can be used to further understand the internal structure and evolution of gas giants like Jupiter and Saturn, which can in turn inform our observations of gas giant exoplanets.

References:

[1] https://exoplanetarchive.ipac.caltech.edu/ [2] Guillot, Tristan. (2005). *Annu. Rev. Earth Planet. Sci.* 33, 493-530. [3] Wahl, S. M., Hubbard et al., (2017). *Geophysical Research Letters*, *44*(10), 4649-4659. [4] Wilson, Hugh F., and Burkhard Militzer. (2012) *Physical Review Letters* 108.11, 111101. [5] Goncharov et al., (2010). *Review of Scientific Instruments*, *81*(11), 113902. [6] Pépin, C. M. et al., (2014). *Physical review letters*, *113*(26), 265504.

Earth is more than one planet: the many faces of Earth history as analogs for habitable exoplanets.
G. N. Arney[1] [1]NASA Goddard Space Flight Center (giada.n.arney@nasa.gov).

Earth is the best studied planet and the only known world with surface water and a biosphere. Thus, it provides a crucial starting to guide our search for other habitable worlds in other planetary systems. Yet the exoplanets we have thus far discovered have surprised us in many ways, and our first observations of terrestrial planets in their stars habitable zones will unquestionably continue this trend of the unexpected.

To guide our studies of the rich diversity of exoplanets we will someday encounter, it is instructive to consider the different environmental conditions and dominant biospheres that existed during our planet's long history to broaden our understanding of the types of habitable planets that might exist elsewhere. Some phases of Earth history are dramatically different from modern Earth, yet they are still, by definition, "Earth-like." In this presentation, I will provide an overview of what Earth through time tells us about biosignatures and environmental conditions that we might find on exoplanets dissimilar to modern Earth.

For instance, during the Archean (4-2.5 billions of years ago), Earth likely had a flourishing anaerobic biosphere (including methane-producing organisms) and a robust inventory of greenhouse gases to keep the surface temperature clement against the fainter younger sun. The atmosphere lacked the oxygen that is such an important biosignature to modern Earth. Instead, methane was likely present in abundance (2-3 orders of magnitude more than what is in the atmosphere today) as an important greenhouse gas and as a key biosignature of this anoxic environment (e.g. Krissansen-Totton et al. 2018). Methane may have occasionally been present at a high enough abundance to trigger the formation of a global organic haze, dramatically impacting the planet's climate and environmental conditions and acting as a kind of novel, non-gaseous biosignature (e.g. Zerkle et al. 2012; Arney et al 2016). Hazy Archean Earth is arguably the most alien planet we have geochemical data for and so is a useful datapoint for expanding our thinking of the kinds of habitable and inhabited environments that may be possible.

During the Proterozoic, (2.5 billion – 541 million years ago), significant oxygenation of the atmosphere occurred, transforming the chemical character of atmosphere in a powerful way. However, in the mid-Proterozoic, atmospheric oxygen levels may have been only 0.1% of the present atmospheric level, precluding directly detectable oxygen spectral features for remote observations. Instead, ozone, a photochemical byproduct of oxygen, may have been the only indirect spectral evidence of oxygen for this kind of low-O_2 atmosphere (e.g. Schwieterman et al. 2018). This is because ozone has an extremely strong absorption feature at UV wavelengths that is a highly sensitive indicator of low O_2 levels. Nitrous oxide levels may also have occasionally been elevated during the Proterozoic, a potent greenhouse gas and a type of biosignature (Roberson et al. 2011; Buick 2007). Yet methane levels may have been suppressed during the same time period (Olson et al. 2016), diminishing its importance as a biosignature and as a greenhouse gas.

Last but not least, modern Earth is the planet we will always understand best, and it can be used to validate models we will use to constrain and understand the properties of exoplanets. Yet remembering that the atmosphere of modern Earth is representative of only about 13% of Earth's total inhabited history is sobering and urges us to look back in time when we consider what may be possible on other Earth-like worlds.

DIRECT EXPLORATION OF AEROSOLS IN THE EXOPLANET NEXT DOOR: AN IN-SITU INSTRUMENT TO DETERMINE THE CHEMICAL COMPOSITIONS AND PARTICLE SIZE DISTRIBUTIONS OF VENUSIAN CLOUDS AND HAZES.

K. H. Baines[1], J. A. Cutts[1], D. Nikolić[1], S. M. Madzunkov[1], J.-B. Renard[2], O. Mousis[3], L. M. Barge[1], and S. S. Limaye[4], [1] Jet Propulsion Laboratory, California Institute of Technology (4800 Oak Grove Dr., Pasadena, CA, 91109, USA) [kevin.baines@jpl.nasa.gov], [2] LPC2E-CNRS, Université d'Orléans (3A Avenue de la Recherche Scientifique, 45071 Orléans, France), [3] Aix Marseille Univ., CNRS, CNES, LAM, Marseille, France, [4] Space Science and Engineering Center, University of Wisconsin-Madison (Madison, WI 53706, USA)

Introduction: Beyond a significant component of H_2SO_4, the composition of the hazes and clouds within Venus's thick atmosphere is poorly understood. Sulfuric acid clouds and hazes in the ~ 40-70 km altitude range result from photochemical processes involving SO_2 and H_2O. An admixture of constituents is evident by the surprisingly strong UV absorption observed within this cloud environment, providing evidence of poorly-understood chemical - and possibly biotic [1-3] - processes within the clouds.

To understand the cloud chemical and possibly biotic processes, we are developing a lightweight,low-power instrument package to measure, in-situ, both (1) the local gaseous environment and (2) the microphysical properties of attendant Venusian aerosols, including their composition and their number density and size distributions. This device would be used on future aerial missions, including on long-duration (multi-week) balloon missions and on short-duration (several hour) probes to explore the clouds and hazes of Venus, as well as potentially on missions to other cloudy worlds such as Titan, the Ice Giants, and Saturn.

Current requirements include the ability to measure mass ranges from 2 to 300 AMU at <0.02 AMU resolution to, for example, measure the component of iron chloride ($FeCl_3$ - 158 AMU; [4]) and potential biotic species embedded within sulfur acid aerosols. Another requirement, based on the expected saturated equilibrium concentration of HCl in H_2SO_4 aerosols near the 55-km-altitude level [5] is to measure HCl/H_2SO_4 with a mixing ratio of 2×10^{-9} to better than 10% in less than 300 secs. Solution chemistry of H_2SO_4 with HCl and with its sister hydrogen halides HF and HBr [6,7] may produce significant amounts of associated sulfonic acids (e.g., $ClSO_3H$, FSO_3H, $BrSO_3H$) and their daughter products (e.g., $SOCl_2$ and SO_2Cl_2, SOF_2, SO_2F_2 [4, 8]). Other potential species to be measured resident on or dissolved within H_2SO_4 particles include elemental sulfur polymers comprised largely of S_8 together with small admixtures of the metastable allotropes S_4 and S_3 [9,10].

The heart of the aerosol mass spectrometer component of the instrument package is the Quadrupole Ion-Trap Mass Spectrometer (QITMS, [11,12]).The preliminary concept involves an inlet aerodynamic lens [13,14] together with an adjustable piezo-electric aperture that allows only aerosols of a selectable size range within an overall range of 0.3 to 3.0 μm radius into the QITMS. Upon entering the QITMS, aerosols are vaporized by its hot electrode surfaces (~320° C). Notably, the elimination of CO_2 and other gas species provided by the aerodynamic lens increases the trace aerosol species concentration by about 4 orders of magnitude. As a result, to a precision of 10%, trace aerosol species with concentrations relative to the expected dominant H_2SO_4 material of 100 ppb and 2 ppb (corresponding to about 0.01 ppb and 0.2 ppt relative to the ambient atmospheric CO_2) can be measured to 10% precision in <6 secs and <5 minutes, respectively. Beyond pertaining to inorganic materials expected to be present within Venusian hazes and clouds, such precisions would be attained as well for biotic and planetary evolution species of interest such as hydrocarbons, phosphorus compounds, and isotopic ratios of carbon, nitrogen, sulfur, oxygen and hydrogen (i.e., the D/H ratio) found both within aerosol particles and the attendant gaseous environment.

As a front end to the aerodynamic lens, we are considering adding a lightweight, compact nephelometer/particle-counter device being developed at LP2CE-CNRS [15]. Evolved from designs regularly flown on balloons in recent years [16,17], this component will enable the particle number density and size distributions to be determined as well, perhaps indicating, for example, that aerosols involving unexpected molecular species have a distinctly different size and number density than typical particles.

References:

[1] Schulze-Makuch, D. and Irwin, L.N. (2002). *Astrobiology, 2,* 197–202. [2] Schulze-Makuch, D. et al. (2004) *Astrobiology 4*, 11–18. [3] Limaye S. S. et al. (2018) *Astrobiology* 18, #10, 1-18. [4] Krasnopolsky V. A. (2017) *Icarus*, *286*,134-137. [5] Delitsky M. L. and Baines K. H. (2018). *Proc. of the 50th AAS/DPS.* #102.01. [6] Sill, G. T. (1975) *J. Atm. Sci*., *32*, 1201 -

1204. [7] Krasnopolsky V. A. (2017) *Icarus*, *293*, 114-118. [8] Delitsky M. L., Baines K. H. (2015) *Proc. of 47th AAS/DPS.* #217.02. [9]Toon O. B. et al. (1982) *Icarus, 51*, 358 - 373. [10] Hartley K. M., et al. (1989) *Icarus*, 77, 382 - 390. [11] Madzunkov, S. M. and Nikolić, D., 2014. *J. Am. Soc. Mass Spectr*., 25, 1841 - 1852. [12] Avice, G., et al. (2019) *J. Anal. Atomic Spectrom.*, *34*, 104-117. [13] Schreiner, J. et al. (1999) *Science, 283,* 968-970. [14] Cziczo, D. J., et al. (2004) *JGR,* 109, DOI: 10.1029/2003JD004032 [15] Renard, J.-B. et al. (2019). IPPW-2019, Poster A3, Oxford, UK. [16] Renard, J.-B., et al. (2016) *Atmos. Meas. Tech. 9*, 1721-1742 [17] Renard, J.-B., et al. (2016) *Atmos. Meas. Tech., 9*, 3673-3686.

PHOTOMETRIC OBSERVATIONS OF POSSIBLE EXOPLANET TRANSITS AT AUSTIN COLLEGE'S ADAMS OBSERVATORY: GROUND-BASED SUPPORT FOR NASA'S TESS MISSION. D. Baker[1], N. Hannon[1], A. Martin[1], and M. Winterrowd[1], [1]Austin College, Physics Department, 900 North Grand Avenue Suite 61627, Sherman, Texas, 75090, dbaker@austincollege.edu.

Introduction: In 2018, the Transiting Exoplanet Survey Satellite (TESS) began its two-year mission to monitor more than 200,000 stars for transiting exoplanets [1]. Because of the wide field of view and corresponding large pixel size of the TESS telescope, high precision ground-based observations are needed to confirm planetary transits and eliminate false positives [2]. The TESS Follow-up Observing Program Sub Group 1 (TFOP SG1) was developed to coordinate ground-based photometric follow-up observations [3].

The Adams Observatory at Austin College provides ground-based photometric support for the TESS project by contributing to TFOP SG1. Located on the roof of the IDEA Center science building, this facility houses the largest research telescope in north Texas and presents outstanding opportunities for research, education, and public outreach. Research projects at the Adams Observatory include planetary imaging, stellar photometry, and stellar spectroscopy. In addition to TFOP, the Adams Observatory contributes to exoplanet transit observations as a member of the KELT Follow-Up Network [2].

Here, we present a summary of TESS follow-up photometric observations at the Adams Observatory through November 2019. Four TESS targets have been observed: one confirmed planet, one verified planet candidate, and two nearby eclipsing binaries (NEBs).

Equipment: The Adams Observatory uses a 0.61-m f/8 DFM telescope of Ritchey-Chrétien design. When coupled with a Finger Lakes Instruments (FLI) Proline 16803 imager, this system produces a 26' x 26' field of view and a 0.38" pixel scale. Telescope guiding is accomplished with an off-axis SBIG STF-8300M camera, resulting in drift of only a few pixels over a four-hour observing session. Typical seeing conditions range between 1.2" and 2.0". *AstroImageJ* is used for image reduction, photometry, and model fitting [4]. Under optimal conditions, we are able to detect a minimum transit depth of 3.0 ppt, which for an M-dwarf star would indicate an exoplanet with radius ~3 Earth radii.

Results: *Confirmed Planet.* TESS Object of Interest (TOI) 197.01 is a hot Saturn orbiting an oscillating host star [5]. Adams Observatory observations on 06 Nov 2018 in the I filter with 45 sec exposures did not reveal a planetary transit since the expected transit depth of 0.8 ppt was less than the RMS uncertainty ~3.0 ppt of our light curve (not shown). This southern hemisphere star was positioned relatively low in the sky for our northern hemisphere site, thus producing large scatter in our data. Our observations did clear a nearby fainter star of a possible NEB transit, eliminating this potential false positive.

Verified Planet Candidate. TOI 1252.01 was observed on 18 Oct 2019 in the I filter with 180 sec exposures under clear skies (Figure 1). This observation only covered the latter half of the transit and detected a 5.5 ppt dip in the light curve (RMS uncertainty ~1.3 ppt). Orbiting an M-dwarf star, this verified planet candidate has a radius of 4.9 Earth radii and an orbital period of 1.12 days, classifying this candidate as a possible hot Neptune.

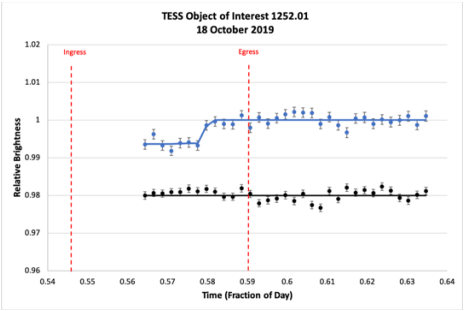

Figure 1. Partial transit of verified planet candidate TOI 1252.01 (blue) vs. nearby comparison star (black). Transit appears to end earlier than predicted.

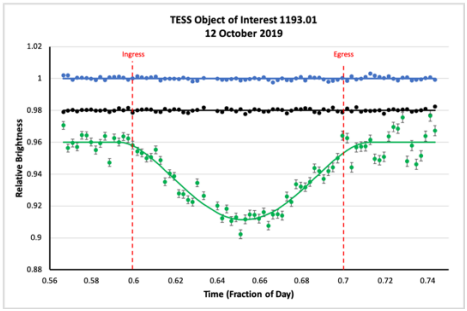

Figure 2. Light curves of TOI 1193.01 target star (blue), nearby comparison star (black), and a fully transiting nearby eclipsing binary (green).

NEBs. TOI 1193.01 was observed on 12 Oct 2019 in the I filter with 180 sec exposures under clear skies with a full Moon (Figure 2). RMS uncertainty on the target star is 0.88 ppt, and no transit was detected on the target. A nearby star 14.5" away shows a 40 ppt V-shaped full transit with the predicted timing, indicative of an NEB. This target has been retired based on these observations.

TOI 1313.01 was observed on 23 Oct 2019 in the R filter with 60 sec exposures under clear skies (Figure 3). RMS uncertainty on the target star is 2.0 ppt, and no transit is detected on the target within this uncertainty. A nearby star 28.2" away shows a 20 ppt full transit with approximately the predicted timing. This target has been expired as an NEB.

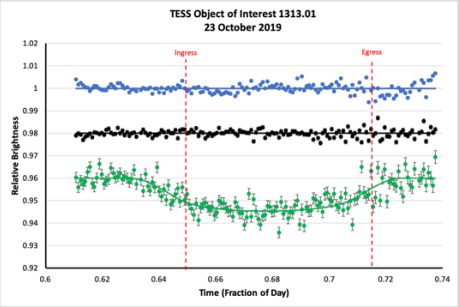

Figure 3. Light curves of TOI 1313.01 target star (blue), nearby comparison star (black), and a fully transiting nearby eclipsing binary (green).

Future Work: In the next year, TESS will complete its observations in the northern hemisphere sky. The need for follow-up ground-based observations will increase considerably. We plan to continue follow-up observations at the Adams Observatory in the coming years, especially in summer 2020. Precision of our measurements should improve as we observe targets closer to zenith, potentially allowing us to detect mini-Neptune sized exoplanets.

References: [1] Ricker G. R. et al. (2015), *JATIS* 1(1), 014003. [2] Collins K. A. et al. (2018), *AJ* 156:234. [3] Collins K. (2019), AAS Meeting, 2019AAS...23314005C. [4] Collins K. et al. (2017), *AJ* 153:77. [5] Huber et al. (2019), *AJ*, 157:245.

TITAN: A HAZY WATERWORLD THAT WE CAN VISIT

Jason W. Barnes[1], Elizabeth P. Turtle[2], Melissa G. Trainer[3], Ralph D. Lorenz[2], Sarah Hörst[4], Shannon M. MacKenzie[2], and the *Dragonfly* Science Team. [1]University of Idaho, Moscow, ID, USA (jwbarnes@uidaho.edu), [2]Johns Hopkins Applied Physics Laboratory, Laurel, MD, USA, [3]NASA Goddard Space Flight Center, Greenbelt, MD, USA, [4]Johns Hopkins University, Baltimore, Maryland, USA

1 INTRODUCTION

There are precious few examples of planets with both distinct surfaces and thick atmospheres in the Solar System: just Venus, Earth, Mars, and Saturn's moon Titan. These four therefore represent our only opportunities to explore close-up the diversity of physical and chemical processes that we expect occur on trillions of extrasolar planets in the Milky Way. Titan's contributions to this endeavor derive from its (1) organic chemistry, (2) interior water ocean, (3) surface-atmosphere interactions, and (4) hazy methane-rich atmosphere.

Titan's particular strength with respect to exoplanets derives from its accessibility. The *Cassini/Huygens* mission explored Titan from Saturn orbit and within the atmosphere, respectively. A future Titan orbiter mission will hopefully follow up on *Cassini*'s discoveries [e.g. 1], providing global imaging and topography, atmospheric measurements and characterization, and gravity probing of the interior.

Dragonfly [2] is a Titan lander mission within the NASA New Frontiers program that was selected for flight on 2019 June 27. Its science themes include prebiotic chemistry, habitability, and a search for biosignatures. To address these themes, *Dragonfly* will sample both water ice and organic sediments within Titan's sand seas' dunes and interdunes. Because prebiotic chemistry or prospective life on Titan might consist of familiar water-based pathways or use liquid methane/ethane as a solvent, sampling both ice and organics provides for a broad-based approach to either. *Dragonfly* carries a mass spectrometer to determine molecular masses of surface materials and a gamma-ray and neutron spectrometer to assess the bulk and inorganic atomic fractions within the regolith, as well as cameras, seismometers, and an atmospheric sensor suite. *Dragonfly* is a giant quadcopter: the entire lander flies. That aerial mobility makes it possible to explore a variety of targets, following up on discoveries that we make along the way like rovers do on Mars.

2 ORGANIC CHEMISTRY

Titan's ubiquitous organic compounds created by photolysis of atmospheric methane set it apart from other Solar System planets. The complexity of Titan's organics exceed that of everywhere else in the Solar System other than Earth itself. Titan therefore serves as an ongoing experiment in abiotic organic synthesis. Entire planets like Titan may be common in extrasolar systems [3, 4, 5].

Figure 1: Artist's conception of *Dragonfly* on the surface of Titan, within an interdune in the Shangri-La sand sea.

On Titan, carbon can interact with liquid water **on the surface**. Cryolava flows and impacts create transient surficial liquid water environments. When organics (sitting on the surface or falling out of the atmosphere) mix with water, the resulting environment simulates what may have happened on the early Earth [6]. *Dragonfly* seeks to answer the question: How far in complexity space have Titan's organics progressed in the absence of biology? Analyzing previously liquid water that mixed with organics could therefore bring insights into prebiotic chemistry unattainable in the terrestrial laboratory and potentially shed light on the origin of life and how that origin may be replicated in extrasolar systems.

3 INTERIOR OCEAN

Extrasolar terrestrial and super-Earth type planets may contain significantly higher water mass fractions than Earth itself. To that end, Titan and its sister ocean worlds of the Solar System provide a tangible analog. *Dragonfly* probes Titan's interior by use of seismometers, electric field measurements, and imaging. Autocorrelation of seismograms of Titanquakes reveal the depth of Titan's solid ice crust, and thereby the depth to the subsurface water ocean mantle [7]. Sufficiently strong quakes could reveal further details of interior structure, allowing for validation of models and serving as a reference point for extrasolar waterworld interior structure as well. We also constrain the depth to the ocean using Titan's Schumann

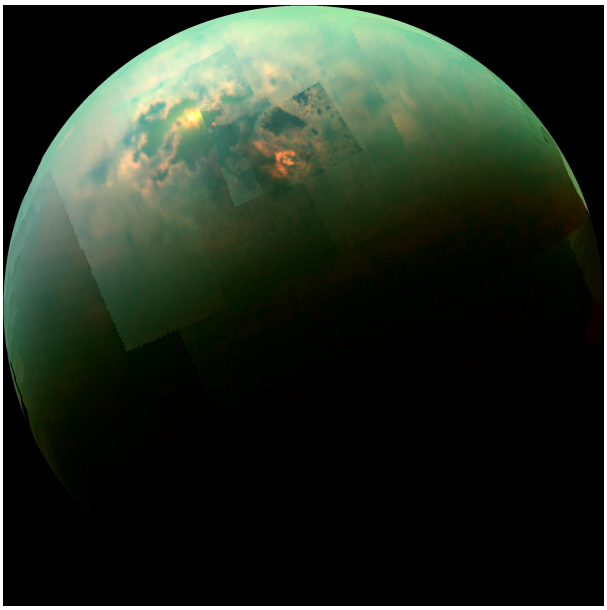

Figure 2: *Cassini* T104 flyby mosaic of Titan's north pole, showing a specular reflection off of Kraken Mare, a liquid hydrocarbon sea.

resonance [8]. *Dragonfly* imaging of landing sites can reveal faulting and other geological process as may mix surface organics with liquid water.

4 SURFACE & ATMOSPHERE

As the only location in the universe with surface lakes other than Earth, Titan allows us to observe how oceanographic processes operate in an extraterrestrial environment [e.g. 9]. Use of sun glints to detect extrasolar planetary oceans [10], for instance, has been tested at Titan from *Cassini* [11].

Because *Dragonfly* will land in Titan's equatorial desert, far from the north polar seas, its primary contribution lies in the characterization of surface and atmospheric processes in-situ. We will not be sending landers to any extrasolar planets while any of us is alive. *Dragonfly* will, however, constrain surface alteration mechanisms, determine their rates, and allow us a second data point for how those processes may vary with differing gravity, atmospheric density, and composition.

5 HAZY METHANE ATMOSPHERE

Titan's nitrogen-methane atmosphere, and the inevitable organic haze that results from its exposure to sunlight, provides insights in to the conditions of early Earth [12]. Prior to the formation of life, methane in Earth's atmosphere may have seeded the surface with organics by similar photolysis under the faint young Sun [13]. Hazes like Titan's may be ubiquitous among extrasolar planets [14]; indeed, the lack of spectroscopic absorption features in some transiting exoplanets has been attributed to high haze opacity. In-situ observation of that haze production at Titan [and in the lab][]2018NatAs...2..303H allows us to constrain the physical and chemical processes at work in a way that complements our very-low-resolution transit spectroscopy of extrasolar planet atmospheres [like GJ1214b 15].

6 CONCLUSION

Titan is an important extrasolar planet analog because it shares important aspects but also because we can visit Titan by spacecraft in our lifetimes. *Cassini* and future Titan orbiters will provide global atmospheric and surface measurements at high resolution. *Dragonfly* will explore Titan as a rotorcraft in a way similar to that achieved at Mars with rovers. As a result, we expect for insights gleaned from its surface mission to be broadly relevant across planetary science discliplines, and in particular for its discoveries to show relevance to the interiors, surfaces, and atmospheres of solid- and liquid-surface extrasolar planets.

References

[1] C. Sotin, et al. (2017) in *LPSC* vol. 48 2306.
[2] R. D. Lorenz, et al. (2018) *Johns Hopkins APL Technical Digest* 374–387.
[3] A. E. Gilliam, et al. (2011) *Planetary and Space Science* 59(9):835 ISSN 0032-0633 doi.
[4] J. Checlair, et al. (2016) *Planetary and Space Science* 129:1 doi.
[5] J. M. Lora, et al. (2018) *ApJ* 853(1):58 doi. arXiv:1712.04069.
[6] C. D. Neish, et al. (2018) *Astrobiology* 18:571 doi.
[7] S. D. Vance, et al. (2018) *Astrobiology* 18(1):37 doi.
[8] C. Béghin, et al. (2007) *Icarus* 191(1):251 doi.
[9] R. D. Lorenz (2014) *GRL* 41(16):5764 doi.
[10] T. D. Robinson, et al. (2010) *ApJ* 721:L67 doi. arXiv:1008.3864.
[11] J. W. Barnes, et al. (2013) *ApJ* 777:161 doi.
[12] M. G. Trainer, et al. (2018) *Astrobiology Science Strategy Whitepaper*.
[13] G. Arney, et al. (2016) *Astrobiology* 16(11):873 doi.arXiv:1610.04515.
[14] T. D. Robinson, et al. (2014) *PNAS* 111(25):9042 doi.arXiv:1406.3314.
[15] Z. K. Berta, et al. (2012) *ApJ* 747(1):35 doi. arXiv:1111.5621.

Physical Oceanography in the Solar System and Beyond. R.K. Barnes[1], J.A.M. Green[2], B.W. Blackledge[2,3], M.J. Way[4], G.D. Egbert[5], and J. Sharples[6]. [1]Astronomy Department, University of Washington, Seattle, WA 98195, rory@astro.washington.edu, [2]School of Ocean Sciences, Bangor University, Menai Bridge, UK, [3]Environmental Futures & Big Data Impact Lab, University of Exeter, Exeter Science Park, EX5 2FS, UK, [4]NASA Goddard Institute for Space Studies, [5]College of Earth, Ocean, and Atmospheric Sciences, Oregon State University, OR, USA, [6]School of Environmental Sciences, University of Liverpool, Liverpool L69 3GP, UK

Introduction: A key controller of a planet's rotational evolution, and hence habitability, is tidal dissipation, which on Earth occurs primarily in the oceans. As the discovery of habitable exoplanets is a primary objective of exoplanet research, it is imperative that we understand how "exo-oceans" behave. Despite this importance, little research has investigated the physical oceanography of worlds other than Earth. This oversight has occurred even though the Earth science community has studied tidal flows in Earth's oceans for over a century and developed sophisticated models that exquisitely match satellite altimetry data, e.g. [1]. Here, we present a) models of tidal effects on exoplanets to motivate the problem [2], b) the application of a physical oceanography model to a putative ancient Venus ocean [3], and c) the application of that model to an ensemble of "alternative Earths" with a range of continental configurations and seafloor properties [4]. We find that oceanic tidal dissipation can span 5 orders of magnitude, revealing that simulating exo-oceans with Earth science tools will provide fundamental insight into exoplanet evolution and habitability.

Methods: To calculate tidal effects on exoplanets we use the "equilibrium tide" model, first derived in [5], which assumes that the line connecting two worlds' centers of mass and the direction of the tidal bulge are not parallel. We consider two cases: one in which the offset is constant in phase (constant-phase-lag, CPL) or constant time in time (constant-time-lag, CTL). We model these tidal effects with the code `VPLanet` [6]. To calculate tidal dissipation in oceans, we use the OSU Tidal Inversion Software (`OTIS`) [7,8], which solves the shallow water equations and can simulate a range of bathymetries, continental shapes, and frequencies.

Exoplanets: Although the possibility of tides driving planetary rotation to synchronous rotation ("tidal locking") is well known [9,10], we have explored a much broader range of assumptions and found that the range of planets that can be affected by tides is much larger than previously realized [2], see Fig. 1. This result assumes that planets can form with obliquities from 0 to π, and rotation rates from 8 hours to 10 days [11]. We find that planets with initially slow rotation periods may tidally lock in the habitable zones (HZs) of Sun-like stars within 10 Gyr, and therefore oceanic tidal effects could affect many habitable exoplanets, including those that will be targeted by direct imaging campaigns. These simple models predict that exoplanets to the left of the dotted line are almost assuredly tidally locked, those to the left of the solid line may be tidally locked, and those to the right of the solid curve are almost assuredly not tidally locked.

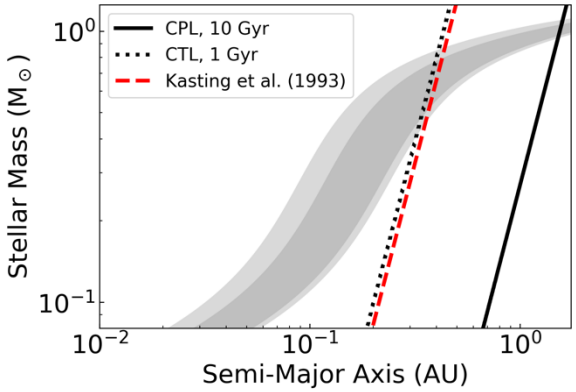

Fig. 1: Timescale to tidally lock as a function of stellar mass and semi-major axis, assuming circular orbits. The HZ from [12] is shown in grey, with light representing the "optimistic" limits and dark the "pessimistic" limits. The dotted line assumes a 0.1 Earth-mass planet, one-tenth of modern Earth's tidal response, a tidal locking time of 1 Gyr, an initial rotation period of 8 hours, an initial obliquity of 60°, and the CTL model. The solid line assumes a 10 Earth-mass planet, modern Earth's tidal response, a tidal locking time of 10 Gyr, an initial rotation period of 10 days, no obliquity, and the CPL model. The red curve is from [12] and assumes a 1 Earth-mass planet with no obliquity, an initial rotation period of 13.5 hours and the CPL model.

Ancient Venus: We next turn to directly modeling a hypothetical ocean on Venus [3]. Although Venus may not have had an ocean [13], it is a known planet with a well-studied surface and therefore serves as a useful fiducial in the quest to understand exo-oceans. We use the elevation data from [14], consider "shallow" (330 m mean depth) and "deep" (830 m mean depth) oceans, and explore a range of prograde and retrograde rotational frequencies. We also consider turbulent ("internal tides," IT) and laminar (noIT) tidal flows. In Fig. 2 we plot the dissipation, torque, and tidal Q (the amount of energy available in the system divided by the energy dissipated in one cycle) of the simulations. These 3 quantities vary by over 4 orders of magnitude depending on assumptions.

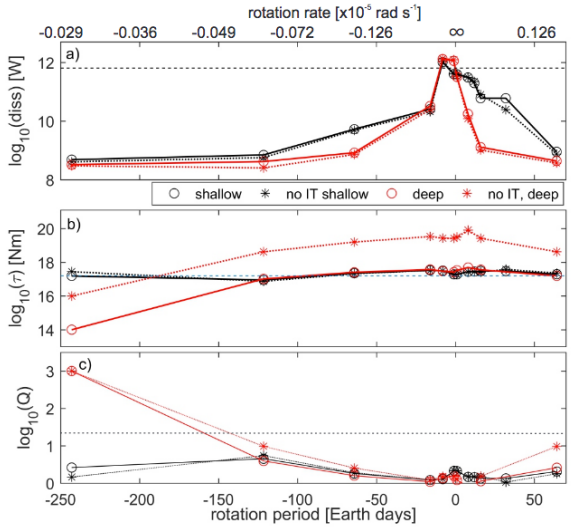

Fig. 2: Tidal effects in an ancient Venusian ocean. Negative rotation rate means retrograde rotation. Modern Earth's values are shown by dotted lines. *Top:* Global dissipation in Watts. *Middle*: Rotational torque induced by tides. *Bottom:* Tidal *Q*.

Alternative Earths: For our final experiment, we consider an Earth-like planet affected by the Sun and Moon, but for a range of continental shapes with fractal coastlines [15], bathymetric "roughness," and rotational frequencies [4]. We considered 111 randomly generated continental configurations and 9 specific configurations designed to test specific scenarios.

In order to characterize the total effect of continent size, ocean basin size, and coastal complexity, we use the non-dimensional value $R = L_{tot}/(A_{ocean})^{0.5}$, where L_{tot} is the total coastline length and A_{ocean} is the ocean basin area. The results of these simulations are shown in Fig. 3 and reveal that, similar to ancient Venus, the dissipation can span 5 orders of magnitude.

Conclusions: Using simple models of tidal effects and a plausible range of initial rotational angular momentum, we find that planets in the HZs of stars up to the mass of the Sun may become tidally locked within 10 Gyr. However, we also find that the tidal locking limit is not well-defined, in part because we only extrapolated from Earth values. This uncertainty motivates the application of `OTIS` to non-Earth worlds to explore the range of tidal dissipation that is possible on exoplanets.

We found that dissipation in an ancient Venusian ocean as well as in an ensemble of Earth-like planets reveals a span of 5 orders of magnitude. Although these simulations greatly expand the number of worlds that have been modeled with modern physical oceanography methods, they still only address a narrow range of possibilities for exoplanets. In the HZs of M dwarf stars, tidal forces and frequencies are orders of magnitude larger than on Earth or Venus due to their closer proximity to their host star. Future research that simulates oceans beyond the Solar System could provide critical insight into the search for life in the universe.

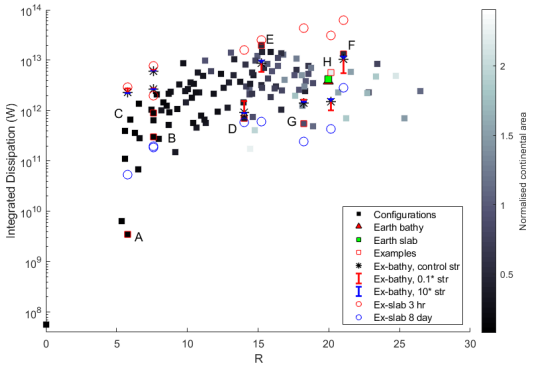

Fig. 3: Tidal dissipation for Earth, but with a range of continental configurations, bathymetries, and rotation periods. The shading corresponds to the amount of land relative to modern Earth. Runs labeled "bathy" include seafloor roughness, while "slab" does not. Squares denote 24 hour rotation period, red circles 3 hours, and blue circles 8 days. Letters denote continental configurations investigated in more detail because they span the parameter space.

Acknowledgments: RB acknowledges support from NASA's Virtual Planetary Laboratory and ROCKE-3D consortium. JAMG acknowledges funding from the Natural Environmental Research Council (MATCH, NE/S009566/1). MJW is thankful for support from the Goddard Space Flight Center's Sellers Exoplanet Environments Collaboration (SEEC), which is funded by the NASA Planetary Science Division's Internal Scientist Funding Model. This work benefited from participation in NASA's Nexus for Exoplanet System Science.

References: [1] Egbert, G.D & Ray, R.D. (2000) *Nature*, 405, 775-778. [2] Barnes, R. (2017) *Cel. Mech. Dyn. Astron.,* 129, 509-536. [3] Green, J.A.M., *et al.,* (2019) *ApJL*, 876, 22. [4] Blackledge, B., *et al*. (2019) *GRL*, submitted. [5] Darwin, G. (1880) *PTRS,* 171, 713-891. [6] Barnes, R. (2019) *PASP*, in press. [7] Egbert, G.D., *et al*. (1994) *JGR*, 99, 24,821-24,852. [8] Egbert, G.D. & Erofeeva, S.Y. (2002) *J. Atm. Ocean Tech.,* 19, 183-204. [9] Dole, S. (1964) *Habitable Planets for Man.* Rand Corp. [10] Kasting, J.F. *et al*., (1993), *Icar.* 101, 108-128. [11] Miguel, Y. & Brunini, A. (2010) *MNRAS,* 406, 1935-1943. [12] Kopparapu, R. *et al.,* (2013) *ApJ,* 765, 131. [13] Way, M.J. *et al.,* (2016) *GRL*, 8376-8383. [14] Ford, P.G. & Pettengill, G.H. (1992) *JGR,* 97, 13103-13114. [15] Goodchild, M.F. & Mark, D.M. (1987) *Ann. Assoc. Am. Geograph.,* 77, 265-278.

Improving Atmospheric Photochemical Models for Cool Rocky Exoplanets with New Low-Temperature Reaction Rate Coefficients

Shiblee R. Barua[1,2] (shiblee.barua@nasa.gov), Paul N. Romani[1]
[1]*NASA Goddard Space Flight Center, 8800 Greenbelt Rd, Greenbelt MD 20771*
[2]*Universities Space Research Association, 7178 Columbia Gateway Dr, Columbia MD 21046*

Nowadays exoplanet atmospheric modeling is focused primarily on giant exoplanets close to their host stars due to their easier detection and characterization by direct imaging. However, the introduction of JWST will enable us to obtain high-quality spectra of exoplanet atmospheres of various sizes and distances from their host star, including low-temperature conditions similar to that of our outer planetary system (*e.g.*, Titan). Reliable interpretation of such spectra will require complex self-consistent photochemical models for which accurate reaction rate coefficients are indispensable. Unfortunately, low-temperature reaction rate coefficients relevant to cool rocky exoplanet atmospheres are currently not well-constrained due to the extreme difficulty in measuring them accurately in the lab. An alternative approach is to employ a high-level *ab initio* quantum chemical method to calculate accurate rate coefficients for radical–radical and radical–neutral reactions relevant to low-temperature atmospheres. We are using this approach to investigate some key reactions that directly impact the production/loss of chemical species such as NH_3, HCN, H_2O, CO, CO_2, C_3H_8, etc. The versatility of our theoretical method enables us to study chemical reactions of modestly sized molecules (*i.e.* less than 40 electrons to keep the computational cost within reach) for any gaseous environment (*e.g.* H_2, He, N_2, NH_3, CH_4, CO_2, O_2, NO_x, SO_x, etc.). In addition, our method covers a wide range of temperatures (10–200K) and pressures (microbar to bars). Our calculated rate coefficients will be made available to the public via established databases and repositories like NASA's Planetary Data System (PDS), Kinetic Database for Astrochemistry (KIDA), Exoplanet Modeling and Analysis Center (EMAC), etc. Modelers can use our rate coefficient data to develop accurate atmospheric photochemical models for cool rocky exoplanets that are to be detected/characterized in the near future by JWST.

Identifying Exo-Earth Candidates in Direct Imaging Data Through Bayesian Classification A. Bixel[1,3] and D. Apai[1,2,3], [1]Steward Observatory, The University of Arizona, [2]Lunar and Planetary Laboratory, The University of Arizona, [3]Earths in Other Solar Systems Team, NASA Nexus for Exoplanet System Science

Introduction: Future space telescopes such as HabEx [1] and LUVOIR [2] could be able to directly image several Earth-sized planets in the habitable zones of nearby stars. Through deep follow-up spectroscopy, astronomers could then determine whether these planets are habitable and search for signs of life. However, these exo-Earth candidates (EECs) would be initially difficult to distinguish from the ~ 10 times as many planets with bulk compositions and surface temperatures not hospitable to life [3]. An efficient survey of nearby planets must therefore rely on a scheme for identifying the most promising candidates for follow-up spectroscopy while rejecting the many potential "false positives".

Methods: In our recent paper [4], we demonstrated a Monte Carlo method for interpreting direct imaging observations of an exoplanet within the context of existing observational and theoretical prior knowledge about exoplanet properties. This allowed us to place constraints on the planet's size, mass, and orbit, and to calculate the probability that it is, in fact, an EEC. For an example of our method's application to a hypothetical exoplanet, see Figure 1. Furthermore, this method can be adapted to incorporate new prior knowledge which may be attained within the coming decade.

Next, using realistic assessments of the targeted host stars and detected planet yield of LUVOIR [2], we conducted a mock survey in which we prioritized planets by the likelihood that they are habitable as inferred from a single epoch of direct imaging data, then submitted them for spectroscopic follow-up observations in order of priority. From this, we calculated the efficiency with which the true EECs were characterized - and potential false positives discarded - over the course of the mock survey.

Discussion: We have shown how our method of prioritizing targets for spectral followup with a single epoch of data is advantageous compared to blind target selection or a simple separation- and magnitude-based cut. We have also estimated the efficiency with which EECs can be identified given additional data - for example, by considering an independent detection through supporting radial velocity observations (e.g., [5]) or by using color information to discriminate between different planet types (e.g., [6]).

Finally, we will discuss the implications of our results for research and instrumentation development in the 2020s, and the survey strategy for space-based imaging missions once they are launched.

Future work: Our published results demonstrate the importance of leveraging prior research to enable future discoveries. Following this theme, we will discuss our ongoing effort to synthesize research in the areas of planet formation, planet statistics, habitability, and quantitative biology into simulations of planetary systems. These simulated systems will contain a diversity of plausible non-habitable, habitable, and inhabited environments, and can be used to formulate testable hypotheses and predict the output of next-generation ground- and space-based surveys.

References:

[1] The HabEx Study Team. 2019, The HabEx Final Report, https://www.jpl.nasa.gov/habex/

[2] The LUVOIR Study Team. 2019, The LUVOIR Final Report, https://asd.gsfc.nasa.gov/luvoir/

[3] Guimond, C. M., & Cowan, N. B. 2018, AJ, 155, 230

[4] Bixel, A., & Apai, D. 2019, ApJ, in press

[5] Dressing, C., Stark, C. C., Plavchan, P., & Lopez, E. 2019, BAAS, 51, 268

[6] Krissansen-Totton, J., Schwieterman, E. W., Charnay, B., et al. 2016, ApJ, 817, 31

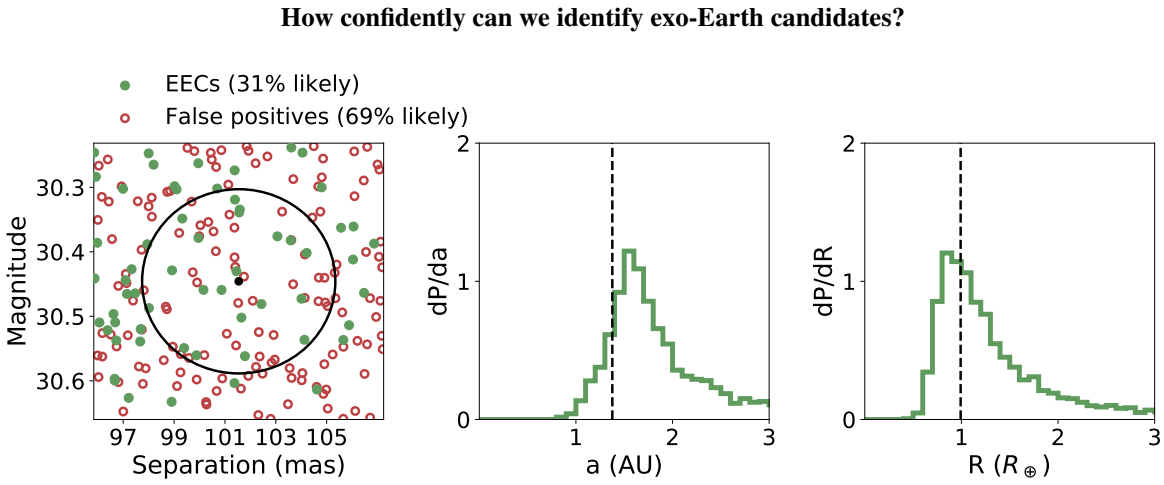

Figure 1: We simulate the detection and characterization of an Earth-sized planet in the middle of the LWHZ of a Solar-mass star at 15 parsecs distance. The planet is in fact an EEC, but the observer can only determine this with 31% confidence. (Left) We compare the planet's observed separation and magnitude to those of several planets drawn from statistical prior distributions, and find that the majority of planets which appear similar to the target are not habitable. (Center/right) Posterior distributions for the planet's semi-major axis and size; the true values are marked with dashed lines. Adapted from [4].

Atmospheric Escape from Mars: Lessons for Studies of Exoplanets. D. Brain[1], M. Chaffin[1], S. Curry[2], H. Egan[1], R. Ramstad[1], B. Jakosky[1], J. Luhmann[2], C. Dong[3], and R. Yelle[4], [1]LASP / University of Colorado (david.brain@colorado.edu), [2]SSL / University of California Berkeley, [3]PPPL / Princeton University, [4]LPL / University of Arizona, [2]SSL / University of California Berkeley.

Introduction: The planet Mars provides an intriguing laboratory for investigations of habitability on exoplanets. Though conditions at the Martian surface today are not well-suited for life, the Martian surface and atmosphere hold many clues that suggest that the necessary conditions for life were present billions of years ago. Habitable surface conditions long ago are thought to require a substantially different atmosphere, implying that much of the Martian atmosphere escaped to space over time. Mars may have been particularly susceptible to escape (compared to Earth) because of its small size and/or its lack of global magnetic field to shield the atmosphere. Each of these differences has implications for the loss rates of both neutral and charged particles over time.

The Mars Atmosphere and Volatile (MAVEN) mission to Mars has provided a wealth of data over the past three years that teach us about atmospheric escape processes and rates both today and over Martian history. These data can be applied (with caution) to situations at other planets both in our solar system and beyond; in a sense Mars is a nearby laboratory for examining issues of atmospheric retention and habitability terrestrial exoplanets.

Atmospheric Escape from Mars: We will begin by reviewing the escape processes active on Mars today, and place them in context with processes thought to be occurring on exoplanets. Further, we will review the amount of atmosphere that could have been removed from Mars over solar system history.

Mars as an Exoplanet: If Mars is a laboratory for exoplanets, one could consider what might happen if a 'Mars' were discovered orbiting a nearby star. Since M Dwarf stars are both particularly numerous and host exoplanets, we choose to consider how Mars might fare if it orbited an M Dwarf.

First, we examine whether the atmosphere of "ExoMars" would hydrodynamically escape and find that, for a Mars in its star's habitable zone, that the exospheric temperature would need to exceed the effective temperature by a factor of 50. Thus, it seems plausible that at least some Mars-like planets orbiting M Dwarves would not lose their atmosphere via hydrodynamic processes.

MAVEN's measurements have enabled estimates of the thermal loss of hydrogen from the Mars extended exosphere, the photochemical loss of oxygen from the thermosphere, and the loss of oxygen ions accelerated by electric fields near Mars. In addition, MAVEN's data have been used to validate models for the loss of atmosphere from the planet. We consider how each of these 'pathways' for atmospheric loss would be changed if: the stellar photon and particle flux were consistent with a typical (such as it is) M Dwarf star, stellar disturbed (i.e. storm) periods were more frequent and more intense, and the planet orbited at a closer distance from the star. We examine the influence of these changes on thermal escape of hydrogen, photochemical escape of oxygen, ion loss, and sputtering. We find that in all cases we expect atmospheric escape to either increase of remain roughly constant. Thus, the timescale for atmospheric retention would be reduced on "ExoMars". This timescale may be ass short as 10's of thousands of years (compared to 100's of millions for present-day Mars), depending upon the activity of the host star.

The Influence of Planetary Magnetic Fields on Atmospheric Retention. D. Brain[1], R. Ramstad[1], H. Egan[1], Y. Dong[1], T. Weber[1], R. Jolitz[1], R. Jarvinen[2], M. Holmstrom[3], K. Seki[4], J. McFadden[5], L. Andersson[1], J. Espley[6], J. Halekas[7], D. Mitchell[5], J. Luhmann[5], and B. Jakosky[1], [1]LASP / University of Colorado (david.brain@lasp.colorado.edu), [2]FMI, Finland, [3]IRF Kiruna, Sweden, [4]University of Tokyo, [3]SSL / University of California Berkeley, [4]NASA GSFC, [5]University of Iowa.

Motivation: Until recently, it had long been assumed that a global magnetic field will shield a planet's atmosphere from being stripped away to space through interactions with the solar wind. Under this assumption, the shut-off of a global dynamo field at Mars contributed to the loss of significant atmosphere – enough to explain the evidence for liquid water on the surface long ago. Similarly, the lack of global magnetic field at Venus may have led to the loss of significant atmospheric oxygen over time.

This assumption has been questioned in recent years, in part based on the similarity in ion escape rates between Venus, Earth, and Mars [1]. It has been instead proposed that the presence of a global magnetic field may even enhance atmospheric escape because the planet presents a larger electromagnetic cross-section to the solar wind than it would otherwise.

Observational inter-planet comparisons, while valuable, are challenging to interpret because planets differ in many ways – Earth and Venus have different atmospheric compositions and rotation rates, for example. Global computer simulations using validated models can provide controlled experiments that isolate only the influence of a planetary magnetic field – but these models must be properly validated. Mars offers a unique opportunity to test the importance of a magnetic field in altering ion escape rates. This is because Mars possesses both magnetized and unmagnetized regions of the crust – allowing a relatively 'controlled' evaluation of the importance of magnetic fields in regulating ion escape in the limit of weak planetary magnetic fields.

In this presentation we will review the evidence 'for' and 'against' magnetic fields playing an important role in atmospheric retention. We will then present results of observational and theoretical analyses ongoing in our group, with emphasis on global plasma modeling and on analysis of data from the Mars Atmosphere and Volatile EvolutioN (MAVEN) mission.

Global Plasma Modeling: A variety of models have been developed for the interaction of the flowing solar wind plasma with unmagnetized objects in the solar system, such as Mars, Venus, and comets. These models are able to compute the escape rate of atmospheric ions from a planet, subject to the various assumptions incorporated into the model. It is now possible to incorporate weak global dipole magnetic fields into the models to determine the influence of planetary magnetic field on escape rate.

We used an open source hybrid plasma model, RHybrid, to simulate ion escape from a Mars-like planet with variable planetary dipole field strength [2]. We examined both the magnetospheric configuration under different dipole strengths, as well as escape rates of O^+ and O_2^+. We found (Figure 1) that atmospheric escape at first increases with increasing planetary field strength, and then decreases at larger field strengths. A weak field provides pathways for ions to escape that would have otherwise gyrated back into the planet, while a stronger field traps planetary ions and prevents them from escaping.

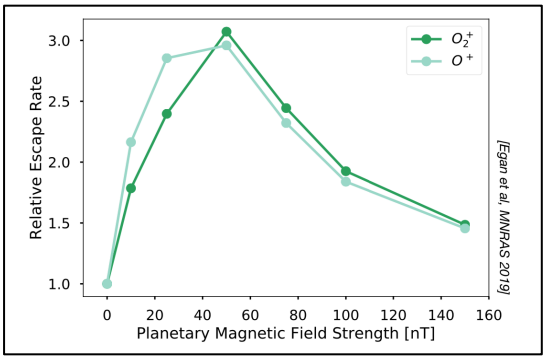

Figure 1: Ion escape rates from a Mars-like planet as a function of planetary magnetic field strength, as simulated by the RHybrid model.

Influence of Mars Crustal Fields: Previous investigators have examined global observations from Mars to determine the variability in ion escape rates as the planet rotates (thereby placing the strong crustal magnetic fields at different positions with respect to the incident shocked solar wind flow) [3,4]. Taken together, these analyses have been inconclusive since one predicts minimal influence of the crustal fields (~20%) and the other predicts a substantial influence. (~2.5x)

Global plasma models have fared similarly. If crustal fields are added to such models then the ion escape rate changes by as much as a factor of 30 or as little as 10%, depending upon the model [e.g. 5,6]. If crustal fields are instead rotated through a day, the variability in ion escape rates ranges from ~10% to 4x, depending upon the model [e.g. 7,8].

Such analyses (both observational and theoretical) are global, and therefore do not necessarily distinguish between ion escape from magnetized and unmagnetized regions. They instead look at the collective effect of crustal fields on the total ion escape from Mars. To truly answer the central question we have posed, a more spatially confined analysis focused on specific magnetized and unmagnetized regions is called for.

We have re-analyzed MAVEN observations of escaping ions, and organized the measured escape rates as a function of the position of the strong southern crustal fields with respect to the incident solar wind flow. We find that crustal fields have no detectable influence on global ion escape (Figure 2). We further find that ion escape is enhanced above crustal fields on the dayside of the planet, but depressed on the nightside. These competing effects average over the course of a Mars rotation.

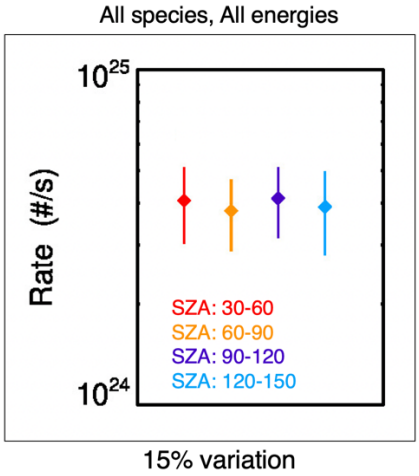

Figure 2: Ion escape rates from Mars as a function of the solar zenith angle (SZA) of the strong southern crustal fields.

Acknowledgments: We acknowledge support from NASA's MAVEN spacecraft mission currently orbiting Mars, and from NASA's Habitable Worlds program.

References: [1] Strangeway, R.S., C.T. Russell, J.G. Luhmann, T.E. Moore, J.C. Foster, S.V. Barabash, and H. Nilsson (2010) *AGU Fall Meeting Abstracts*, #SM33B-S1893. [2] Egan, H., R. Jarvinen, and D. Brain (2019) *MNRAS*, 488, 2108-20. [3] Ramstad, R., S. Barabash, Y. Futaana. H. Nilsson, and M. Holmström (2016) *GRL*, 43(20), 10574-9. [4] Brain, D. A., and 20 co-authors (2016), *AGU Fall Meeting Abstracts,* #P11D-02. [5] Harnett, E. M. and R. M. Winglee (2006) *JGR*, 111, 09213. [6] Brecht, S. H. and S. A. Ledvina (2012) *EPSL*, 64, 175-178. [7] Ma, Y., A. F. Nagy, I. V. Sokolov, and K. C. Hansen (2004) *JGR*, 109, 07211. [8] Fang, X., M. W. Liemohn, A. F. Nagy, J. G. Luhmann, and Y. Ma (2010) *Icarus*, 206, 130-8.

EXOPLANET CRUST COMPOSITIONS AS DETERMINED BY PETROLOGICAL EXPERIMENTS.

K. K. Brugman[1], M. G. Phillips[1], and C. B. Till[1], [1]School of Earth and Space Exploration, Arizona State University, 781 Terrace Mall Tempe, AZ, 85287-6004 USA.

Introduction: Over 4,000 exoplanets have been discovered, with active missions such as TESS and TRAPPIST aiming to double this number in the next few years. Key questions driving the field of exoplanet research require an understanding of their surface environments: what is the composition of the surface? What minerals and rock types are available for surface geochemical reactions that could potentially could support life? Recent investigations have highlighted our ability to measure exoplanet atmosphere compositions (e.g., [1, 2, 3]) but observations of exoplanetary surface chemistries (i.e., crusts) remain forthcoming. Investigations of these planets from outside our solar system have primarily utilized tools from the fields of astronomy and geophysics. However, exoplanet science is no longer an inchoate field, and answering the aforementioned questions necessitates applying methods from the field of igneous petrology. Our work uses established methods from experimental petrology to investigate the compositions of likely exoplanet mantle melts, which are the building blocks for the planet's crust. This study addresses a lack of experimental data on igneous exoplanetary systems, and our results could be used to constrain current geochemical models which are almost exclusively calibrated on terrestrial systems.

Methods: We focused on super-Earths (exoplanets with radius $\leq 1.5\ R_{Earth}$) with an Earth-like adiabatic gradient and compositions based on the spectral compositions of known stars in our galaxy (Fig. 1). A host star's composition can be used as a first order proxy to an exoplanet's composition, as demonstrated by the relationship between Earth and the Sun [4, 5, 6]. We exploit this relationship to examine the range of likely bulk silicate compositions for exoplanets, which may vary significantly relative to our star, particularly in Mg, Fe, Al, Ca, and Si [7], elements critical in rock-forming minerals. As most stars have molar Mg/Si from 0.5–2.0 (Fig. 1), bulk silicate exoplanet starting compositions were focused in this range. To determine the effect of this variation on exoplanet mantle solidi, we conducted piston-cylinder experiments over 1–2 GPa and 1100–1475°C on two non-Earth silicate exoplanet compositions.

Our first exoplanet bulk composition explores the effect of a higher Mg/Si relative to Earth (1.42 vs. 1.06 [8]) and represents the high Mg end member of exoplanets [6]. Our second composition has an Mg/Si (0.93) similar to that of Earth, but a higher Ca/Al (1.81 vs. 1.07) to represent a system where clinopyroxene is favored to crystallize over garnet.

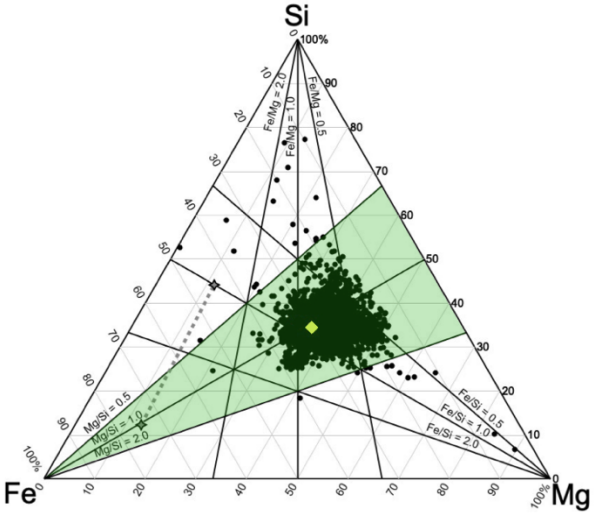

Figure 1: *Ternary of molar compositions of known stars (black circles) in our galaxy in Fe-Si-Mg space. Our sun is plotted as a yellow diamond. Solid lines delineate areas of equal molar ratios. After [9].*

Results: Initial results using our experimentally-derived solidi, as well as calculated exoplanetary adiabatic gradients and mantle potential temperatures, indicate that anhydrous exoplanet mantle phase proportions and melt compositions do deviate from that of Earth, and we compare these to rocky planet melts from our solar system. Our experimental melt compositions can be used to predict differences in crust compositions of exoplanets with similar bulk compositions to those explored here, and may have implications for the sustainability of density-driven plate tectonics on other worlds.

References: [1] Koll D. D. B. et al. (2019) arXiv:1907.13138. [2] Lustig-Yaeger J. (2019) *AJ*, 158(1), 28. [3] Mansfield M. et al. (2019) arXiv:1907.13150. [4] Desch S. et al. (2014). Report on the NASA Astrobiology Workshop Without Walls: Stellar Stoichiometry. [5] Young P. A. et al. (2014), *Astrobiology*, 14(7), 603–626. [6] Unterborn C. T. et al. (2017), arXiv:1706.10282. [7] Hinkel N. R. et al. (2014), *AJ*, 148(3), 54. [8] Hart S. R. and Zindler A. (1986) *Chem. Geo.* 57, 247–267. [9] Unterborn C. T. and Panero W. R. (2019) *JGR: Planets,* 124(7), 1704-1716.

THE GEOLOGY OF EXOPLANETS WITH THIN, BRITTLE LITHOSPHERES: LESSONS FROM VENUS.

Paul K. Byrne[1], Michael J. Heap[2], Sami Mikhail[3,4], Bradford J. Foley[5], and Richard C. Ghail[6], [1]Planetary Research Group, Department of Marine, Earth, and Atmospheric Sciences, North Carolina State University, Raleigh, NC, USA (paul.byrne@ncsu.edu), [2]Institut de Physique de Globe de Strasbourg (UMR 7516 CNRS, Université de Strasbourg/EOST), Strasbourg, France, [3]The School of Earth and Environmental Sciences, The University of St. Andrews, UK, [4]The Center for Exoplanet Science, The University of St. Andrews, UK, [5]Department of Geosciences, Pennsylvania State University, PA, USA, [6]Department of Earth Sciences, Royal Holloway, University of London, Surrey, UK.

Introduction: The uppermost, rigid portion of a solid planetary body is termed the lithosphere [e.g., 1]. The lithosphere usually comprises a relatively cold, upper region where brittle deformation occurs, and a relatively warm, lower region that responds to stress in a ductile manner [e.g., 2]. In the brittle lithosphere, tectonic deformation is accomplished by localized fracturing processes, commonly forming shear fractures (i.e., faults). In the ductile regime, deformation is dominantly accommodated by distributed plastic flow mechanisms such as dislocation glide or diffusion creep [e.g., 3]. The region in the lithosphere where brittle behavior gives way to ductile deformation is the brittle–ductile transition (BDT), the depth interval of which is controlled primarily by temperature and strain rate.

The thickness of the brittle lithosphere plays a major role in the geological evolution and behavior of a planetary body, including for example its heat flux [4], style of tectonic deformation [5], and even the evolution of any atmosphere present [6]. Absent in situ geophysical (e.g., seismic and/or heat flux) data, however, there is no direct measure of the depth of the BDT within a planetary body's lithosphere. Instead, this depth can be estimated by forward modeling of the penetration depths of tectonic structures [7], matching models of flexurally induced strains to geological observations [8], and studies of topography–gravity admittance and correlation spectra [9].

Gravity and Lithospheric Thickness: A wealth of laboratory data show that the failure mode of material is strongly influenced by both temperature and pressure. For example, low lithostatic pressure, P, promotes brittle failure in rock [10]. Since P is a function of surface gravitational acceleration, g, a less massive body but with otherwise similar composition, heat flux, and strain rate will have a deeper BDT, and thus a thicker brittle lithosphere, than a body with greater mass—with concomitant implications for volcanic, tectonic, and thermal properties and evolution [11].

It is therefore possible to place estimates on the BDT depth interval within a differentiated, terrestrial body simply from knowledge of its gravitational acceleration (or, if g is not measured directly, its mass), with that depth further affected by some combination of heat flux, atmospheric conditions, and incident stellar radiation. With this technique we have published BDT depth estimates for Venus [6] and Mars [11]; here, we extend our approach to considerations of lithospheric structure and behavior for rocky planets in orbit about other stars.

Rock Experimental Data: We compiled published data for rock deformation experiments with basalt and diabase samples, performed at high temperatures and over a wide range of pressures [11]. (These lithologies are appropriate for the majority of the Terran lithosphere, and probably the majority of the Venus and Mars lithospheres [12,13].) For a body with chondritic relative K–U–Th abundances and an assumed thermal gradient of 25 K/km, this approach yielded a predicted transition from brittle to ductile failure at a depth of ~25 km for Earth [11]—consistent with a BDT interval depth of 10–40 km for oceanic lithosphere calculated with yield strength envelopes [3]. That same thermal gradient predicts a brittle lithospheric thickness for Mars of 30–40 km, with BDT depths of as little as ~25 km and as much as ~100 km for thermal gradients of 40 K/km and 5 K/km, respectively [11]. These findings for Mars are in agreement with the range of estimates for both brittle lithospheric thickness and heat flow derived from inversion of present-day tectonic structures [e.g., 14], and demonstrate the control on failure mode by surface gravitational acceleration alone.

Brittle Lithospheres in Exoplanets: To estimate the depth interval of BDTs in extrasolar planets, we follow a simple, analytical approach that only requires that g be known. Assuming a differentiated, chondritic body, we take a rock density, ρ, of 3,000 $kg \cdot m^{-3}$ and, instead of a given thermal gradient, we regard the transition from brittle to ductile failure as occurring at a pressure of 300 MPa (which is the case for basalt at about 300 K [15]). We therefore place the BDT in an exoplanet's lithosphere at a depth, z, where the lithostatic pressure is 300 MPa, calculated from $P = \rho \cdot g \cdot z$. Gravitational acceleration, in turn, is found with $g = G \cdot M / r^2$, where G is the gravitational constant (6.674×10^{-11} $m^3 \cdot kg^{-1} \cdot s^{-2}$), M is planetary mass, and r is planetary radius.

We consider five exoplanets for which mass estimates are available, and which, on the basis of the relationship between mass and volume, have densities equal to or greater than the terrestrial planets in the Solar System. These selected exoplanets include Kepler-36b [16], Kepler-99b, Kepler-113b, and Kepler-406c [17],

Table 1. *Calculated BDT depths in select exoplanets.*

Exoplanet	$M_\oplus$ [a]	g (m·s^{-2})	Z[b] (km)	Ref.
Kepler-36b	3.9±0.2	17.0±1.1	**5.9±0.4**	[16]
Kepler-99b	6.2±1.3	28.5.±8.9	**3.9±1.2**	[17]
Kepler-113b	11.7±4.2	35.5±14.4	**3.4±1.4**	[17]
Kepler-406c	2.7±1.8	38.7±27.2	**5.1±3.6**	[17]
K2-3d	7.5±3.0	37.0±22.2	**2.7±1.0**	[18]

[a]$M_\oplus$ is mass of Earth; [b]z is depth within the lithosphere with a thermal gradient of 25 K/km where the overburden pressure is 300 MPa.

and K2-3d [18]. With estimates of mass and radius for these bodies, we first calculate g and then determine the depths within their lithospheres (assumed to mechanically correspond to basalt) where the overburden pressure is 300 MPa (***Table 1***). (We treat g as invariant over the depth ranges we consider here.)

This approach returns a range of BDT depth estimates for each planet (as a function of measurement uncertainty of planetary mass and radius). Nonetheless, none of these worlds' predicted BDTs is situated deeper than about 10 km (and several are within 2 km of the surface). Such a depth is comparable to the minimum BDT depth for Terran oceanic lithosphere [3], but substantially less than for continental settings on Earth [e.g., 19] and for the lithospheres of Mercury [7], the Moon [8], or Mars [11].

Other Controls on BDT Depth: Factors additional to g influence the depth range of the BDT within planetary lithospheres. For example, the relative abundances of heat-producing elements within a body will influence heat flux, with a low thermal gradient leading to a proportionately deeper BDT [e.g., 11]. Therefore, a thermal gradient greater than 25 K/km will yield yet shallower transition depth ranges than those we give in ***Table 1***. In the Archaean, the Terran heat flux was up to three times greater than today [20]; a rocky exoplanet that orbits a relatively young star (e.g., the 1.5-Gyr old Kepler-99 [17]) might have a similarly elevated thermal gradient compared with present-day Earth, and thus a proportionately thinner lithosphere.

Atmospheric mass and composition, as well as type, age, and distance to host star, also influence BDT depth. For example, atmospheric pressure and temperature on the Venus surface is 9.2 MPa and 735 K, respectively, and stellar irradiance is almost twice that of Earth. Together, these conditions place the Venus BDT, at least in the lowlands, at a depth range of ~2–12 km [6,21] comparable to those we calculate for the five exoplanets we assess here. It follows, then, that combinations of mass, atmospheric pressure and composition, and instellation are capable of producing conditions on a planetary body where the lithosphere is thin or even entirely absent.

Thin-Lithosphere Planets: Earth oceanic-style plate tectonics may not operate on a world with a thin lithosphere, as any plates present would likely be too thin to subduct. A fragmented, horizontally mobile lithosphere could therefore resemble the "block tectonics" pattern of deformation that characterizes much of the Venus lowlands [22] (***Figure 1***). Where mobile blocks collide on Venus, low-relief shortening structures ensue, in contrast to the major orogenic systems of convergent plates on Earth. The inference of a lack of high-standing terrain on worlds with thin lithospheres can be tested by future efforts to search for exoplanet topography [23].

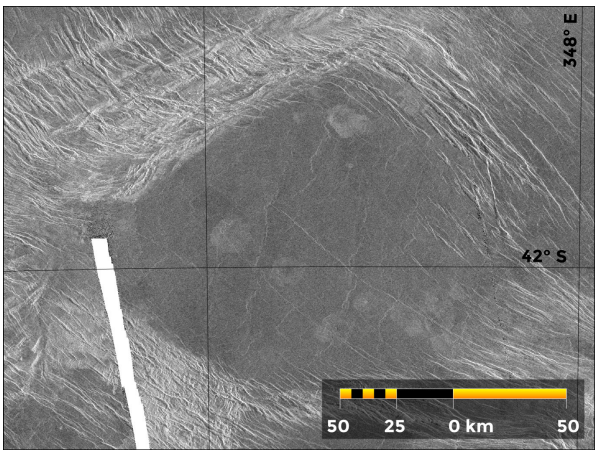

Figure 1. *This example of a mobile block on Venus features shortening structures along the southwestern margin with relief of only a few hundred meters [22].*

References: [1] Phillips R. J. et al. (1997) in *Venus II*, Bougher S. W. et al. (eds.) Univ. Arizona Press, pp. 1163–1204. [2] Kohlstedt D. L. and Mackwell S. J. (2010) in *Planetary Tectonics*, Watters T. R. and Schultz R. A. (eds.) Cambridge Univ. Press, pp. 397–456. [3] Kohlstedt D. L. et al. (1995) *J. Geophys. Res.*, *100*, 17,587–17,602. [4] Moresi L. and Solomotov V. (1998) *Geophys. J. Int.*, *133*, 669–682. [5] Byrne P. K. (2014) *Nat. Geosci.*, *7*, 301–307. [6] Mikhail S. and Heap M. J. (2017) *Phys. Earth Planet. In.*, 268, 18–34. [7] Egea-González I. et al. (2012) *Planet. Space Sci.*, 60, 193–198. [8] Solomon S. C. and Head J. W. (1980) *Rev. Geophys. Space Phys.*, 18, 107–141. [9] Turcotte D. L. et al. (1981) *J. Geophys. Res.*, *86*, 3951–3959. [10] Wong T.-f. and Baud P. (2012) *J. Struct. Geol.*, *44*, 25–53. [11] Heap M. J. et al. (2017) *Icarus*, *281*, 103–114. [12] Surkov Yu. A. et al. (1983) *JGR*, *88*, Suppl., A481–A493. [13] McSween H. Y. et al. (2009) *Science*, *324*, 736–739. [14] Solomon S. C. and Head J. W. (1990) *J. Geophys. Res.*, *95*, 11,073–11,083. [15] Violay M. et al. (2012) *JGR*, *117*, B03213. [16] Hadden S. and Lithwick Y. (2017) *Astron. J.*, *154*, 1, pp. 22. [17] Marcy G. W. (2014) *Astrophys. J. Suppl.*, *210*, 2, pp. 70. [18] Dai F. et al. (2016) *Astrophys. J.*, *823*, 2, pp. 16. [19] Yuan H. and Romanowicz B. (2010) *Nature*, *466*, 1063–1068. [20] Arevalo R. et al. (2009) *Earth Planet. Sci. Lett.*, *278*, 361–369. [21] Ghail R. C. (2015) *Planet. Space Sci.*, *113–114*, 2–9. [22] Byrne P. K. et al. (2018) *LPS*, *49*, abstract 1935. [23] McTier M. A. and Kipping D. M. (2018) *Month. Not. Roy. Astron. Soc.*, *475*, 4978–4895.

ARE THERE MASSIVE PLANET OR BROWN DWARF COMPANIONS LURKING IN THE NOISE?

Adolfo. S. Carvalho[1], Christopher M. Johns-Krull[1], and Lisa Prato[2], [1]Rice University, Department of Physics and Astronomy, Houston, TX 77005, [2]Lowell Observatory, 1400 Mars Road, Flagstaff, AZ 86001.

Introduction: We have been performing radial velocity (RV) monitoring of a large number of T Tauri stars – young, roughly solar mass pre-main sequence stars – since 2004. To date this program has identified the first planetary mass companion to a young star still surrounded by its protoplanetary disk [1]. For the other monitored stars, if we assume no detected companions in the systems, we identify the measured RV variability as stellar jitter and compute upper limits for undetected companion masses as a function of separations from the host star.

Motivation: Studies in the last two decades have shown how remarkably common it is for large planets to be found around nearby stars. Surprisingly, these radial velocity searches have found few brown dwarf (BD - an object more massive than a planet but less massive than a star) companions to main sequence stars. It is not clearly understood whether the lack of BDs around main sequence stars is due to evolutionary or formation processes: for example, it has been suggested that BDs in these systems might migrate inward toward the star during the protoplanetary disk phase and merge with the central host star while the system is young [2]. If this is the case, searches might find a relatively large number of these elusive companions orbiting young stars, particularly with more massive disks.

In 2004 we initiated an optical RV search for low mass companions to young stars, and so far have not detected any BD companions in our sample. Here, we seek place limits on the mass of undetected companions to our program stars to determine to what extent BD companions may be hidden by the relatively large RV scatter of young stars.

Data: We have made observations of ~50 T Tauri stars spanning the years 2004-2018. We use high resolution optical spectra obtained with the McDonald Observatory's 2.7m Harlan J. Smith telescope coupled to the Robert G. Tull cross dispersed coudé echelle spectrograph [3]. A 1.2" slit was used to deliver a spectral resolution ($\lambda/\delta\lambda$ = 60,000) and the spectra were recorded on a Tektronix 2080x2048 CCD. A total of 54-55 full spectral orders were recorded on the CCD for each observation. Observations were made roughly each night of a given 5-10 night observing run. Thorium-Argon lamp spectra were recorded before and after each observation to serve as references for instrumental shifts and to determine the wavelength scale for the observations. The spectra were reduced using a custom package of IDL echelle reduction routines based on procedures described by [4]. RV standards were observed every night and their RMS scatter (~140 kms^{-1}) is added in quadrature to measured RV uncertainty for each observation to account for the uncertainty intrinsic to the measurement method.

The RVs are calculated using a Cross-Correlation Function (CCF) based analysis as described by [5]. A reference for the CCF analysis is chosen from the set of observations to be the observation with the greatest signal-to-noise ratio. We select 9-11 orders from each observation and compute the CCF between the observation and the reference. The CCF peak is then fitted with a gaussian, from which we determine the relative shift of the two observations. The pixel shift is converted into a radial velocity using the wavelength scale and the Doppler formula. A similar procedure applied to the Thorium-Argon spectra is used to account for instrumental shift. The RVs from the different orders are then averaged and the standard deviation of the mean of the values from each order is taken to be the uncertainty in the measurement.

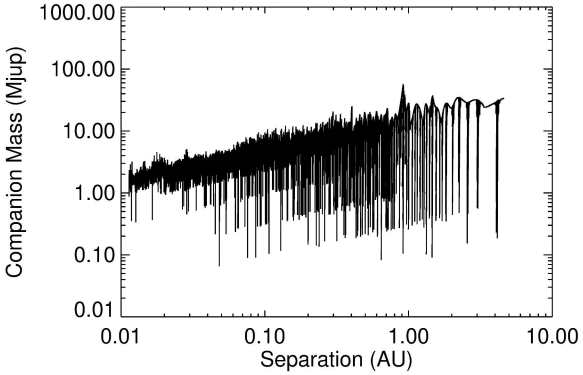

Figure 1: 2σ companion mass upper limits as a function of orbital separation for BP Tau

Analysis for Unseen Companions: To place an upper limit on undetected companions at a given orbital separation, we follow the procedure described in [6] and summarized here. We phase fold the RVs to 10^4 periods ranging from 0.5 days to 4000 days. The resulting RV signature is then fitted with a sinusoid via least squares. We use the measured RV amplitude and add 2σ to get a conservative upper limit for the maximum allowed RV amplitude at the given period.

To convert the RV amplitude to a companion mass, we must assume a mass for the host star. The mass of the host star is taken from the isochrones of [7] using the literature spectral type of the host and the age of the cluster to which it belongs. For BP Tau shown in Figure 1, we take the we assume a temperature of 4200K from its K5 spectral type and age of ~2 Myr to get a mass of ~0.8$M_{\odot}$.

Results: We present preliminary results of our analysis as plots demonstrating our computed detection limits. The conservative upper limits we calculate for undetected companions at various separations from BP Tau are show in Figure 1. We are able to exclude BD mass companions out to just beyond 1 AU for most stars.

References: [1] Johns-Krull C. M. et al. (2016) *ApJ*, 826, 206. [2] Armitage P. J. and Bonnell I. A. (2002) *MNRAS*, 330, L11. [3] Tull R. G. et al. (1995), *PASP*, 107. [4] Hinkle K. et al. (2000), *Visible Infrared Atlas Arcturus Spectr. 3727-9300*. [5] Tonry J. and Davis M. (1979), *AJ*, 84:10. [6] Boyajian T.S. et al. (2016), *MNRAS*, 457, 3988. [7] Baraffe I. et al. (2015), *A&A*, 577, A42.

EXOPLANET AND SOLAR SYSTEM SCIENCE WITH THE JAMES WEBB SPACE TELESCOPE. K. D. Colón[1,2], [1]NASA Goddard Space Flight Center, Exoplanets and Stellar Astrophysics Laboratory, Greenbelt, Maryland, USA, 20771; [2]Deputy Project Scientist for Exoplanet Science for the James Webb Space Telescope; knicole.colon@nasa.gov.

Abstract: The James Webb Space Telescope (JWST) will be the next premier space-based facility for near- and mid-infrared astronomy over 0.6-28.5 microns [1, 2]. The 6.5-meter telescope will be placed at the Earth-Sun Lagrange 2 point and will be equipped with four state-of-the-art instruments that include capabilities for imaging, spectroscopy, and coronagraphy. JWST will offer unprecedented sensitivity enabling detailed studies of transiting exoplanets and their atmospheres. It will also provide new views of exoplanet systems and debris disks via direct imaging. In addition, JWST will have the capability to study solar system objects ranging from asteroids, comets, near-Earth objects, trans-Neptunian objects, Kuiper Belt objects, Mars, Jupiter, and the other gas giants along with several of the moons orbiting the outer planets. We will provide an overview and status update of the observatory, its capabilities for exoplanet and solar system studies, and details about the Early Release Science (ERS) and Guaranteed Time Observations (GTO) programs (including the specific exoplanets and solar system bodies to be targeted, the science goals of the programs, and the timeline for observations). We will also discuss the scientific connections that can be made between the planned solar system and exoplanet observations. In addition, we will provide an overview of the first call for General Observer (GO) proposals, which will be released in January 2020 with a submission deadline of 1 May 2020. JWST is scheduled for launch in Spring 2021 and is an international collaboration between the National Aeronautics and Space Administration (NASA), the European Space Agency (ESA), and the Canadian Space Agency (CSA).

References: [1] http://www.stsci.edu/jwst. [2] https://jwst-docs.stsci.edu/.

ATMOSPHERIC ESCAPE AT MARS AND VENUS: PAST, PRESENT AND FUTURE. S. M. Curry[1] and J. G. Luhmann[1], [1]University of California, Berkeley, Space Sciences Laboratory (smcurry@berkeley.edu), 7 Gauss Way, Berkeley, CA 94720

Introduction: Earth, Venus and Mars formed at similar times, yet their atmospheres have evolved drastically differently. Venus's upper atmosphere, or exosphere, hosts several atomic species such as hydrogen, helium, oxygen, carbon, and argon, some of which are energized in the upper atmosphere to escape energies or ionized and carried away from the planet. Mars' atmosphere has a similar mainly carbon dioxide makeup, but the present day atmospheric pressure is significantly less than that of Venus.

So how is atmospheric escape at different at Venus and Mars? Both Venus and Mars lack a global dipole magnetic field, which may expose their atmospheres to scavenging more so than a planet like Earth [1]. *However at Venus, as opposed to Mars, virtually all significant present day atmospheric escape of heavy constituents is in the form of ions.* At Mars, photochemical escape is currently the main channel for atmospheric escape [2]. This is the process where molecules are photodissociated and obtain enough energy to exceed the escape velocity. However, Venus is roughly 7x more massive than Mars, and subsequently its gravitational well impedes photochemical escape. The sheer difference in their size and proximity to the sun have profound effects on their atmospheric evolution, which we will discuss at length.

Relevance to Exoplanets. Throughout the inner heliosphere, the evolution of the solar or stellar wind interaction is a critical topic for terrestrial planets since the solar (stellar) wind interacts directly with the planetary atmosphere to drive atmospheric escape. A star's activity plays a critical role in the evolution of terrestrial atmospheres, with extreme EUV and X-ray fluxes, as well as a more intense solar wind and higher occurrences of powerful solar transient events. At CO_2 planets, if you follow the oxygen, you can follow the water. Evidence of liquid water is present at Earth, Mars and Venus, and the presence of liquid water directly contributed to habitable conditions at Earth (see Figure 1). Additionally, volcanism has been active at all three of these terrestrial planets, which serves as an atmospheric source as well as a catalyst for the water and carbon cycle. Understanding how the atmospheres of our terrestrial neighbors evolve with respect to our sun may tell us how and when a rocky planet may be able to sustain an atmosphere with sufficient pressure to maintain liquid water.

We currently have multiple assets at both Mars and Venus that are able to observe atmospheric dynamics and escape. Because in-situ measurements of exoplanetary atmospheres are unlikely in our lifetime, it is critical to use the natural planetary laboratory in our own back yard to understand how atmospheres, and water, evolve and influence potential habitability. With the upcoming James Webb Space Telescope (JWST) mission, future observations of Earth-sized planets will only increase our understanding of atmospheric composition and the relationship a planetary atmosphere has with its host star.

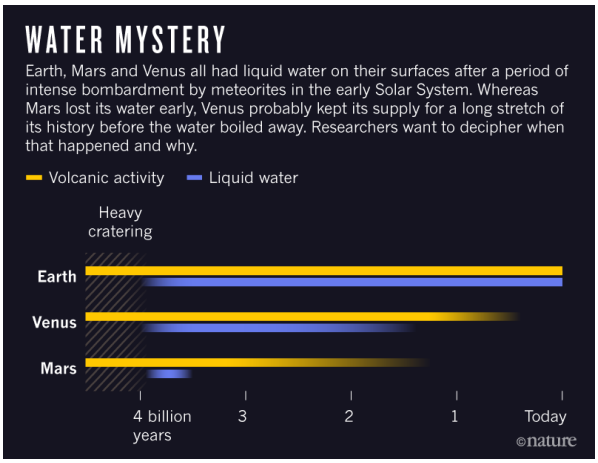

Image courtesy of Darby Dyar, Nature

Results: We will present Pioneer Venus Orbiter (PVO) and Venus Express (VEX) observations of Venus' ion loss throughout solar cycle 22, 23 and 24. We will also present the most recent observations during the Parker Solar Probe (PSP) flybys of Venus. We will compare the Venusian picture of atmospheric escape to that at Mars by presenting Mars Express (MEX) and Mars Atmosphere and Volatile Evolution (MAVEN) measurements. Using a composite of in-situ observations at Mars and Venus, we will construct a global picture of atmospheric escape, ion precipitation, and magnetic topology throughout the last three solar cycles. We will extrapolate these results to conditions when our sun was younger and more active, serving as an analogue .

References:

[1] Curry S.M., Luhmann J., Ma Y., Liemohn M., Dong C., Hara T. Comparative pick-up ion distributions at Mars and Venus: Consequences for atmospheric deposition and escape. *Planetary and Space Science.* 2015;115:35-47.

[2] Jakoskey et al., (2018). Loss of the Martian atmosphere to space: Present-day loss rates determined

from MAVEN observations and integrated loss through time. *Icarus*, **315**, 146– 157.

A TRANSITING OUTER GIANT EXOPLANET POISED FOR COMPARATIVE PLANETOLOGY WITH JUPITER AND SATURN. P. A. Dalba[1,2] and P. Tamburo[3]. [1]Department of Earth and Planetary Sciences, University of California Riverside, pdalba@ucr.edu; [2]NSF Astronomy and Astrophysics Postdoctoral Fellow; [3]Department of Astronomy, Boston University.

Introduction: Outer Jovian planets are excellent candidates for comparative investigations between the Solar System and exoplanets. In the Solar System, the dynamics of Jupiter and Saturn likely sculpted the planets' orbital configurations [1,2] and influenced the properties of the Earth, specifically related to the delivery of volatiles, the impact rates of minor bodies, and the development of life [3,4,5]. In exoplanetary systems, evidence exists for the substantial migration of Jovian planets [6]. A full understanding of the mechanisms dictating this migration will come with repercussions for the occurrence rates and architectures of systems hosting giant exoplanets.

Although the discovery of exoplanets has so far been dominated by the transit method, outer Jovian planets are more readily discovered by radial velocity (RV) surveys. Unfortunately, atmospheric characterization of RV exoplanets (that do not transit) awaits the next generation of direct imaging observatories.

Alternatively, follow-up characterization of *transiting* Jovian-analog exoplanets is feasible. *Cassini* observations demonstrated the amenability of Saturn-analog exoplanets to transmission spectroscopy [7]. Also, repeated transit observations offer an opportunity to detect and characterize exomoons [8]. However, the low transit probability of an outer Jovian-analog exoplanet is a major obstacle to their characterization and to efforts to conduct comparative planetology with the Solar System giant planets.

Kepler-167e, A Jupiter-analog Exoplanet: The four-year observational baseline of the primary *Kepler* mission enabled the discovery of Kepler-167e, a 0.9-$R_{Jupiter}$ exoplanet orbiting a K dwarf host star once every ~1,071 days [9]. Kepler-167e has been branded as a Jupiter-analog because of its size, its low eccentricity, and its Jupiter-like stellar insolation. *Kepler* observed only two transits of Kepler-167e, which did not allow for the detection of transit timing variations (TTVs). Around 50% of *Kepler*'s long-period transiting exoplanets and candidates exhibit TTVs of at least 2–40 hours [10]. These variations are difficult to characterize with only a few observed transits and, for many cases, leave an insuperable uncertainty on the timing of future transits.

***Spitzer* Observations:** We conducted a high-risk-high-reward observing campaign to detect an additional transit of Kepler-167e [11]. We monitored Kepler-167 with the *Spitzer Space Telescope* for 10 hours under program 14047 (PI: P. Dalba). The observations were timed to capture a portion of the transit including egress and out-of-transit baseline in the absence of TTVs.

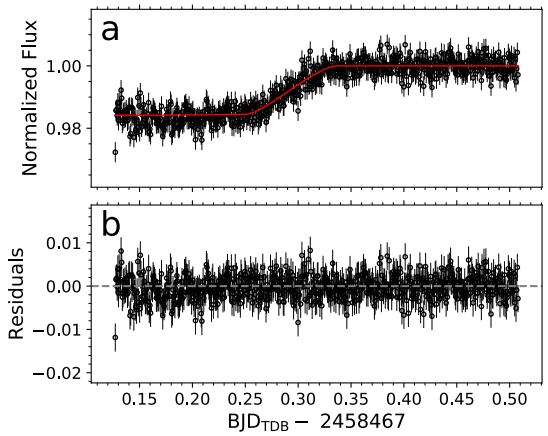

Figure 1: (a) *Spitzer* time-series observations of Kepler-167 with the best-fit partial transit model, and (b) residuals between the data and the model [11].

Figure 1 shows *Spitzer* observations (after the removal of systematics) and the best-fit transit model. Our observations captured the egress of Kepler-167e and confirmed the linear ephemeris of this unprecedented outer transiting exoplanet.

Results: We combined the timing of the two *Kepler* transits and the partial *Spitzer* transit to refine the ephemeris of Kepler-167e and predict future transit times. The orbital period and epoch we report is consistent with the previous estimate [9], but these parameters no longer contain an unaccounted for source of uncertainty due to the unknown influence of TTVs. By comparing the time intervals between subsequent transits, we ruled out TTVs of order 11, 34, and 57 minutes to 1σ, 3σ, and 5σ significance, respectively. As a result, we are now able to predict the future transit times of Kepler-167e to better than 6 minutes precision through the year 2030, thereby making this target accessible to the *James Webb Space Telescope* (*JWST*).

An Unprecedented Opportunity: The transiting nature of Kepler-167e makes it a remarkably improbable target for follow-up characterization. It is a member of a small group of transiting exoplanets that orbit their host stars from beyond the water ice line. Kepler-167e's many similarities to Jupiter make it a benchmark for future comparative planetology investigations.

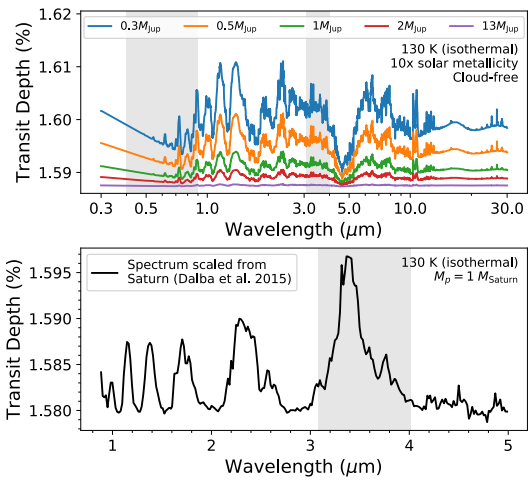

Figure 2: Several possible transmission spectra for Kepler-167e. (Top) The transit spectra are modeled with Exo-Transmit [12] for a variety of planet masses. (Bottom) The transit spectra is scaled from that of Saturn (as if it were a transiting exoplanet [7]) assuming a planet mass of 1 M_{Saturn} [11].

The next steps in the characterization of Kepler-167e are the measurement of its mass and the investigation of its atmosphere via transmission spectroscopy (i.e., the wavelength dependence of its transit depth). Figure 2 shows several possible transmission spectra for Kepler-167e. The top panel shows models made with Exo-Transmit [12] for several masses and assuming a 130-K isothermal, cloud-free atmosphere. At this temperature, many of the features are indicative of CH_4 absorption. For H_2O, deeper layers of the atmosphere act as a cold trap, condensing it into a cloud layer. Similarly, NH_3 likely condenses (as is the case on Jupiter and Saturn). As expected, the size of the features scales strongly with mass. For the 0.3-$M_{Jupiter}$ scenario, the peaks of the 1–2 μm CH_4 features are ~200 parts per million (ppm) above the deep 5 μm window, indicating the potential amenability of Kepler-167e to joint transmission spectroscopy with the *Hubble Space Telescope* and *JWST*.

In the bottom panel of Figure 2, we draw analogy to the Solar System by scaling the reconstructed transmission spectrum of Saturn [7] to Kepler-167e assuming a mass equal to that of Saturn. The 50–75 ppm features blueward of 3 μm are caused by CH_4 absorption, while the largest feature near 3.4 μm indicates additional opacity from larger hydrocarbons produced via CH_4 photolysis [7]. If similar hydrocarbon photochemistry is ongoing in the atmosphere of Kepler-167e, it can potentially be identified and characterized with near-IR transmission spectroscopy with *JWST*.

References: [1] Tsiganis K. et al. (2005) *Natur., 435*, 459. [2] Morbidelli A. et al. (2007) *AJ, 134*, 1790. [3] Zahnle K. J. and Sleep, N. H. (1997) in *Comets and the Origin and Evolution of Life*, New York: Springer, 175. [4] Morbidelli A. et al. (2000) *Meteoritics & Planet. Sci., 35*, 1309. [5] Horner J. et al. (2010) *IJAsB, 9*, 1. [6] Lin D. N. C. et al. (1996) *Natur., 380*, 606. [7] Dalba P. A. et al. (2015) *ApJ, 814*, 154. [8] Kipping D. M. (2011) *MNRAS, 416*, 689. [9] Kipping D. M. et al. (2016) *ApJ, 820*, 112. [10] Wang J. et al. (2015) *ApJ, 815*, 127. [11] Dalba P. A. and Tamburo P. (2019) *ApJ Let., 873*, L17. [12] Kempton E. M. R. et al. (2017) *PASP, 129*, 044402.

PEBBLE ACCRETION BY BODIES ON ECCENTRIC ORBITS AND THE MASS RATIOS OF EXOPLANETS Steven Desch[1], Alan Jackson[1], Chuhong Mai[1], and Jessica Noviello[1] [1]School of Earth and Space Exploration, Arizona State University, PO Box 871404, Tempe AZ, 85287-1404 (steve.desch@asu.edu).

Introduction: In the last decade, several lines of evidence—from our own solar system and from studies of exoplanets—have converged to suggest that growth of planets is extraordinarily fast. In our own solar system, Hf-W dating of Mars shows it was an embryo formed between 1 and 3 Myr after CAIs (calcium-rich, aluminum-rich inclusions) [1]. The isotopic dichotomy of the solar system [2], reduced water content inside the snow line [3] and the concentration of CAIs in carbonaceous chondrites [4] have all been explained by invoking formation of Jupiter's ~20-30 M_E core in < 1 Myr. Ingassing of nebula gas into the magma oceans of the Earth [5,6] and Theia [7] explain their low-D/H hydrogen reservoirs and their He and Ne isotopic abundances. This requires them to achieve masses of several × 0.1 M_E in < 3 Myr. In exoplanetary systems, many super-Earths accreted substantial hydrogen-rich atmospheres [8,9], requiring them to grow to several Earth masses within < 3 Myr [10]. The gaps in young protoplanetary disks (sometimes ~ 10^5 yr, like HL Tau) observed by the Atacama Large Millimeter Array, may be due to massive (tens of Earth masses) planets [11]. Overall, planets in our solar system and others demand accretion rates of at least 10^{-6} M_E yr^{-1}.

Recent astrophysical modeling suggests a path for rapidly turning micron-sized dust into planets thousands of km in diameter. Fast coagulation produces millimeter-sized particles (precursors of compactified dust, or melted chondrules). For conditions in the inner disk, their Stokes number (the ratio of aerodynamic stopping time to orbital time) is St ~ 10^{-3}. Turbulence then concentrates these into aggregates up to ~10 cm in size [12], with St ~ 0.01 – 0.1. These particles are intermittently but rapidly collected into ~100-km objects by streaming instability [13]. The very largest of these objects, those several ×100 km in diameter, can grow rapidly by pebble accretion. This aerodynamic process relies on drag to slow particles (especially those with St ~ 0.01 – 0.1) in the vicinity of a growing planet, allowing it to capture almost all such particles entering the planet's Hill sphere [14]. Growth at rates of at least 10^{-6} M_E yr^{-1} appear possible.

As successful as pebble accretion is, the theory appears incomplete at present. An important constraint from observations is that exoplanets in multiple-planet systems (observed in transits by Kepler and followed up by radial velocity measurements) appear to be similar in orbital period ratios and in size, and therefore also mass [15]. The growth of planets by pebble accretion in the Hill regime scales as $dM_p/dt \sim M_p^{2/3}$ [14], so the mass ratios between embryos should decrease with time very slowly, making it difficult to reconcile with the peas-in-a-pod result. We propose a modification of pebble accretion involving embryos on eccentric orbits that leads to embryos growing to similar sizes.

Growth on circular orbits: Growth of embryos on circular orbits proceeds as follows. Pebbles with St ~0.01-0.1 entering an embryo's Hill sphere with radius $R_H = a\,(M_p / 3M_\odot)^{1/3}$ are accreted with high efficiency, assuming they have scale height < R_H. Pebbles are assumed to sweep into the Hill sphere at velocity $V_H = R_H\Omega_K$, $\Omega_K = (GM_\odot/a^3)^{1/2}$, due to Keplerian shear across the Hill radius. The embryo sweeps up pebble mass at a rate $dM_p/dt = 2\,R_H\,\Sigma_p\,V_H$, where Σ_p is the surface density of pebbles (St~0.01–0.1 solids). This yields $dM_p/dt \sim 47\,(\Sigma_p / 1\text{ g cm}^{-2})\,(M_p / 1\,M_E)^{2/3}\,M_E\,\text{Myr}^{-1}$ at 1 AU. This is such a high accretion rate, an embryo will quickly (~100 years) sweep up the mass in its torus, $2\pi a\,(2\,R_H)\,\Sigma_p = 0.0047\,(\Sigma_p / 1\text{ g cm}^{-2})\,(M_p / 1\,M_E)^{1/3}\,M_E$, and will grow only if a pebble flux can feed its torus. [A surface density Σ_p = 1 g cm^{-2} of pebbles corresponds to 20% of all solids if the gas surface density is 1000 g cm^{-2}.] The radial drift of pebbles is $dM_p/dt = (2\pi a)\,\Sigma_p\,V_{pr}$, where $V_{pr} = -\text{St}\,(\eta V_K) / (1+\text{St}^2)$, and $\eta = -(C^2/V_K^2)\,d\ln P / d\ln r$ [16]. But only a fraction of these, $(2R_H/V_{pr})(V_H/2\pi a)$ (which is < 1 if St ≥ 0.01 and $M_p \le 1\,M_E$), are accreted before drifting through the annulus entirely, yielding the same result: $dM_p/dt = 2\,R_H\,\Sigma_p\,V_H$. Thus $dM_p/dt \sim M_p^{2/3}$ and larger planets should grow faster than small ones. Integrating the growth equation, assuming Σ_p = 1 g cm^{-2} at 1 AU, a 0.5 M_E planet would grow to 13.2 M_E in only 10^5 yr, and a 2.0 M_E planet would grow to 22.6 M_E in the same time.

Growth on eccentric orbits: Growth by pebble accretion is faster for an embryo on an eccentric orbit instead of a circular one. In a frame co-moving with the embryo, the embryo makes epicyclic orbits with radial excursions ±*ae*, where *e* is the eccentricity. The embryo and pebbles have relative velocity ~ $eV_K = ea\Omega_K$, several km/s. Analogous to the circular case, immediately after being put onto an eccentric orbit, embryos grow as $dM_p/dt = 2R_H\,\Sigma_p\,eV_K$, accreting a high fraction of the pebbles in its epicyclic torus in one orbit [17]. Thereafter it grows at the rate pebbles in the annulus between $a(1-e)$ and $a(1+e)$ can drift into the torus. Pressure support of gas makes it orbit at an azimuthal

velocity $\eta V_K/2$ slower than the embryo, and the azimuthal velocities of pebbles differ from Keplerian by ~ $(-\eta V_K/2) / (1 + St^2)$ [16]. Typically $\eta \sim 10^{-3}$; in the models of [4], $\eta = 3 \times 10^{-3}$. Within a time $2\pi a / (\eta V_K/2) \sim 2\eta^{-1}$ orbits, the embryo sweeps up the entire annulus of area $\approx 2\pi a$ ($2ae$). The mass accretion rate while it is sweeping up the annulus is $dM_p/dt = (ae)\ \Sigma_p\ (\eta V_K) / (1+St^2)$. A correction would have to be made if the Hill sphere were small enough that the pebbles could cross the torus width in less than one orbit, i.e., if $2R_H / (\eta V_K/2) < 2\pi / \Omega_K$, or $M_p < [157\ \eta]^3\ M_E \sim 0.0034\ M_E$; but as long as an embryo is at least this large, it will sweep up pebbles at the rate $dM_p/dt \approx (ae)\ \Sigma_p\ (\eta V_K)$. An embryo will sweep up the entire pebble mass of the annulus, $\Delta M = (2\pi a)(2ae)\ \Sigma_p = 0.05\ (\Sigma_p / 1\ g\ cm^{-2})\ (e / 0.1)\ M_E$ in less than 10^3 yr.

As with circular orbits, continued embryo growth relies on radial drift of pebbles. Pebbles are brought into the annulus at a rate $dM_p/dt = (2\pi a)\ \Sigma_p\ V_{pr}$, where $V_{pr} = -St\ (\eta V_K)/(1+St^2)$. The fraction of these that are accreted is 100% if $St < e/2\pi$, and $dM_p/dt \approx 2\pi a\ \Sigma_p\ St\ \eta V_K$; but is $e/(2\pi St)$ if $St > e/2\pi$, and $dM_p/dt = ae\ \Sigma_p\ \eta V_K$, as before. Either generally exceeds the circular orbit pebble accretion rate = $2\ R_H\ \Sigma_p\ V_H$, because the embryo can sweep up pebbles from a larger area, and because pebbles are swept up with greater efficiency.

Embryos may accrete at the circular orbit rate until they are scattered onto an eccentric orbit. While on eccentric orbits, before their orbits are damped, an embryo can quickly accrete all of the pebbles in its annulus. At 1 AU in a disk model with gas densities like those of [4], $\tau = 0.1\ (M_p/0.5\ M_E)^{1/3}$ Myr for small embryos $M_p < 0.5\ M_E$ in the gas drag regime, and $\tau = 0.1\ (M_p/\ 0.5\ M_E)^{-1}$ Myr for larger embryos in the disk torque regime [18]. Embryos generally will accrete all the pebbles in their annulus before their eccentricities damp, gaining mass $\Delta M = (2\pi a)(2ae)\ \Sigma_p = 0.05\ (\Sigma_p / 1\ g\ cm^{-2})\ (e / 0.1)\ M_E$ in $< 10^3$ yr. Thereafter they grow at rates dependent on the pebble flux. Integrating the coupled differential equations for growth dM_p/dt and damping $de/dt \sim -e\ M_p$, for $St > e/2\pi$, embryos grow linearly in time, but for durations that depend on their initial masses. A 0.5 M_E embryo set on an e=0.1 orbit will circularize in ~0.022 Myr and will grow to mass 10.1 M_E. A 2.0 M_E embryo will circularize in ~0.019 Myr and will grow to 10.3 M_E. In the case with $St < e/2\pi$, embryos may gain mass as their eccentricities damp, at rate $dM_p/dt \approx (ae)\ \Sigma_p\ (\eta V_K)$. Solving the coupled differential equations for growth $dM_p/dt \sim e$ and damping $de/dt \sim -e\ M_p$, we find that being scattered onto an orbit with eccentricity e, will cause a 0.5 M_E embryo to reach mass $M_p = 3.80\ (\Sigma_p / 1\ g\ cm^{-2})^{1/2}\ (e / 0.1)^{1/2}\ M_E$, and a 2.0 M_E embryo to reach mass $M_p = 4.26\ (\Sigma_p / 1\ g\ cm^{-2})^{1/2}\ (e / 0.1)^{1/2}\ M_E$, both within $\sim 5 \times 10^4$ yr. Once an embryo's orbit has circularized, it will continue to accrete at the circular pebble accretion rate, $dM_p/dt = 2\ R_H\ \Sigma_p\ V_H$.

System Architecture: In systems with embryos growing by pebble accretion on circular orbits, $dM_p/dt \sim M_p^{2/3}$, and the mass ratio of two embryos tends to decease with time, but slowly. In the example above, over 0.1 Myr, the mass ratio of two embryos decreased from (2.0)/(0.5) = 4.0, to (22.6)/(13.2) = 1.7. Embryos scattered onto eccentric orbits will accrete by pebble accretion more rapidly than if they were on circular orbits, at rates independent of mass, at least until their eccentricities damp. In the one example above, with $St > e/2\pi$, the mass ratio of two embryos decreased from (2.0)/(0.5) = 4.0, to (10.3)/(10.1) = 1.02. In the other case, with $St < e/2\pi$, the mass ratio decreased from (2.0)/(0.5) = 4.0, to (4.26)/(3.80) = 1.12. Embryos are only transiently on eccentric orbits, after being scattered; but while they are, the small embryos tend to grow more rapidly and catch up in mass with the larger embryos. By the time they each circularize, they will have attained masses much more similar than if they grew at the circular orbit pebble accretion rate. The tendency of exoplanets in the same system to have similar masses [8] may best be explained if a significant fraction of their growth occurs after they are scattered onto eccentric orbits.

References: [1] N. Dauphas and A. Pourmand (2011) *Nature* 473, 489-492. [2] T. S. Kruijer, C. Burkhardt, G. Budde, and T. Kleine (2017) *PNAS* 114, 6712-6716. [3] A. Morbidelli et al. (2016) *Icarus* 267, 368-376. [4] S. J. Desch, A. Kalyaan, and C. M. O'D. Alexander (2018) *Ap.J.S.* 238, 11-41. [5] J. Wu et al. (2018) *JGR* 123, 2691-2712. [6] C. Williams and S. Mukhopadhyay (2019) *Nature* 565, 78-81. [7] S. J. Desch and K. L. Robinson (2019) *Chemie der Erde*, in press. [8] L. M. Weiss and G. W. Marcy (2014) *Ap.J.L.* 783, L6-12. [9] B. J. Fulton et al. (2017) *A.J.* 154, 109-127. [10] A. Stokl, E. Dorfi, and H. Lammer (2015) *A&A* 576, 87-96. [11] R. Dong, Z. Zhaohuan, B. Whitney (2015) *Ap.J.* 809, 93-110. [12] J. I. Simon et al. (2018) *EPSL* 494, 69-82. [13] A. N. Youdin and J. Goodman (2005) *Ap.J.* 620, 459-469. [14] M. Lambrechts and A. Johansen (2012) *A&A* 544, 32-44 . [15] Weiss et al. 2018. [16] T. Takeuchi and D. N. C. Lin (2002) *Ap.J.* 581, 1344-1355. [17] B. Liu and C. Ormel (2018) *A&A* 615, 138-152. [18] M. Morris, A. C. Boley, S. J. Desch and T. Athanassiadou (2012), *Ap.J.* 752, 27-43.

LUVOIR, Exoplanets, and Exoplanets in our Back Yard. S. D.. Domagal-goldman[1] and the LUVOIR concept study team, [1]NASA Goddard Space Flight Center, Greenbelt, MD, USA. shawn.goldman@nasa.gov

Are we alone? What diversity of worlds exists beyond our Solar System? How can that diversity enhance our understanding of the planetary processes in our Solar System? How did the Universe lead to the creation of this diversity of worlds?

These are questions that can be answered by LUVOIR - the Large UV/Optical/Infrared Surveyor. LUVOIR is a concept for a powerful observatory in the tradition of the Hubble Space Telescope, spanning the far-UV to the near-infrared, and would enable revolutionary advances in our understanding of exoplanet science, planetary science, and astrophysics.

LUVOIR will create a great leap in exoplanet science, with direct images and spectra of rocky Earth-sized exoplanets in the habitable zones of other stars. These data will allow a wide range of investigations, including analysis of rocky planet atmospheres and their surfaces, discovery of potentially habitable exoplanets, and a search for global biospheres. A key goal for LUVOIR is to conduct these studies on a large sample of potentially habitable exoplanets to constrain the frequency of habitable conditions. Enabling this requires a large-aperture space telescope, and the LUVOIR team has studied two variants: LUVOIR-A (15-m mirror) and LUVOIR-B (8-m mirror).

The large aperture of LUVOIR would also enable groundbreaking observations of the Solar System with sensitive, high spatial resolution remote sensing over long time baselines and a broad wavelength range. This will enable observations of the chemistry, mineralogy, and weather of a variety of targets, with quality approaching that of a fly-by mission but over a much longer (5+ years) monitoring timeline. LUVOIR-A will resolve features as small as 25 km at Jupiter and 232 km at 40 AU.

We will review LUVOIR's ability to conduct exoplanet and Solar System observations. This includes a search for "Earth-like" worlds that will also deliver high-quality observations of a wide variety of non-habitable exoplanets, ushering in a revolution in our understanding of planet formation, evolution, and comparative planetology. We will showcase some examples of LUVOIR Solar System remote sensing, review the observatory designs, and describe the concept study process that has led to the LUVOIR concept.

Acknowledgments: This presentation will summarize some of the work of the LUVOIR Concept Study, which was enabled by the work of hundreds of scientists, engineers, and technologists from across the globe. The work on this was also funded by NASA, in support of the studies of future strategic astrophysics assets as inputs to the Astro2020 Decadal Survey.

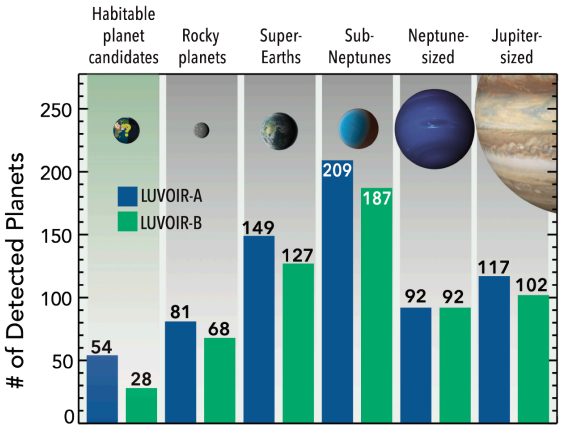

Figure 1. *LUVOIR will discover dozens of habitable planet candidates and hundreds of other kinds of exoplanets. The chart shows exoplanet detection yields from an initial 2-year survey optimized for habitable planet candidates with LUVOIR-A (blue bars) and -B (green bars). The first column shows the expected yields of habitable planet candidates. Non-habitable planets are detected concurrently during the 2-year survey. Color photometry is obtained for all planets. Orbits and partial spectra capable of detecting water vapor and/or methane are obtained for all habitable planet candidates. Credit: C. Stark (STScI) / J. Friedlander (NASA GSFC)*

Role of Planetary Obliquity in Regulating Atmospheric Losses: G-dwarf vs. M-dwarf Earth-like Exoplanets.

C. F. Dong[1], Z. G. Huang[2], M. Lingam[3,4], [1]Princeton University (dcfy@princeton.edu), [2]University of Michigan, [3]Harvard-Cfa, [4]Florida Tech

Introduction: Over the past decade, much attention has been directed toward understanding what factors contribute to exoplanetary habitability [1]. In particular, it is widely accepted that orbital parameters play a major role in governing habitability [2]. One of the chief orbital parameters is the obliquity (axial tilt). The fact that Earth's obliquity is subject to only mild fluctuations is believed to play a vital role in maintaining its stable climate.

Exoplanets around M-dwarfs are typically anticipated to have very low (or zero) obliquities due to rapid tidal energy dissipation. This effect may be particularly pronounced for the inner planets of multi-planet systems such as the Kepler-186 system. Nevertheless, there are mechanisms that permit the existence of high obliquity M-dwarf exoplanets. Perhaps the most famous among them are the "Cassini states" that involve the precession of the planet's spin and orbital angular momenta at the same rate; the Moon has an non-zero obliquity of 6.7◦ due to this reason. Hence, it is feasible for certain M-dwarf exoplanets to have high obliquities [3,4].

Another factor that plays a vital role in regulating surficial habitability is the presence of an atmosphere. Moreover, an atmosphere also permits the detection of biosignature gases (e.g., molecular oxygen) via spectroscopy. Recent numerical and theoretical studies indicate that both magnetized and unmagnetized planets around M-dwarfs might be particularly susceptible to the depletion of ∼ 1 bar planetary atmospheres over sub-Gyr timescales due to the high ultraviolet fluxes and intense stellar winds they experience [5-9].

In view of the preceding discussion, it is worthwhile asking the question: how does obliquity regulate atmospheric escape rates? It is, however, important to note that the rotational and magnetic axes of Earth are separated only by ∼ 10◦. Hence, it is plausible that these two axes are potentially aligned for Earth-like planets as well, viz., the angle between the two might be fairly small. In this study, we opt to perform a parametric analysis of how magnetic obliquity (i.e. the angle between the magnetic axis and orbital axis) affects the atmospheric ion loss from magnetized exoplanets.

Method: In our Solar system, the most sophisticated codes tend to use magnetohydrodynamic (MHD) models for modeling the interactions of the solar wind with both magnetized (such as Earth) and unmagnetized (such as Mars and Venus) planets. We use the BATS-R-US MHD model that has been well validated and applied to different solar system objects to study the atmosperhic loss from exoplanets [5-9]. For the stellar wind parameters (such as the stellar wind velocity, density and magnetic field), we adopt the AWSoM model to simulate those parameters based on the observed magnetograms of M-dwarf stars [7].

Results: We focus on two distinct examples due to their astrobiological relevance [10]: an Earth-like planet around a solar-type star and an Earth-like planet around a late-type M-dwarf using TRAPPIST-1 as a proxy. There are several interesting features that stand out in both cases, viz., solar-type stars and late M-dwarfs.

First, the atmospheric ion escape rate is $\sim 10^{26}$ s^{-1} in the case of G-dwarf Earth-like planets, whereas the escape rate increases to $\sim 10^{28}$ s^{-1} for M-dwarf planets due to the extreme stellar wind conditions and high energy radiations in the close-in habitable zones (HZs) [9]. In other words, a ∼ 1 bar atmosphere of an Earth-like planet would take $O(10^{10})$ yrs to be depleted for a G-type star and $O(10^{8})$ yrs for an M-dwarf based on normal stellar wind conditions.

Second, the variation in the atmospheric ion escape rates is virtually independent of the magnetic obliquity for an Earth-analog around a solar-type star. We find that the total variation is less than 10% (see Figure 1). In contrast, when we consider an Earth-like planet around a late Mdwarf, we determine that the variation is modest (but non-negligible); in quantitative terms, the maximum escape rate is more than twice (or 200%) the minimum value. The chief reason why the obliquity plays a weak role in determining the escape rate for solar-type stars stems from the temperate stellar wind and radiation in HZs.

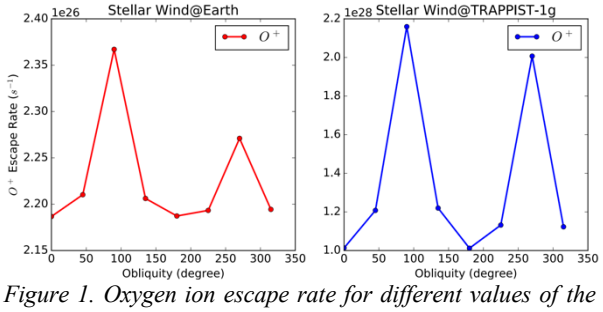

Figure 1. Oxygen ion escape rate for different values of the planetary (magnetic) obliquity. Note the different scales of the vertical axis in the two panels [9].

As shown in Figures 2 and 3, the magnetosphere of the G-dwarf planet is larger than that of the M-dwarf planet; therefore, regardless of magnetic obliquity's

value, the ionosphere does not experience much difference. On the other hand, for an Earth-analog around TRAPPIST-1, the dual effect of the compressed magnetosphere and high energy radiation makes the ion sources (e.g., electron impact ionization and charge exchange) more sensitive to the magnetic configuration.

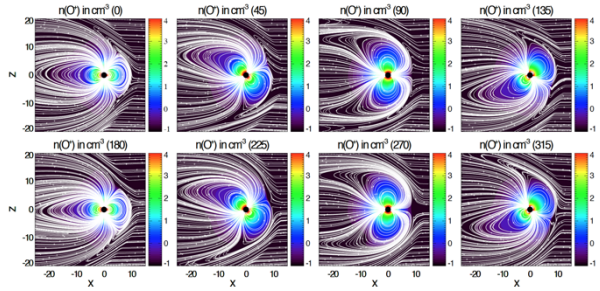

Figure 2. The logarithmic scale contour plots of the O^+ ion with magnetic field lines (in white) in the meridional plane for a magnetized Earth-like planet orbiting around a solar-type star. Different plots correspond to different planetary magnetic obliquities [9].

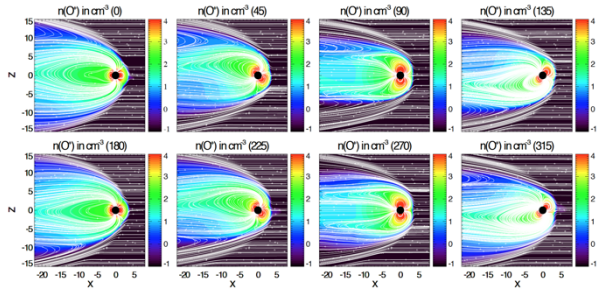

Figure 3. A magnetized Earth-like planet (with different magnetic obliquities) orbiting around TRAPPIST-1 [9].

Third, we see that the maximal ion escape rate is attained at a magnetic obliquity of 90◦ whereas the minimum occurs at 0◦ or 180◦ (Figure 1). While the atmospheric escape rates at 0◦ and 180◦ are nearly the same, there is a clear distinction between 90◦ and 270◦. The reason behind the latter behavior has to do with the relative orientation of the interplanetary magnetic field (IMF) and the planetary magnetic field. At the magnetic obliquity of 90◦, the IMF can directly connect to the dayside planetary surface due to the field polarity, whereas the IMF can only connect to the nightside surface at the magnetic obliquity of 270◦; see the third column of Figure 2. Therefore, stellar wind particles, especially electrons (with relatively low energy) can be transported along the field lines and ionize the atomic oxygen in the upper atmosphere via impacts as shown in Figure 4.

Conclusions: We found that the maximum escape rates arose at obliquities of 90◦ or 270◦ (depending on field polarities), whereas the minimum rates were attained at 0◦ or 180◦. The reason is that the cusp (comprising open field lines) faces the stellar wind at obliquities of 90◦ or 270◦, and allows the stellar wind particles to deposit their energy in the planetary upper atmosphere. For Earth-like planets around solar-type stars, it is found that the escape rate is virtually independent of the obliquity. On the other hand, for late M-dwarfs, we determined that the escape rate varies by more than a factor of ∼ 2.

From our simulations, we found that the timescale required to deplete a ∼ 1 bar Earth-like atmosphere is $O(10^{10})$ and $O(10^{8})$ yrs, for solar-type stars and late M-dwarfs, respectively. If we assume that the source of atmospheric oxygen is water from oceans, we find that the mass of Earth's oceans (M_{oc}) cannot be depleted over the main-sequence lifetime of a solar-type star. In contrast, for a late M-dwarf we determine that Moc could be depleted over a timescale of $O(10^{10})$ yrs, which is shorter than the star's lifetime.

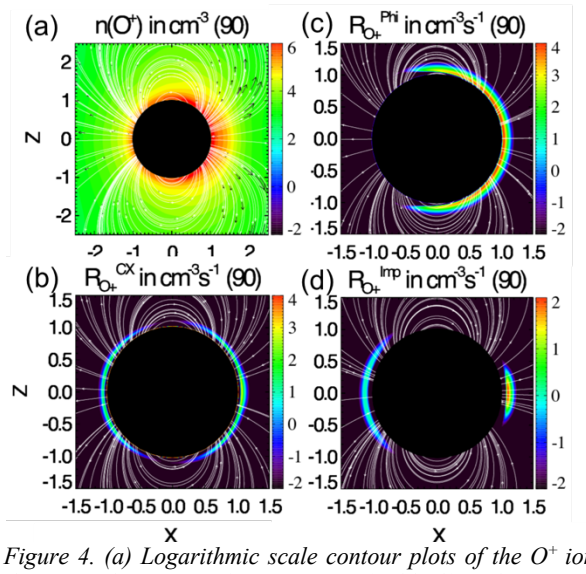

Figure 4. (a) Logarithmic scale contour plots of the O^+ ion density with O^+ ion velocity vectors (in black) and magnetic field lines (in white) in the meridional plane for the M-dwarf planet with obliquity of 90◦. The black arrows depict both the direction and the magnitude of O^+ ion velocities. (b)-(d): Logarithmic scale contour plots of the photoionization rate $R_{O^+}{}^{Phi}$, electron impact ionization rate $R_{O^+}{}^{Imp}$, and charge exchange rate $R_{O^+}{}^{CX}$ (with stellar wind protons) of O^+ ions [9].

References: [1] Cockell, C. S. et al. 2016, *Astrobiology*, 16, 89. [2] Shields, A. L. et al., A. 2016, *PhR*, 663, 1 [3] Shan, Y. & Li, G. 2018, *AJ*, 155, 237. [4] Millholland, S., & Laughlin, G. 2019, *NatAs*, 3, 424. [5] Dong, C., et al. 2017a, *ApJL*, 847, L4. [6] Dong, C., et al. 2017b, *ApJL*, 837, L26. [7] Dong, C., et al. 2018a, *PNAS*, 115, 260. [8] Dong, C. et al. 2018b, *ApJL*, 859, L14. [9] Dong, C et al. 2019 *ApJL*, 882, L16. [10] Lingam, M. et al. 2019, *RvMP*, 91, 021002.

Earth as an Exoplanet: A Two-dimensional Alien Map

Siteng Fan[1], Cheng Li[1], Jia-Zheng Li[1], Stuart Bartlett[1], Jonathan H. Jiang[2], Vijay Natraj[2], David Crisp[2], and Yuk L. Yung[1,2]

[1] Division of Geological and Planetary Sciences, California Institute of Technology, Pasadena, CA 91125, USA

[2] Jet Propulsion Laboratory, California Institute of Technology, Pasadena, CA 91109, USA

(stfan@gps.caltech.edu)

Introduction: Since the first exoplanet was detected [1], approximately 4000 more have been confirmed (NASA Exoplanet Archive, exoplanetarchive.ipac.caltech.edu). Among these exoplanets, a number of them have similar properties to Earth and may be habitable, e.g., TRAPPIST-1e [2]. However, existing measurements are still not adequate to determine whether or not these planets can support life. A geological and climate system that supports all three phases of water is critical to life on Earth's surface. The presence of atmospheric water vapor, clouds, and surface oceans could therefore serve as biosignatures that can be observed from a distance, and are also among the indicators for habitability. Identifying surface features and clouds on exoplanets is thus essential in this context.

Earth is the only known planet that harbors life. Remote sensing observations of Earth can therefore serve as proxies for a habitable exoplanet, as seen from the perspective of hypothetical distant observers. A number of such studies have been performed using snapshots of Earth obtained by the Galileo spacecraft [3,4] and two daily light curves obtained by the Deep Impact spacecraft [5-7]. Despite interference from clouds, two-dimensional (2D) surface maps of exoplanet surfaces can be constructed using time-resolved spectra together with orbital and viewing geometry information, which in principle can be derived from light curves and other observables. In this work, we reanalyze the two-year DSCOVR/Earth Polychromatic Imaging Camera (EPIC) observations [8] to study the Earth as a proxy exoplanet. We integrate over the disk of the Earth to reduce each image to a single point source in order to simulate the light curve of a distant exoplanet. We report the first 2D surface map of this proxy cloudy exoplanet reconstructed from its single-point light curves, without making any assumptions about its spectral features.

Observations: Disk-integrated light curves analyzed in this work are derived from Earth's images obtained by DSCOVR's Earth Polychromatic Imaging Camera (EPIC) during the years 2016 and 2017. The DSCOVR spacecraft is positioned at the first Sun-Earth Lagrangian point (L1), viewing the sunlit face of Earth from a distance of about 10^6 km. From this vantage point, DSCOVR views the entire disk of Earth, illuminated near local noon. This provides an ideal geometry for studying the Earth as a proxy exoplanet seen near opposition relative to its parent star. Because the observations are all near full-phase configuration, similar to those near secondary eclipse (when the planet is blocked by the star), the phase-angle effect [8] is not considered in this work. The EPIC instrument images the Earth every 68–110 minutes, returning a total of 9740 frames over a two-year period (2016–2017), with a 2048 × 2048 charge-coupled device (CCD) in 10 narrowband channels (317, 325, 340, 388, 443, 552, 680, 688, 764, and 779 nm), which are selected primarily for investigations of the Earth's climate. We integrate the spatially resolved images over the Earth's disk to simulate observations of an exoplanet that is detected as a point source. Due to considerable difference among the channels, we normalize the time series of reflection spectra to yield zero means and unit standard deviations. This is done in order to give each channel equal importance, because the wavelengths are likely to be different for future exoplanet observations.

Result: We use the singular value decomposition (SVD) to decompose the time series into principal components (PCs), and then separate the influences of different reflective surfaces. Given that the singular values are the square roots of the variance along corresponding dimensions, the first two PCs contain 96.2% of the variation of the scaled light curves. In order to interpret the physical meaning of the PCs, we include two metrics based on ground truth, the averaged land and cloud fractions of the Earth's sun-lit face. We use a machine learning method, Gradient Boosted Regression Trees [9], to analyze the relationship between the two metrics and the PCs. Model result shows that between the first two PCs (hereafter, PC1 and PC2) changes in the land fraction are independent of PC1 and mostly correlated with PC2 (r^2 = 0.91). For the cloud fraction, the two PCs contribute comparably. Given the strong correlation between PC2 and surface features, the comparable importance of PC1 and PC2 for clouds suggests that the clouds consist of two types: surface-independent clouds and surface-correlated clouds, due to the orthogonality of SVD. Some changes in clouds can correlate temporally with the surfaces underneath. The importance of clouds in PC2 is likely to be due to these surface-correlated clouds. Converse-

ly, PC1 contributes the largest variation to the light curves via surface-independent clouds that are not correlated with the land fraction.

Although convoluted, information on the spatial distribution of different types of surfaces and clouds is fully contained in the time series of an observed planet's light curves. As discussed above, we separate the clouds from surface features using SVD. Surface information about the Earth is mostly contained in PC2 with a strong linear correlation. Here we report the first 2D surface map of Earth (Figure 1) that is reconstructed from single-point light curves. For the purpose of retrieving the map, the viewing geometry is assumed to be known in this work and obtained from DSCOVR navigation data based on maneuvers that took place during the two-year observation period. It can, in principle, also be derived using light curves and other data (e.g., radial velocity, transit timing). In the construction of Earth's surface map, spectral features of reflective surfaces are assumed to be unknown in order to facilitate generalization for future Earth-like exoplanet observations. We make the minimal assumptions that the incoming solar flux is uniform and known, and that the entire surface of the proxy exoplanet acts as a Lambertian reflector. Although Earth's ocean is strongly non-Lambertian, we still employ the Lambertian assumption because we assume that the surface properties are unknown. With these assumptions, constructing the Earth's surface map becomes a linear regression problem. The quantity derived in the map is the value of PC2, which has a positive linear correlation with the land fraction as noted above. Coastlines in the reconstructed map are determined by the median value of PC2, which is consistent with the minimal assumption of the overall land fraction being unknown.

Summary: Spectrally dependent, single-point light curves of the Earth were analyzed as observations of a proxy exoplanet. SVD analysis suggests that the majority of the information is captured by two principal components. The first captures the non-periodic behavior of surface-independent clouds. The second describes more periodic surface albedo structure. Using the fact that SVD separates the clouds from the surface, we derive the first 2D surface map of the Earth, acting as a proxy exoplanet, from single-point light curves, assuming only that the surface acts as a Lambertian reflector. The geometry is assumed to be known in the analysis, but in principle it can be derived directly from light curves. This study serves as a baseline for analyzing observations of Earth-like exoplanets with unknown surfaces and possible clouds, enabling future assessments of habitability.

References: [1] Campbell, B., Walker, G. A. H., & Yang, S. 1988, ApJ, 331, 902. [2] Gillon, M., Triaud, A. H. M. J., Demory, B.-O., et al. 2017, Nature, 542, 456. [3] Sagan, C., Thompson, W. R., Carlson, R., et al. 1993, Nature, 365, 715. [4] Geissler, P., Thompson, W. R., Greenberg, R., et al. 1995, J. Geophys. Res., 100, 16895. [5] Cowan, N. B., Agol, E., Meadows, V. S., et al. 2009, ApJ, 700, 915. [6] Cowan, N. B., Robinson, T., Livengood, T. A., et al. 2011, ApJ, 731, 76. [7] Cowan, N. B., & Strait, T. E. 2013, ApJ, 765, L17. [8] Jiang, J. H., Zhai, A. J., Herman, J., et al. 2018, AJ, 156, 26. [9] Friedman, J. H. 2001, The annals of Statistics, 29, 1189. [10] Fan, S., Li, C., Li, J.-Z., et al. 2019, ApJL, 882, L1.

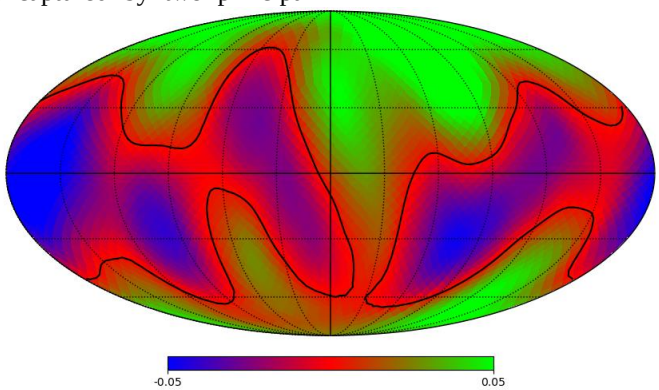

Figure 1. Surface map of Earth, which serves as a proxy exoplanet, reconstructed from multi-wavelength light curves. The contour of median is denoted as the black line. [10]

CONSTRAINING THE IONOSPHERIC IMPACTS OF EXOPLANET HOST STAR EMISSION. A. O. Farrish[1], D. Alexander[1], A. M. Sciola[1], F. Toffoletto[1], and W. T. Barnes[2] [1]Rice University Department of Physics and Astronomy, 6100 Main St., Houston, Texas 77005; [2]Lockheed Martin Solar and Astrophysics Laboratory, 3251 Hanover Street, B/252, Palo Alto, CA 94304; Alison.O.Farrish@rice.edu.

Introduction: We present a study of the impact on exoplanet ionospheric composition and electric conductance of high-energy XUV emission from the host star. In particular, we compare forcing of ionospheric conditions by variations in stellar emission over cycle timescales and across a range of stellar magnetic activity.

We employ a surface flux transport (SFT) model [1-3] in order to simulate the detailed magnetic structure and dynamics of exoplanet host star photospheres. In coupling the SFT model with a potential-field source surface (PFSS) [4] extrapolation of coronal field, and with a suite of forward-modeling tools for the derivation of coronal X-ray and EUV emission [5], we simulate self-consistently the magnetic structure and energetic budget of host star surfaces and coronae. In particular, our modeling framework can be used to determine magnetic field structure and plasma emission of a host star with finely-gridded 3-dimensional spatial information as well as complete temporal coverage over stellar cycle timescales.

In order to constrain exoplanet space physics environments with an eye toward questions of habitability, we examine the relation between host star X-ray and EUV emission and planetary ionospheric response. We employ a relation between stellar emission input to the planetary environment and changes in ionospheric conductance, Joule heating, and the resulting radio emission [6,7]. We aim to explore the conditions of star-planet interaction that might lead to observable radio signatures of exoplanet magnetic activity. Radio emission signatures from exoplanet systems, if found, would contribute greatly to our understanding of the ionospheric and magnetospheric behavior of planets outside of our Solar System.

References:

[1] Schrijver, C. J. 2001, ApJ, 547, 475. [2] Schrijver, C. J., DeRosa, M. L., & Title, A. M. 2003, ApJ, 590, 493. [3] Farrish, A. O. et al. 2019, ApJ. [4] Schatten, K. H., Wilcox, J. M., & Ness, N. F. 1969, SoPh, 6, 442. [5] Bradshaw, S. J., and Cargill, P. J. 2013, ApJ, 770, 1. [6] Zarka, P. Planetary and Space Science 55 (2007) 598–617. [7] Sciola, A. M., et al. 2019 (in prep.)

TRAPPIST-1 HABITABLE ATMOSPHERE INTERCOMPARISON (THAI). MOTIVATIONS AND PROTOCOL VERSION 1.0. T. J. Fauchez[1,2,3], M. Turbet[4,5], E. T. Wolf, I. Boutle, M. J. Way, A. D. Del Genio, N. J. Mayne, K. Tsigaridis, R. K. Kopparapu, J. Yang, F. Forget, A. Mandell, and S. D. Domagal Goldman, [1]Goddard Earth Sciences Technology and Research (GESTAR), Universities Space Research Association (USRA), Columbia, Maryland, USA, [2]NASA Goddard Space Flight Center, Greenbelt, Maryland, USA,[3]GSFC Sellers Exoplanet Environments Collaboration, [4]Laboratoire de Météorologie Dynamique, IPSL, Sorbonne Universités, UPMC Univ Paris 06, CNRS, 4 Place Jussieu, 75005 Paris, France, [5]Observatoire Astronomique de l'Université de Genève, Université de Genève, Chemin des Maillettes 51, 1290 Versoix, Switzerland.

Introduction: TRAPPIST-1 is one of the most promising targets for follow-up observations due to the depths of the planetary transit signals. The transits of the seven rocky planets in this system are relatively deep because the system is located about 12~pc away, and the star is star is relatively small (0.121 R), even for an M-type star. Among the star's seven planets, three orbit within the Habitable Zone where surface temperatures would allow surface water to exist. Amongst these three habitable zone planets, TRAPPIST-1e has been identified, by previous 3-D climate simulations, as the most habitable planet, for which surface liquid water can be present for an extended set of atmospheric configurations. TRAPPIST-1e is therefore considered the favorite target for atmospheric characterization by transmission spectroscopy with JWST. This has all caused a considerable amount of interest in TRAPPIST-1E, and simulations thereof, in order to derive constraints on its possible atmosphere and serve as a guideline for future observations.

In this context, the modeling of its potential atmosphere is an essential step prior to observation. Global Climate Models (GCMs) offer the most detailed way to simulate planetary atmospheres. However, intrinsic differences exist between GCMs which can lead to different climate prediction and thus observability of gas and/or cloud features in transmission and thermal emission spectra. Such differences should preferably be known prior to observations.

We present a planetary GCM intercomparison protocol and preliminary results [1] using TRAPPIST-1e as a benchmark and four different simulations. The four test cases included two land planets composed of a modern Earth and a pure CO_2 atmospheres, respectively, and two aqua planets with the same compositions. While our focus is TRAPPIST-1e, the methodology is applicable to other rocky exoplanets in the Habitable Zone. Currently, there are four participating models (LMDG, ROCKE-3D, ExoCAM, UM), however this protocol is intended to let other teams participate as well.

Acknowledgments: Goddard affiliates are thankful for support from GSFC Sellers Exoplanet Environments Collaboration (SEEC), which is funded by the NASA Planetary Science Divisions Internal Scientist Funding Model. M.T. acknowledges the use of the computing resources on OCCIGEN (CINES, French National HPC).\\

This project has received funding from the European Union's Horizon 2020 research and innovation program under the Marie Sklodowska-Curie Grant Agreement No. 832738/ESCAPE. M.W. and A.D. acknowledge funding from the NASA Astrobiology Program through participation in the Nexus for Exoplanet System Science (NExSS).The THAI GCM intercomparison team is grateful to the Anong's THAI Cuisine restaurant in Laramie for hosting its first meeting on November 15, 2017.

References:

[1] Fauchez, T., Turbet, M., Wolf, E. T., Boutle, I., Way, M. J., Del Genio, A. D., Mayne, N. J., Tsigaridis, K., Kopparapu, R. K., Yang, J., Forget, F., Mandell, A., and Domagal Goldman, S. D.: TRAPPIST-1 Habitable Atmosphere Intercomparison (THAI). Motivations and protocol, Geosci. Model Dev. Discuss., https://doi.org/10.5194/gmd-2019-166, in review, 2019.

Study of Barnard's Star B as an Analog for Titan-like Exoplanets. Ryan Felton[1,2](26felton@cua.edu), Shawn Domagal-Goldman[2], Giada Arney[2], Peter Gao[3], Juan Lora[4], Geronimo Villanueva[2], [1]Catholic University of America, [2]NASA Goddard Space Flight Center, [3]UC Berkeley, [4]Yale University

Introduction: Titan is currently unique in many ways: it is a rocky/terrestrial planet outside the snow line of the solar system but with a thick atmosphere; that atmosphere exhibits cycles of evaporation and precipitation, an optically thick haze, and a reducing chemical composition. As such, Titan serves as an example of potential exoplanets that are dissimilar from Earth in many ways, and as we improve our studies of Titan it will be necessary to apply what we have learned to potential "Titan-like" exoplanets to provide context for our search for potentially "Earth-like" worlds.

Recent radial velocity measurements of Barnard's Star [1] have shown the potential for there to be a planet – Barnard's Star b – with a minimum mass of 3.2 Me, and an orbiting with a semimajor axis near the snow-line of the system. In other words, the size and orbital properties of Barnard b are somewhat Titan-like in nature: Barnard b is a potentially rocky planet with a thick atmosphere above it, orbiting at a distance at which methane and ethane could condense. Further, Barnard's Star is 1.8 parsecs from the Sun, which is close enough to allow direct-imaging of this world with a large space-based telescope such as LUVOIR-A.

In this presentation, we present simulations of the observational features of Titan, as an exoplanet, using the known properties of Barnard b and the performance of LUVOIR's coronagraph (ECLIPS). These simulations were done using the Planetary Spectrum Generator (PSG) [2] to produce synthetic reflectance spectrum of a Titan-like Barnard's Star b. First, we discuss our efforts to validate PSG against previous Titan observations for transit and reflection spectroscopy [3]. We discuss some of the validation issues encountered and how they were mitigated. We then present simulations for Barnard's Star b, pointing out the observable features of that planet, and top-level conclusions we could make based on those simulated observations. We increased the complexity of the simulated atmosphere by adding hydrocarbon gas abundance profiles that were calculated by the Titan Atmospheric Model (TAM) and the photochemical models KINETICS [4] and Atmos. We highlight which of these gases can be detected in the spectra and also discuss how uncertainties on Barnard b's radius could influence these conclusions. Figure. 1 shows the synthetic direct imaging spectra of a Titan-like Barnard's Star b being observed with LUVOIR-A.

The results of this study tell us that potentially Titan-like exoplanets are characterizable with a large space-based telescope. Our next goal is to study a wider range of planetary properties, including planet size, chemical composition, and orbital semimajor axis.

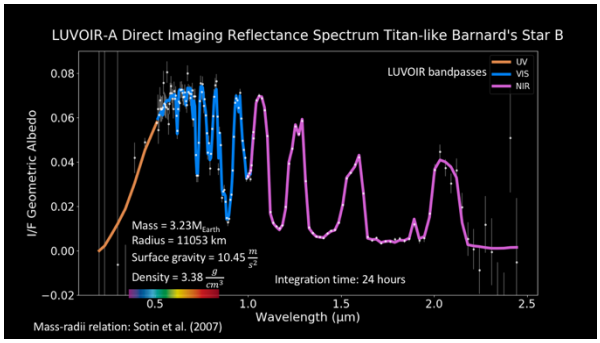

Figure 1. Synthetic spectra of Barnard's Star B assuming a minimum mass of 3.2 Me and a corresponding radius of 11053 km. A portion of the UV, all of the visible and a section of the near-infrared is observable when noise is considered.

References:

[1] Ribas et al. (2018), *Nature,* 563, 365-368.

[2] Villanueva et al. (2018), *Journal of Quantitative Spectroscopy and Radiative Transfer*, Vol. 217, 86-104.

[3] McCord et al. (2006), *Planetary and Space Science*, Vol. 54, Issue 15, 1524-1539.

[4] Lora et al. (2017), *The Astrophysical Journal,* 853.

DIRECT DETECTION OF CO IN THE PLANET AROUND CI TAU: PLANET FORMATION CONSTRAINTS FROM A YOUNG HOT JUPITER. Laura Flagg[1], Christopher Johns-Krull[1], Larissa Nofi[2], Joe Llama[3], Lisa Prato[3], Kendall Sullivan[4], Daniel T. Jaffe[4], and G. N. Mace[4], [1]Department of Physics and Astronomy, Rice University, 6100 Main St. MS-108, Houston, TX 77005, USA, Institute for Astronomy, University of Hawai'i at Mânoa, 2680 Woodlawn Drive, Honolulu, HI 96822, USA, [3]Lowell Observatory, 1400 W Mars Hill Road, Flagstaff, AZ 86001, USA, [4]McDonald Observatory and the Department of Astronomy, The University of Texas at Austin, Austin, TX 78712, USA.

Introduction: The first hot Jupiter was discovered in 1995. After nearly a quarter century, the origin of these close in massive planets remains a mystery [1]. More generally, the primary mechanisms by which giant planets form – core accretion or gravitational instability – is not firmly established [2]. Different formation models for giant planets differ substantially in the physical parameters expected at young ages [3]. Observing very young, newly formed planets, such as a candidate ~11 M_J planet in a 9 day orbit around the ~2 Myr old T Tauri star CI Tau [4], is perhaps the best way to test the various models.

Methods: We analyzed a total of 40 K band spectra of CI Tau obtained with the IGRINS spectrometer at the 2.7 m Harlan J. Smith telescope of McDonald Observatory and the 4.3 m DCT of Lowell Observatory. We focused on 4 orders of the echelle format which contain numerous CO lines between 2.3 and 2.4 microns. After removing telluric and stellar lines, we used the orbit of the star to shift the lines expected from the planet to the systemic velocity and then co-added spectra from different epochs. We cross correlated this co-added spectrum with a template of the expected planetary spectrum

Results: Figure 1 shows the cross correlation significance with a peak (5.7σ) at the expected location of CI Tau b based on the discovery paper [4]. This indicates a direct detection of CO in the planet's atmosphere, confirming the existence of the planet and allowing us to directly study its properties. Based on the planet's measured velocity amplitude, we calculate a mass of 11.6 M_J for CI Tau b.

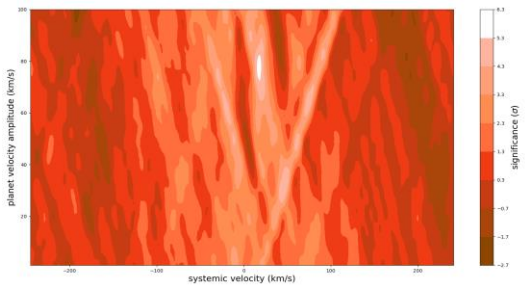

Figure 1: The cross-correlation function significance plotted as a function of planet velocity amplitude and systemic velocity.

We also estimated the contrast ratio between the star and the planet. Combined with the K-band magnitude of CI Tau and the Gaia distance to the star, we estimate the absolute K-band magnitude of CI Tau b at 8.17. CI Tau b is the youngest confirmed exoplanet as well as the first exoplanet around a T Tauri star with a directly determined, model-independent, dynamical mass.

Conclusions: Figure 2 shows the absolute K band magnitude vs age for a sample of young planet candidates including CI Tau b, as well as hot & cold start planet models [3]. Only Beta Pic b and CI Tau b have independent measurements of their mass and brightness and these strongly favor hot start models. Follow up work to detect H_2O and CH_4 will be done to constrain the planet's composition and link this to the nature of gas giant planet formation.

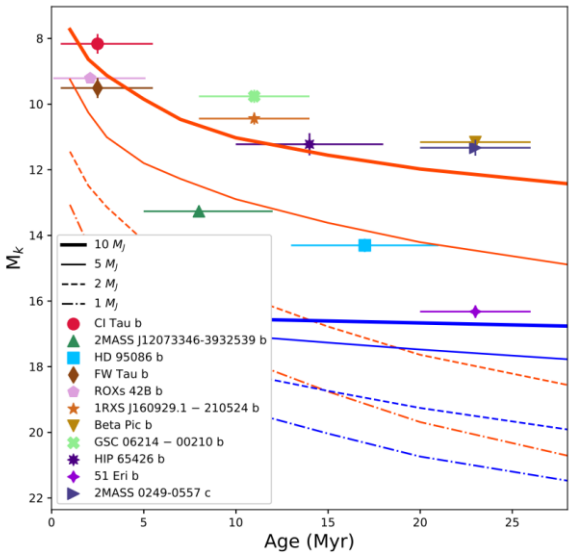

Figure 2: A sample of known young planets giving their K band absolute magnitude vs age. Also shown are hot (red) & cold (blue) start models [3].

References: [1] Dawson, R. & Johnson, J. 2018, *ARAA*, 56, 175. [2] Helled, R. et al. 2014, *PPVI*, 643. [3] Spiegel & Burrows 2012, *ApJ*, 745, 174. [4] Johns-Krull et al. 2016, *ApJ*, 826, 206.

VENUS FLAGSHIP MISSION PLANETARY DECADAL STUDY, A MISSION TO THE CLOSEST EXOPLANET M. S. Gilmore[1] and P. M. Beauchamp[2], S. R. Kane[3,4] and the 2019 Venus Flagship Study Science Team[4], [1]Department of Earth and Environmental Sciences, Wesleyan University, 265 Church St. Middletown CT 06459, mgilmore@wesleyan.edu. [2]Jet Propulsion Laboratory, California Institute of Technology, 4800 Oak Grove Drive, Pasadena, CA 91109, patricia.m.beauchamp@jpl.nasa.gov. [3]Department of Earth and Planetary Sciences, University of California, Riverside, CA, USA. [4]S. Atreya, Univ. of Michigan, P. Boston, NASA Ames, M. Bullock, Science & Technology Corp, S. Curry, UC Berkeley, R. Herrick, Univ. of Alaska, J. M. Jackson, Caltech, S. Kane, UC Riverside, A. Santos, NASA Glenn, D. Stevenson, Caltech, C. Wilson, Oxford Univ., J. Luhmann, UC Berkeley, R. Lillis, UC Berkeley, J. Knicely, Univ. of Alaska.

Introduction: More than any other known planet, Venus is essential to our understanding of the evolution and habitability of Earth-sized planets in the solar system and throughout the galaxy. Volatile elements have strong influence on the evolutionary paths of rocky bodies and are critical to understanding planetary evolution. It is clear that Venus experienced a very different volatile element history than the Earth, resulting in a different evolutionary path. The science objectives of the Venus Flagship Mission (VFM) focus on understanding volatiles on Venus. The mission concept's science goals, similar to those for other solar system bodies that were shaped by volatiles such as Mars and Europa, are: to 1) assess the volatile reservoirs, inventory, and cycles over Venus history, and 2) use the understanding of the environments created by and availability of these volatiles to constrain the habitability of Venus. The VFM aims to address two critical questions for planetary science: How, if at all, did Venus evolve through a habitable phase? What circumstances affect how volatiles shape habitable worlds?

Relevance to Exoplanets. Venus is the most Earth-like planet, yet at some point in planetary history there was a bifurcation between the two: Earth has been continually habitable since the end-Hadean, whereas Venus became uninhabitable. Indeed, Venus is the type-planet for a world that has transitioned from habitable and Earth-like conditions through the inner edge of the Habitable Zone (HZ); thus it provides a natural laboratory to study the evolution of habitability. At the present time, exoplanet detection methods are increasingly sensitive to terrestrial planets, resulting in a much needed collaboration between the exoplanetary science and planetary science communities to leverage the terrestrial body data within the solar system. In fact, the dependence of exoplanetary science on solar system studies runs deep, and influences all aspects of exoplanetary data, from orbits and formation, to atmospheres and interiors. A critical aspect of exoplanetary science to keep in mind is that, unlike the solar system, we will never obtain in situ data for exoplanet surface environments and thus exoplanet environments may only be inferred indirectly from other measurables, such as planetary mass, radius, orbital information, and atmospheric composition. The inference of those environments in turn are derived from detailed models constructed using the direct measurables obtained from observations of and missions to solar system bodies [1, 2]. Thus, whilst ever we struggle to understand the fundamental properties of terrestrial objects within the solar system, the task of characterizing the surface environments of Earth-sized planets around other stars will remain proportionally inaccessible. If we seek to understand habitability, proper understanding of the boundaries of the HZ are necessary, exploring both habitable and uninhabitable environments. Furthermore, current and near-future exoplanet detection missions are biased towards close-in planets, so the most suitable targets for the James Webb Space Telescope (JWST) are more likely to be Venus-like planets than Earth-like planets. The further study and understanding of the evolution of Venus' atmosphere and its present state provides a unique opportunity to complement the interpretation of these exoplanet observations.

Objectives and Overview. The VFM concept study seeks to design a flagship class that mission enables us to understand the: 1) History of volatiles and liquid water on Venus and determine if Venus was habitable, 2) composition and climatological history of the surface of Venus and the present-day couplings between the surface and atmosphere and 3) geologic history of Venus and whether Venus is active today.

The proposed VFM concept comprises an Orbiter with several instruments (near infrared spectrometer, radar, gravity measurements), two (or more) SmallSats that carry magnetometers and ion analyzers, and two Landers/Probes capable of measuring atmospheric chemical composition, isotopic ratios, pressure, temperature, as well as obtaining 1-μm descent images below ~5 km altitude. Once landed, a panoramic camera would sweep the horizon, and instruments, such as the Planetary Instrument for X-ray Lithochemistry or Raman/Laser Induced Breakdown Spectroscopy, would be used to measure the rock chemis-

try and mineralogy at nominally two sites. The landers would target the basaltic plains that comprise the bulk of the surface, and tessera terrain, which provide the only access to rocks from the first 80% of the history of the planet. One lander would carry a longer-lasting technology demonstration, the Long-Lived In- Situ Solar System Explorer, which measures surface temperature, pressure, wind and atmospheric chemistry as a function of time. The proposed study will also examine the possibility of detecting ground

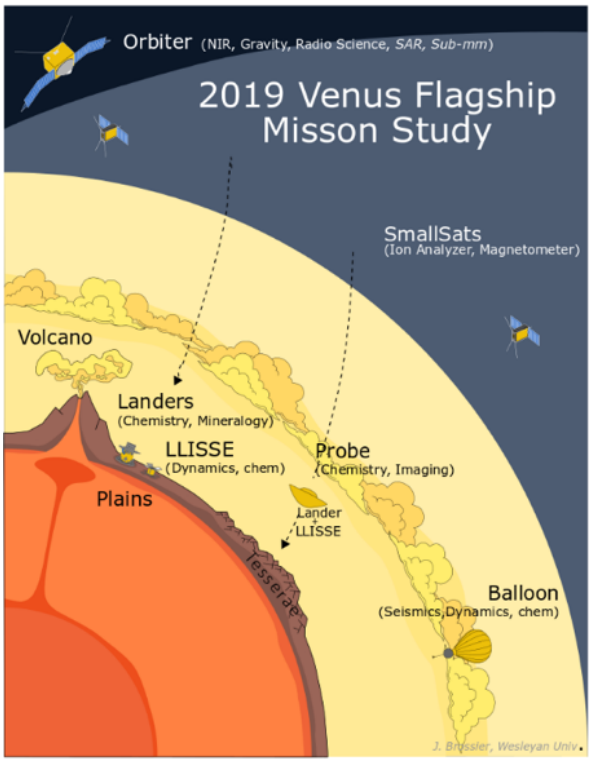

motions via a landed seismometer or by an infrasound technique from aerial platforms.

A Venus Flagship mission, similar to prior flagship missions such as Galileo and Cassini, would accomplish scientific discoveries greater than the sum of what is possible with the individual instruments, employing synergistic observations that work together to answer the 'big questions' relating to Venus' evolutionary path. Our proposed mission could be the first mission to trace volatile inventory, phase, movement, reservoirs and loss over Venus history. Specifically, it will provide the first measurements of the isotopes and inventory of all major atmospheric noble gases, the first measurement of the isotopes and volatile content of rocks, and the first measurement of the chemistry of the oldest rocks on Venus, the first measurement of global sur-face composition from orbit, the first measurement of interior structure and remanent magnetism, the first modern, multiple measurements of lower atmosphere in situ and over time via orbital spectroscopy, the first deployment of SmallSats at Venus and simultaneous measurements of the exosphere. Although we will be specifying a point-design, we will provide a range of mission implementation strategies at a number of cost points that can address significant science goals. This study will also evaluate and make recommendations for future technology investments and maturation schedules.

Studying Venus as an Exoplanet. We are seeking community feedback regarding science requirements and critical measurements that will address fundamental questions for both intrinsic Venus and exoplanet analog science. For example, atmospheric modeling of exoplanets is of critical importance and an improved sampling of pressure, temperature, composition, and dynamics of the Venusian atmosphere as a function of latitude and altitude would aid enormously in our ability to study exoplanetary atmospheres. In particular, new direct measurements of D/H ratios within and below the clouds are needed to better constrain the volume of water present in Venus' history. Combined with D/H, isotopic measurements in the atmosphere would yield insights into the origins and fate of the Venusian atmosphere. Further measurements of the Venusian deep atmosphere will allow a detailed study of the atmospheric chemistry that occurs at very high temperature and pressures. Such deep atmosphere measurements are important for exoplanet atmospheric studies because the deep atmosphere of exoplanets will be inferred from models that use data that samples the upper atmosphere via transmission spectroscopy [3, 4].

Acknowledgments: This project is supported through a NASA Planetary Mission Concept Studies grant 80NSSC20K0123.

References. [1] Fuji, Y., Kimura, J., Dohm, J., & Ohtake, M. (2014). Geology and photometric variation of solar system bodies with minor atmospheres: Implications for solid exoplanets. Astrobiology, 14(9), 753–768. https://doi.org/10.1089/ast.2014.1165 [2] J.H. Madden and L. Kaltenegger. Astrobiology. Dec 2018. http://doi.org/10.1089/ast.2017.1763 [3] Hu, R., Seager, S., & Bains, W. (2012). Photochemistry in terrestrial exoplanet atmospheres. I. Photochemistry model and benchmark cases. Ap.J., 761(2), 166. https://doi.org/10.1088/0004-637X/761/2/166; [4] Forget, F., & Leconte, J. (2014). Possible climates on terrestrial exoplanets. Philosophical Transactions of the Royal Society, 372(2014), 20130084. https://doi.org/10.1098/rsta.2013.0084.

COMPARING MODELS OF THE EARTH AS AN EXOPLANET TO EARTHSHINE OBSERVATIONS.

K. E. Gordon[1] and T. Karalidi[1] [1]Department of Physics, Planetary Sciences Group, University of Central Florida, Orlando, FL 32816 – ke14gordon@knights.ucf.edu

Introduction: Recent technological advancements and improved observing techniques have allowed for the detection of >4000 planets orbiting stars outside of the Solar System [NASA Exoplanet Archive]. These extrasolar planets, or exoplanets, can range in size and physical properties from large, hot gas giants to small, cooler rocky planets. Indeed, the rocky exoplanets provide for more intriguing studies as astronomers strive to discover life on distant worlds. However, to know whether a rocky exoplanet is habitable, we have to characterize its atmosphere and surface. Currently, transit spectroscopy and direct detection of planetary flux are the most widely used techniques for performing these characterizations. While proven successful for the gaseous giant exoplanets, Earth-sized exoplanets are slightly more challenging, as their planetary flux received during their transit is usually small compared to that of their host star [4].

Polarimetry is widely becoming recognized as a powerful technique for enhancing the contrast between a star and an exoplanet, and thus improving upon the direct detection of exoplanets. The reason for this is that, when integrated over the stellar disk, the light of a solar type star can be considered to be unpolarized, whereas the starlight that has been reflected by a planet will usually be polarized due to scattering within the planetary atmosphere off of gas, aerosol, and cloud particles and/or reflection by the surface (if one exists) [6]. The signal for the polarized light of the exoplanet is far more sensitive than its reflected flux, and therefore polarimetry can enhance the contrast between a planet and its star by a factor of ~ 10^4 - 10^5 [2].

The real power of polarimetry is in its ability to characterize the physical properties of exoplanets. This is because the state of the polarization of the light from the planet is dependent on the composition and structure of the planetary atmosphere and surface (if present), being affected by properties such as the cloud optical thickness, cloud top pressure, cloud altitude, and surface albedo [2].

Various groups ([2], [3], [6]) have theoretically studied the optical linear polarimetric signal of an Earth-like planet as functions of orbital phase and wavelength. These studies have shown that the disk integrated signal of exoplanets should still preserve crucial information on the planetary composition such as the signal of the Vegetation Red Edge and the ocean glint. Observations of the Earth itself will provide important data that can then be used to test these predictions. One of the easiest ways to view the Earth as an exoplanet is by observing and analyzing the earthshine, which is the sunlight scattered by the dayside Earth and reflected by the nightside of the Moon [1].

This project aims to validate the accuracy of these theoretical models of Earth-like planets. Using Earth atmospheric and surface data taken by the Moderate Resolution Imaging Spectroradiometer (MODIS) instrument aboard the Terra and Aqua satellites, as well as surface albedo spectra from the EcoStress Spectral Library, we can create a very detailed model of the Earth. Then, using this model data as input for a radiative transfer algorithm that models horizontally homogeneous exoplanets, we can generate the flux and linear polarization spectra for the model exoplanet Earth, which we can then compare to actual Earthshine observations taken by [1]. If the code produces similar results to the earthshine data, then we can begin to confidently say that these theoretical predictions are true and accurate. These comparisons could then help inform the search for habitable exoplanets and lead to improvements on the characterizations of signals from other worlds.

Observations: Optical (0.4 − 0.9 μm) and near-infrared (0.9 − 2.3 μm) linear spectropolarimetric data of the earthshine were acquired by observing the nightside of the waxing Moon. The data have high spectral resolution (2.51 nm in the optical, and 1.83 and 2.91 nm in the near-infrared) that can resolve molecular species present in the Earth atmosphere, particularly when it comes to cloud features. These spectra were taken using the Andalucía Faint Object Spectrograph and Camera (ALFOSC) of the 2.56-m Nordic Optical Telescope (NOT) and the Long-slit Intermediate Resolution Infrared Spectrograph (LIRIS) of the 4.2-m William Herschel Telescope (WHT), respectively. The date of observation was 2013 May 18 [1]. Although the optical and NIR data were taken on the same night at the same time, the two instruments were not able to point exactly at the same area of the Moon. This leads to a slight offset between the average values of the continuum of the optical data versus the continuum of the NIR data around 1.0 μm.

Modeling Techniques: To create our model Earth we use data from the Moderate Resolution Imaging Spectroradiometer (MODIS) instrument aboard the Terra and Aqua NASA satellites, which are in constant Earth orbit and view the entire Earth's surface every 1 to 2 days. In particular, we use the MODIS Level 3

Atmosphere Gridded Product for the cloud optical thickness, cloud top pressure, and cloud altitude properties, and the MODIS Level 3 Land Cover Types Yearly Global Product to determine the surface features. Once we have determined the type of surface from the Land Cover Product, we use surface albedo spectra for each type of surface from the NASA JPL EcoStress Spectral Library. We use data from these products collected on 2013 May 18, the same day as the earthshine data, so that the most accurate comparisons can be made. We then grid this data to make an atmosphere map and a surface map of the Earth with a spatial resolution of 2° x 2°. Once the model Earth has been created, we use the data for each of the 2° x 2° pixels as input in our radiative transfer code to produce the model flux and linear polarization spectra for that pixel. Finally, we sum up the pixels statistically to create a final spectrum for the exoplanet Earth.

The radiative transfer calculations in our code are based on the adding-doubling algorithm described in [5], which fully includes single and multiple scattering by gases and cloud and aerosol particles. The clouds for the exoplanet Earth pixel atmosphere are modelled as horizontally homogeneous, locally plane-parallel layers of scattering particles, which allows surface features to show up in the reflected light even if the planet is fully covered by clouds [6]. The code then combines this adding-doubling algorithm with a fast, numerical disk integration algorithm to integrate the reflected light across the whole pixel [2].

Current Results and Ongoing Work: We present here the preliminary results of our project. Gridded maps have been generated for our exoplanet Earth model using the MODIS and EcoStress data, displaying the cloud and land properties as observed on 2013 May 18. We also plot the resulting flux and linear polarization spectra for a few chosen pixels of our model, as functions of wavelength and planetary phase angle. As expected from previous studies, we see strong differences between the spectra for pixels with cloudy atmospheres versus pixels with clear atmospheres, and we can also observe surface features in the resulting spectra. We also plot the earthshine data taken in [1], which we are planning to match with our model.

Additional work is being done currently to finish computing the radiative transfer code on all of our exoplanet Earth pixels and generate the resulting flux and polarization spectra for each pixel. Once all of the runs have been completed, we can combine all of the pixels of the model to create the final linear polarization spectra for this exoplanet Earth.

Earthshine can be a bit tricky to work with, and it has been shown in previous studies that the scattered, polarized light from Earth can become slightly depolarized upon reflection off of the lunar surface. Therefore, before we compare our results to the Earthshine observations, we will also scan the parameter space for the Moon depolarization factor and apply this to the Earthshine data. We expect to see correlations between our model spectra and the observed earthshine spectra from [1], thus bridging the gap between theoretical and observational data of an Earth-like exoplanet.

In addition to our results and comparisons, other groups throughout the exoplanet community are attempting to make comparisons between exoplanet Earth model data and the Earthshine data from [1] using other radiative transfer codes. By comparing our results and comparisons with the outputs of the codes and the comparisons made from these other groups, everyone involved can see where improvements need to be made in the different existing models, thus helping to improve the overall accuracy of the exoplanet modeling community.

References: [1] Miles-Páez P. A. et al. (2014) *A&A, 562,* L5. [2] Karalidi T. et al. (2011) *A&A, 530,* A69. [3] Karalidi T. et al. (2012) *A&A, 546,* A56. [4] Karalidi T. et al. (2012) *Planetary and Space Science, 74*, 202-207. [5] de Haan J. F. et al. (1987) *A&A, 183,* 371-391. [6] Stam D. M. (2008) *A&A, 482*, 989-1007.

FORMATION OF ROCKY PLANETS AND SUPER-EARTHS IN SYSTEMS WITH MIGRATING GIANT PLANETS.

N. Haghighipour[1], [1]Institute for Astronomy, University of Hawaii-Manoa, 2680 Woodlawn Drive, Honolulu, HI 96822, USA, nader@ifa.hawaii.edu

Introduction: It is widely accepted that planet migration is an integral part of the formation and dynamical evolution of planetary systems. As the type and rate of migration vary with the mass of the planet and the stage of its formation, planet migration manifests itself differently during the formation of planetary systems. A survey of the currently known extrasolar planets indicates that while in some systems giant planet migration hindered the formation of rocky planets and resulted in systems with lonely hot-Jupiters, in others, close-in giant planets co-exist peacefully with small super-Earths and terrestrial-class bodies.

With an interested in the formation of rocky planets, and with an eye on those in the Habitable Zone, we started a major initiative on understanding the effect of giant planet migration on the formation of these bodies. The goal of the project is to determine the connection between the type, number, and rate of the migration of giant planet(s) and the mass, frequency, size distribution, and orbital assembly of the final super-Earth and rocky bodies. We have carried out several hundred simulations of the late stage of terrestrial planet formation in systems with migrating giant planets. Simulations have been carried out for different masses and migration rates of the giant planets, different mass distribution and surface density profile of the disk, and different masses of the central star. We have determined their final planetary assemblies, and studied the connection between the migrating planet and the size distribution, planet frequency and water content of the final bodies.

Figure 1 shows samples of our results. Here, the late stage of terrestrial planet formation has been simulated with 1, 2, and 3 migrating giant planets. The central star is Sun-like and giant planets are Jupiter-mass. As shown here, a variety of different outcomes appear. The top panel shows the giant planet and a super-Earth in a mean-motion resonance, and a super-Mars interior to their orbits. The middle panel shows a three-body resonance between two giant planets and a 2 Earth-mass super-Earth. The bottom panel shows the formation of an Earth-mass and two super-Mars planets.

In this talk, we present details of our calculations and discuss the results. We will also present an analysis of the frequency of the planets in the HZ and a comparison between the outcomes of our simulations and the results of planet formation models in our solar system as well as the currently known extrasolar planets.

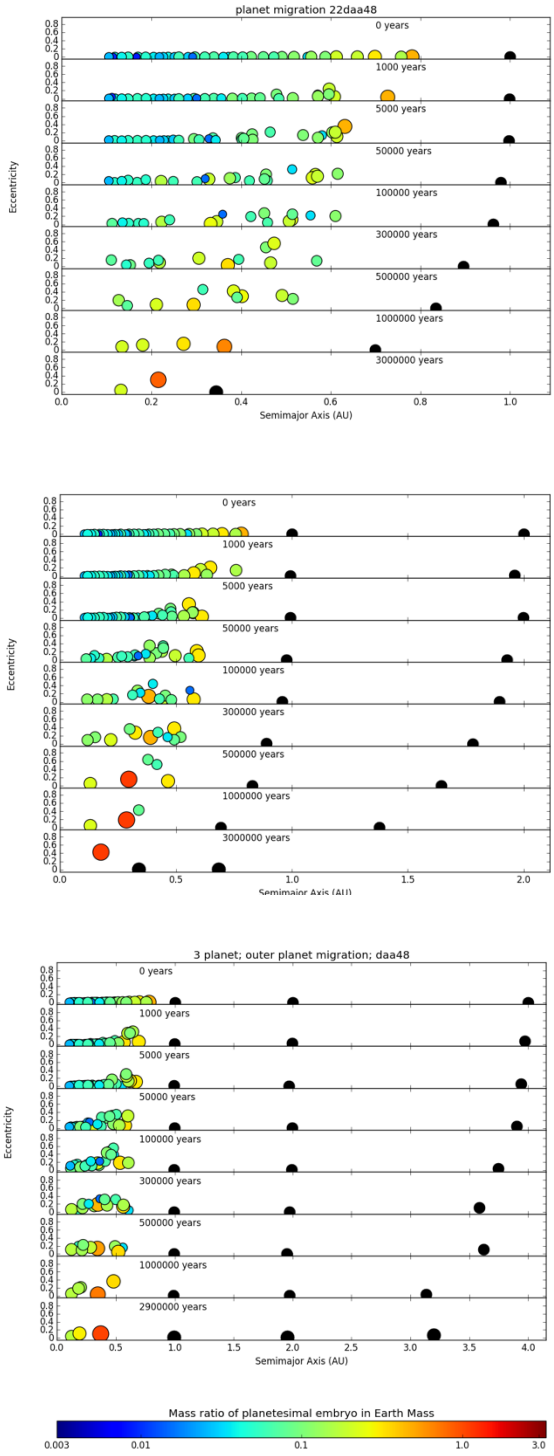

Figure 1. Late stage of terrestrial planet formation around a Sun-like star with 1, 2, and 3 migrating giant planets.

Exploring Exoplanetary Atmospheres from Laboratory Simulations

Chao He[1], Sarah M. Hörst[1,2], Nikole K. Lewis[3], Julianne I. Moses[4], Eliza Miller-Ricci Kempton[5], Patricia A. McGuiggan[1], Mark S. Marley[6], Caroline V. Morley[7], Jeff A. Valenti[2], Véronique Vuitton[8], and Xinting Yu[1,9]
[1]Johns Hopkins University, Baltimore, MD, USA (**che13@jhu.edu**), [2]Space Telescope Science Institute, Baltimore, MD, USA, [3]Cornell University, Ithaca, NY, USA, [4]Space Science Institute, Boulder, CO, USA, [5]University of Maryland, College Park, MD, USA, [6]NASA Ames Research Center, Mountain View, CA, USA, [7]University of Texas at Austin, Austin, TX, USA, [8]Université Grenoble Alpes, Grenoble, France, [9]University of California Santa Cruz, Santa Cruz, CA, USA.

Introduction: The majority of discovered exoplanets (over 4,000 by November, 2019) are super-Earths and mini-Neptunes (with size or mass between Earth's and Neptune's), and their atmospheres are expected to exhibit a wide variety of atmospheric compositions. Clouds and/or hazes are likely to be present in these atmospheres as they exist in every solar system planetary atmosphere. However, the photochemical processes for haze formation in these exoplanet atmospheres remain largely unknown as the atmospheric phase space has not been explored previously. To understand haze formation in these atmospheres, we have conducted a series of laboratory experiments simulating a range of atmospheric compositions at four different temperatures (300, 400, 600, and 800 K) [1,2,3,4].

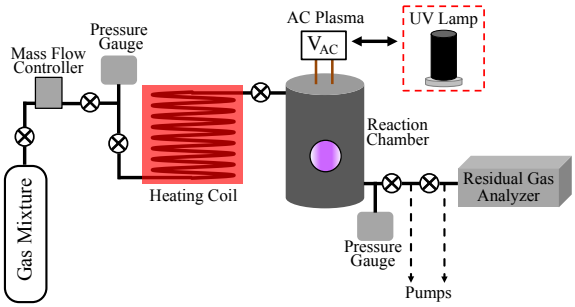

Figure 1: Schematic of the PHAZER setup.

Experimental Setup: We carried out the experiments using the PHAZER setup (Figure 1) at Johns Hopkins University [5], which allows us to conduct simulation experiments over a broad range of atmospheric parameters with two different energy sources (AC plasma or FUV photons). Figure 2 shows the initial gas mixtures for our experiments, which is prepared from high-purity gases. The gas mixture flows through a heating coil that heats the gas mixture to the required experimental temperature, and then flows into the chamber where the heated gas mixture is exposed to AC plasma, or UV photons. The gas flowing out the chamber is monitored with a Residual Gas Analyzer (RGA, a quadrupole mass spectrometer). We run the experiment for 72 hr, and collect the solid samples in a dry (<0.1 ppm H_2O), oxygen free (<0.1 ppm O_2) N_2 glove box.

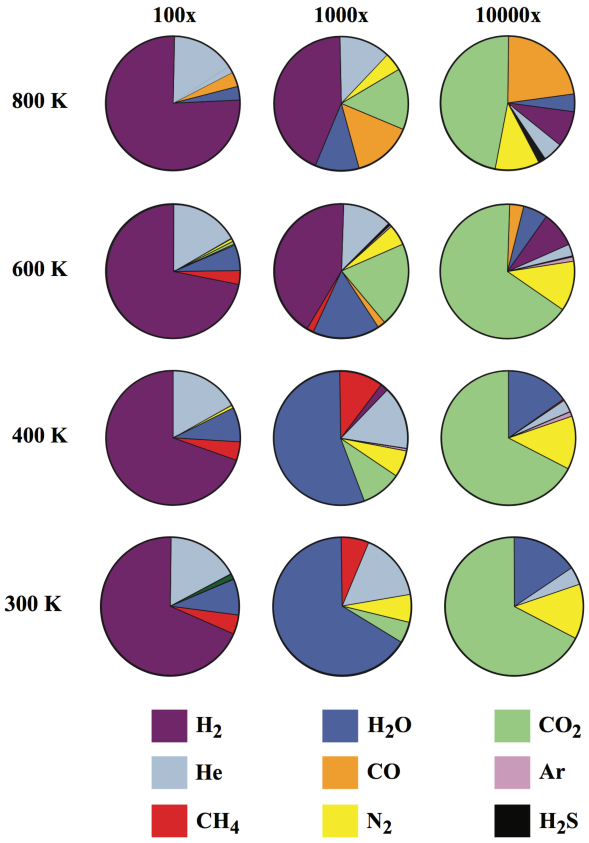

Figure 2: Initial gas mixtures used in the experiments, which span a range of temperatures (300-800 K) and initial gas mixtures (100 to 10,000x solar metallicity).

Results and Conclusions: The mass spectra of the gas phase show the compositional changes during the experiments, suggesting that distinct chemical processes happen in the experiments as a function of different initial gas mixture and different energy sources (plasma or UV photons). We identified new gas products that could be indicative to photochemistry and haze formation in these atmospheres [1]. All simulated atmospheres resulted in haze formation with both energy sources, but the production rates varied substantially with different conditions [2,3,4]. The resulting haze particles display different properties, such as color, size distribution, particle density, and composi-

tion. Our laboratory results indicate that complex atmospheric photochemistry can happen and produce new gas products and haze particles in diverse exoplanet atmospheres, including compounds (O_2 and organics) that could be falsely identified as biosignatures.

References:

[1] He, C. et al. (2019) *ACS Earth and Space Chemistry,* 3, 39-50*,*

[2] He, C. et al. (2018) *Astronomical Journal,* 156, 38.

[3] He, C. et al. (2018) *Astrophysical Journal Letters*, 856:L3.

[4] Hörst, S.M. et al. (2018) *Nature Astronomy,* 2, 303-306.

[5] He, C. et al. (2017) *Astrophysical Journal Letters*, 841:L31.

THE SOLAR SYSTEM AS AN EXOPLANET GUIDE: FINDINGS, SURPRISES AND CAVEATS FROM THE FIRST PHASE OF HUMAN AND ROBOTIC EXPLORATION. James W. Head[1], [1]Department of Earth, Environmental and Planetary Sciences, Brown University, Providence, RI USA (james_hea@brown.edu).

Introduction: Sixty years of space exploration has provided unprecedented knowledge of, and perspectives on, the origin and evolution of our Solar System. This initial phase of human and robotic exploration has both confirmed and rejected previous theories, revealed completely new information, and unveiled sobering new insights into the reality of the multiple paths of planetary formation and evolution, all of which can be applied to the exploration of exoplanets and other planetary systems. We are in the early stages of an unprecedented period of mutual, bilateral education and learning.

Opportunities for the Solar System Community: Other planetary systems offer untold numbers of individual examples of planets, systems of planets, and stars. Exploration of this huge parameter space is yet another framework for increased understanding of the origin and evolution of our Solar System. It can also assist in the development of future Solar System exploration strategies.

Opportunities for the Exoplanet Community: The Solar System provides a rich and accessible record of the origin, evolution and fate of a small number of planets and satellites. The lessons learned from initial assumptions and evolving outcomes is both instructive and sobering, and provides a template for exploring and understanding other planets and planetary systems.

Findings and Surprises from Terrestrial Planet Exploration: Planetary formation and early evolution: The original Laplacian theory of nebular condensation and planetary formation predicted a relatively orderly trend in temperature and pressure decay from the interior of the solar nebula, consistent with the first-order observations of the high-density of Mercury, the water-rich habitable zone, and the distinctive differences between terrestrial planets and gas giants (Fig. 1). More recent studies of the order of planet formation and its effects on planetary migration as well as the role of giant impacts in stripping planetary crusts have significantly modified this simple picture. Problems have also arisen in accounting for the small size and volatile abundances on Mars. The Venus D/H ratio suggests significantly more water on Venus than Earth. Formation and evolution of planetary crusts: Planetary crusts turned out to be distinctly un-Earth-like (Fig. 2) with primary crust generated by accretionary energy, producing magma oceans and a plagioclase flotation crust on the Moon, and secondary crusts by partial melting of the mantle. Not fully understood is the transition from primary to secondary crusts on bodies where plagioclase flotation is unlikely (Earth, Venus, Mercury). Tectonic systems and heat-loss mechanisms: The terrestrial planets, including "Earth-like" Venus, do not have multiple lithospheric plates and plate tectonics, instead being characterized by single global lithospheric plates ("one-plate planets") and losing heat by conduction (Fig. 3). The role of size in planetary evolution: Small planets (Mercury, Mars) and the Moon lost heat efficiently due to the high surface area to volume ratio, stabilizing lithospheres that thickened with time. Internal structure and mantle convection: The first-order internal structure of the terrestrial planets is known but the details of mantle composition, convection scale-lengths, and history, are not uniformly known or understood. Planetary scale and crustal and magnetic fields have been detected but the cause of their generation, and the nature and timing of their evolution and/or demise is not well known. Spin-axis/orbital parameters: Variations in planetary obliquity, eccentricity and precession have been shown to have a significant influence on climate and the migration of volatile species; deposits from huge tropical mountain water-ice glaciers and smaller polar CO_2 glaciers have been observed on Mars. The huge Tharsis rise on Mars is likely to have caused True Polar Wander (TPW), but the timing and magnitude is debated. Petrogenetic evolution: The compositions, including volatile content, and percent partial melting, of mantles producing secondary crusts are likely to have been quite different from the Earth, and to have varied over the course of geologic time. Details of terrestrial planet mantle evolution are largely unknown. Planetary processes: Impact cratering has clearly played a major role in all aspects of early planetary history, including primary crust formation. The volumes, styles and flux of planetary volcanism varied significantly throughout history, related to initial volatile content, lithospheric heat loss mechanisms, and planetary compositional layering. Tectonic style and importance varied substantially with one-plate planets dominated by vertical processes (uplift, loading, flexure) in contrast to the lateral plate tectonics of Earth. Planetary atmospheres: First order observations have been made on current atmospheres of Earth, Venus and Mars, but great uncertainty exists about their formation and evolution. How do we distinguish primary and secondary atmospheres, what are the major processes and rates of acquisition and loss to space, how did Venus acquire and retain its 'runaway greenhouse' atmosphere, was early Mars 'warm and wet' or 'cold and icy' and how did it evolve to its current state, what role did the evolving Sun have on

climate and atmospheric retention, how do stochastic processes such as impact cratering influence atmospheric formation, evolution and loss. Geological history: The early-stabilized lithospheres of the small planetary bodies Moon, Mercury and Mars have provided an invaluable record of the impact, volcanic and tectonic processes that may have operated on Earth and Venus in their earlier, largely missing history (Fig. 4). Habitability: Exploration of Mars and the outer planet satellites has led to new perspectives on possible environments conducive to the formation and evolution of life.

Planetary Perspectives and Questions: Mercury: Did a major impact strip the early crust, producing the observed high Fe/Si ratio? How does small mantle convective scale-length influence the generation, ascent and eruption of secondary crust? Venus: What plausible evolutionary pathways can lead to the loss of the majority of its history by recent crustal resurfacing and to the currently observed state of the atmosphere? Earth: What are the effects of the formation of the Moon on the internal structure and subsequent evolution of Earth, and can this account for observed Earth-Venus differences? Moon: How can a body accreting from the aftermath of a Mars-sized impact into proto-Earth retain volatiles? Mars: What is the nature and evolution of the early atmosphere and the climate, and what accounts for the transition from primary to secondary atmosphere, and to that of today?

Some Perspectives and Caveats: Terracentrism: We know the (recent) Earth so well that we view everything through this lens; it took decades to appreciate the role of impacts in Earth history. As Rodney Brooks has said, the *retreat* from specialness has become a *route*! Uniformitarianism: This concept has served geologists well in the last centuries, weaning us from Usher-ian and biblical deluge interpretations, but has built in a distaste for the inevitable stochastic processes. The Role of Stochastic Processes: Punctuated, stochastic events are a fundamental part of planetary evolution. The Promise and Pitfalls of Paradigms: Paradigms are essential in making sense out of a complex Universe, but Kuhn-ian revolutions are inevitable and necessary; keep an eye out for those data that don't fit the paradigm. The Space-Time Continuum: We spend virtually all of our time in the lower left-hand corner; spend time in *deep space* and *deep time*. Don't forget option d): When considering multiple interpretations, it could be: "None of the above". Venus (Fig. 4) turned out to be that way!

Summary: The lessons learned from initial assumptions and evolving outcomes in the exploration of the Solar System provide a template for exploring and understanding other planets and planetary systems. Mutual interactions between the two communities will provide an improved understanding of both our Solar System and exoplanets and exoplanetary systems.

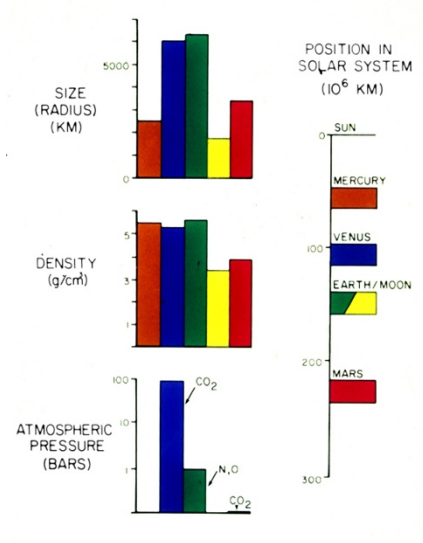

Fig. 1. Variations in planetary position, other factors.

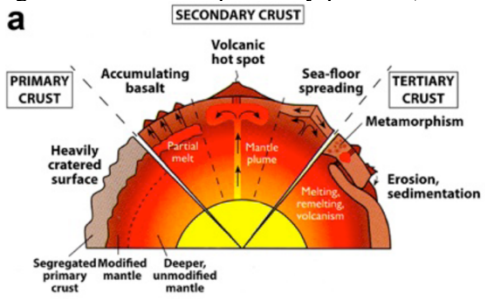

Fig. 2. Origin and evoution of planetary crusts.

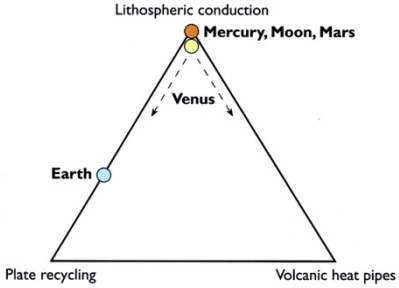

Figure 3. Mechanisms of planetary heat loss. The position of ancient Venus is unknown.

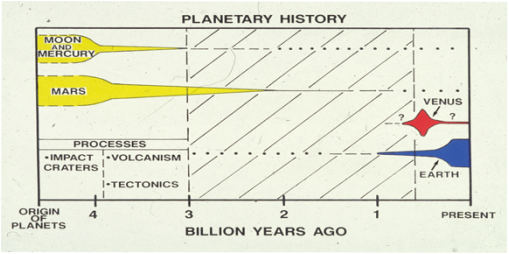

Fig. 4. Geological evolution of the terrestrial planets; width of line represents estimated amount preserved today dating from that time.

VENUS AS AN EXOPLANET LABORATORY: THE MANY PATHWAYS TO VENUS-LIKE EXOPLANETS AND HOW TO MAKE ENDS MEET. James W. Head[1], Stephen R. Kane[2], Robin D. Wordsworth[3] and Stephen W. Parman[1], [1]Department of Earth, Environmental and Planetary Sciences, Brown University, Providence, RI USA (james_hea@brown.edu), [2]Department of Earth and Planetary Sciences, University of California, Riverside, CA USA, [3]School of Engineering and Applied Sciences, Harvard University, Cambridge, MA, USA.

Introduction: Sixty years of Solar System exploration has provided new insights into the reality of the multiple pathways of planetary formation and evolution that can be applied to the exploration of exoplanets and other planetary systems. In this contribution we focus on how our current knowledge of Venus can be applied to interpret and understand the family of currently known Venus-like exoplanets [1]. What key questions can we identify that will aid us in interpreting the extremely large parameter space represented by the presence of dozens of Venus-like planets occurring in multiple planetary systems around other stars?

Current Knowledge: We know several things about the nature of Venus, and these represent "temporal bookends" on its history and evolution. At the earliest end, we rely on models for the formation and early evolution of Venus based on planetary evolution analogs, and the possibility of a water-rich early history with the presence of oceans, based on Pioneer/Venus D/H data [2]. At the most recent end, we know the general nature of its current "runaway greenhouse"-like, CO_2-dominant atmosphere, and the geologic processes and sequence of events representing the most recent 10-20% of its history [2,3]. The nature of the intervening period of evolution of the interior, surface and atmosphere, the majority of the history of Venus, is unknown. What are the different pathways between these bookends? How can they be predicted and distinguished, and used as a guide to the exploration and understanding of Venus-like planets in other planetary systems? In turn, how can the observed array of Venus-like exoplanets inform us of the candidate pathways that might have characterized the missing chapters in Venus' history?

Working Backward in Time: Global data from the Magellan Mission enabled construction of a global geologic map [3] and a synthesis of the nature and sequence of volcanic and tectonic processes operating there. These data showed that 1) there was a paucity of superposed impact craters, 2) the average age of the surface was less than a billion years, 3) the current crater population was not easily distinguishable from a spatially random one, 4) most craters were not significantly modified, and 5) there was no evidence of active plate tectonics. Detailed and global geologic mapping of stratigraphic sequences showed that the geological history of Venus can be characterized by three basic consecutive phases: Phase I represents the period prior to the formation age of the geomorphological/geological units on the surface and occupies the majority of the history of Venus. The observed geologic record starts with Phase II, comprised of two regimes, an initial global tectonic regime interpreted to have formed the tesserae (~7.3% of Venus). The second regime in Phase 2, the global volcanic regime, starts with emplacement of volcanic plains dotted with thousands of small shield volcanoes, and is immediately followed by regional plains interpreted to have been emplaced as flood basalts (~61.3%). Thus, the vast majority of the observed surface geologic units on Venus (80.7%) formed over a relatively short period of time. Phase III represents a distinctive change in style, an extended period of global network rifting; volcanism continues to today [4], primarily characterized by lobate lava flows associated with the rifts. In summary, the geological record consists of the majority of history that leaves no geological/geomorphological record (Phase I), followed by Phase II, a period of intense global tectonic deformation and global volcanic resurfacing over 60% of the planet, followed by Phase III, relative quiescence and development of a global rifting system linking several broad rises. Although active plate tectonics was not observed, the young age of the surface of Venus strongly suggested that a significant global change had taken place. Each candidate model to explain the transition in geologic and geodynamic history from the observed record back in time (Fig. 2) has significant implications for the atmosphere. 1) Equilibrium volcanic resurfacing called on random volcanic resurfacing to bury craters and constantly maintain an average crater surface age; no unusual inputs to the atmosphere were envisioned. 2) Global volcanic resurfacing that ended abruptly was called on to explain the obliteration of previous craters and the preservation of observed craters; this would clearly be accompanied by extremely high fluxes of volcanic gases. 3) Volcanic heat-pipe mechanisms on a one-plate planet were suggested to explain the observations; this would imply a constant and significant input of volcanic gases into the atmosphere. 4) A uniformitarian-evolutionary temporal change from mobile-lid to stagnant lid convection was called upon to explain the lack of plate tectonics in late Venus history; this would imply a cessation of recycling of crust into the mantle (possibly including ocean-related volatiles in earlier history), and resulting changes in rates and types of vol-

canic inputs into the atmosphere. 5) Catastrophic-episodic model called on either episodic vigorous plate tectonics or global overturn of a depleted mantle layer, leading to intense crustal deformation rapidly followed by massive fertile mantle upwelling, melting and a pulse of global volcanism, followed by relative quiescence; the catastrophic global outpouring of lava would have significant input into the atmosphere.

Critical Outstanding Questions: We now identify a series of fundamental questions that can help guide an improved understanding of the multiple pathways that might have been taken by Venus throughout its evolution. We focus on those questions that might have specific predictions about the nature of the atmosphere and climate, and those that can aid in the development of observational and instrumental strategies for the discovery and understanding of Venus-like exoplanets. 1. Current Atmosphere: What is the cause of the current "runaway greenhouse" state of the atmosphere of Venus? What are the distinctive signatures of this current atmospheric and climate state that might be recognized in exoplanets? 2. Atmosphere-Surface Buffering: What is the range of atmosphere-surface processes that can buffer the current atmosphere and what is their predicted stability? 3. Recent Phase III Geological History: Is the geologically recent rate of volcanism (Phase III) inferred from the geologic record sufficient to maintain the atmosphere in its current state? Over what time scales? If volatile input into the current atmosphere is episodic, what rates and repose periods are required to maintain its stability? 4. Recent Phase II Geological History: Is the degassing associated with the geologically rapid global volcanic resurfacing observed in Phase II sufficient to produce the currently observed atmosphere? If so, does this provide clues to the more detailed nature of the resurfacing event? If not, does this provide clues to the nature of the ambient atmosphere before the Phase II event? If the intense crustal deformation implied by the Phase II tessera formation exposes voluminous fresh bedrock, what is the effect on atmospheric buffering? 5. Nature of the Venus Mantle: What is the parameter space predicted for the Venus mantle for composition, convective style, petrogenesis, percent partial melting, volatile content and volatile release? 6. Ancient Phase I Geological History and Pathways to the Present: What are the petrogenetic processes, characteristics, outgassing rates and pathways predicted for the following plausible states for the Phase I history of Venus: a) one-plate planet dominated by vertical accretion of secondary crust; b) episodic global overturn of vertically accreting secondary crust, accompanied by upwelling and pressure-release melting of fertile mantle; c) mobile-lid plate tectonics regime with subduction, and with and without oceans; d) episodic plate tectonics and/or depleted mantle layer overturn; e) Io-like advective hot-spot heat loss with distributed centers of volcanism; f) sequential combinations of the above? Which pathways can account for the Pioneer-Venus D/H ratios? 7. Stochastic Processes: What is the role of stochastic processes? What are the effects of basin-scale impact processes on the formation, retention and characteristics of primary and secondary atmospheres? What is the effect of cometary inputs to the atmosphere instantaneously and over time? Can any of these signals be recognized in the residual atmosphere? 8. Integrated Atmospheric and Climate History: How do each of these multiple states contribute to the origin and evolution of the atmosphere? What is the most likely sequence for the history of Venus? Which of these states produce unique atmospheric signatures that might be recognized on Venus-like exoplanets? How does atmospheric structure/composition influence atmospheric loss rates? 9. Habitability: Which of these states and evolutionary sequences might be most conducive to the formation and evolution of life? Are any unique or distinctive signatures of these states and pathways predicted for the atmosphere? 10. Relation to Earth History: What lessons for Venus can be learned from the evolving understanding of Earth history? 11. Implication for Venus Exploration: How can these fundamental questions guide the current and future exploration of Venus? What are the outstanding questions that can be addressed on decadal timescales? 12. Implications for Exploration of Venus-like Exoplanets: What are the distinctive and unique atmospheric signatures that might be associated with these multiple pathways, and how can these be applied to the exploration and demographics of Venus-like exoplanets?

References: 1. Kane et al. 10.1029/2019JE005939; 2. Taylor & Grinspoon, 10.1029/2008JE003316; 3. Ivanov & Head, 10.1016/j.pss.2011.07.008, 10.1016/j.pss.2013.04.018, 10.1016/j.pss.2015.03.016; 4. Shalygin et al. 10.1002/2015/GL064088.

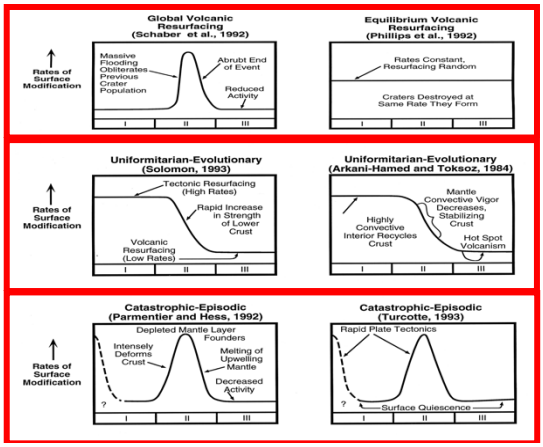

Fig. 1. Venus transitional scenarios (References in 3).

EXPLORING THE LOWER PLANET SIZE BOUNDARY OF PLANETARY HABITABILITY.

Michelle L. Hill[1] & Stephen R. Kane[1]
[1]University of California, Riverside, Department of Earth Sciences, CA 92521, USA
mhill012@ucr.edu

The search for exoplanets has been more successful than could ever have been imagined prior to the detection of the first exoplanet: today there are over 4000 confirmed planets and many more awaiting confirmation. While the abundance of planet discoveries outside our solar system has been a huge benefit to the study of exoplanets, it has caused an extra problem in the search for habitable planets: Of the many targets in the habitable zone of their star, which are the best candidates to observe to try and detect signs of life? With limited resources for follow-up observations it is important to find ways to refine the list of potentially habitable planets to those that are the most likely to be habitable. This project aims to help refine this list by exploring the lower planet size limit of habitability. While there have been many studies that have attempted to determine the size at which a rocky planet will become a gas giant, very few have looked at the lower size boundary of potentially habitable terrestrial planets. While there is evidence to suggest that Mars was only able to retain surface liquid water for the first ~0.5 Gyrs, we are far from understanding how surface water retention varies as a function of planet size. What surface pressure is needed to maintain sufficient atmospheric volatile's so that liquid water can exist on the surface of the planet? How small can a planet be and still retain sufficient atmosphere to support life? At what size does cooling of a planet reduce its magnetic field so it can no longer effectively protect its atmosphere from solar winds? And when will the cooling of the planet reduce the tectonic plate motion to a point where carbon cycling is no longer sufficient? These are examples of some the questions that are being addressed in this project. We start by developing scaling laws for the smaller than Earth, or "sub-Earth" sized planets to determine what we can expect for planets between Mars and Earth size. These scaling laws include expected changes in a planet's interior composition, atmospheric composition, surface pressure, planet cooling and subsequent tectonic plate immobility, and methods of atmospheric escape. These Scaling Laws will then be tested using exoplanet modelling tools: ROCKE-3D [1] and VPLanet [2]. ROCKE-3D (Resolving Orbital and Climate Keys of Earth and Extraterrestrial Environments with Dynamics) is a three-dimensional General Circulation Model (GCM) that models the atmospheres of Earth, the terrestrial Solar System planets and rocky exoplanets (See Figure 1). VPLanet is a 1D model that simulates tidal heating, atmospheric loss, radiogenic heating, magnetic field generation, and climate of planets. Using both VPLanet and ROCKE-3D in conjunction with the scaling laws developed in the beginning of the project, the internal and external processes of Earth that are thought to be essential to maintaining habitable conditions will be explored for sub-Earth sized planets. Preliminary simulation results and scaling laws will be presented in this poster along with an outline of the next steps in the project.

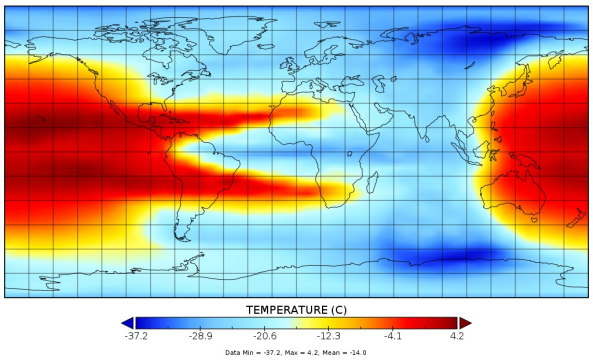

Figure 1: *A ROCKE-3D simulation output of the mean surface temperature of TRAPPIST-1 e, a sub-Earth sized planet in the HZ of its star. Here the simulated planet is tidally locked, resulting in an uneven distribution of heat on the surface of the planet. By varying many parameters that can affect Earths habitability, ROCKE-3D can help place constraints on planetary habitability scenarios.*

References:

[1] Way, M. J., Aleinov, I., Amundsen, D. S., et al. 2017, The Astrophysical Journal Supplement Series, Vol. 231, 12

[2] Barnes, R., Luger, R., Deitrick, R., et al. 2019, Proceedings of the Astronomical Society of the Pacific, accepted for publication.

THE PLANETARY LIFE EQUATION. N. R. Izenberg, Johns Hopkins University Applied Physics Laboratory, Laurel, MD, USA, (noam.izenberg@jhuapl.edu)

Introduction: One of the biggest questions of, and motivators for, exploring the solar system and beyond is whether life currently exists, or now-extinct life once existed, on worlds beyond ours. Given the proximity of the rocky planets of our solar system, Venus, Mars, and the most extreme environments of Earth are obvious targets for the first attempts to answer these questions via direct exploration, with concomitant implications for how we think of exoplanets.

Studies of extreme environments on Earth have shown just how adaptable is life as we do know it. Mars has been the target of many life-related investigations. Venus has not, yet there may be compelling reasons to think about extant life on the second planet, and lessons to learn from there about searching for life elsewhere in the solar system and beyond.

Precursor - The Venus Life Equation: Our current state of knowledge of the past and present climate of Venus suggests that the planet may once have had an extended period – perhaps 1-2 billion years – where a water ocean and a land ocean interface could have existed on the surface, in conditions possibly resembling those of Archaean Earth [1]. Also, although today Venus' surface is far from hospitable to life as we know it, there is a zone of the Venus middle atmosphere, at around 55 km altitude, just above the sulfuric acid cloud layer, where the conditions are more Earthlike than anywhere else in the solar system [2]. The question of whether life could have – or could still – exist on the Earth's closest neighbor is more open today than it's ever been.

What if we approached the question of present-day life on Venus in a similar manner as Drake Equation [3], treating the possibility of current life on Venus (including the planet's atmosphere in the word "on") as an exercise in informal probability – seeking qualitatively the likelihood or chance of the answer being nonzero.

The working version of the Venus Life Equation is expressed as:

$$\boldsymbol{L} = O * P * A * S$$

where L is the likelihood (zero to 1) of there being life currently in some Venus ecosystem, O (origination) is the chance life ever began on Venus, P (proliferation) is the chance life filled all available, or all critical ecological niches on Venus before conditions began to become increasingly hostile, A (adaptation) is the probability life could evolve as fast as or faster than conditions on the surface became, to terrestrial reckoning, uninhabitable, and S (stability) is the chance that there are sufficient essential accessible ingredients in some Venus environment to sustain life processes today.

The Venus Life Equation is an ongoing pre-decadal White Paper project [4] and its variables are currently being refined. For example, life on Venus could have originated in one of two ways: independent abiogenesis, or importation from elsewhere (panspermia - the most likely candidate being Earth), which could be termed subfactors O_A and O_P respectively. Howerver, is O the sum of those subfactors, or instead the net probability that life originated either way (e.g. $O = 1- ((1- O_A) * (1- O_P))$? Whether life originated on Venus independent of Earth depends on how "easy" is abiogenesis, or in other words: is O_A a trivial number (less than 0.0001?) a significant possibility (0.1 or greater?), or something in between?

Each of the other Venus Life Equation factors similarly comprises subfactors. The first iteration of the equation (see [4] for details) resulted in

$\boldsymbol{L} = 0.5 * 0.6 * 0.5 * 0.2 = \mathbf{0.03}$ *(low)* or
$\boldsymbol{L} = 0.5 * 0.8 * 0.5 * 0.5 = \mathbf{0.1}$ *(high)*

or a 3% to 10% chance life exists today on Venus (most likely in the upper troposphere). Whether the assumptions or variables are realistic and where they fail are subjects for discussion and debate. However, results like this for Venus motivate, and may help justify new avenues of research and calls for direct measurements of the planet in new missions. For example, the stability factor (*S*) depends on subfactors like the availability of the resources required by life processes (*e.g.,* for terrestrial life, the availability over time of the elements C H N O P and S), the availability of a solvent in which reactions can take place, and an environment that is protected enough from destructive heat/cold/radiation, and others. In-situ measurements in the Venus atmosphere and clouds can put real constraints on *S* and drive the entire Venus Life Equation towards zero (if we find some essential ingredient completely missing and *S* goes to zero), or as high as 20% (if all ingredients are there in abundance and *S* approaches 1).

Planetary Life Equation: Each of the factors used for Venus can be adapted, possibly with different or additional subfactors, to a more generalized Planetary Life Equation. For example, generalizing beyond Venus, but still within the solar system near to Earth we can debate whether we *need* a separate start to life or whether panspermia (presumably from early Earth, but cases can be made for life originating elsewhere in the solar system) is a reasonable probability – likely with O_P decreasing the farther one gets from home. For exoplanets, unless we want to talk about interstellar panspermia, *O* pretty much must rely on O_A not being infinitesimal.

Additionally, for our solar system's ocean worlds, or exoplanets, *S* may have similar or very different subfactors; life on exoplanets may indeed not be life as we know it, and may require different resources.

In this most general case, the Planetary life equation's four main factors are the same as for the Venus Life Equation. The $\boldsymbol{L}$ in the Planetary Life Equation now also helps solve for $\boldsymbol{f_l}$ of the Drake Equation: the fraction of planets in our galaxy that actually develop life [4]. While the Venus Life Equation is currently being refined (*e.g.*, the current iterations of factors *P* and *A* may not be completely independent as variables), the working version of the equation for Venus provides an early blueprint for how we might reasonably estimate the probabilities for life on other worlds.

Acknowledgements: This abstract builds on the ongoing work of the Venus Life Equation pre-Decadal White Paper group: Diana Gentry, David J. Smith, Martha Gilmore, Grzegorz Slowik, David Grisnpoon, Mark Bullock, Penny Boston.

References:

[1] Way *et al*., 2016 *JGR* 43(16) 8376-8383.
[2] Limaye *et al*., 2018 *Astrobiology*, 18(9), 1181-1198.
[3] Burchell 2006, *Int. J. Astrobio,* 5(3) 243-250.
[4] Izenberg *et al*., 2020, https://is.gd/vd4JE7 (location of Latest version of Venus Life Equation White Paper).

STAR HELIX: MULTIPLE EARTH-TRANSIT CUBESAT. N. R. Izenberg[1], K. B. Stevenson[1], K. E. Mandt[1], R. S. Miller[1], R. Nikoukar[1], B. Kilpatrick[2], E. M. May[1], K. S. Sotzen[1]. [1]Johns Hopkins University Applied Physics Laboratory, Laurel, MD, USA, [2]Space Telescope Science Institute, Baltimore, MD, USA. (noam.izenberg@jhuapl.edu)

Star Helix is a proposed study project for a cubesat that would travel away from the Earth on one of several possible trajectories and tailored to observe multiple transits of the Earth across the Sun. There is no better way to understand how an Earth-like exoplanet appears as it transits across a Sun-like star than to actually observe the Earth as if it *were* an exoplanet. Star Helix is meant to be a low-cost mission that will either ping-pong across the the Earth-Sun line as it travels away from Earth, or spiral outward from the Earth in an expanding orbit, creating multiple transit opportunities to observe with a near-UV to near-IR spectrometer.

Over these wavelengths (approximately 200 nm to 2500 nm), Star Helix will be sensitive to atmospheric habitability indicators and biosignatures such as H_2O, O_2, O_3, and CH_4. The ever-changing weather and seasonal patterns of the Earth, and decreasing relative angular size of the planet relative to the Sun, as well as speed of transit, will make each transit unique - as if each represents a different Earth-like exoplanet. The science value of real observations within the solar system of the best possible "Earth-analog exoplanet" will be to show how a world we know is both habitable and inhabited actually looks in transit, provide empirical constraints on predicitive models, and demonstrate the variability to be expected for an Earth-like world. By constraining the spatial and temporal variability, this study will be able to assess the feasibility of stacking dozens of transits to derive atmospheric abundances of potentially habitable exoplanets transiting nearby stars. A variety of trade studies will be explored, from orbital design to instrument constraints for a Sun-looking spectrometer.

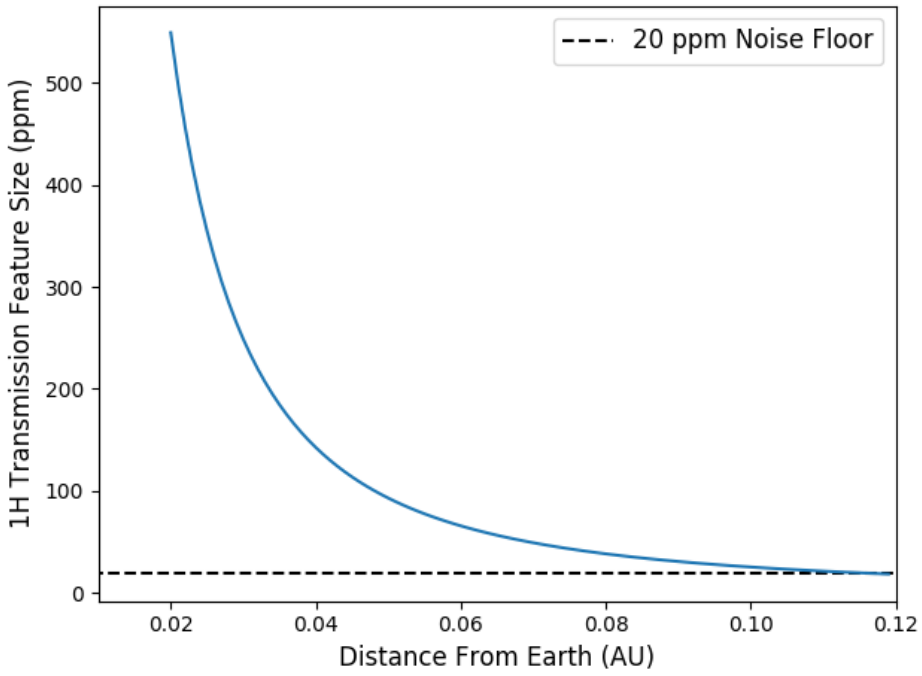

Figure 1: One scale height spectral feature size as Earth transits the Sun from various distances. Within 0.1 AU of the Earth, a cubsat would achieve sufficient signal to detect signs of life within Earth's atmosphere.

THE MAGNETIC FIELD OF THE PLANET HOSTING YOUNG STAR CI TAU. Christopher M. Johns-Krull[1], Kimberly R. Sokal[2], Gregory N. Mace[2], Larissa Nofi[3], L. Prato[4], Jae-Joon Lee[5], and Daniel T. Jaffe[2] [1]Department of Physics & Astronomy, Rice University, 6100 Main St., Houston TX 77005, USA, [2]Department of Astronomy, The University of Texas at Austin, Austin, TX 78712, USA, [3]IfA, University of Hawaii, 2680 Woodlawn Dr., Honolulu, HI 96822, USA, [4]Lowell Observatory, 1400 Mars Hill Road, Flagstaff, AZ 86001, USA, [5]KASI, 776 Daedeokdae-ro, Yuseong-gu, Daejeon 34055, Korea.

Introduction: Strong stellar magnetic fields play a fundamental role in the pre-main sequence (PMS) and early main sequence evolution of late type stars. It is now well established that the interaction of the newly formed star, also known as a T Tauri star (TTS), with its disk is strongly regulated by the stellar magnetic field. This interaction is described principally by the magnetospheric accretion paradigm [1]. In magnetospheric accretion, the large scale component of the stellar field truncates the accretion disk at or near the co-rotation radius, redirecting the path of accreting disk material so that it flows along the stellar magnetic field lines to the surface of the star. It is usually assumed that the footprints of the stellar magnetic field, which take part in the accretion process, are anchored at high latitude so that accretion occurs near the stellar poles.

Stellar magnetic fields may also have important effects on the planet formation process itself, for example the observed pileup of planets on very close orbits and the likelihood of planets being habitable. Hot Jupiters, roughly Jupiter mass planets in very close orbits around their host stars, have a peak in their distribution at ~ 0.04 au [2,3]. It is now well accepted that these planets must form significantly further out in the disk and migrate in through some mechanism [4, 5]. The stellar magnetosphere can cause inner disk truncation, which then halts inward migration and leads to a pileup of hot Jupiters [6, 2]. High energy radiation resulting from the stellar magnetic activity also potentially plays an important role in disk ionization structure and chemistry [7, 8], which influences the environment where planets form and potentially migrate. Once planets do form, the stellar magnetic field likely plays a significant role in the potential habitability of worlds around other stars, again through the impact of high energy radiation resulting from the magnetic activity which is then incident on planetary atmospheres [9]. As a result, it is important to know the magnetic properties of young stars that are in the process of forming, or have recently formed, planets.

Recently, [10] announced CI Tau b as an ~ 11 M_{Jup} planet in a possibly eccentric orbit around the Classical (disk bearing) TTS CI Tau. The K2 lightcurve of CI Tau shows additional support for the planetary interpretation of the RV signals observed from CI Tau [11]. As an ~2 Myr old star with a close, massive planet, this system may have much to reveal about planet formation and migration. Here, we seek to measure the global magnetic field properties of this star.

Observations: Zeeman broadening of K-band Ti I lines is an excellent way to measure the magnetic field strength on low mass young stars [12, 13] and has been used to measure the field strengths of close to 3 dozen young systems to date. We analyze a high signal-to-noise IGRINS spectrum of CI Tau, produced by combining IGRINS spectra from 10 separate nights. IGRINS (Immersion GRating INfrared Spectrometer) is an extremely powerful instrument that provides a large spectral grasp with high throughput [14]. The 10 observations of CI Tau were obtained with IGRINS on the 4.3m Discovery Channel Telescope of Lowell Observatory over the years of 2016 – 2017. The airmass of CI Tau varied per visit and ranged from 1.02 to 1.275. An A0V telluric standard was observed at a similar airmass either prior or following CI Tau on every night. All targets were nodded along the slit in an ABBA pattern. We use the IGRINS pipeline package (version 2.1 alpha 3, [15]) to produce a one-dimensional, telluric-corrected spectrum with wavelength solutions derived from OH night sky emission lines at shorter wavelengths and telluric absorption lines at wavelengths greater than 2.2 μm. The telluric correction is then performed by dividing the target spectrum by the A0V telluric standard and multiplying by a standard Vega model

Analysis: We used MoogStokes [16] and SYNTHMAG [17] to analyze the K-band line profiles of CI Tau, focusing on the Ti I lines near 2.22 μm to measure the mean magnetic field. Both analyses gave consistent field strengths. When using SYNTHMAG, we used multiple field components to model the lines, fitting for the filling factor of 0, 2, 4, and 6 kG field. The sum of the filling factor multiplied by the field strength is then the mean field. The infrared veiling (continuum emission from the disk) is an additional free parameter. The best fit SYNTHMAG model is shown in Figure 1, and this fit yields a mean magnetic field of 2.26 ± 0.06 kG. The best fit using MoogStokes gives a mean field of 2.15 ± 0.15 kG.

Once the mean field of CI Tau is determined, we attempt to put our results into context by comparing

the field of CI Tau to fields measured on numerous additional pre-main sequence stars. CI Tau's mean field is very typical of other low mass pre-main sequence stars as can be seen in Figure 2. This figure also shows a curious observation – there appears to be a division in the field strengths for pre-main sequence stars that are fully convective versus those that have developed a radiative core. At a given effective temperature, fully convective stars have lower average field strengths compared to those with radiative cores. In addition, there is some evidence for a clustering of fully convective stars near this boundary which may be dictated by equipartition arguments for a convectively generated dynamo field (see Figure 2). It is clear from the measurements that the surface fields observed in these stars are significantly stronger than equipartition predictions at the surface, indicating any dynamo that is operating must be anchored well below the surface.

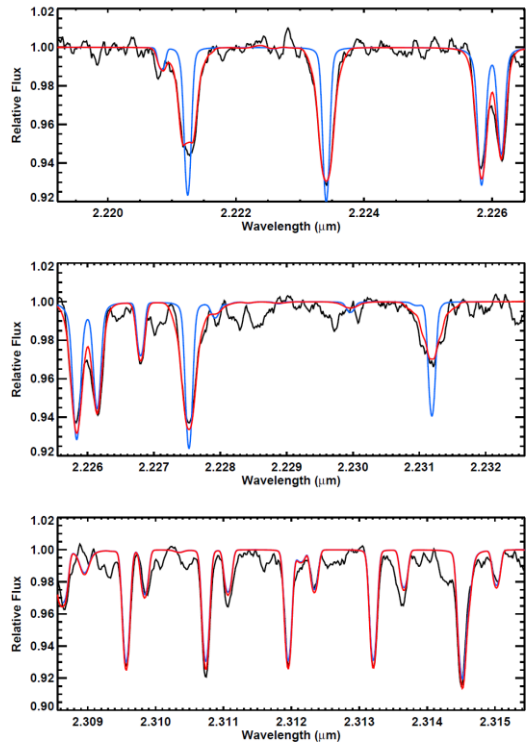

Figure 1: The observed spectrum of CI Tau is shown in black. The best fit model spectrum with no magnetic field is shown in blue, while the best fit spectrum with a mean field of 2.25 kG is shown in red.

Conclusions: Using IGRINS observations of CI Tau, we present an extremely high signal-to-noise combined spectrum that spans from 1.5 to 2.5 μm and has a spectral resolving power of R = 45,000. At these NIR wavelengths, the Zeeman effect is enhanced compared to the optical. Magnetic broadening is evident in the magnetically sensitive Ti I lines near 2.22 μm in the spectrum of CI Tau and is clearly the result of a strong magnetic field present in this young star. We measure the mean surface magnetic field strength of CI Tau to be B ~ 2.25 kG using a blind comparison of two different modeling techniques. CI Tau appears to be a perfectly ordinary TTS in the context of this analysis. Its mean surface magnetic field strength is similar to other TTSs nearby in the Hertzsprung-Russell diagram. Interestingly, we find that plotting the mean surface magnetic field strength versus the effective temperature for TTSs results in an apparent trend suggestive of some physical change.

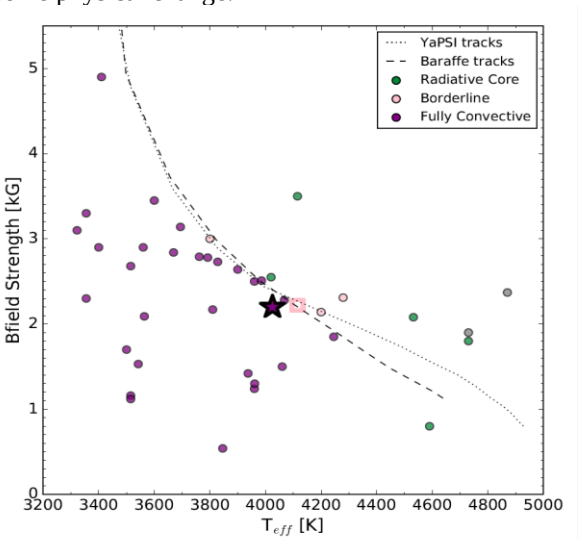

Figure 2: Mean magnetic field versus effective temperature for several TTSs. CI Tau is shown with the star. Equipartition field predictions are shown for two evolutionary tracks, with the fields normalized to one star at the boundary.

References: [1] Bouvier J. et al. (2007) *PPV*, 479. [2] Baruteau C. et al. (2014) *PPVI*, 667. [3] Heller R. (2019) *A&A*, 628, 42. [4] Lin, D. and Papaloizou J. (1986) *ApJ*, 309, 846. [5] Naoz S. (2011) *Nature*, 473, 187. [6] Lin D. et al. (1996) *Nature*, 380, 606. [7] Glassgold A. et al. (1997) *ApJ*, 480, 344. [8] Dullemond C. and Monnier J. (2010) *ARAA*, 48, 205. [9] Kaltenegger L. et al. (2010) *Astrobiology*, 10, 103. [10] Johns-Krull C. M. et al. (2016) *ApJ*, 826, 206. [11] Biddle L. et al. (2018) *ApJL*, 853, L34. [12] Johns-Krull C. M. et al. (1999) *ApJ*, 516, 900. [13] Johns-Krull C. M. (2007) *ApJ*, 664, 975. [14] Park C. et al. (2014) *SPIE*, 9147, 1. [15] Lee J. and Gulikson K. (2016) doi:10.5281/zenodo.56067. [16] Deen C. (2013) *AJ*, 146, 51 [17] Piskunov N. (1999) *Astrophysics and Space Science Library*, 243, 515.

From Mobile Lid to Stagnant Lid Mantle Convection: Variations in Solar Luminosity, Climate Evolution, and the Temporal Variability in Tectonic Style on Venus

Walter S. Kiefer[1] and Matthew B. Weller[2], [1]Lunar and Planetary Institute/USRA, 3600 Bay Area Blvd., Houston TX 77058, kiefer@lpi.usra.edu, [2]Dept. of Earth, Environmental, and Planetary Sciences, Brown University, Providence RI, mbweller@brown.edu

Evidence for Transition in Convective Style on Venus

One of the most profound questions in planetary science involves the apparent divergence in tectonic style between Earth and Venus. Understanding the cause of this divergence may also be relevant for some "Earth-like" exoplanet systems. Venus and Earth are similar in size and presumably in composition, and therefore would be expected to have similar patterns of heat loss and convective style. Indeed, Venus likely once did have a mobile lithosphere. The high topography and folded mountain belts of western Ishtar Terra, including the Lakshmi Planum plateau and the mountain belts Maxwell, Akna, and Freyja Montes, are similar in both geomorphology and dimensions to the Tibetan Plateau and Himalaya Mountains on Earth. Western Ishtar is supported by thickened crust, implying tectonic transport of crust over distances of at least several thousand km [1-4]. The complexly deformed tessera are the stratigraphically oldest preserved tectonic units on Venus. Structural relationships in Tellus Regio indicate that it formed by lateral transport and assembly of at least three distinct tessera blocks [5].

On the other hand, present day Venus is much less active than present day Earth. Gravity observations indicate that Atla Regio and Beta Regio are supported by upwelling mantle plumes [6, 7], but there are no obvious hotspot tracks associated with either plume. The Devana Chasma rift system is thermally supported and must be geologically young [8] but shows evidence for only 10-20 km of extension, similar to continental rifts on Earth [9, 10]. The recent volcanism rate is likely in the range 0.5-4 km^3/yr [11, 12], which is less than 20% of the current Earth volcanism rate. The low volcanism rate is consistent with the moderate degree of post-impact filling on the floors of large Venus craters [13].

Collectively, these observations suggest that Venus has evolved from an Earth-like, mobile lithosphere toward a present-day lithosphere that is sluggish or stagnant with limited surface motions. The high viscosity of the cold, near-surface lithosphere will impose a stagnant lid boundary condition on mantle convection [14] unless the buoyancy forces in the upper thermal boundary layer of the convecting mantle exceed the brittle strength of the lithosphere [15, 16]. Assuming based on the geologic evidence that Venus had a mobile lithosphere at some point in its history, it could transition to a stagnant lid either due to a reduction in the buoyancy force driving convective flow or due to an increase in the frictional force on faults that resists lithospheric motion. Both changes are plausible consequences of the Sun's evolution over time.

Effects of Solar Evolution on Planetary Tectonic Evolution

As a natural consequence of stellar evolution, the Sun's luminosity has increased by ~30% over the age of the Solar System, in turn increasing the radiative equilibrium temperature at Venus's orbit. A likely consequence is the loss of liquid water from the surface; the elevated D/H isotopic ratio measured by the Pioneer Venus Large Probe is consistent with substantial water loss over Venus history [17]. Pore fluids such as water in the crust support a portion of the normal stress on faults and thus reduce frictional fault strength [18]; loss of liquid water from the surface would increase fault friction and thus help push Venus from a mobile lithosphere towards a stagnant lithosphere. Increasing the surface temperature acts to thin the mantle's upper thermal boundary layer, reducing the buoyancy force that drives motion of the lithosphere, which also pushes Venus towards a more stagnant lithosphere [19]. Clearly, these two processes can act simultaneously and mutually reinforce one another.

Evolution of Convective Style on Venus

We have recently explored the consequences of a climate-driven change in lithospheric conditions on Venus for the evolution of the style of mantle convection over time on Venus [20]. The models are calculated in in three-dimensional spherical geometry and initially have lithospheric fault parameters (modeled here as plastic yielding) that are consistent with a mobile lid. At time t=0, the parameters are changed by a small amount in a direction that favors development of a stagnant lithosphere. The results shown here (Figure 1) assume an 8% increase in fault friction, but a 5% increase in the surface temperature has a similar effect on the evolution.

The results in Figure 1 are scaled to the overturn time of mantle convection, which is ~100 million years for a planet whose convective vigor is similar

to present-day Earth. Initially, convection remains relatively mobile (mobility index > 1 in Figure 1). However, due to the lithosphere's increased resistance to faulting, the degree of mobility oscillates, with large decreases at t=6, 9, 11, 12, and 14; at t= 9 and 14, the lithosphere becomes fully stagnant for ~100 Ma before resuming some degree of surface motion. In some of these events, the lithosphere is stagnant on one side of the planet and mobile on the other side. At t=16, the lithosphere becomes fully stagnant for the remainder of the model evolution. There are correlated changes in the characteristic mantle flow velocity, surface and core heat flux, and magmatic production rate (Figure 1). The complexity of the convective transition in the model has strong similarities to the geology and geophysics of Venus [20], suggesting that this mechanism is relevant to the divergence in tectonic evolution between Venus and Earth. A similar mechanism might play a key evolutionary role in exoplanet systems with T_{surf} ~100°C.

References: [1] Kiefer and Hager, JGR Planets 96, 20,967-20,980, 1991. [2] Kaula et al., JGR Planets 97, 16,085-16,120, 1992. [3] Ivanov and Head, Planet. Space Sci. 56, 1949-1966, 2008. [4] Harris and Bedard, pp. 215-291 in *Evolution of Archean Crust and Early Life*, Springer-Verlag, 2014. [5] Gilmore and Head, Planet. Space Sci. 154, 5-20, 2018. [6] Kiefer and Hager, JGR Planets 96, 20,947-20,966, 1991. [7] Smrekar et al., pp. 845-878 in *Venus II*, Univ. Arizona Press, 1997. [8] Kiefer and Peterson, Geophys. Res. Lett., doi:10.1029/2002GL015672, 2003. [9] Rathbun et al., JGR Planets 104, 1917-1927, 1999. [10] Kiefer and Swafford, J. Struc. Geo. 28, 2144-2155, 2006. [11] Grimm and Hess, pp. 1205-1244 in *Venus II*, Univ. Arizona Press, 1997. [12] Stofan et al., Icarus 173, 312-321, 2005. [13] Herrick and Rumpf, JGR Planets, doi:10.1029/2010JE003722, 2011. [14] Solomatov and Moresi, JGR Planets 101, 4737-4753, 1996. [15] Weller et al., Earth Planet. Sci. Lett. 420, 85-94, 2015. [16] Weller and Lenardic, Geosci. Frontiers 9, 91-102, 2018. [17] Grinspoon, Nature 363, 428-431, 1993. [18] Hubbert and Rubey, GSA Bulletin 70, 115-166, 1959. [19] Lenardic et al., Earth Planet. Sci. Lett. 271, 34-42, 2008. [20] Weller and Kiefer, JGR Planets, doi:10.1029/2019JE005960, in press, 2019.

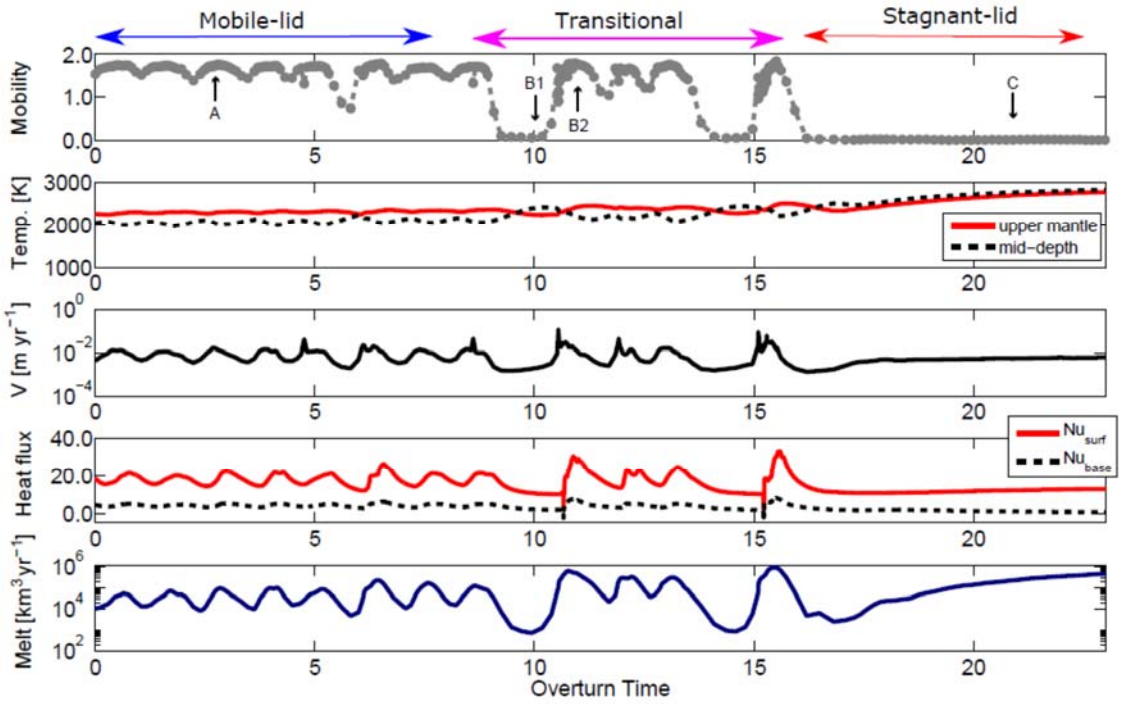

Figure 1: Representative evolution of the Venus mantle during the transition from mobile lid to stagnant lid convection. Results show the mobility index (~0 is stagnant, > 1 is mobile surface), interior temperature, RMS convective velocity, surface and core heat flux, and magma production rate. Fault friction is changed at time 0, and the transition to a fully stagnant lid convection system takes about 16 convective overturns (~1.6 billion years assuming a convective vigor typical of present-day Earth). Based on Figure 2 of Weller and Kiefer [20].

High Solubility of Mg in H_2O at High Pressures and its Implications for the Interiors of Water-rich Planets.

Taehyun Kim[1], Sang-Heon Shim[2], Vitali Prakapenka[3], Hanns-Peter Liermann[4], Sergio Speziale[5], Yongjae Lee[1,6,*], [1]Department of Earth System Sciences, Yonsei University, Seoul, 03722, Republic of Korea, ppower306@yonsei.ac.kr, [2]School of Earth and Space Exploration, Arizona State University, Tempe, Arizona, 85287, U.S.A., SHDShim@asu.edu, [3]GeoSoilEnviroCars, University of Chicago, Chicago, Illinois, 60439, U.S.A., [4]Photon Sciences, Deutsches Elektronen-Synchrotron (DESY), Hamburg, Germany, [5]GFZ, German Research Centre for Geosciences, 14473, Potsdam, Germany, [6]Center for High Pressure Science and Technology Advanced Research, Shanghai, 201203, China, *yongjaelee@yonsei.ac.kr.

Introduction: Our solar system has two large H_2O-rich bodies, Uranus and Neptune. Recent studies have also shown that water-rich exoplanets are common in our galaxy, typically categorized as sub-Neptunes [1-2]. In standard models, water-rich planets have separate layers of ice/fluid, rocky mantle, and metallic core. However, recent studies have proposed the existence of heavy elements in the ice/fluid layer of Uranus [3-4], challenging the conventional view. Therefore, it is important to understand the reactions between H_2O and rock-forming minerals at high pressures and high temperatures under H_2O saturated conditions.

Methods: We have performed laser-heated diamond-anvil cell experiments on two starting compositions: $(Mg_{0.9},Fe_{0.1})_2SiO_4$ olivine and $(Mg_{0.9},Fe_{0.1})O$ ferropericlase [5]. The thin compressed foils of these starting materials were loaded in a diamond-anvil cell under water-saturated conditions. We conducted laser heating combined with X-ray diffraction measurements at beamline 13-IDD of the GSECARS at APS and at beamline P02.2 at PETRA-III. Our dataset covers both solid-solid and solid-liquid reactions at pressures between 20 and 80 GPa. After high-pressure experiments, we conducted chemical and textural analysis using focused ion beam (FIB) and scanning electron microscope (SEM) at Yonsei University.

Results: During laser heating, Si-rich high-pressure phases were formed, such as $(Mg,Fe)SiO_3$ akimotoite or bridgmanite, stishovite, and phase D $[MgSi_2O_4(OH)_2]$, from the high Mg/Si ratio of starting composition $[(Mg_{0.9},Fe_{0.1})_2SiO_4$: olivine]. Some hydrous minerals were also identified, such as ε-FeOOH and brucite $[Mg(OH)_2]$. The formation of Si-rich phases from Mg-rich starting composition suggests dissolve of Mg^{++} into H_2O liquid during laser heating at high pressure. This was also found for $(Mg_{0.9},Fe_{0.1})O$ ferropericlase starting material. The peak intensity of ferropericlase was dramatically decreased at high pressure and high temperature conditions. In both starting materials, $Mg(OH)_2$ peak intensity increased upon temperature quench. Our SEM-EDS analysis of the recovered samples showed dome structures at the laser heated spots (Fig. 1). The dome structures were porous while the foil beneath them were still dense. Chemical analysis showed that the domes are Mg-rich while the layers below the domes are Si-rich. The morphology of the mineral grains forming the dome structures suggests that they are brucite, $Mg(OH)_2$.

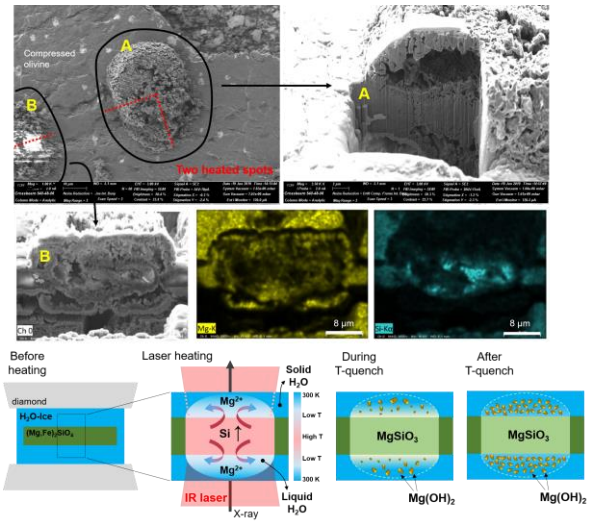

Figure 1. SEM-FIB analysis of the laser-heated spots in the recovered sample from $(Mg,Fe)_2SiO_4$ + H_2O experiments. Spot A was heated at 31 GPa and 1500 K, and Spot B was heated at 33 GPa and 1800 K. We cut vertically along the red-dashed lines in the top left image. We found dome structure which likely results from precipitation of $Mg(OH)_2$ from Mg-dissolved H_2O liquid during temperature quench.

Discussion: The textural and chemical analysis combined with XRD data indicates that liquid H_2O leached out Mg^{++} preferentially from silicate during laser heating (Fig. 1), making Mg^{++} dissolved in high-temperature fluid. Upon temperature quench, because of the reduced solubility of Mg^{++} in solid H_2O at lower temperature, it becomes precipitated as brucite. Such precipitation resulted in the observed porous dome structures at the laser-heated spots. This process leaves the silicate layer originally loaded in the diamond-anvil

cell deficient in Mg but rich in Si after reaction with H_2O.

Combined with the recent demonstration of H_2O solubility in solid SiO2 (Shim *et al.*), we propose H_2O would contain Mg while making the rocky layer deficient in Mg but rich in Si. The rocky layer would also be significantly hydrated. Such reactions would favor "fuzzy" boundary between ice and rock layers. Also, if these reactions are pressure dependent (or depth), mixing and de-mixing of ice and rock at various planetary-thermal conditions will have important implications for the convection and geochemical cycle of water-rich planets.

Acknowledgements: This work was supported by the Leader Researcher program (NRF-2018R1A3B1052042) of the Korean Ministry of Science, ICT and Planning (MSIP). This work has also been supported by NASA (80NSSC18K0353) and NSF (EAR1338810) (PI: Shim). The results reported herein benefit from NASA's Nexus for Exoplanet System Science (NExSS) research coordination network. S.-H.S. was also supported by the Keck foundation. GSECARS is supported by the National Science Foundation - Earth Sciences (EAR - 1634415) and Department of Energy- GeoSciences (DE-FG02-94ER14466). We also acknowledge DESY (Hamburg, Germany), a member of the Helmholtz Association HGF, for the provision of experimental facilities.

References: [1] D. Spiegel et al. (2014) *PNAS*, 111 (35), 12622-12627. [2] C. Unterborn et al. (2018) *Nature astronomy*, 2, 297–302. [3] J. Monteux et al. (2018) *Space Sci. Rev.*, 214: 39. [4] R. Helled and T. Guillot (2018) arXiv:1705.09320 [astro-ph.EP]. [5] H. Marquardt et al. (2009) Science, 324 (5924), 224-226.

Strange New Worlds: R. K. Kopparapu[1,2,3], [1]NASA Goddard, [2]Sellers Exoplanet Environment Collaboration, [3]Virtual Planetary Laboratory

Introduction: In the search for exo-Earth candidates, we have, and continue to, detect a multitude of exoplanets that are not found in our Solar system. The most common type of planets in our Galaxy are objects between the size of our Earth and Neptune, which are not found around the Sun. Furthermore, these planets are found around a variety of stellar spectral types, at varying distances, indicating different formation mechanisms, and distinct atmospheric physics.

I will discuss a classification scheme for exoplanets in planetary radius and stellar flux bins, based on chemical species' condensation sequences in planetary atmospheres. The order of condensation of these species represents the order in which the boundaries of classification scheme are defined.

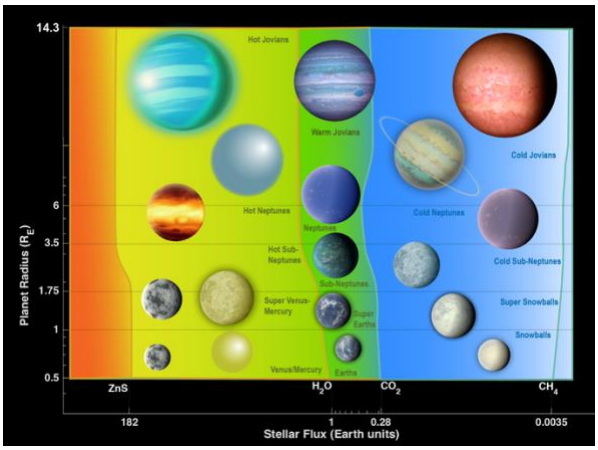

Fig. 1: The boundaries of the boxes represent the regions where different chemical species are condensing in the atmosphere of that particular sized planet at that stellar flux, according to equilibrium chemistry calculations. The radius division is from Fulton et al. (2017) for super-Earths and sub-Neptunes, and from Chen & Kipping (2016) for the upper limit on Jovians.

The boundaries of this classification scheme are illustrated in Fig. 1. The respective classes of planets are also shown, grouped together according to their relative sizes and incident stellar flux. This classification scheme has been used to estimate the exo-Earth yields from direct imaging surveys (Kopparapu et al. 2018). However, these boundaries can also be used to classify any new discoveries for comparative planetology with Solar system planets.

In the near-term, transit spectroscopy characterization of terrestrial planet atmospheres is within reach with JWST. The transit method has a dramatic bias toward the detection of planets that are closer to the host star than farther away. Consequently, "Venus zone" was proposed, where inner boundary uses the atmospheric erosion limit, and the outer boundary in terms of the runaway greenhouse limit (Kane et al. 2014).

I will provide updates to Venus zone limits for planets around M-dwarf stars, considering recent results from 3-D climate models and different planetary masses.

References:

[1] Fulton, B. J. (2017) *ApJ, 152,* 109. [2] Chen & Kipping (2016) ApJ., *834*,17. [3] Kopparapu, R. K. (2018) *ApJ*, 856, 122

TRANSITS IN THE SOLAR SYSTEM AND COMPOSITION OF EXOPLANET ATMOSPHERES

P. E. Laine[1], [1]Departments of Physics and Computer Science and Information Systems, P.O. Box 3 5, FI-4001 4 University of Jyväskylä, Finland, pauli.e.laine@jyu.fi.

Introduction: Our knowledge about exoplanets depends on very limited measurements and resolution. Atmospheric compositions are limited only to hot Jupiters and Neptunes. Detection of possible biosignatures on Earth-sized planets is not possible today. However, upcoming space missions, e.g. TESS, JWST, CHEOPS, and PLATO will give us unprecedented access to exoplanet light curves and other observations.

Before the new results arrive, it could be useful to collect the only known living planet's and other well-known planet's light curves and spectra for the future comparison and habitability modeling. For this, we need to seek possibilities to measure Earth's and other terrestrial planet's transits, occultations, and reflections from different locations in the Solar System. I will present some past events and experiments, potential locations and events, probes, and their instruments that could be used, as well some limitations and challenges..

DIVERSITY IN THE COMPOSITIONS OF FLUIDS GENERATED FROM THE SERPENTINIZATION OF OLIVINE- AND ORTHOPYROXENE-BEARING ROCKS. J. M. Leong and E. L. Shock, Arizona State University (jmleong@asu.edu)

Introduction: The crust is directly involved in the habitability of a planet. Interaction between water and rocks that compose the crust mobilizes nutrients and facilitates the transfer of energy from the lithosphere to the biosphere. On Earth, a pertinent example is when serpentinization of ultramafic rocks yields reduced and alkaline fluids. These reduced fluids support chemotrophic communities [*e.g.*, ref. 1] and the abiotic synthesis of organic compounds [*e.g.*, ref. 2], and thus are attractive for their potential to support life outside our own planet – in ocean worlds in the outer solar system and in exoplanets beyond.

Spectroscopic surveys of stars in the solar neighborhood reveal variabilities in stellar elemental abundance [3, 4]. This diversity could potentially extend to the compositions of the interiors of terrestrial exoplanets [*e.g.*, refs. 5, 6]. Variabilities in the mineral compositions (olivine- *vs* orthopyroxene-rich) predicted for the upper mantles of exoplanets hosted in stellar systems with differing Mg/Si ratios [6] can lead to varying crustal compositions. Ultimately, aqueous alteration of the crust of terrestrial exoplanets will yield diverse compositions of fluids and gases that can support chemotrophic life as well as contribute to differing atmospheric signatures. This work explores this diversity through simulations of water-rock interactions that involve olivine- and orthopyroxene-bearing igneous rocks of variable compositions.

Methods: We used the speciation and reaction path code, EQ3/6 [7], to simulate interactions between water and rock and track the evolution of fluids and minerals as aqueous alteration progresses. We first simulate systems with varying contributions from olivine and orthopyroxene to explore outcomes of the differing Mg/Si compositions of the reacting rocks [8]. To further explore contributions from other rock-forming elements, we then performed simulations involving numerous olivine- and pyroxene-bearing rock types with compositions ranging from what is known from harzburgitic to picritic rocks on Earth. These calculations include a model serpentine solid solution with various Fe^{+3}-bearing components as informed by Mössbauer and X-ray absorption spectroscopic measurements [*e.g.*, refs. 9, 10]. Calculations simulate low-temperature conditions (<100°C) pervasive in most of serpentinizing aquifers on Earth, and perhaps in icy ocean worlds in the solar system.

Results: Results show that serpentine is stable at most simulated conditions and starting bulk compositions. These results allude to the pervasive occurrence of serpentine as observed in several terrestrial bodies, meteorites, and other planetary materials in our solar system. However, the compositions of fluids and gases arising from the serpentinization of various olivine- and orthopyroxene-bearing rocks differ. Alteration of olivine-rich rocks results in fluids that are more enriched in H_2 than those resulting from alteration of orthopyroxene-rich rocks. These predictions corroborate natural observations wherein fluids hosted in olivine-rich rocks are among the most H_2-rich and reduced in Earth. All rocks used in the model have similar ferrous iron content (FeO ~ 10 wt %) and intuitively, similar potentials in generating H_2 as its production is tied to the coupled oxidation of Fe^{+2} in rocks and the reduction of H_2O to H_2. However, redox reactions are also controlled by the abundance of non-redox-sensitive elements. Rocks enriched in Mg (olivine-rich rocks) favor the formation of Fe^{+3}-bearing serpentine and magnetite over Fe^{+2}-bearing serpentine and talc that are stable in orthopyroxene-rich rocks, and thus dictates how much of the starting iron can be oxidized and the amount of H_2 generated. Results of simulations also show a transition of the dominant precipitating secondary phases from serpentine to Fe^{+2}-bearing chlorite and clay minerals as the reacting rocks become more picritic in composition. As a consequence, alteration of these rocks would result in much less H_2 than that resulting from alteration of ultramafic rocks.

Concluding Thoughts: Despite variations in rock compositions, all of the examples studied reveal a pattern wherein non-redox sensitive components of rocks (*e.g.*, Mg, Si, Al) dictate the stabilities of Fe-bearing minerals and therefore the redox processes that generate reduced species during aqueous alteration. Fluxes of reduced gas from water-rock interactions could contribute to the compositions of exoplanetary atmospheres. Thus, these simulations can potentially inform future measurements of atmospheric biosignatures. For example, the alteration of the crust of Mg-rich (or olivine-rich) exoplanets would result in large fluxes of H_2 that can potentially draw O_2 to very low levels. On the other hand, a H_2-rich atmosphere would favor CH_4 formation, either microbially or abiotically. Aside from redox-sensitive species, calculations also reveal

lithological regimes that lead to contrasting aqueous compositions (*e.g.*, pH, silica activity) and mineralization that can serve as tracers of water-rock interactions during planetary exploration. Ultimately this work provides a framework for exploring the origins of fluid and gas compositions, particularly their redox state, that can result from the varied crustal compositions of various water-bearing terrestrial bodies in the solar system and beyond.

References:

[1] Schrenk, M. et al. (2013) *Rev Mineral Geochem*, *75*, 575-606. [2] McCollom, T. M. and Seewald, J. S. (2007) *Chemical Reviews*, *107*(2), 382-401. [3] Hinkel, N. R. et al. (2014) T*he Astronomical Journal*, *148*(3), 54. [4] Brewer, J.M. and Fischer, D.A. (2016) *The Astrophysical Journal*, *831*(1), 20. [5] Carter-Bond, J.C. et al. (2012) *The Astrophysical Journal Letters*, *747*(1), L2. [6] Hinkel, N.R. and Unterborn, C.T. (2018) *The Astrophysical Journal*, *853*(1), 83. [7] Wolery T. and Jarek R. (2003) *Sandia National Laboratories*. [8] Leong, J.M. and Shock, E.L. (in press) *American Journal of Science*. [9] O'Hanley, D.S. and Dyar, M.D. (1993) *American Mineralogist*, *78*(3-4), 391-404. [10] Andreani, M. et al. (2013) *Lithos*, *178*, 70-83.

Title: Direct Imaging of Exoplanets Beyond Radial Velocity Limits

Authors: Zhexing Li[1], Stephen Kane[1], Neil Zimmerman[2], and Margaret Turnbull[3]

Affiliations:
[1] Department of Earth and Planetary Sciences, University of California, Riverside; (zli245@ucr.edu)
[2] NASA Goddard Space Flight Center
[3] SETI Institute

Radial Velocity (RV) has been an extremely useful tool for discovering and following up exoplanetary systems, but is mostly limited to planets with masses similar to solar system gas giants or even heavier, and planets that are relatively close to their host stars. With the advent of new spectrographs, we can foresee the RV precision being pushed towards lower mass regime. However, planets such as those that are further out from the host stars and Earth-sized terrestrial counterparts that lie in the habitable zone (HZ) around the stars remain below the detection threshold of RV. Future space-based direct imaging missions such as WFIRST, however, offer a pathway for such detections. With the contrast ratio of 10^{-9} for the coronagraph instrument (CGI) and 10^{-10} for the starshade, further out low mass planets around nearby stars could be revealed through imaging, offering us a way to study terrestrial planet atmosphere and habitability. Here, we investigate the parameter space within which planets are unlikely to be detected by RV in the near future due to precision limitation, but are possible to be discovered using WFIRST CGI and starshade. These directly imaged planets will provide discoveries of sub-giant planets at long orbital periods and even terrestrial planets in the HZ, as well as opportunities for atmospheric characterization in the low incident flux regime.

Procedure For Observing Rocky Exoplanets To Maximize the Likelihood of Atmospheric Oxygen Biosignatures Carey M. Lisse[1], Steven J. Desch[2], Cayman T. Unterborn[2], Stephen R. Kane[3], Patrick R. Young[2], Hilairy E. Hartnett[2,4], Natalie R. Hinkel[5], Sang-Heon Shim[2], Eric E. Mamajek[6], [1]Applied Physics Laboratory, Johns Hopkins University, 11100 Johns Hopkins Rd., Laurel, MD 20723 carey.lisse@jhuapl.edu, [2]School of Earth and Space Exploration, Arizona State University, PO Box 871404, Tempe AZ 85287---1404 steven.desch@asu.edu, cunterbo@asu.edu, patrick.young.1@asu.edu, [3]Department of Earth and Planetary Sciences, University of California, Riverside, 900 University Ave., Riverside CA 92521 skane@ucr.edu, [4]School of Molecular Sciences, Arizona State University, PO Box 871604, Tempe, AZ 85287-1604 h.hartnett@asu.edu, [5]Southwest Research Institute, San Antonio, TX, USA 28510 natalie.hinkel@gmail.com, [6]Jet Propulsion Laboratory, 4800 Oak Grove Drive MS 321-100, Pasadena, CA 91109-8099 mamajek@jpl.nasa.gov

Introduction: The first observations of exoplanet biosignature molecules are likely to be hotly debated and argued throughout the astrobiological community; therefore it is critical to obtain the clearest, most interpretable biosignature information possible. We thus present a gated observational strategy to help prioritize exoplanet oxygen biosignature observations.

Our strategy triage-ranks exoplanets for more difficult follow-up observations based on the likelihood of avoiding planets for which atmospheric O_2 is a false positive or inconclusive signature of life. It starts with the most easily obtained observational data (stellar flux and planetary orbital semimajor axis) that places an exoplanet in its system Habitable Zone (HZ). We then require that the primary star not have excessive high energy photon (XUV) flux, so that a present-day exoplanet atmosphere is likely. If so then the observer should obtain the planetary mass & radius and the host star elemental abundances to high accuracy, to determine if the exoplanet has a core/mantle/crust structure consistent with a relatively shallow surface ocean capable of supporting hydrological chemical cycles. If so, then this should be followed up by 3-color reflectance photometry and low resolution optical transmission spectroscopy to search for the presence of an optically thin Earth-like atmosphere. If and only if an optically thin atmosphere is found should long duration high resolution infrared transmission spectroscopy then be performed to search for biomarker molecule detections. Assuming that atmospheric water and carbon dioxide are found present at low (and not runaway greenhouse) 10^2 – 10^4 ppm levels, the final, most difficult step requires that a detailed multi-color exoplanet optical lightcurve be obtained to search for evidence of color variability due to the presence of both surface land and surface water.

Exoplanets that fail some of these steps might be habitable - but since their life would not be *detectable*, they should be avoided during the first searches for exosystem life.

Figure 1: Flowchart describing an observational campaign designed to efficiently find planets with oxygen in their atmospheres due to ongoing biological processes, i.e., planets for which oxygen would be a biosignature. The observations range from those currently being undertaken, to those requiring future ground- and space based observations. The least time and resource intensive observations possible for large numbers of planets are listed first, at top, and the most expensive and difficult measurements possible for only a handful of exoplanets are at bottom, in the last part of the flowchart.

Solar System Planet Test: In this paper we will describe in more detail each of the measurement assessment steps to be done on a potential life bearing exoplanet. We will then show, by example, how these steps could be used to determine the life-bearing planets in our solar system.

Using accurate planetary masses and radii obtained for planets Venus through Neptune, the first two steps of our logical prescription would remove all but Venus, Earth, and Mars from further considera-

tion. Only the Earth, with atmospheric mixing ratios of ~20% O_2 and ppm levels of CH_4, would make it to completely through the flowchart to the last step and the search for lightcurve color variability due to land and water rotating through the observer's telescope beam. Mars would survive any triaging/culling until the fourth step, where the abundance of radioactives and interior modeling would reveal it to be a small planet with a cold surface and a frozen lithosphere. It would also fail at the next two steps as its atmosphere is much too tenuous to produce bluish Earth-like colors and a variation in transit depth with wavelength signature. And it would fail again at the last step, when only 0.17% O_2 (Franz *et al.* 2017, Hartogh *et al.* 2010) and ppb to sub-ppb levels of CH_4 (Webster *et al.* 2015, 2018) are detected. Venus would survive until the fifth and sixth steps, when its yellowish reflectance and lack of transit depth variability in multi-color lightcurves determines it supports an incredibly thick non-O_2 + H_2O haze. This would have been determined after only spending enough observing time to obtain multi-color Venus transit lightcurves (i.e., much observing time will have been saved to use on other, more promising worlds in other systems). If one were to ignore these issues and press onto perform high resolution IR molecular spectroscopy as per the final step, the > 1 bar of CO_2 (Barker & Perry 1975, Cochran *et al.* 1977) and the PPM levels of O_2 (< $8x\ 10^{-5}$, Spinrad & Richardson 1965; < $3x10^{-6}$, Mills 1999) detected would eliminate it from further contention.

Acknowledgments: The authors gratefully acknowledge the support and input of the NASA Nexus for Exoplanet System Science (NExSS) research coordination network sponsored by NASA's Science Mission Directorate in the making of this paper.

References: Franz, H.B. *et al.* 2017, *Planetary and Space Science* **138**, 44; [2]Hartogh, P. *et al.* 2010, *Astron. Astrophys.* **521**, L49; [3] Webster, C.R. *et al.* 2015, *Science* **347**, 415; [4] Webster, C.R. *et al.* 2018, *Science* **360**, 10; [5] Barker, E. S. & Perry, M. A. 1975, *Icarus* **25**, 282; [6] Cochran, W. D., Trafton, L. M., & Macy, W.W. 1977, *Astron Astrophys.* **58**, 345; [7] Spinrad, H. & Richardson, E. H., 1965, *Astrophys J.* **141**, 282; [8] Mills, F.P. 1999, *J Geophys Res.* **104,** 30757

LESSONS FROM VENUS ON OCEANS AND THE SULFUR CYCLE: SULFATE AEROSOL HAZES AND SO_2 GAS AS CONSTRAINTS ON ROCKY EXOPLANETS' SURFACE LIQUID WATER.

K. Loftus[1*], R. D. Wordsworth[1], C. V. Morley[2]. [1]Department of Earth and Planetary Sciences, Harvard University, Cambridge, MA, 02138, US; [2]Department of Astronomy, University of Texas at Austin, Austin, TX, 78712, US; [*]kloftus@g.harvard.edu.

Introduction: Despite surface liquid water's importance to habitability (e.g., [1], [2]), observationally diagnosing its presence or absence on exoplanets is still an open problem (e.g., [3]). Inspired within the Solar System by the differing sulfur cycles on Venus and Earth, we investigate thick sulfate (H_2SO_4-H_2O) aerosol haze and high trace mixing ratios of SO_2 gas as observable atmospheric features whose sustained existence is linked to the near absence of surface liquid water.

Methods: We examine the fundamentals of the sulfur cycle on a rocky planet with an ocean and an atmosphere in which the dominant forms of sulfur are SO_2 gas and H_2SO_4–H_2O aerosols, as on Earth and Venus (Figure 1). We build a simple but robust model of the wet, oxidized sulfur cycle to determine the critical amounts of sulfur in the atmosphere-ocean system required for detectable levels of SO_2 and a detectable haze layer.

Our modeling approach begins with the critical SO_2 mixing ratio for observational detection of atmospheric SO_2 or the critical aerosol optical depth for detection of a haze layer. Working backwards, we then calculate the critical number of sulfur atoms in the atmosphere and ocean system necessary for detection. Finally, we compare this critical value to the expected number of surface sulfur atoms to evaluate whether observable SO_2 buildup or observable haze formation is likely.

For each parameter in our model, we consider both the best reasonable estimate from Solar System analogs and the limiting scenario that promotes conditions for observable sulfur. The latter presents the most challenging conditions for our hypothesis and allows us to stringently test our hypothesis in the face of a vast planetary parameter space.

Results: The presence of liquid water on an oxidized planet strongly influences its sulfur cycle—particularly the planet's ability to sustain an optically thick H_2SO_4-H_2O haze layer or a high trace mixing ratio of SO_2 gas. Detectable levels of both H_2SO_4-H_2O aerosols and SO_2 gas require SO_2 in the upper atmosphere, but the presence of an ocean restricts the availability of SO_2 in the atmosphere. For expected ocean pHs, exponentially more SO_2 is stored in the ocean than in the atmosphere because of basic chemical properties of aqueous SO_2 (Figure 2).

Within the ocean, the dissolved products of SO_2 are thermodynamically unstable [4]-[6] and thus short lived on geologic timescales. Recent outgassing must supply both the SO_2 present in the atmosphere necessary for observation and the accompanying amount of aqueous sulfur implied by the size of the ocean. Our calculations of this process suggest the buildup of observable atmospheric sulfur is incompatible with the presence of oceans (Figures 3 and 4).

Conclusion: Via a quantitative model of the wet, oxidized sulfur cycle, we have shown that neither observable H_2SO_4-H_2O haze layers nor observable levels of SO_2 are likely compatible with significant surface liquid water ($> 10^{-3}$ Earth ocean masses). Despite the uncertainties involved in modeling exoplanet processes, this incompatibility seems to persist even in the most extreme physical conditions to promote SO_2 buildup and haze formation. Thus, we propose the observational detection of H_2SO_4-H_2O haze and SO_2 gas as two new constraints on surface liquid water.

References: [1] Scalo J. et al. (2007) *Astrobiology*, *7(1)*, 85-166. [2] Kasting J. F. (2012) *Princeton UP*. [3] Cowan N. B. (2012) *ApJL, 752(1)*, L3. [4] Ermakov A. et al. (2001) *Kinetics and Catalysis*, *42(4)*, 479–489. [5] Guekezian M. et al. (1997) *Analytical Letters*, *30(7)*, 1423–1436. [6] Karchmer J. H. ed. (1970) *Wiley-Interscience*.

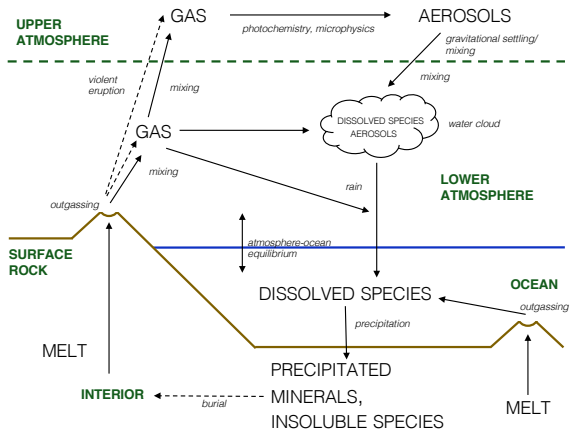

Figure 1: Schematic of the major components of the sulfur cycle on a planet with an ocean and active hydrological cycle.

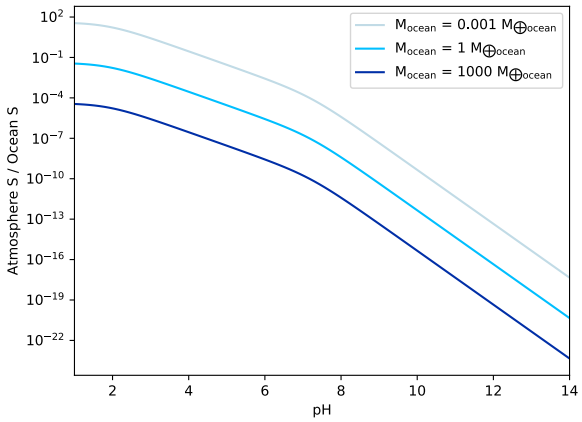

Figure 2: The ratio of sulfur in SO_2 in the atmosphere compared to sulfur in S(IV)—dissolved aqueous SO_2 products—in the ocean as a function of ocean pH and ocean mass relative to Earth's. The ocean and atmosphere are assumed to be in equilibrium and the ocean saturated with S(IV).

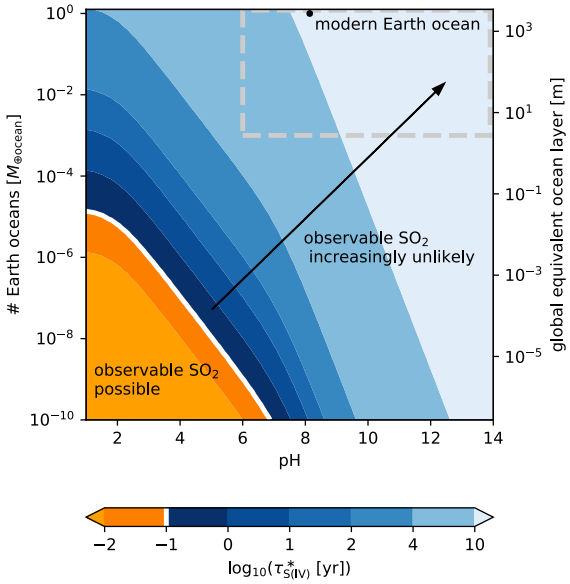

Figure 3: Contours of the critical lifetime of aqueous S(IV) $\tau^*_{S(IV)}$ necessary for observable mixing ratios of SO_2 versus ocean pH and mass (in Earth ocean masses). Aqueous S(IV) is known to be unstable, but its decay kinetics are poorly constrained. The white contour indicates a reasonable timescale for $\tau^*_{S(IV)}$ from present aqueous redox sulfur chemistry experimental results [5]. For ocean pHs and total masses below this line, observable SO_2 is possible. Above this line, observable SO_2 grows increasingly unlikely. The dashed gray lines indicate ocean parameters of interest (from a reasonable pH limit of 6 and a low-liquid-water threshold of 0.001 Earth oceans). Model results are shown for our best-guess model parameters.

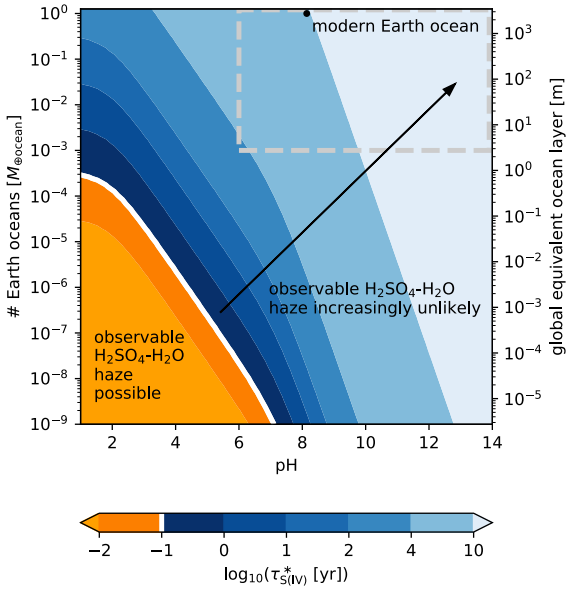

Figure 4: Same as Figure 3 except for an observable H_2SO_4–H_2O haze layer.

PHOTOCHEMISTRY AND STAR-ATMOSPHERE INTERACTION IN THE TRAPPIST-1 SYSTEM. A. Luspay-Kuti[1], K. E. Mandt[1], K. A. Sorathia[1], V. G. Merkin[1], K. B. Stevenson[1], A. M. Rymer[1]. [1]Johns Hopkins University Applied Physics Laboratory (Laurel, MD 20723 USA, Adrienn.Luspay-Kuti@jhuapl.edu).

Introduction: Understanding processes relevant to exoplanetary atmospheres and how they influence the evolution of the atmosphere over time is critical to assess their ability to retain water, and potentially support life. With the increasing number of rocky exoplanets being discovered in the habitable zones – regions where liquid water can exist on the surface – of their stars and the upcoming James Webb Space Telescope (JWST), understanding how the atmospheres of rocky exoplanets evolve is especially timely.

Star-planet interactions are one of the key contributors to how an atmosphere evolves over time. Understanding the solar wind-magnetosphere-ionosphere-thermosphere coupling is a critical step in understanding how a stellar wind may impact the upper regions of a planetary atmosphere. Energy input from the host star into the atmosphere leads to atmospheric escape, which in turn affects the stability of the atmosphere. In addition, stellar radiation initiates photochemistry, resulting in a change in atmospheric structure and composition over time. While there is great value in looking at these processes independently, a more physically accurate representation would involve considering photochemistry and star-atmosphere interactions in unison.

In this work, we will present our approach to *provide detailed photochemical modeling of a variety of potential atmospheric pressures and compositions for TRAPPIST-1e, and combine the results from our photochemical model with a model of star-exoplanetary atmosphere interaction*.

The TRAPPIST-1 planetary system consists of seven terrestrial-sized temperate exoplanets, of which at least three are within their star's habitable zone [1, 2]. The middle planet (e) is considered to represent the best chance for a habitable ocean-covered world in the system [3]. As such, TRAPPIST-1e is a highly favorable target for atmospheric characterization by JWST, which will allow for testing our model results against future observations.

Methods: To model the composition and structure of the atmosphere of TRAPPIST-1e, we used our Exoplanet Atmospheric Model (ExAM). ExAM is a 1-D photochemical model that was originally developed and validated for the atmosphere of Titan [4-7]. The original photochemical model has since been adapted and validated for Pluto, Triton, and Mars [8-11].

ExAM couples the neutral and ion chemistry by solving the continuity equation at each 10 km grid from the surface to a user-defined upper boundary. We include a total of 53 neutral and 35 ion species to model the photochemistry.

If an atmosphere around TRAPPIST-1e does indeed exist, its parameters are currently unknown. Therefore, we will conduct pilot studies by varying the atmospheric composition, the temperature profile, and the surface pressure, including parameters of an Earth-like atmosphere.

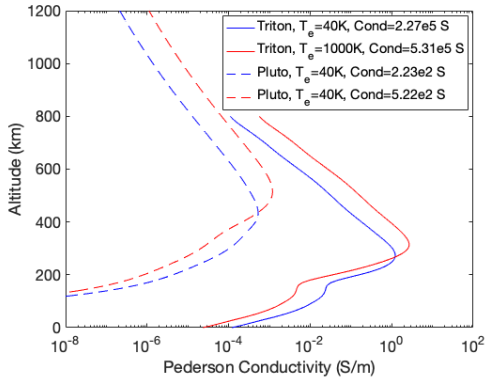

Fig. 1. Examples of extreme cases of Pedersen conductivity profiles for Triton and Pluto calculated with the heritage model of ExAM. The column-integrated conductivity is shown in the figure legend. This parameter is essential for understanding star-planet interaction at a level required to constrain escape rates when a magnetosphere is present.

We calculate the ionospheric conductivity and outflow from ExAM results. We then feed the altitude-integrated Pedersen conductivity (Fig. 1) into the Grid Agnostic MHD for Extended Research Applications (Gamera), which we will adapt for the TRAPPIST-1 system. Gamera is a new magnetohydrodynamic simulation tool building and improving upon the high-heritage Lyon-Fedder-Mobarry (LFM) code [12]. It has minimal external library dependence, high degree of optimization, OpenMP parallelism allowing use of heterogeneous architectures, and multiple numerics upgrades. Gamera is unique in its use of very high-order schemes, arbitrary hexahedral meshes, and intrinsic divergence conservation methods to solve MHD equations [13-15]. The current applications of Gamera include the terrestrial magnetosphere (Fig. 2), the inner heliosphere/solar wind, magnetospheres of outer planets, current sheets and reconnection, and MHD instabilities. It allows easy adaptation to different geometries and initial/boundary conditions via user files making its adaptation to the

TRAPPIST-1 system. The primary current applications are the terrestrial magnetosphere, the inner heliosphere/solar wind, magnetospheres of outer planets, current sheets and reconnection, and MHD instabilities (e.g, Kelvin-Helmholtz and Rayleigh-Taylor.)

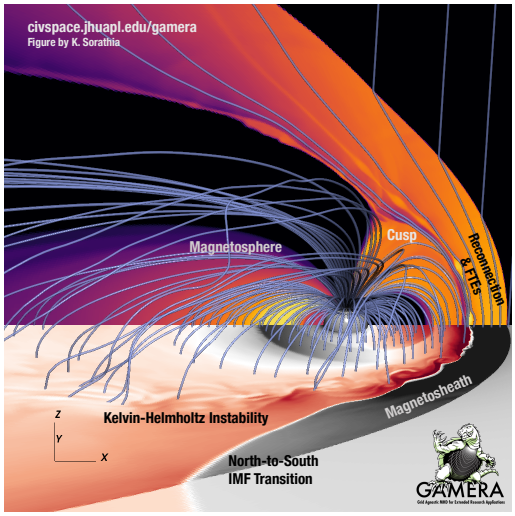

Fig. 2. High-resolution simulation of the terrestrial magnetosphere with our Gamera MHD code.

The combination of photochemical and star-planet interaction models as we do in this work will help better understand the relevant physical processes controlling the composition and structure of exoplanetary atmospheres.

References: [1] Gillon M. et al. (2016) *Nature, 533,* 221–224. [2] Gillon M. et al. (2017) *Nature, 542,* 456-460. [3] Wolf E. T. (2017) *ApJL,* 839, L1. [4] de la Haye V. et al. (2008) *Icarus,* 197, 110-136. [5] Mandt K. E. et al. (2012) *JGR*, 117, E10. [6] Luspay-Kuti A. et al. (2015) *ApJL*, 801, L14. [7] Luspay-Kuti et al. (2016) *ApJ*, 823, 163. [8] Luspay-Kuti A. et al. (2017) *MNRAS*, 472, 104-117. [9] Mandt K. E. et al. (2017), *MNRAS*, 472, 118-128. [10] Mandt K. E. et al. (2015), *Icarus*, *254*, 259-261. [11] Mandt K. E. et al. (2016) *PSS, 130*, 104-109. [12] Lyon J. G. et al. (2004) *Journal of Atmospheric and Solar-Terrestrial Physics*, 66, 133. [13] Merkin V. G. and Lyon J. G. (2010) *JGR*, 115, A10202. [14] Zhang B. et al. (2018) *J. Comput. Phys.*, 376, 276-294. [15] Zhang et al. (2019) *ApJ Suppl. Ser.*, 244, 20.

PEAS: THE PLANET AS EXOPLANET ANALOG SPECTROGRAPH. E. C. Martin[1] and A. J. Skemer[1], [1]Department of Astronomy & Astrophysics, University of California, Santa Cruz, CA (emilymartin@ucsc.edu)

Introduction: Exoplanets are abundant in our galaxy and yet characterizing them remains a technical challenge. Solar System planets provide an opportunity to test the practical limitations of exoplanet observations with high signal-to-noise data, and ancillary data (such as 2D maps and in situ measurements) that we cannot access for exoplanets. However, data on Solar System planets differ from exoplanets in that Solar System planets are spatially resolved while exoplanets are all unresolved point-sources.

There have been several recent efforts to validate techniques for interpreting exoplanet observations by binning images of Solar System planets to a single pixel: For example, Cowan et al. [1] used images from the EPOXI mission to study Earth's globally averaged properties as it rotated; Mayorga et al. [2] used data from the Cassini spacecraft's fly-by of Jupiter to observe globally averaged reflected light phase curves; and Karalidi et al. [3] imaged Jupiter with the Hubble Space Telescope in the UV and red-optical as a test of their methods for determining spot size and location on exoplanet atmospheres. However, there is a dearth of disk-integrated spectra of Solar System planets from modern equipment.

We present a novel instrument designed to observe Solar System planets as though they are exoplanets, the Planet as Exoplanet Analog Spectrograph (PEAS). PEAS consists of a dedicated 0.5-m PlaneWave Telescope and off-the-shelf optics, which will be located at Lick Observatory. PEAS uses an integrating sphere to disk-integrate light from the Solar System planets before it is dispersed in a fiber-fed spectrograph, producing spatially mixed light more similar to the spectra we can obtain from exoplanets. PEAS will obtain optical and infrared spectra and imaging of Solar System planets, which will then be analyzed using exoplanet modeling tools, in order to validate and test those tools. Here we describe the science goals and general system design of the PEAS instrument.

Science Goals:

Short term:

- Produce an atlas of Solar System planet spectra and images observed by PEAS to serve as comparison to ground-truth observations from space missions
- Measure atmospheric compositions and trace elemental abundances, compared to in situ or fly-by measurements of Solar System planets
- Produce 2D surface maps of Venus, Mars, Jupiter, Saturn, Uranus, Neptune
- Produce fiducial measurements that will be used to plan instruments for future exoplanet missions, such as HabEx/LUVOIR and TMT.

Long term:

- Time-series observations of Solar System planets to explore variability and weather patterns on planets
- Comparison to historical data (e.g. [4])
- Study planetary seismology (oscillation modes) of Solar System planets

PEAS Instrument Design Planetary light collected by the telescope will be split into a spectrograph system and an imaging system for simultaneous observations. Our innovative approach uses an integrating sphere to turn the spatially-resolved planet light into disk-integrated light before it is dispersed inside a fiber-fed spectrograph. The modular design allows for easy changes to the spectrograph and imaging systems as we iterate on the observational and analysis techniques. For example, we can swap out the beam splitter, fiber optic cable, spectrograph, and imaging camera, to optimize observations in different wavelength ranges and resolving powers. We will continuously modify the instrument to perform new experiments as we work to achieve a comprehensive understanding of the optimal observational and analysis combinations. Continuous feedback between the instrument configurations, observations, and theoretical interpretations will be critical for determining which combination of observations and theoretical interpretations produce accurate depictions of our Solar System planets.

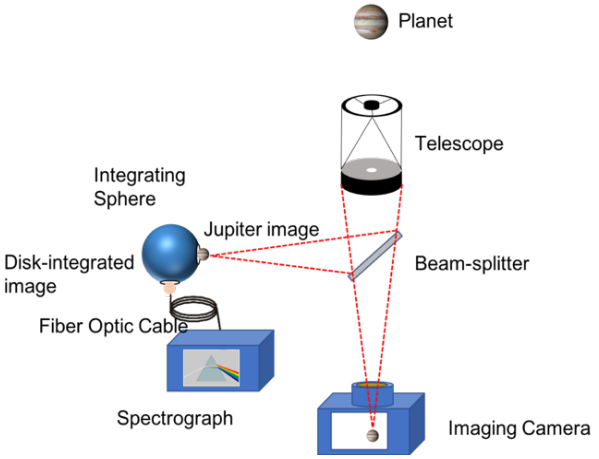

Figure 1. PEAS instrument layout

References: [1] N. B. Cowan, et al. (2009) *ApJ, 700,* 915–923. [2] L. C. Mayorga, et al. (2016) *AJ, 152*, 209–220. [3] T. Karalidi, et al. (2015) *ApJ, 814,* 65–82. [4] F. C. Gillett et al. (1969) *ApJ, 157,* 925–934.

REFLECTED LIGHT OBSERVATIONS OF THE GALILEAN SATELLITES FROM CASSINI: A TESTBED FOR COLD TERRESTRIAL EXOPLANETS. L. C. Mayorga[1], D. Charbonneau[1], and D. P. Thorngren[2,3], [1]Center for Astrophysics | Harvard & Smithsonian, Cambridge, MA, USA, [2]Department of Physics, University of California, Santa Cruz, CA, USA, [3]Exoplanet Research Institute (iREX), University of Montréal, QC, Canada. *Corresponding Author: laura.mayorga@cfa.harvard.edu*

Abstract: For terrestrial exoplanets with thin atmospheres or no atmospheres, the surface will contribute to the reflected light signal of the planet. Measurement of the variety of disk-integrated brightness of bodies in the Solar System, and the variation with illumination and wavelength, is essential for both planning imaging observations of directly imaged exoplanets and interpreting the eventual data sets. Here, we measure the change in brightness of the Galilean satellites as a function of planetocentric longitude, illumination phase angle, and wavelength. Despite the similarity in size and density between the moons, surface inhomogeneities result in significant changes in the disk-integrated reflectivity with planetocentric longitude and phase angle. We present the expected contrast ratios of these surfaces as if they had occurred on icy terrestrial Earth-sized exoplanets and discuss the implications on the necessary sensitivity of future direct-imaging missions.

Introduction: Direct imaging missions are presently the only technology with potential to characterize exo-Earths in the habitable zones of nearby solar-type stars in reflected light. However, it is unlikely that we will ever be able to resolve the disks of these planets to understand the underlying processes that shape their atmospheres and surfaces. Thus, the Solar System is the only place where we can understand the connections between unresolved local variations in reflectivity and color and the disk-integrated observations that we actually observe, as has been done for the gas giants and other solar system bodies with thick atmospheres [1–3].

For thin atmospheres to atmosphereless bodies, the surface is a critical component because of its potential to contribute to the reflected light observed [4–6]. For direct imaging missions, planets are most often observed only partially illuminated and it is critical to consider and benchmark the reflectivity of planets at partial phase geometries. Here, we use the Galilean satellites as a representative sample of surfaces possible on icy terrestrial exoplanets and observe them in the same manner that exoplanets will be studied in the future with reflected light.

Methods: While on route to Saturn, the *Cassini*/Imaging Science Subsystem (ISS) took tens of thousands of images of Jupiter during a flyby spanning from 2000 October to 2001 March. The field of view of the ISS cameras, the Wide and Narrow Angle Camera (WAC and NAC), were sufficiently large that the Galilean satellites often appear in images targeting Jupiter itself. After reducing the images with `Cisscalv3.9` [7] and identifying the moon locations with `SPICE` [8,9], we perform aperture photometry on roughly 5,000 images. The data span a range of wavelengths from 400–950 nm and predominantly phase angles from 0°–25°, with some constraining observations near 60°–140°. Although the data were taken in many filters, coverage is best in the six filters shown in ***Table 1***.

Table 1. Number of observations in a filter for a given moon and the filter's effective wavelength in nm.

Moon	Filter						Total
	VIO	BL1	GRN	RED	CB2	CB3	
	420	463[a]	568[a]	647	752	939	
Io	585	170	676	565	328	188	2363
Europa	622	105	668	599	343	130	2386
Ganymede	574	124	635	564	293	202	2283
Callisto	396	19	394	373	123	3	1276
						Number of WAC Images	3300
						Number of NAC images	329

[a]The NAC effective wavelengths differ slightly from the WAC.

We iteratively fit the orbital phase curves with a polynomial (starting with a simple 3rd order) and the rotation variations at low phase angles (14°–24°) with a simple orange slice model of `N` longitudinal slices using `PlanetSlicer` [10], a modified version of the phase function inversion mapping technique [11]. The rotational variations are then removed from the orbital phase curve at phase angles smaller than 25° and the process is repeated. In this way, we are able to disentangle illumination variations from rotational variations.

Results: All of the Galilean satellites readily display rotational modulations. A simple Lomb-Scargle Periodogram readily reproduces the rotation periods of all of the satellites except Callisto, whose variations are of order the scatter in the data while also poorly sampling all longitudes. The amplitudes of the rotational variations at low phase angles range from roughly 5%–40%, where Europa exhibits the largest variations in the VIO filter. A rudimentary composite of the inverted orange slice maps is in agreement with broad features

present in the mosaics produced by the US Geological Survey with *Voyager* and *Galileo* data [12–15]. At high phase angles (90°–130°) the data coverage is poor for all of the moons, but the minimal data present for Io in GRN suggests that the morphology of the variations can be markedly different and a factor of 2 larger in amplitude.

The illumination variations of each moon show a steep fall off at low phase angles; this cuspy behavior is known as the *opposition effect* and has yet to be observed in an exoplanet. The moons are also much darker than would be predicted by the classical Lambertian model by 33%–55%, depending on the wavelength and the moon. The contrast curve in GRN of an Earth-sized version of each Galilean satellite with a potential rotational modulation is shown in ***Figure 2***.

At low phase angles, we are able to use the VIO, GRN, and RED filters to compute colors as in [1,16]. Io is demonstrably redder than the other three satellites, which is due to the volcanism present on its surface. Despite their similar colors, the other three satellites track different paths through color space, suggesting that color variations with illumination phase angle may be able to differentiate them in direct-imaging observations. The color variations with rotation are not significantly larger than the noise ellipses except in the case of Io, where the compositional variations in sulfur compounds and silicates vary across its surface [17].

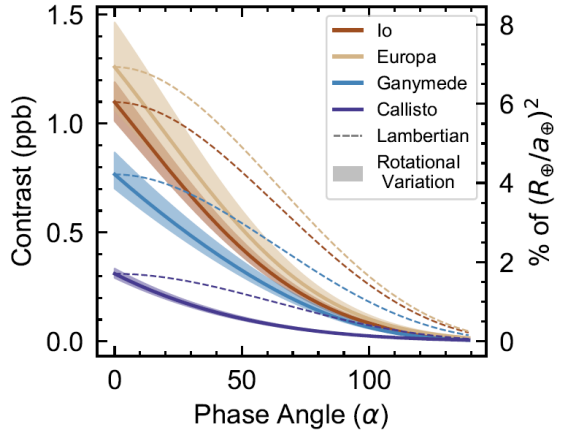

Figure 1. The contrast curve of Io (red), Europa (tan), Ganymede (blue), and Callisto (purple) as if they were 1 $R_\oplus$ around a Sun-like star at 1 AU as compared to the predictions of the Lambertian model (dashed). The rotational variations as measured at low phase angles are shown as a shaded region.

Conclusions: Since the Galilean satellites have little to no atmosphere, we have been able to isolate reflectivity variations as a function of illumination and rotation. If they had thick atmospheres and/or bright water clouds like Earth, such variations would be entangled with the temporal and spatial variations due to weather. It is important to consider the potential contamination into the reflected or emitted light signal of a terrestrial exoplanet by the surface. Should instrumentation be precise enough to isolate the reflected light from an exoplanet, our analysis of the varied surfaces of the Galilean satellites indicate that the planet's rotation period can be inferred from the surface compositional variations that cause the brightness and color variations over the course of the planet's rotation.

Future flagship missions, such as *LUVOIR* and *HabEx*, will be able to image warm and colder Earth-sized planets. Through long-term monitoring, rotational and orbital light curves can be interpreted to infer underlying surface and weather phenomena. We have demonstrated here that Earth-sized exoplanets with Galilean-like surfaces will require 10^{-10}–10^{-11} contrast ratios to detect and undergo variations of order 10^{-11}–10^{-12} with longitude. With sufficient precision, we can begin to characterize their surfaces and disentangle their atmospheres in reflected light observations.

Acknowledgments: The Cassini/ISS data was obtained from the Planetary Data System.

References: [1] Mayorga, L. C. et al. (2016) *AJ*, 152 (6), 209. [2] Dyudina, U. A. et al. (2005) *ApJ*, 618 (2), 973–986. [3] Dyudina, U. et al. (2016) *ApJ*, 822 (2), 76. [4] Cowan, N. B. et al. (2009) *ApJ*, 700 (2), 915–923. [5] Robinson, T. D. and Reinhard, C. T. (2018). [6] Fujii, Y. et al. (2010) *ApJ*, 715 (2), 866–880. [7] Knowles, B. (2016). [8] Acton, C. et al. (2018) *P&SS*, 150 (2017), 9–12. [9] Annex, A. (2017), 2017 (1986), 2. [10] Thorngren, D. P. (2019). [11] Cowan, N. B. and Agol, E. (2008) *ApJ*, 678 (2), L129–L132. [12] Williams, D. A. et al. (2011) *Icarus*, 214 (1), 91–112. [13] US Geological Survey (2002) *U.S. Geol. Surv. Geol. Investig. Ser.*, I–2757. [14] US Geological Survey (2003) *U.S. Geol. Surv. Geol. Investig. Ser.*, I– 2762. [15] US Geological Survey (2001) *U.S. Geol. Surv. Geol. Investig. Ser.*, I–2770. [16] Cahoy, K. L. et al. (2010) *ApJ*, 724 (1), 189–214. [17] Geissler, P. E. et al. (1999) *Icarus*, 140 (2), 265–282.

TIDAL HEATING: LESSONS FROM IO AND THE JOVIAN SYSTEM; RELEVANCE TO EXOPLANETS.

A.S. McEwen[1], K. de Kleer[2], R.S. Park[3], C.J. Bierson[4], A.G. Davies[3], D. DellaGiustina[1], A.I. Ermakov[3], J. Fuller[2], C. Hamilton[1], C. Harris[5], H. Hay[1], J. Keane[2], L. Kestay[6], K. Khurana[7], K. Kirby[8], V. Lainey[9], I. Matsuyama[3], K.E. Mandt[8], C. McCarthy[10], F. Nimmo[4], M. Panning[3], A. Pommier[11], J. Rathbun[12], G. Steinbrügge[13], D. Stevenson[2], V.C. Tsai[2], and E. Turtle[8], [1]University of Arizona, Tucson, AZ 85721; [2]California Institute of Technology, Pasadena, CA 91125; [3]Jet Propulsion Laboratory, California Institute of Technology, Pasadena, CA 91109; [4]University of California – Santa Cruz, Santa Cruz, CA 95064; [5]University of Michigan, Ann Arbor, MI 48109; [6]US Geological Survey, Flagstaff, AZ 86001; [7]University of California – Los Angeles, CA 90095; [8]Applied Physics Laboratory, Johns Hopkins University, Laurel, MD 20723; [9]IMCCE, F-75014 Paris, France; [10]Columbia University, Palisades, NY 10964; [11]University of California – San Diego, La Jolla, CA 92093; [12]Planetary Science Institute; [13]University of Texas at Austin, Austin, TX 78705.

Introduction: Tidal heating is a fundamental process in the evolution of many worlds across our Solar System and beyond. Tidal heating can produce magma oceans in rocky worlds, a key step in the evolution of Earth-like planets. Tidal dissipation can also control how and where energy is transferred between the icy and liquid-water regions of ocean worlds, directly impacting their habitability. This process also drives the orbital evolution of these bodies. Despite its broad ranging importance, there remain fundamental gaps in our understanding of tidal heating and coupled orbital evolution. To address this, the Keck Institute for Space Studies (KISS) workshop "Tidal Heating: Lessons from Io and the Jovian System" was held in late 2018 [1]. The objective of the workshop was to integrate recent advances in theory, laboratory studies, telescopic/spacecraft data, and instrumentation, to construct a path forward for understanding tidal heating and its influence on the evolution of planetary systems.

The Jovian system provides the greatest potential for advances in our understanding of tidal heating in the next few decades because of the 4:2:1 Laplace resonance of Io, Europa, and Ganymede; and because NASA's *Europa Clipper* and ESA's *Jupiter Icy Moons Explorer (JUICE)* missions will provide in-depth studies of Europa and Ganymede in the 2030s, and the Juno mission is studying Jupiter in depth.

Advances from the Saturnian System: Precise measurements of the Saturnian moon orbits, largely based on *Cassini* radio tracking during close encounters, have revealed outward migration rates much faster than expected [2]. Extrapolating this migration measurement backwards in time with a constant tidal dissipation parameter, Q, implies that the Saturnian moons formed recently, in far less time than the lifetime of the solar system. Alternatively, Fuller *et al.* [3] proposed a new theory for tidally excited systems, based on the idea that the internal structures of gas giant planets can evolve on timescales comparable to their ages, causing the frequencies of a planetary oscillation mode to gradually change. This evolution enables "resonance locking" in which a planetary oscillation mode stays nearly resonant with the forcing created by a moon's orbital period, producing outward migration of the moon that occurs over a timescale comparable to the age of the solar system. This model predicts similar migration timescales but different Q values for each moon, matching the Saturnian system, and can be tested by astrometry in the Jupiter system.

Relevance to Exoplanets: Tidal heating of exoplanets and their satellites significantly enlarges the total habitable volume in the galaxy. As exoplanets continue to be confirmed and characterized, researchers are increasingly studying tidal heating of exoplanets. For example, seven roughly Earth-sized planets orbit close to TRAPPIST-1, with periods of a few Earth days and with nonzero eccentricities. Barr *et al.* [4] concluded that two of these planets undergo sufficient tidal heating to support magma oceans and the other five could maintain water oceans.

Five Key Questions about Tidal Heating: The KISS report [1] identified five key questions about tidal heating to drive future research:

Q1: What do volcanic eruptions tell us about the interiors of tidally heated bodies? Active eruptions from tidally-heated worlds in our backyard include Io, Enceladus, and maybe Europa and Triton. Volcanism provides information about interiors that are otherwise inaccessible via remote sensing, as well as evidence that there is sufficient internal energy to melt the interior. When combined with laboratory experiments under controlled pressure and temperature, eruptive products can constrain temperature and pressure with depth.

Q2: How is tidal dissipation partitioned between solid and liquid materials? Tidal energy can be dissipated as heat in both the solid and liquid regions of a body. The dissipation response of planetary materials depends on their microstructural characteristics, such as grain size and melt distribution, as well as on the timescales of forcing. If forcing occurs at high frequency, planetary materials respond via instantaneous elastic deformation. If forcing occurs at very low frequency, in a quasi–steady state manner, materials respond with permanent viscous deformation. On timescales most relevant to tidal flexing

of planetary materials, the response is anelastic, with a time lag between an applied stress and the resulting deformation. Decades of experimental studies have rarely been designed for the type of forcing relevant to tidally heated worlds. For instance, it is not clear under what conditions tidal stress could alter existing grain sizes and/or melt distributions within the material being stressed.

For icy worlds, the three-dimensional distribution of tidal heating may impact the dynamical and chemical behavior of the ocean through the introduction of gradients in temperature and salinity. Ocean tide dissipation produces significantly different patterns of heat flow than that in the solid regions [5].

Q3: Does Io have a magma ocean that mechanically decouples the lithosphere from the deep interior? To understand Io's dynamics, such as where tidal heating occurs in the interior, we need to better understand its interior structure. Observations collected during close spacecraft flybys can determine whether Io has a magma ocean or another melt distribution. One means to study this is from magnetic measurements, similar to Galileo [6] but with better data on Io's plasma environment, flybys optimized to the best times and places for measuring variations in the magnetic field, and new laboratory measurements of electrical conductivities of relevant planetary materials. Measuring the composition of erupting lava provides an independent constraint on degree of mantle melting.

Another method to investigate Io's interior is with gravity science, in which the tidal Love numbers k_2 and h_2 express how a body's gravitational potential responds on a tidal timescale and its radial surface deformation, respectively. Each of these variables alone can confirm or reject the hypothesis of a liquid layer decoupled from the lithosphere because their values are roughly 5 times larger if Io possesses a magma ocean and detached lithosphere [7]. Libration amplitude provides an independent test for a detached lithosphere. If there is a continuous liquid layer within Io and the overlying lithosphere is rigid (as is thought to be needed to support tall mountains), libration amplitudes greater than 0.5 km are expected [8].

Q4: Is the Jupiter/Laplace System in equilibrium? Tidal heating in the Io–Europa–Ganymede system is exquisitely coupled and driven by the Laplace resonance. The resonance excites the moons' eccentricities, while tidal heating circularizes the orbits. In order to understand the evolution of any of the moons, we must investigate all of them. Two possible resonance scenarios have been proposed: one in which orbital eccentricity and total heat produced is constant and one with periodic variations in eccentricity and heat production. These questions can be answered by measuring how orbits are changing and measuring heat flow.

Q5: Can stable isotopes inform long-term evolution? We lack knowledge about the long-term evolution of tidally-heated systems, in part because their geologic activity destroys the older geologic record. Isotope ratios, which preserve long-term records of processes, provide a potential window into these histories. If processes lead to the preferential loss of certain isotopes, significant fractionation of a species may occur over the age of a satellite. However, to draw robust conclusions, we must understand the current and past processes that affect the fractionation of these species, as well as the primordial isotope ratios.

Avenues for Progress: The most promising avenues to address these questions include a new spacecraft mission making close flybys of Io [9], missions orbiting and landing on ocean worlds, technology developments to enable advanced techniques, closer coupling between laboratory experiments and tidal heating theory, and advances in Earth-based telescopic observations. An Io mission should: characterize volcanic processes to measure heat flow and lava compositions and temperatures (Q1); test interior models via a set of geophysical measurements coupled with laboratory experiments and theory (Q2 and Q3); measure the rate of Io's orbital migration (*i.e.,* to complement similar measurements expected at Europa and Ganymede) to measure the total energy production of the Jovian system (Q4); and measure stable isotopes and mass loss processes in Io's atmosphere and plumes (Q5). In the longer-term, seismology and interferometric synthetic aperture radar are promising avenues for future exploration, but require advanced power systems and lower mass for outer Solar System operations.

References: [1] de Kleer, K. et al. (2019), http://kiss.caltech.edu/final_reports/Tidal_Heating_final_report.pdf. [2] Lainey, V. et al. (2017) Icarus 281, 286. [3] Fuller, J. et al. (2016), *MNRAS 458*(4), 3,867. [4] Barr, A.C. et al. (2018) Astr.&Astophy. 613, A37. [5] Hay, H. and I. Matsuyama (2019) *Icarus*, 319, 68. [6] Khurana, K. et al., *Science*, 6034, 2011. [7] Bierson, C. J., and F. Nimmo (2016) JGR-Planets 121.11, 2211. [8] Van Hoolst, T. et al. (2018), Fall AGU abstract P51E-2929. [9] McEwen, A.S. et al (2019), 50th LPSC, #1316.

Acknowledgements: This work is supported by the W.M. Keck Institute for Space Studies and was carried out in part at the Jet Propulsion Laboratory, California Institute of Technology, under contract with NASA.

ATMOSPHERIC CHEMISTRY ON PRESENT-DAY VENUS AND EARTH: UNRESOLVED ISSUES AND IMPLICATIONS FOR EXTRASOLAR PLANETS. F. P. Mills[1,2,3], C. D. Parkinson[2], K. L. Jessup[4], Y. L. Yung[5], E. Marcq[6], and A. C. Vandaele[7], [1]Fenner School of Environment and Society, Australian National University, Canberra, ACT, Australia, [2]Space Science Institute, Boulder CO, USA, [3]McDonald Observatory, University of Texas Austin, Austin, TX, USA, [4]Southwest Research Institute, Boulder CO, USA, [5]Division of Geological and Planetary Sciences, California Institute of Technology, Pasadena, CA, USA, [6]Laboratoire Atmosphères, Milieux, Observations Spatiales, Université de Versailles, Guyancourt, France, [7]Royal Belgian Institute for Space Aeronomy. Brussels, Belgium.

Introduction: The major foci for studies to date of atmospheric chemistry on potential/actual terrestrial-like extrasolar planets has been identification of biosignatures and habitability assessment [e.g., 1-7]. While major portions of atmospheric composition parameter space remain unexplored, there is an extremely large degree of overlap between abiotic and biotic atmospheric signatures. Given this high degree of overlap, even if a portion of atmospheric composition parameter space is found that is uniquely biotic, then one must also determine whether that uniquely biotic portion of atmospheric composition parameter space is common to all habitable or inhabited planets.

Significantly less attention has been given to assessing the atmospheric chemistry implications of atmospheric composition observations on extrasolar planets. This is an area in which solar system studies can provide extremely valuable insight. For terrestrial-like exoplanets, the atmospheric chemistry on Earth and Venus is particularly relevant and important.

Venus' atmosphere is 96.5% CO_2 and 3.5% N_2 with trace abundances of SO_2, OCS, H_2O, HCl, HF, and HBr, as well as their photochemical and lightning-induced products. The global clouds are composed at least partly of concentrated sulfuric acid. The surface pressure is 90 bar and surface temperatures exceed 700 K. Atmospheric chemistry transitions from ion chemistry through photochemistry to thermal equilibrium chemistry with heterogeneous chemistry likely throughout the atmosphere.

Earth's atmosphere is 78% N2 and 21% O2 with trace abundances of SO_2, OCS, H_2O, HCl, HF, HBr, and N_2O, as well as their photochemical and lightning-induced products. Clouds are patchy and have compositions that vary from liquid and solid water in the troposphere to sulfur, hydrogen, and nitrogen ternary compounds in the stratosphere and mesosphere. Ion and photochemistry occur throughout the atmosphere, as does heterogeneous chemistry.

Current understanding of Venusian atmospheric chemistry: Three major chemical cycles have been identified: the carbon dioxide, sulfur oxidation, and polysulfur cycles [e.g., 8,9], Fig. 1. The carbon dioxide cycle includes CO_2 photolysis, transport of a significant fraction of CO and O to the night side, production of O_2, and conversion of CO and O_2 to CO_2, mostly via chlorine catalyzed pathways. The sulfur oxidation cycle comprises transport upward of OCS, SO_2, and H_2O, oxidation to H_2SO_4, condensation to form the global 30-km thick cloud layers, and sulfuric acid rain. The polysulfur cycle involves the upward transport of OCS and SO_2, disproportionation and production of S_x (x=2-8), and downward transport of S_x to react with CO and SO_3. There is solid evidence for the carbon dioxide and sulfur oxidation cycles; the polysulfur cycle is more speculative but plausible. Alternatively, sulfur chemistry on Venus has been conceptually divided into fast and slow atmospheric cycles and a geological cycle [e.g., 10-12]. Recent work suggests the ternary SO_2-H_2O-H_2SO_4 system may bifurcate depending on the relative abundances of H_2O and SO_2 [13].

Key outstanding issues in Venusian atmospheric chemistry: Despite this general understanding, five decades of spacecraft observations, and 200 years of Earth-based observations, numerous significant unresolved issues remain. One is the means by which CO_2 is stabilized over geologic time - models predict abundances a factor of 10 larger than the observational upper limit [e.g., 14,15]. Another is the lack of consistency among models of the chemistry and microphysics in different regions, especially in the cloud layers, where the mixing ratios of many important trace species change by orders of magnitude within several vertical scale heights, and at the surface [10]. A third is the mechanism(s) creating an inversion layer in SO_2 abundances in the mesosphere, Fig. 2 [16,17,18].

Earth atmospheric chemistry: Chemical cycles on Earth, as elsewhere, predominantly involve trace (radical) species whose abundances may be at the ppm to ppt level. The chemistry occurring in each portion of the Earth's atmosphere is strongly influenced by the energy of available photons and the reservoir species present.

The primary radical species are typically grouped into families based on the relatively short lifetimes for conversions between members of a family and rela-

tively long lifetimes for loss from a family: odd oxygen (O_x = $O(^3P)$ + $O(^1D)$ + O_3), odd hydrogen (HO_x = H + OH + HO_2), odd chlorine (Cl_x = Cl + ClO + HOCl and Cl_y = Cl_x + HCl + $ClONO_2$ = reactive chlorine), and odd nitrogen (NO_x = N + NO + NO_2 + NO_3 + 2 * N_2O_5 +HO_2NO_2 and NO_y = NO_x + HNO_3 + PAN + HONO + organic nitrates, etc, = reactive nitrogen), with similar definitions for SO_x, Br_x, Br_y, etc [19].

Species that are reasonably diagnostic of the importance of each of these families in the middle atmospheres on Earth and/or Venus, which are also potentially detectable on extrasolar terrestrial-like planets, are CO_2 or O_2, O_3, H_2O, HCl, N_2O, and SO_2. Adding DCl would provide a D/H measure that is less directly affected by condensation fractionation and variable cloud cover than HDO. In addition to their potential utility for extrasolar planetary atmosphere simulations, monitoring the abundances of most of these species on hemispheric spatial scales on Earth and Venus would be diagnostic of decadal scale atmospheric changes.

References: [1] Meadows V. S. et al. (2018) *AsBio 18*, 630. [2] Arney G. et al (2016) *AsBio 16*, 873. [3] Grenfell J. L. (2017) *Phys. Rep. 713*, 1. [4] Harman C. E. et al. (2018) *ApJ 866*, 56. [5] Tian F. (2015) *Earth Plan. Sci. Lett. 432*, 126. [6] Segura A. (2007) *A&A 472*, 665. [7] Domagal-Goldman S. D. et al. (2014) *ApJ 792*, 90. [8] Mills F. P. et al. (2007) *Exploring Venus as a Terrestrial Planet*, 73-100. [9] Yung Y. L. et al. (2009) *J. Geophys. Res., 114*, E00B34. [10] Marcq E. et al. (2018) *Space Sci, Rev. 214*, 10. [11] Krasnopolsky V. A. (2013) *Icarus, 225*, 570-580. [12] Krasnopolsky V. A. (2012) *Icarus, 218*, 230-246. [13] Parkinson C. D. (2015) *Planet. Space Sci., 113-114*, 226-236. [14] Mills and Allen (2007), *Planet. Space Sci.,55*, 1729-1740. [15] Krasnopolsky V. A. (2006) *Planet. Space Sci., 54*, 1352-1359. [16] Vandaele A. C. et al. (2017) *Icarus, 295*, 16-33. [17] Jessup K. L. et al. (2015) *Icarus, 258*, 309-336. [18] Mills F. P. et al. (2018) *VENERA-D Venus Modeling Workshop Oct 5-7 2017 Proceedings*, 59-62. [19] Brasseur G. and Solomon S. (1984) *Aeronomy of the Middle Atmosphere*, D. Reidel Publishing. [20] Mills F P. et al (2019) 50th LPSC Abst. 2374 (LPI Contrib. No. 2132).

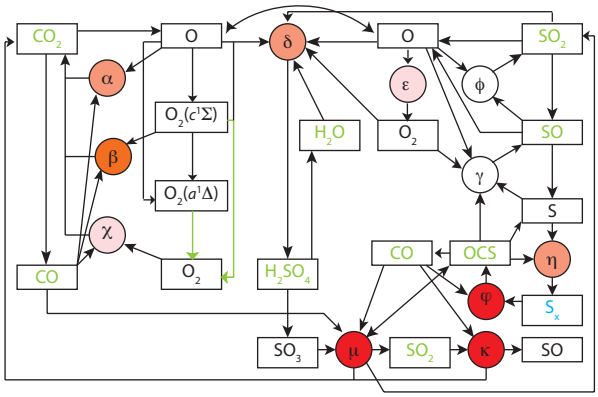

Fig. 1. Schematic diagram for the atmospheric chemistry on Venus. Catalytic schemes are indicated by the Greek letters in circles. The degree of laboratory confirmation is indicated by the lightness of the shade of red. The darkest red have received no confirmation. [16]

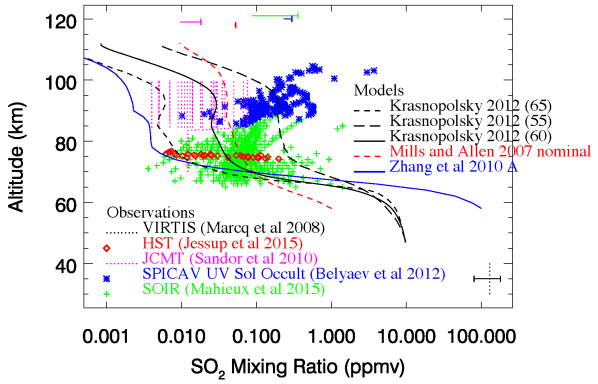

Fig. 2. Observed and modeled SO_2. Only models using standard chemistry are shown. [20]

Terrestrial Planetary Atmospheres and Climate Extremes: From Earth to Titan. J. L. Mitchell[1], [1]Atmospheric and Oceanic Sciences, Earth, Planetary & Space Sciences, UCLA.

Introduction: Venus, Earth and Mars appear to tell a compelling and complete story about the climate of terrestrial planets. Venus likely had a water ocean, but flying too close to the Sun, lost it all in a runaway greenhouse [1]. Earth somehow escaped the frigid doom of perpetual snowball when the Sun was young and dim [2]. Mars might have once had an ocean and thick atmosphere, but the climate atmosphere collapsed and/or was lost to space. Together, they provide fundamental insights into the nature of planetary habitability in the inner Solar System [3]. In the outer Solar System, however, Titan provides a counterpoint of a nearly-dry, "terraplanet" climate state with almost all of the condensable methane in vapor form, and thereby opens a new window into our understanding of the climates of terrestrial planets. In fact, Titan is much like a very warm version of Earth; condensable methane vapor is as abundant in supply as water would be if Earth's surface temperatures were considerably higher. But Titan is also very dry, with a limited supply of polar liquid reservoirs, and has very limited and sporadic cloud cover. From a comparative perspective, and given these novel features, what new insights do we gain about the climate of Earth when Titan is added to the Venus-Earth-Mars climate triptych?

Methods: We will summarize preliminary results from our numerical experiments with the primary goal to determine how an Earth-like climate with abundant surface liquids, relatively low amounts of water vapor, and partial cloud cover would transition to a Titan-like climate with limited liquids, more abundant water vapor and limited cloud cover. Our experiment has three, primary control parameters: 1) the rotation rate; 2) the saturation vapor pressure; and 3) the amount of water in the (assumed land) reservoir. Our prior work has focused solely on the effect of varying rotation rate, for instance on the position of a seasonal ITCZ [4], or the emergence of strong superrotation [5]. This program is a natural extension of these studies, but now makes use of a hierarchy of climate models from 1D and 3D radiative-convective equilibrium to GCM simulations of the climate, and adds two dimensions to the parameter space exploration (surface liquids and saturation vapor pressure). Although we expect a primary distinguishing factor between climate states to be the coverage, height, mass, etc. of clouds produced in the model, our preliminary results will focus on the circulation and convection changes accompanying changes in our control parameters rather than the clouds.

Bibliography:

[1] Ingersoll, Andrew P. "The runaway greenhouse: A history of water on Venus." *Journal of the atmospheric sciences* 26.6 (1969): 1191-1198.

[2] Wolf, E. T., and O. B. Toon. "The evolution of habitable climates under the brightening Sun." *Journal of Geophysical Research: Atmospheres* 120.12 (2015): 5775-5794.

[3] Kasting, James F., Daniel P. Whitmire, and Ray T. Reynolds. "Habitable zones around main sequence stars." *Icarus* 101.1 (1993): 108-128.

[4] Faulk, Sean, Jonathan Mitchell, and Simona Bordoni. "Effects of rotation rate and seasonal forcing on the ITCZ extent in planetary atmospheres." *Journal of the Atmospheric Sciences* 74.3 (2017): 665-678.

[5] Mitchell, Jonathan L., and Geoffrey K. Vallis. "The transition to superrotation in terrestrial atmospheres." *Journal of Geophysical Research: Planets* 115.E12 (2010).

Chemistry of Laboratory Exoplanet Hazes. S. E. Moran[1], S. M. Hörst[1], V. Vuitton[2], C. He[1], N. K. Lewis[3], N. Bishop[4], L. Flandinet[2], J. I. Moses[5], F.-R. Orthous-Daunay[2], J. Sebree[4], and C. Wolters[2], [1]Department of Earth and Planetary Sciences, Johns Hopkins University, 3400 N. Charles St, Baltimore, MD 21218 (smoran14@jhu.edu); [2]Institute of Planetology and Astrophysics Grenoble, Université Grenoble Alps, Grenoble, FR; [3]Department of Astronomy and Carl Sagan Institute, 122 Sciences Drive, Ithaca, NY 14853; [4]Department of Chemistry and Biochemistry, University of Northern Iowa, IA; [5]Space Science Institute, Boulder, CO 80301

Introduction:

Hazes, solid particles resulting from photochemistry, are found in all planetary atmospheres across the solar system; evidence exists that they contribute significantly to the observed spectra of transiting exoplanets as well [1, 2]. Little is known about the chemistries or optical properties of such exoplanet hazes, posing a challenge for observers and modelers to properly interpret data from current facilities such as the Hubble Space Telescope or future observatories such as the James Webb Space Telescope, Wide Field Infrared Survey Telescope, and the next generation of both space- and ground-based telescopes. Moreover, laboratory haze studies of solar system atmospheres, namely that of Titan, have shown incredible chemical complexity – even the suggestion that Titan's atmosphere is capable of considerable prebiotic chemistry, possibly generating amino acids and nucleotide bases [3].

Hazes made in the laboratory can provide critical inputs for exoplanet atmospheric chemistry and the resulting impacts on observations. Conditions in exoplanet atmospheres range dramatically in temperature, stellar radiation, and bulk atmospheric composition, so a wide range of haze outcomes is possible. The possible haze scenarios will require dedicated laboratory investigation to understand, particularly regarding exoplanets for which there is no solar system analogue such as super-Earths and mini-Neptunes.

Methods:

PHAZER production of exoplanet hazes

With the Planetary HAZE Research chamber at Johns Hopkins University, we simulated nine distinct exoplanet atmospheres relevant to super-Earth and mini-Neptunes under two energy inputs, an AC plasma discharge and a UV photon lamp. We performed experiments at three temperatures (300 K, 400 K, and 600 K) and under three compositional regimes (100x/hydrogen-rich, 1000x/water-rich, and 10000x/carbon dioxide-rich). All experiments generated measurable solid particles [4] and showed variance in color [5], particle size [6], and gas phase chemistry [7].

Orbitrap™ Mass Spectrometry of exoplanet hazes

The resulting solid particles from the PHAZER chamber were subjected to very high resolution Orbitrap™ mass spectrometry. We measured the solubility of the particles in various solvents, the concentrations of C, H, N, and O in the hazes in both positive and negative ion modes up to 1000 amu, and the presence of specific molecules of prebiotic interest.

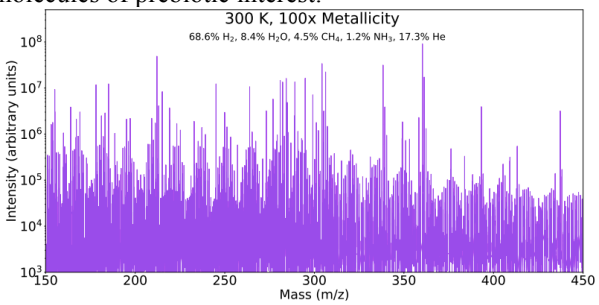

Fig. 1. Mass spectrum of the 300 K, hydrogen-rich haze particles.

Results and Discussion:

Solubility of exoplanet hazes

The laboratory-produced exoplanet hazes displayed a wide range of solubility behavior when tested in methanol (CH_3OH, polar), toluene (C_7H_8, non-polar), dichloromethane (CH_2Cl_2, polar), and hexane (C_6H_{14}, non-polar). All were at least somewhat soluble in polar solvents, suggesting that such hazes might act as good cloud condensation nuclei in worlds with condensable species in their atmospheres that are also polar (such as water). The most readily soluble hazes were all produced from the water-rich starting gas compositions. Notably, the only soluble hydrogen-rich solid was also the only 100x mixture to contain a nitrogen-bearing molecule (in the form of NH_3).

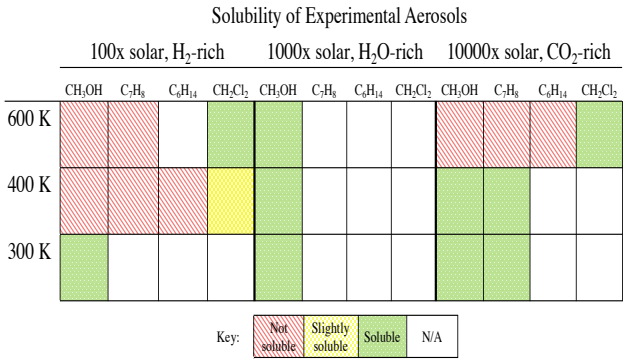

Fig 2.The solubility behavior of each haze analogue, showing that all exoplanet hazes were at least slightly soluble in polar solvents.

Prebiotic molecular formulae in exoplanet hazes

In the exoplanet hazes from the laboratory which were significantly soluble (i.e., they are marked as a green box in Fig. 2), further analysis was performed on the resulting mass spectra. For each set of samples, a wide variety of molecular formulae were detected. Potential identifications include those with prebiotic connotations, such as simple sugars, amino acids, and nucleobases.

Molecular detections from Orbitrap mass spectra alone are highly degenerate, and confirmation of any prebiotic molecules will require further follow-up analyses, such as High Performance Liquid Chromatography (HPLC). However, gas phase results of these same experimental atmospheres [7] show gas phase products consistent with known chemical pathways that produce both the simple sugar molecules observed as well as higher order organics, like amino acids.

Bulk chemistry of exoplanet hazes

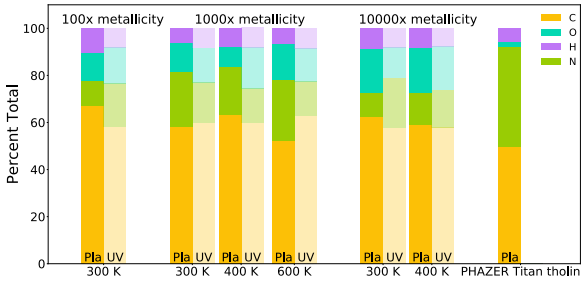

Fig. 3. Bulk composition of exoplanet haze analogues. Comparison to PHAZER lab Titan tholin is provided as a point of comparison.

All the exoplanet hazes produced in the PHAZER chamber showed significant oxygen incorporation in the solid products, especially in contrast to hazes from PHAZER Titan experiments (see Fig 3). However, the oxygen present in the solid sample is not merely a direct reflection of the bulk oxygen content in the starting gas mixtures. The most oxygen-rich solid sample from the 1000x starting gas mixtures actually came from the least oxygen-rich gas mixture (the 600 K). This 600 K/1000x sample notably was the only one of the 1000x condition to have carbon monoxide (CO) in the starting gas mixture, suggesting that a) the molecular carrier of the atoms in play matters for the subsequent chemistry and b) we replicate results showing CO increases oxygen incorporation into solid particles resulting from photochemistry [8]. The hydrogen concentration in the haze samples, on the other hand, does seem to more directly correspond to the amount of hydrogen present in the starting gas mixtures.

Additionally, the two types of energy source (either UV or AC plasma) used to initiate photochemical-like reactions produced hazes with similar bulk compositions within experimental error. Differences in composition may result from the lower energy density of the UV lamp as compared to the plasma, following previous measurements of both exoplanet and Titan-like hazes [7, 9]. The effect of the type of radiation (as, for example, a proxy for different stellar type host stars) requires careful follow-up to fully understand and extrapolate to other worlds and the stars around which they orbit.

References:

[1] Marley, M. S. et al. (2013) *in Comparative Climatology of Terrestrial Planets, University of Arizona Press,* 367. [2] Sing, D. K. et al. (2016) *Nature 529,* 7594. [3] Hörst et al. (2012) *Astrobiology 9,* 809. [4] Hörst et al. (2018) *Nature Astronomy 2*, 303. [5] He et al. (2018) *ApJL 856 (1)*, L3. [6] He et al. (2018) *AJ 156 (1)*, 38. [7] He et al. (2019) *ACS Earth and Space Chemistry 3 (1),* 39. [8]. Hörst and Tolbert (2014) *ApJ 781 (1)*, 5. [9]. Sebree et al. (2018) *ApJ 865 (2)*, 133.

Exoplanet Atmospheric Chemistry and Composition: Some Lessons Learned from Solar-System Giant Planets.
Julianne I. Moses, Space Science Institute, Boulder, CO (jmoses@spacescience.org).

Introduction: Exoplanet observations to date reveal an amazing diversity of planetary sizes, bulk densities, and orbital properties [e.g., 1-4], far beyond what occurs in our own solar system. Exoplanet atmospheres are expected to be equally diverse. However, the same chemical and physical principles that govern the behavior of the planetary atmospheres in our own solar system also operate in exoplanet atmospheres, albeit under potentially different environmental conditions. Theoretical models designed for solar-system planets can therefore help predict atmospheric properties on exoplanets, and lessons learned from a half century of *in situ* and Earth-based observations of solar-system planetary atmospheres can help guide our interpretation of exoplanet observations. Here, I describe some key lessons garnered from studies of Jupiter, Saturn, Uranus, and Neptune that are applicable to exoplanets.

Lesson 1: Condensation at depth removes elements from observable regions of the atmosphere. The sequestering of elements deep within an atmosphere means that determinations of the bulk elemental composition of an exoplanet atmosphere from spectral observations could be difficult, depending on the planet's thermal structure, atmospheric thickness, and relative abundance of different elements. For example, on our solar-system giant planets, metals and silicates condense deep in the troposphere and are not seen in atmospheric spectra. Even water condenses on our giant planets, complicating the determination of the planetary bulk oxygen abundance, and obstructing the clues to planet-formation mechanisms that this information could provide. Water is not expected to condense on hotter, close-in, transiting giant exoplanets, but some oxygen and other elements can still be tied up in refractory condensates at depth.

Lesson 2: Atmospheric photochemistry is complex. Despite the great distance of our giant planets from the Sun, photochemistry operates efficiently, producing a host of disequilibrium products [e.g., 5]. Photochemistry is also expected to operate in exoplanet atmospheres, removing some expected equilibrium atmospheric constituents and producing new, unexpected disequilibrium ones.

Lesson 3: Photochemistry produces hazes on giant planets (but not as efficiently as on Titan): The photolysis of methane in giant-planet upper atmospheres leads to the production of heavy organics, some of which can condense to form hazes, affecting the spectrum at visible and ultraviolet wavelengths. The relative efficiency of haze production depends on the atmospheric composition; the thermal structure; the type, spectrum, and flux of the dissociating energy source (e.g., UV, energetic electrons, protons); and the mean molecular mass of the background atmosphere compared with the main photochemical "parent" species.

Lesson 4: Photochemical products affect the planetary spectrum. On our giant planets, spectral features from hydrocarbon photochemical products dominate mid-infrared spectra, and photochemically produced gases and hazes affect UV spectra. Theoretical models of disequilibrium exoplanet chemistry will be needed to accurately predict and interpret atmospheric spectra from exoplanets.

Lesson 5: Photochemical products affect the atmospheric thermal structure. Gas-phase photochemical products such as C_2H_2, C_2H_6, and H_3^+ control the cooling rates in our giant-planet middle atmospheres and thermospheres, and aerosols can contribute to heating. Disequilibrium chemical products might also influence the thermal structure of exoplanet atmospheres.

Lesson 6: Giant planets have warm stratospheres (and sometimes we're not sure why). Stratospheric heating on our giant planets predominantly derives from absorption of solar radiation in near-IR bands of CH_4. Jupiter and Saturn seem reasonably close to radiative equilibrium in models that consider heating in the near-IR bands of methane plus shorter-wavelength aerosol absorption, and cooling from H_2-H_2 and H_2-He continuum, CH_4, C_2H_2, C_2H_6 [6-8], but such models do not work well for Uranus and Neptune. Are the models missing a heat source, such as gravity-wave breaking? Something else? The observed aerosols are not optically thick enough, large enough, or dark enough to explain the discrepancy. If this unknown process also occurs on exoplanets, stratospheric thermal inversions may also be present, affecting IR transit and eclipse spectra.

Lesson 7: Giant planets have hot thermospheres (and we don't understand why). We still do not understand the mechanism(s) responsible for the high-temperature thermospheres on our giant planets. The same process(es) could be operating in exoplanet thermospheres. Even when stellar heating alone is considered, close-in transiting giant exoplanets should have very hot thermospheres, with H and H^+ rather than H_2 dominating, with important implications for atmospheric escape and short-wavelength observations. Any close-in terrestrial exoplanet that contains abundant hydrogen-containing species such as H_2O would also have a very hot H-dominated thermosphere.

Lesson 8: Giant planets have magnetic fields and aurora. The influx of solar and magnetospheric energetic particles affects atmospheric chemistry, temperatures, spectra, and haze formation on our giant planets. It is still not clear how global these consequences are on our giant planets, as opposed to being constrained to high latitudes. Do tidally locked giant exoplanets have dynamos and magnetic fields? If so, are there observational consequences?

Lesson 9: Ion chemistry matters. As on Titan, ion chemistry on the giant planets is important for the production of heavy hydrocarbons and refractory photochemical hazes. For example, the C_6H_6 distribution on Saturn suggests that both solar EUV-driven ion chemistry and auroral chemistry are critical to benzene formation [9]. Ion chemistry is often ignored in exoplanet atmospheric chemical modeling. It shouldn't be.

Lesson 10. Seasonally dependent chemistry matters. The stratospheric composition of Saturn and Neptune, at least, changes significantly with season due to variable photochemistry [10,11]. If an exoplanet has an axial tilt or an eccentric orbit, the time-dependent seasonal forcing could affect atmospheric temperatures and chemistry. As with our giant planets, significant phase lags might exist at higher pressures (lower altitudes).

Lesson 11. Atmospheric circulation matters. Spatially resolved observations of hydrocarbon meridional distributions on our giant planets are often at odds with photochemical model predictions [10,12-13]. Combined with temperature retrievals, circulation patterns can be inferred from the model-data mismatch. Atmospheric circulation on exoplanets will also affect the 3D thermal structure and global distribution of atmospheric constituents, affecting spectral observations.

Lesson 12: Wave activity and vertical mixing (eddy K_{zz}) matters. The strength of atmospheric mixing has a strong influence on the chemical composition of our giant planets. The pressure at which methane is photolyzed affects the C_2H_6/C_2H_2 ratio and other aspects of the hydrocarbon chemistry, as well as the overall column abundance of products. Strong mixing = more abundant products and strong spectral features; weak mixing = less abundant products, weaker spectral features (e.g., Neptune versus Uranus). Wave mixing matters more than incident solar flux, methane abundance, or any other single factor. Unfortunately, it is difficult to predict K_{zz} from first principles [e.g., 14]. Wave activity and "mixing" will also be important for the distribution of species on extrasolar giant planets.

Lesson 13. Transport-induced quenching of disequilibrium atmospheric constituents matters. Species that are more abundant in thermochemical equilibrium at high pressures and temperatures at depth in an atmosphere can be dragged up into cooler high-altitude regions if the transport is faster than chemical interconversion [e.g.,15-17]. This "quenching" process explains the presence of CO and PH_3 in Jupiter's troposphere, for example. Transport-induced quenching may be extremely important on exoplanets, especially those with thick, deep, atmospheres whose thermal structure lies near a boundary between different dominant forms of an element. Horizontal quenching is also possible due to strong zonal or meridional winds [e.g., 18].

Lesson 14. Atmospheric composition is affected by external material. External influx of material from interplanetary dust, cometary impacts, & ring/satellite debris brings in elements to the observable portions of giant-planet atmospheres that would not otherwise be present there [e.g., 19]. Close-in transiting exoplanets will be affected by gravitational focusing of external debris by their central star, potentially leading to a high influx rate. The degree to which external material could affect the observable atmospheric composition of exoplanets is unclear and has not been explored to date.

Conclusions. Many processes that affect the composition and structure of our solar-system giant planets are also expected to operate on extrasolar planets. These processes should be considered when making predictions about spectral behavior or interpreting observations from exoplanets.

Acknowledgments: Support from the NASA Solar System Workings program is gratefully acknowledged. The content in this abstract was motivated by my talk from the ISSI workshop "Understanding the Diversity of Planetary Atmospheres," November 2018, Bern, Switzerland.

References: [1] Borucki, W. J. et al. (2011), *ApJ, 728*, 117. [2] Marcy, G. W. et al. (2014), *ApJS, 210*, 20. [3] Neil, A. R. & Rogers, L. A. (2019), arXiv:1911.03582. [4] Jontoff-Hutter, D. (2019), *Ann. Rev. Earth Planet. Sci., 47*, 141. [5] Moses, J. I. et al. (2005), *JGR, 110*, E08001. [6] Yelle, R. V. et al. (2001), *Icarus, 152*, 331. [7] Zhang, X. et al. (2013), *PSS, 88*, 3. [8] Guerlet, S. et al. (2014), *Icarus, 248*, 110. [9] Koskinen, T. et al. (2016), *GRL, 43*, 7895. [10] Fletcher, L. N. et al. (2017), in *Saturn in the 21st Century* (K. Baines, F. M. Flasar, N. Krupp, T. Stallard, eds.), Cambridge. [11] Moses, J. I. et al. (2018), *Icarus, 307*, 124. [12] Moses, J. I. & Greathouse, T. K. (2005), *JGR, 110*, E09007. [13] Guerlet, S. et al. (2010), *Icarus, 209*, 682. [14] Zhang, X. & Showman, A. P. (2018a,b), *ApJ, 866*, 1, & *ApJ, 866*, 2. [15] Prinn, R. G. & Barshay, S. S. (1977), *Science, 198*, 1031. [16] Lodders, K. & Fegley, B., Jr., Icarus, 155, 393. [17] Visscher, C. & Moses, J. I. (2011), ApJ, 738, 72. [18] Agundez, M. et al. (2014), A&A 564, A73. [19] Moses, J. I. & Poppe, A. R. (2017), *Icarus, 297*, 33.

LEARNING A PLANET'S DEEP INTERIOR SECRETS FROM ITS EXTERNAL GRAVITY FIELD: A NEW APPROACH FOR EMPIRICAL PLANET MODELING. N. Movshovitz[1], J. J. Fortney1, C. Mankovich[1], D. Thorngren[1], and R. Helled[2] [1]University of California, Santa Cruz, [2]University of Zurich, Switzerland.

Introduction: One piece of information that is available for many solar system bodies, but is as yet outside the realm of possibility for exoplanets, is an approximate description of their gravity fields. This requires a visit by spacecraft; an orbiter is best but even a single fly by will provide valuable data. Gravity data is so valuable because it is one of very few ways we have of probing the deep interior of a planet, in principle through to the center. If our solar system giant planets are used as proxies for understanding giant exoplanets, it is essential to understand the interior structure of these planets in as much detail as possible, as well as limits to our ability to interpret these interior structures.

But gravity data is not only hard won but also difficult to interpret. There are two problems. The first is that connecting the interior structure to the gravity data is a forward-modeling task: an interior model is created first, and then its gravity is computed and compared with the observed field. Inevitably, this introduces model specific assumptions that will limit, often quite severely, the robustness of the results. Many published studies of Jupiter and Saturn interiors for example are based on models with three compositionally homogenous layers and an adiabatic thermal profile. These are good models, but they are only a subset of possible interior structures.

The second problem is that the gravity field is a non-unique feature of the interior mass distribution. In other words, a continuum of interior structures are consistent with a measured gravity field, particularly given the finite precision to which the gravity is known.

How can we best remove this degeneracy and narrow down the range of possible planetary structures implied by a measured gravity field? Can we at the same time satisfy a competing preference for generality? Here we present preliminary findings from a theoretical attempt to answer this question, focusing on Saturn and on the solar system's ice giants, Neptune and Uranus.

We use Saturn to demonstrate how empirical models, interior density profiles created without reference to an assumed composition and thermal state, allow exploration of a much wider range of possible interior structures, using the gravity data obtained during Cassini's Grand Finale orbits [1].

We then use toy models of Uranus and Neptune constructed in a Markov-Chain Monte Carlo process that ensures we explore all structures, and only such structures, that are consistent with an arbitrarily precisely given gravity. By varying that precision level we can determine how much our knowledge of a planet can improve with improved gravity data.

Composition agnostic models of Saturn's interior: Traditionally, studies of Saturn's interior begin by assuming some realistic but necessarily simple structure defined by a small number of physical variables, and then proceed to tune these parameters to match the model to Saturn's observed properties, namely its mass, equatorial radius, and gravitational potential field represented by the coefficients of its expansion in Legendre functions. A common model is one of the planet comprising three layers, an upper envelope, a lower envelope, and a core, with homogeneous composition and adiabatic thermal gradient inside each layer. It's a potentially physically sound model, and allows derivation of tight constraints on things like the heavy element abundance in the planet, but the host of a priori ad hoc assumptions that go into the model limit the strength of such inferences.

Here we present constraints on Saturn's interior derived by setting the planet's gravity field as a likelihood function driving a Markov-chain Monte Carlo sampling of the space of so called *empirical* models. These are models where the interior density profile is explicitly varied, rather then derive from an assumed composition, thermal state, and material equations of state as in traditional models. Constraints on interior structure derived in this way framework are necessarily less informative, but are also less biased and more general.

Figure 1 below shows a sample from the posterior distribution of these empirical models, obtained by MCMC. We find that the outer half of Saturn's radius is relatively well constrained and the density suggests a significant metal enrichment, in line with atmospheric abundances from remote sensing [2]. As expected, the inner half of the planet's radius is less well-constrained by gravity, but we generally find solutions that include a significant density enhancement, which can be interpreted as a core, although this core is often lower in density and larger in radial extent than typically found by standard models. This is consistent with a dilute core and/or composition gradients [3-4].

Limitations of gravity as interior probe: Whichever model we use for the interior structure, a comparison with gravity data yields a range of solutions, rather than a single answer. There are two reasons. First,

gravity data, like all observational data, is of finite precision. Second, the external gravity field is an integrated quantity. Even when measured with extreme precision it may not uniquely define the density structure.

Gravitational potential coefficients are available for Uranus and Neptune, but with much larger error bars than those for Saturn and Jupiter. We can only set very loose constraints on their interior density based on these. Instead we derive increasingly narrower distributions of interior models by using the sampling of empirical models approach, as for Saturn, but with very simple models and by artificially increasing the assumed precision of the known gravity field. We thus determine the accuracy required of hypothetical future measurements, such as from a 2030s/2040s space mission to visit one or both of the ice giants.

References: [1] Iess, L., Militzer, B., Kaspi, Y., Nicholson, P., Durante, D., Racioppa, P., … Zannoni, M. (2019) Science, 2965. [2] Atreya, S. K., Crida, A., Guillot, T., Lunine, J. I., Madhusudhan, N., & Mousis, O. (2016) ArXiv E-Prints 1606.04510. [3] Helled, R., & Stevenson, D. J. (2017), The Astrophysical Journal Letters, 840(1), L4. [4] Leconte, J., & Chabrier, G. (2012), Astronomy & Astrophysics, 20, 1–13. [5] Mankovich, C., Marley, M. S., Fortney, J. J., & Movshovitz, N. (2019), The Astrophysical Journal, 871(1).

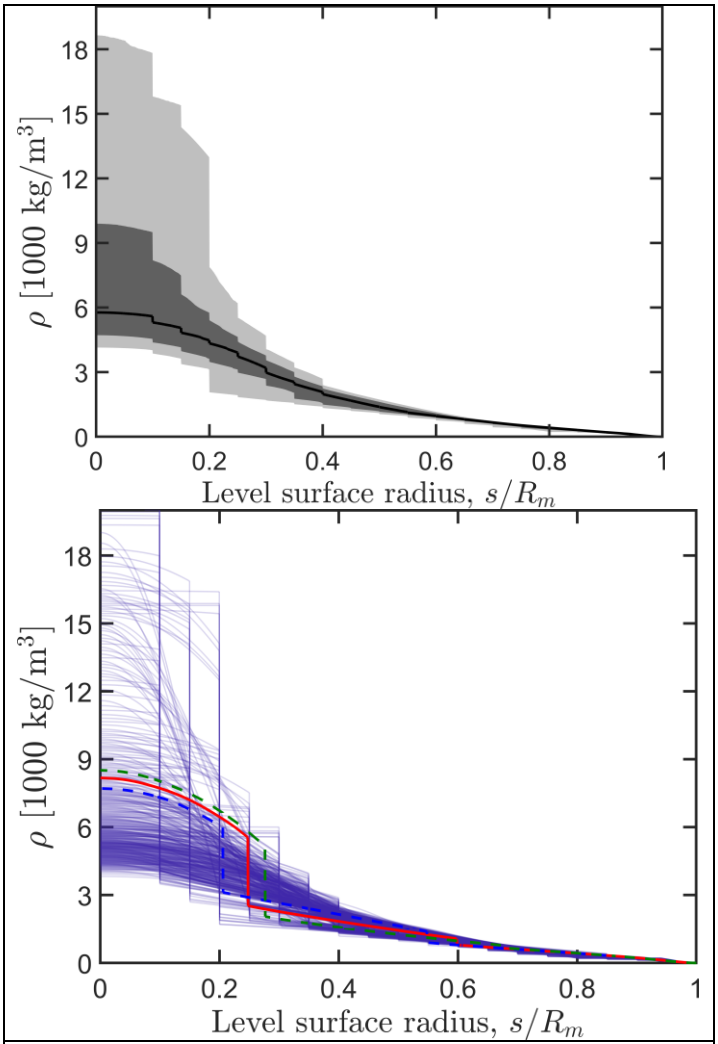

Figure 1. Visualization of the posterior probability distribution of Saturn interior density profiles. Top: The thick black line is the sample-median of density on each level surface. The dark gray shaded region includes values between the 16th and 84th percentiles of the sample and the light gray shaded region includes all values between the 2nd and 98th percentiles. Bottom: Several hundred profiles covering the sampled range. By nature of the MCMC algorithm regions of the figure where lines are closer together correspond to high likelihood areas of parameter space. For comparison, three profiles derived by physical models with a pure H2O core [5] are overlaid.

TESTING ACCRETION MODELS AGAINST THE "PEAS IN A POD" OBSERVATION OF EXOPLANETS. J. L. Noviello[1], S. J. Desch[1], A. P. Jackson[1]. [1]School of Earth and Space Exploration, Arizona State University, Tempe, AZ, USA, 85287. Jessica.Noviello@ASU.edu.

Introduction: Exoplanets have been found in myriad sizes and periodicities orbiting hundreds of stars, but there is evidence that these characteristics are well-ordered within exoplanet systems. Weiss et al. [1] found strong evidence in the California-*Kepler* Survey (CKS) dataset that the planets within each multi-planet system are relatively equal in size and orbital spacing, a finding they call the "peas in a pod" model [1]. A series of bootstrap analyses that created and analyzed synthetic radius and period ratios of randomly selected planets did not recover the observed correlations between masses or periods of neighboring planets. They interpreted this result to support *in situ* formation of planets via runaway growth, specifically that the multi-planet systems in the CKS dataset have masses that reflect densities in the disk, and are not attributable to stochastic growth by hierarchical accretion; and that the period spacings reflect formation conditions in the disk, and have not been affected by significant differential migration or orbital scattering [1].

These conclusions, that the masses and periods of CKS planets reflect formation in the disk, appears more consistent with growth by pebble accretion than hierarchical growth. Traditional models [2,3,7] assume growth by pairwise collisions between small bodies. Due to the stochastic nature of hierarchical growth, no strong correlations are expected between masses or orbital spacings of neighboring planets. In pebble accretion models [4-5], planetesimals grow to planet-sizes within a few Myr, thanks to a combination of gravitational focusing and aerodynamic drag of small (< meter-sized) particles accreted directly from the disk. As planets accrete directly from the disk in pebble accretion models, it is hypothesized that they would yield the best match to the peas-in-a-pod observation [1].

We test various formation models to see if they reproduce the peas-in-a-pod pattern. Recovering the patterns detailed in [1] could help validate or rule out formation models and motivate future work in a particular direction. As a baseline before including pebble accretion, we first consider the case of purely hierarchical growth.

Data and Methods: We examine a set of 60 N-body simulations run with the Mercury N-body code [6]. All simulations begin initially with 15 embryos of 0.15 Earth mass and 150 planetesimals of 0.015 Earth mass for a total of 4.5 Earth masses of material initially. The embryos and planetesimals are distributed between 0.4 and 4 AU from a 1 solar mass star. In addition a Jupiter-mass planet is placed at 5.2 AU. The simulations were run for 100 Myr. In half of the simulations the bodies are spaced evenly while in the other half the semi-major axis is chosen randomly. We find no difference between the two sets of initial conditions. Note that while these initial conditions are known not to perfectly reproduce the Solar system (producing a Mars analogue that is significantly too large) the goal here is not to reproduce the Solar system but to produce a roughly analogous system of terrestrial planets.

Each of the 60 iterations of the N-body simulation produced at least two planets in addition to the Jupiter-mass planet, which we did not include in subsequent analyses. In total the simulations produced 199 planets which translated into 139 pairs of planets.

Comparative calculations: The output of these 60 iterations included the orbital semi-major axes of these planets and the masses of these planets in units of solar mass. The masses were converted into Earth masses, which were then used to calculate approximate planet radius using three different parameterizations [8, 9]. This enables direct comparison to the observations in [1]. We note that the CKS survey is reasonably complete down to radii of 0.4 Earth radii. We then graphed different attributes of planet pairs, where the inner planet is P_1 and the outer planet in the pair is P_2 and continued until no more planets in the system remained. For each iteration with M planets, $M–1$ planet pairs were calculated.

Next, we performed linear regressions on the following planet attributes: 1) The mass of P_1 against the mass of P_2; 2) The period ratios of P_3/P_2 against P_2/P_1; 3) The log vs. log of the mass ratios P_3/P_2 and P_2/P_1; and 4) The log vs. log of the period ratios P_3/P_2 and P_2/P_1. Here planet 1 could be any of M-2 planets, and planets 2 and 3 are the next two planets farther out. In items 3 and 4, the linear slope is interpreted as an exponent in a power law equation.

Finally, we report the full equation of the linear model and the goodness-of-fit of the linear model to the data as r_2. We also include a p-value of the Pearson r_2 coefficient, with a significance level of $\alpha = 0.05$.

Results: In all graphs produced from the simulations, we did not recover evidence of the "peas in pod" model reported in [1]. If the model planets followed the equally-sized and equally-spaced pattern,

then they would have a linear slope of around 1 in all graphs and a high r^2. None of the graphs revealed a statistically significant correlation and had slopes significantly different from 1. Figures 1 and 2 show two of the graphs produced using the data from the Mercury code. The boundaries shown in Fig. 1 are artificial and created by the predetermined minimum size of the planetary embryos of the simulation (0.15 Earth masses), and the radius calculation was taken from [8].

Discussion: The model presented here shows insufficient agreement with the observations of [1]. There is not a strong tendency for adjacent planets to have similar masses. This suggests that stochastic accretion does not dominate planet growth in the CKS samples, but this work is very preliminary. To fully test the model we must consider the observational selection effects, including the efficiency with which embryos of various radii are detected at different orbital distances, and whether multiple planets in a system can be simultaneously detected in a transit survey, by comparing their mutual inclinations. A more careful analysis would consider only the most easily observed planets in each simulation. We will present these more carefully constructed analyses at the meeting.

We find comparisons between the peas-in-a-pod findings and the predicted planet mass and period ratios to be a useful measure of the success of a planet formation model. Our preliminary results point the way to comparisons between pure N-body models and models incorporating pebble accretion, that will allow us to assess the relative contributions of these modes.

Future work: We will consider the planetesimal data from multiple sources that form planets under different accretion conditions. We will put the data through a data reduction pipeline as close to identical as the one used in [1] to analyze the CKS data. We will determine which model produces planets with the closest similarities to the CKS system and to what extent the predictions align with the observations. This will guide future analysis of planetary formation processes and identify which processes are more likely to be at work in a young solar system.

References: [1] Weiss, L. M., et al. (2018), *AJ, 155:48*. [2] Kokubo, E, Ida, S (1998), Icarus, 131, 171 [3] Raymond, S. N., et al. (2004), Icarus, 168, 1–17. [4] Lambrechts, M. and Johansen, A. (2012), A&A, 544, A32. [5] Lambrechts, M., et al. (2014), A&A, 572, A35. [6] Chambers, J. E. (1999), MNRAS, 304, 793–799. [7] Kenyon, S, Bromley, B (2006), AJ, 131, 1837 [8] Chiang, E. and Laughlin, G. (2013), MNRAS, 431, 3444–3455. [9] Chen, J. and Kipping, D. M. (2017), MNRAS, 473, 2753–2759.

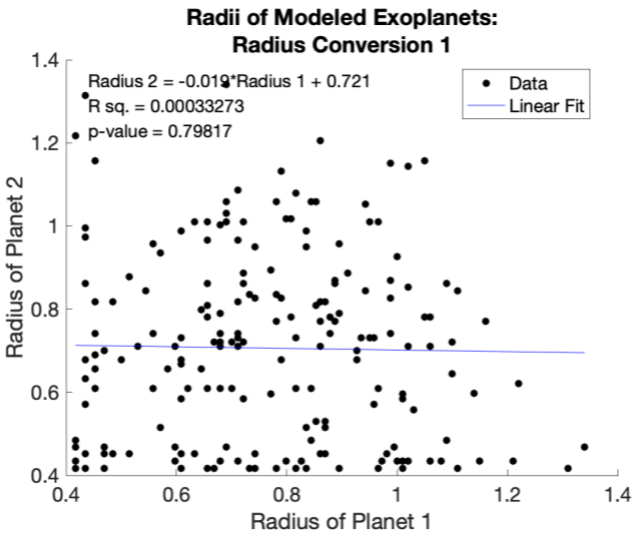

Figure 1: Plotting radius vs. radius of adjacent planets under one conversion calculation from mass to radius from [8]. This plot shows wide scatter and minimal correlation between the radii of planets within a pair, contrary to the results of [1].

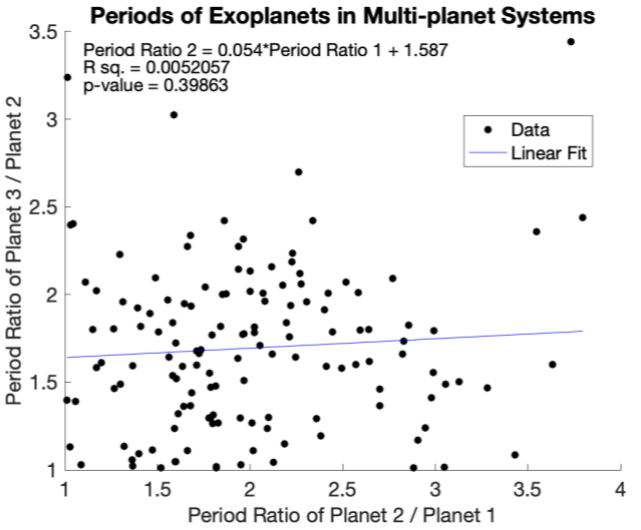

Figure 2: Plotting the period ratios of sequential planet pairs. This plot also shows wide scatter and minimal correlation between the radii of planets within a pair, contrary to the results of [1].

Identifying Potential Venus Analogs from Exoplanet Discoveries

Colby Ostberg, Stephen R. Kane
University of California, Riverside, CA, USA

Abstract

With a radius of $0.95R_{Earth}$ and a mass of $0.85M_{Earth}$, Venus is the most analogous planet to Earth in the solar system. Study of Venus and Venus-like exoplanets is invaluable in understanding factors that determine a planet's habitability throughout its evolution. Fortunately, many Venus-analogs are expected to soon be discovered as the recently launched Transiting Exoplanet Survey Satellite (TESS) mission is sensitive to planets in close proximity to their host stars. TESS is predicted to discover hundreds of terrestrial planets within the inner boundary of their host star's Habitable Zone (HZ), placing them in the 'Venus Zone' (VZ), defined by Kane et al. (2014). TESS in tandem with the launch of the James Webb Space Telescope in the coming years will allow for the characterization of these planets' atmospheres, providing a better understanding of atmospheric compositions of planets inside the VZ. This will help delineate the primary factors that determine whether a planet develops sustainable temperate surface conditions, or if it would be pushed into a runaway greenhouse state, leading to a more well-defined outer boundary for the VZ. Here we provide a progress report on discoveries from the TESS mission, identification of planets in the VZ, and methods used to determine runaway greenhouse scenarios. The observed properties of these planets will be applied to Global Climate Models, such as ROCKE-3D, to better constrain the boundaries of the HZ and VZ, and study the atmospheric demographics of terrestrial planets.

DETECTION OF EXO-MOONS OR DEBRIS ORBITING EXOPLANETS. A.V. Oza[1], S. Charnoz[2], and R.E. Johnson[3]
[1]Physikalisches Institut, University of Bern, Gesellschaftsstrasse 6, CH-3012 Bern, Switzerland, apurva.oza@space.unibe.ch, [2]IPGP, Sorbonne Universités, Paris, France, charnoz@ipgp.fr, [3]U. of Virginia, Charlottesville, 22904 & Physics, NYU, NY, NY 10012, rej@virginia.edu

Introduction: Extrasolar satellites, ring material or plasma tori, features generally too small to be directly detected at present by nominal searches of close in planets, can in principle be detected using our understanding and modeling of solar system observations [1,2,3]. For instance, as is the case at the most active body in the solar system, Io (Fig.1), we describe how alkali gas transmission spectra could be a signature of the geological activity venting from an exo-Io orbiting a hot Jupiter or the sputtering of orbiting debris [2]. Alternatively, a dusty exoring fueled by the disintegration of a small satellite might account for the large rates thought to be due to escape at a close-in system [2]. At present, extended absorption features at several systems have been interpreted as features of a gas giant atmosphere .

Although planets orbiting at larger distances from their stars are more likely to exhibit such features [1], analyzing a number of close-in gas giants hosting robust alkaline detections, we confirm that an Io-sized satellite can be stable against orbital decay [4] with the tidal energy driving mass-loss rates order of magnitude higher than Io's supply to Jupiter's Na exosphere [2]. The consequence is that potential exo-Io column densities or, possibly dusty exoring column densities, can be more than sufficient to account for the observed equivalent width of an exoplanet transmission spectrum with the high-altitude Na observations at WASP-49b used as an example [2]. Furthermore, the requirements for tidal stability, situate a putative rocky exomoon dangerously close to the gas giant's Roche limit [2,4]. Ongoing tidal disintegration of a rocky core may then be revealed as a *metallic* gas signature in transit [5]. Therefore, comparative planetology, using the solar system observations to infer the presence of satellites or rings, can be critical to understanding exoplanet observations [1,2].

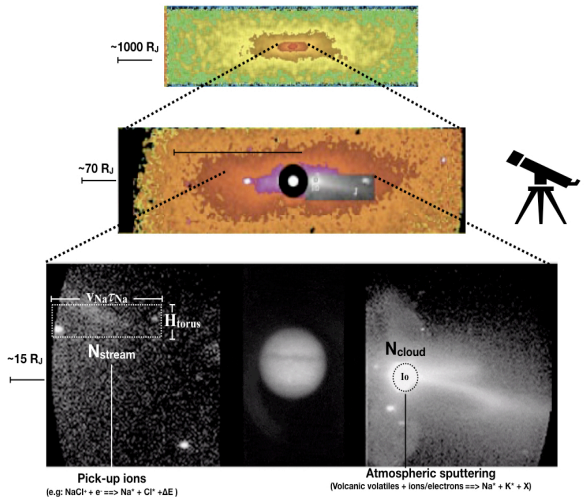

Fig. 1 Architecture of a sodium exosphere imaged at the Jupiter system can be used as a guide to understand the presence of a moon or a toroidal feature around an exoplanet [2].

References: [1] Johnson, R.E., & P.J. Huggins, Toroidal Atmospheres around Extrasolar Planets. Pub.Astron.Soc.Pacific (PASP) 118, 1136-1143 (2006) [2] Oza, A.V. R.E. Johnson, E. Lellouch, & 12 authors. Sodium and Potassium Signatures of Volcanic Satellites Orbiting Close-in Gas Giant Exoplanets. ApJ. 885:168 https://doi.org/10.3847/1538-4357/ab40cc (2019). [3] Charnoz, S, R.M. Canup, A. Crida, L. Dones. The Origin of Planetary Ring Systems, in Planetary Rings Systems, M. S. Tiscareno and C.D. Murray Eds, Cambridge University Press (2018). [4] Cassidy, T.A., R. Mendez, P. Arras, R.E. Johnson, M.F. Skrutskie, Massive Satellites of Close-In Gas Giant Exoplanets ApJ. 704, 1341-1348 (2009). [5] Hoeijmakers, H.J., D. Ehrenreich, D. Kitzmann & 16 co-authors. A spectral survey of an ultra-hot Jupiter. A&A, 627, A165 (2019)

L 98-59: A Benchmark System of Terrestrial Planets for Future Atmospheric Characterization. **Daria Pidhorodetska[1,2]**, Sarah Moran[3], Thomas Fauchez[1,4], Ravi Kopparapu[1], Knicole Colon[1], Elisa Quintana[1], Geronimo Villanueva[1], and Shawn Domagal-Goldman[1]
(1) NASA Goddard Space Flight Center (8800 Greenbelt Road, Greenbelt, MD 20771, USA) (2) CRESST/UMBC (1000 Hilltop Cir, Baltimore, MD 21250, USA) (3) Department of Earth and Planetary Sciences, Johns Hopkins University (Baltimore, MD 21218, USA) (4) Goddard Earth Sciences Technology and Research (GESTAR), Universities Space Research Association (Columbia, MD 21046, USA)

1. Introduction

L 98-59 is an M3 dwarf (M∗ = 0.3M) that hosts three terrestrial-sized planets recently discovered by TESS. The host star is bright (K = 7.1) and nearby (10.6 pc), making the system a prime target for follow-up characterization with Hubble and the upcoming James Webb Space Telescope. Herein, we present the plausibility of these planets having atmospheres that are dominated by either H_2, H_2O, CO_2, or O_2, while exploring the possibilities of the presence of clouds and hazes. The L 98-59 planets orbit close to their star with insolations ranging from 4 to 21 X that of Earth, placing the planets in the Venus-zone (Kane et al. 2014). These planets might therefore be Venus-analogs. L 98-59 is near the TESS continuous viewing zone and will be observed for an additional 3 months (∼160 days total), providing a wealth of information on the three currently known planets as well as the potential to reveal additional longer-period planets. In contrast to the highly active M-dwarf TRAPPIST-1 (M ∗ = 0.08M), the host star in the L 98-59 system shows no evidence for stellar activity in the TESS data (Kostov et al. 2019a) and is likely a relatively quiet M-dwarf with a low level of XUV activity. The XUV fluxes impingent upon these planets is sufficiently

low to allow for a sustainable atmosphere around each of these worlds, given their masses. With upcoming HST observations occurring in the near-term, modeling efforts show what we can expect to measure, while exploring the additional information that can be uncovered with observations using JWST. Transiting multi-planet systems provide ideal laboratories for comparative planetary studies, and the L 98-59 system offers a unique opportunity to study an exciting system of terrestrial planets that may exhibit features similar to the planets in our Solar System.

2. Methods

Although there is a significant parameter space to be explored regarding the potential atmospheric scenarios for this planetary system, this work considers just a few of those possibilities. These include the modeling of atmospheres that are dominated by H_2, H_2O, CO_2, or O_2, along with considering the presence of clouds and hazes. Each atmospheric configuration is created within the Planetary Spectrum Generator (PSG), an online radiative-transfer suite that computes synthetic transit spectra for a wide range of objects such as planets, moons, comets, and asteroids (Villanueva et al. 2018). In addition, PSG allows the user to explore many different instrument modes across a multitude of observatories. The atmospheres considered here do not represent the full spectrum of potential outcomes, but are merely a representation of atmospheres which have been motivated by their ability to produce measurable spectra, given the known planetary parameters.

3. Results

Preliminary results highlight the strength of the SNR of the system compared to other nearby terrestrial exoplanets. In addition, initial highlights focus on the feasibility to detect the presence of an atmosphere with HST/WFC3 in merely one transit, while follow-up observations to detect additional features that may be present in a water-dominated atmosphere are noted as feasible with one transit using JWST/NIRSpec.

4. Preliminary Figures

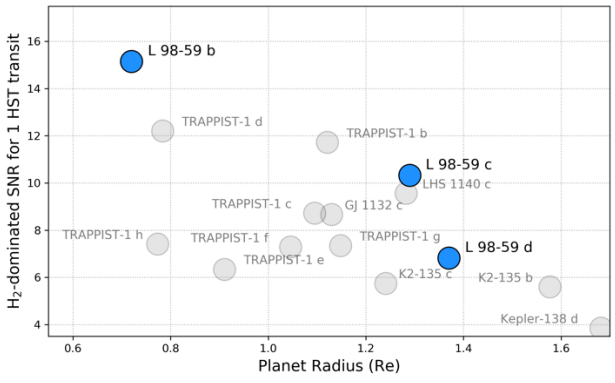

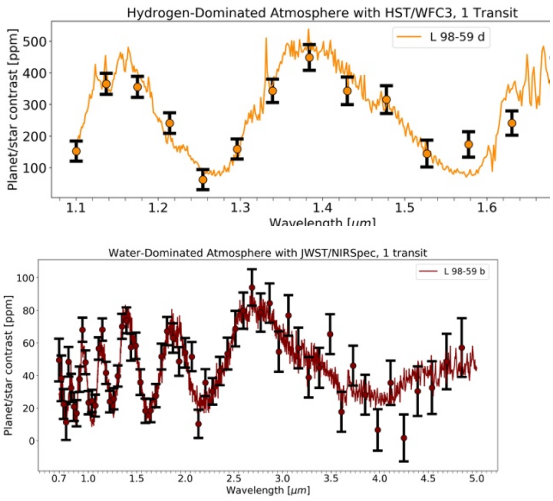
Hydrogen-Dominated Atmosphere with HST/WFC3, 1 Transit
L 98-59 d
Planet/star contrast [ppm]
500
400
300
200
100
1.1
1.2
1.3
1.4
1.5
1.6
Wavelength [μm]

Water-Dominated Atmosphere with JWST/NIRSpec, 1 transit
L 98-59 b
Planet/star contrast [ppm]
100
80
60
40
20
0
0.7
1.0
1.5
2.0
2.5
3.0
3.5
4.0
4.5
5.0
Wavelength [μm]

A POTENTIAL STRATIFICATION OF THE CORE OF MARS CAUSED BY HYDROGEN. H. Piet[1], K. Leinenweber[1], E. Greenberg[2], S. Chariton[2], V. B. Prakapenka[2], P. R. Buseck[1], and S.-H. Shim[1]
[1]Arizona State University, Tempe, USA, [2]University of Chicago, Chicago, USA

Abstract: We study the phase relations in the Fe-S-H system under pressures and temperatures relevant to the Martian core. We find that H-bearing alloys and S-bearing alloys would be immiscible in the core of Mars potentially causing its stratification.

Introduction: The Earth's core mainly consists of an iron-nickel alloy enriched with light elements [1]. Candidate light elements are silicon, oxygen, sulfur, carbon and hydrogen given their natural abundance and solubility in core-forming materials [2]. Geophysical observables, such as density, provide us with some constraints on the amount of light elements in the core. However, the abundance of each light element in the core remains a matter of debate.

In the case of Mars, geophysical constraints are limited and its core density remains to be constrained. However, given the nature of core formation, it is likely that the core of Mars (just like Earth's core) contains light elements as well. From SNC meteorites, there is strong evidence that sulfur is a major alloying component in the core of Mars, with an estimated abundance around 3-15% [3].

Hydrogen is the most abundant element in the solar nebula from which planets accreted. As such, it is important to consider its presence in the interior of planets, including cores. However, this element has not received the appreciation of other light elements in the study of Earth's core composition because of i) its high volatility and ii) the challenges associated with its experimental study. Recent experimental developments have highlighted that hydrogen's affinity for metals is strongly enhanced with pressure [4, 5]. Core formation being a high-pressure process [6], it is therefore possible for planetary cores to incorporate a significant amount of hydrogen during their formation.

In this study, we investigate phase relations in the Fe–S–H system at the pressures and temperatures relevant to the Martian core. We then discuss the potential geophysical implications.

Experimental methods: To simulate the high pressures and temperatures in the core of Mars, we use the laser-heated diamond anvil cell. Samples of Fe_3S, FeS or FeS_2 compositions were loaded into the sample chamber together with H_2 gas using a hydrogen gas loading facility at ASU. First, we compressed the diamond-anvil cell to target pressures ranging between 28 and 50 GPa. To reduce diamond anvil embrittlement from hydrogen, we then conducted pulsed laser-heating to temperatures in the 1000–3100 K range. Phase identification was performed at in-situ high pressure and high temperature using synchrotron X-ray diffraction at the GSECARS sector of the Advanced Photon Source.

Phase relations in the Fe-S-H system and implications for Mars core: Upon heating at high pressure, we observed the formation of separate iron sulfide and iron hydride phases, e.g. $FeS + H_2 = Fe_3S + FeS_2 + FeH_2$. The same behavior is observed for $FeS_2 + H_2$ and $Fe_3S + H_2$ as well. Measured unit-cell volumes of the phases suggest that hydrogen is not incorporated into iron sulfides, and the amount of sulfur in hydride should be very low. We observed the formation of FeH_2 at pressures as low as 27 GPa, which may require a small amount of S in the structure of FeH_2 since S-free FeH_2 does not form below 67 GPa [4].

In the $Fe_3S + H_2$ system – the most relevant to Mars core composition – we observed the formation of FeS and FeH upon heating, similarly to more sulfur rich compositions. We also found the formation of a new phase with a crystal structure similar to that of FeH_2 but with a significantly bigger volume. Our data suggest that the new phase might be a more Fe-rich phase than Fe_3S. Its structure, however, remains to be revolved.

The formation of separate FeS and FeH phases at pressure and temperature relevant to the Martian core suggests immiscibility of FeS and FeH alloys. The density difference between light H-bearing alloys and heavier S-bearing alloys could lead to a stratification of the core. Such stratification could influence the strength and scale of convection in the core, providing a potential mineralogical explanation for the early shutdown of Mars geodynamo [7].

References:

[1] Birch F. (1952) *JGR, 57,* 227–286.
[2] Poirier J. (1994) *PEPI, 85,* 319–337.
[3] Dreibus G. and Wänke H. (1985), *Meteoritics*, 20, 367–382.
[4] Pépin C. et al. (2014), *PRL, 113,* 1–5.
[5] Pépin C. et al. (2017), *Science, 357,* 382–385.
[6] Wade J. and Wood B. J. (2005), *EPSL, 236,* 78–95.
[7] Lillis R. J. et al. (2013), *JGR, 118,* 1488–1511.

THE OL DOINYO LENGAI VOLCANO, TANZANIA, AS AN ANALOGUE FOR CARBON PLANETS. J. Radebaugh[1] , R. Barnes[2], and J. Keith[1]. [1]Department of Geological Sciences, Brigham Young University, Provo, UT 84602, janirad@byu.edu. [2]The University of Washington Department of Astronomy and Physics, Seattle, WA.

Introduction: Recent stellar observations and models of exoplanet compositions have revealed the possibility of carbon-rich nebular environments that could lead to the creation of "carbon planets" (e.g., [1, 2]). Such objects would have high amounts of carbon in their interiors and on their surfaces, similar to the graphite observed on Mercury, but very different from the vast majority of Earth's surface.

The Ol Doinyo Lengai (ODL) volcano of Tanzania is currently erupting carbon-rich lavas, or carbonatites, in the summit crater (Fig. 1). These lavas are unique on Earth, but may be analogous to those that would erupt onto the surface of a carbon planet, making ODL to our knowledge the first field analogue of an exoplanet. Detailed studies of the lava flow textures, landscape, lava colors and albedos, and how these change with atmospheric composition, would reveal characteristics expected when observing carbon planets in various stages of internal and atmospheric evolution.

Fig. 1. The caldera floor of ODL in 2001, with active (black), recently cooled (white) and older (brown) flows. Lavas are fluid, but some steep landforms occur.

Carbon Planets: The possibility of carbon planets was first raised by Kuchner & Seager [3], who argued that a C/O ratio in excess of 0.98 could result in a condensation sequence that favored the formation of C-rich planetesimals (see also [4]). Detailed cosmochemical and N-body simulations by Bond et al. [2, 5] found that when C/O > 0.8 in the disk, then some planets may form with large carbon abundances, including cases in which the primordial carbon abundance of a planet in the habitable zone (HZ) was larger than 75%! While these results suggest that some planets may be extremely carbon-rich, significant ambiguity remains (see, e.g. [6, 7, 8, 9]). Nonetheless, the existence of carbon planets remains a viable possibility.

The scenario of carbon planets orbiting M dwarf stars is particularly intriguing because of the possibility of an oxygen-rich atmosphere. The planet may spend millions or even billions of years closer to the star than the HZ due to the slow luminosity decline of the star during the pre-main sequence (e.g. [10]). During this period, the planet is in a runaway greenhouse, and water can reach the stratosphere and be photolyzed by high-energy radiation. The liberated hydrogen may then escape while the heavier oxygen atoms remain. This process can result in large, oxygen-rich atmospheres [11]. It is unknown how the oxygen interacts with carbon-rich surfaces, so the longevity of a carbon planet oxygen atmosphere, the resultant surface features such as albedo, and the final composition of the atmosphere are also unknown. Studies of how the carbonatite lava flows of ODL are impacted by Earth's oxygen-rich atmosphere would yield important information for carbon planetary surfaces.

On the other hand, habitable planets orbiting G dwarfs may experience a similar atmospheric evolution as Earth, i.e. the early atmosphere may have been reducing, like Earth's Archaean atmosphere. Studies of how the carbon-rich lava flows of ODL would interact with an Archaean-like atmosphere could provide critical insight into how Archean chemistries led to conditions right for life.

Carbon-rich lavas of ODL: The Ol Doinyo Lengai volcano of Tanzania is in the East African Rift Zone, where the crust is thin and heat flux is high. Quiet, fluid eruptions of carbonatites emerge from discrete centers on the generally flat caldera floor and gradually fill up the crater [12]. The carbonatite lavas are thought to be produced from melt segregation, either from strongly peralkaline nephelenite magmas through extreme fractionation [13], or from a high-silica, low FeO, high K/Na source [14], or from more typical silicate fractional crystallization [15]. These carbonatite lava production mechanisms, along with direct, carbon-rich source melting, could all exist in carbon-rich planetary interiors.

The ODL lavas are dominantly composed of Na_2O, K_2O, CaO and CO_2 with minor Ba, Sr, Cl, F, P, S [16]. They have similar flow morphologies as basalts and tend to also erupt from fissures and cones (Fig. 1), but they are cooler, with a maximum eruption temperature of 593° C [17], and are an order of magnitude less viscous than basalt (0.3-120 Pa s, with gas-rich lavas having higher viscosity; [18]). The lavas are highly varied in color, erupting as black and changing within 24 hours (not precisely measured) to white, presumably as the lava is exposed to atmospheric oxygen [12] (Fig. 2).

More detailed field observations of how quickly this color change occurs, and if lavas protected from the atmosphere remain black (or if they devitrify and form microlites, similar to obsidian), would reveal the level of atmospheric control on the carbonatite lava albedo.

Fig. 2. Carbonatite lava flow in ODL crater. Liquid lava is red, recently solidified lava is black.

Carbon Planet Tectonism and Heat Release: The atmospheric evolution of a carbon planet depends critically on geochemical processes that are intimately tied to the tectonic expression. On Earth, plate tectonics cycles carbon dioxide into and out of the atmosphere to maintain a quasi-stable mean surface temperature [19]. Plate tectonics appears to require a mobile mantle and decoupling of the lithosphere by an asthenosphere. Strictly carbon-based lavas, such as the carbonatites of ODL, have low melting temperatures and viscosities, and thus the solid form found in the deep mantle may readily convect. If conditions are right for an asthenosphere, perhaps the lithosphere can move on top of this layer and subduct.

In carbon planets with significant Si, SiC may exist as a dominant mantle and crustal component, which is a stiff, high-melting-temperature, and much more insulating material [17]. This material is not likely to be mobile enough to enable sufficient mantle convection to produce plate tectonics, nor would the crust readily move and bend. These worlds may be more like Io than Earth, in which there is heat pipe or advection-style heat release [20, 21], expressed as isolated surface volcanic centers and hot spots [22]. Under this model of heat release, over time, the planet completely volcanically resurfaces and crustal materials are returned to the mantle through burial and subsidence (similar to Io) to re-melt and begin the process again. This enables significant transfer of crustal solids and volatiles from the surface to the interior and vice versa.

Carbon Planet Atmospheric Evolution: Plate tectonics and the heat pipe mechanism both cause the burial and recycling of atmospheric volatiles trapped in the crust. This depletes the atmosphere of toxic levels of oxygen and an overabundance of CO_2 and creates a habitable environment. Foley & Smye [24] derived a model for the geochemical evolution of such a "hot spot planet" in which water and CO_2 are outgassed and then reincorporated into the mantle. Should carbon-rich planets be unlikely or unable to transport internal energy via plate tectonics or the heat pipe mode, gases may build in the atmosphere and ultimately trigger a runaway greenhouse that removes all water from the surface, rendering it uninhabitable. This is the case on Venus, where neither plate tectonics nor the heat pipe mechanism appear to have been operating for billions of years, and CO_2 has been expelled to the atmosphere rather than recycled.

Habitable Carbon Planets: The surface environment of a carbon planet depends on the atmospheric composition, surface composition, and stellar radiation. Bond et al. [2] suggest that carbon planets will be dark, which is also seen in the color of newly erupted carbonatites at ODL (Fig. 2). Prior to the rise of O_2 on Earth, ODL-type lava flows may have in fact remained dark. On the other hand, the surfaces of oxygen-rich carbon planets may have whiter (high albedo) surfaces, as the initially black lavas gradually change to white (Fig. 2). An analysis of carbonatite's chemical reactions and color changes with different atmospheres could help us predict and interpret planetary albedo, possibly related to oxygen levels. Crucially, free oxygen may prevent the development of large biomolecules because it is so reactive. Therefore, it is critical to measure the rate at which carbon-rich surfaces can absorb oxygen, relative to the rate at which it is produced by water photolysis, to determine if habitable conditions can exist on carbon planets.

Exoplanet in our backyard: The ODL volcano is a rare and unique opportunity to study potential materials and processes on carbon planets. Analyses of the lava flow characteristics, and especially how those materials interact with Earth's current and Archean atmospheres, will help us predict and interpret observations of the surfaces of carbon planets.

References: [1] Seager & Kuchner (2005). [2] Bond et al. (2010). [3] Kuchner & Seager (2005). [4] Lodders (2003). [5] Bond et al. (2008). [6] Teske et al. (2013). [7] Nissen et al. (2014). [8] Wilson et al. (2016). [9] Brewer & Fischer (2016). [10] Baraffe et al. (2015). [11] Luger & Barnes (2015). [12] Dawson et al. (1995a). [13] Peterson et al. (1995). [14] Sweeney et al. (1995). [15] de Moor et al. (2013). [16] Dawson et al. (1995b). [17] Pinkerton et al. (1995). [18] Dawson et al. (1990). [19] Walker et al. (1981). [20] O'Reilly & Davies (1981). [21] Moore (2001). [22] Lopes et al. (1999). [23] Schenk & Bulmer (1998). [24] Foley & Smye (2018).

IO AS AN EXTREME EXOPLANET ANALOGUE. J. Radebaugh[1] , A. S. McEwen[2], D. Ragozzine[3], J. T. Keane[4], A.G. Davies[5], K. de Kleer[4], C. W. Hamilton[2], F. Nimmo[6], A. Pommier[7], P. Wurz[8] and the IVO Mission Science Team. [1]Department of Geological Sciences, Brigham Young University, S-389 ESC, Provo, UT 84602, janirad@byu.edu. [2]Lunar and Planetary Laboratory, University of Arizona, Tucson, AZ. [3]Department of Physics and Astronomy, Brigham Young University, Provo, UT. [4]California Institute of Technology, Pasadena, CA. [5]NASA Jet Propulsion Laboratory, Pasadena, CA. [6]University of California Santa Cruz, CA. [7]University of California San Diego, CA. [8]University of Bern, Switzerland.

Introduction: Jupiter's moon Io is the most tidally heated world in the solar system. Its surface (Fig. 1) is mottled by hundreds of continually erupting silicate volcanoes, producing towering plumes and polluting the rest of the Jovian system with sulfur and other volatiles. The tidal energy is so great that it may produce a global, subsurface magma ocean—akin to the early Earth.

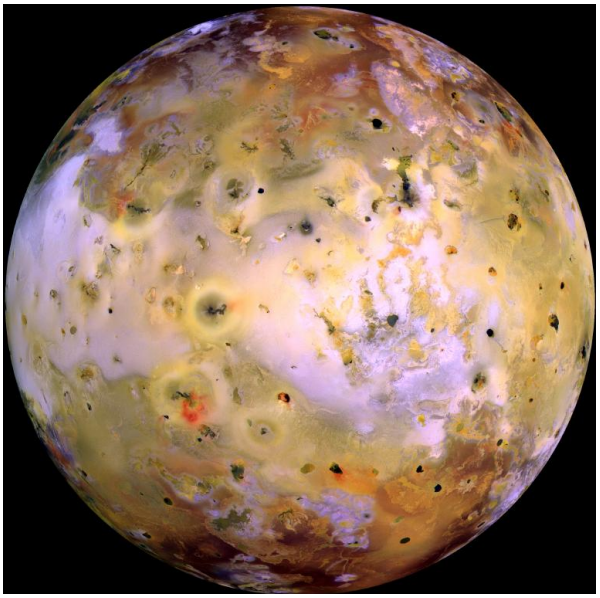

Fig. 1. Io in false color as seen by Galileo. All dark spots are recent or active volcanic eruptions.

Io is an important analogue to a key group of superheated exoplanets—including worlds powered by tidal heating, extreme insolation, abundant heat-producing radionuclides, or left-over accretional energy. Such objects have been termed "lava worlds", "highly volcanic planets" and "magma ocean worlds" [1]. This makes Io a high-value target for understanding the generation and transfer of large amounts of heat, the longevity of bodies in resonance orbits, and the evolution of planetary interiors and surfaces with high volcanic output. Io has been studied extensively from Earth and space-based assets, and there are notable similarities between Io and several exoplanets. In this work, we outline potential synergies between Io and exoplanets, and some key observations that may address outstanding science problems for both classes of worlds.

Heat Generation: Io's tidal heat is maintained by a 1:2:4 mean motion Laplace resonance [2] between Io, Europa, and Ganymede. This forces eccentricity in the orbits of each moon, resulting in tidal deformation and dissipation. Every 42 hours, Io's shape is deformed by as much as hundreds of meters, generating significant frictional heating of the interior silicate rocks and a surface heat flux 40 times that of Earth. Exoplanet observations have revealed mean motion resonances, or near-commensurabilities, in many well-characterized multi-planet systems [3, 4, 5, 6]. TRAPPIST-1 has multiple terrestrial planets in Laplace-like resonances. Tidal heating models suggest that the innermost world (TRAPPIST-1b) may have a heat flow as high as Io's [7, 8], potentially producing a magma ocean [9]. Furthermore, ancient resonances are likely [10]. Observations of exoplanets like those in the TRAPPIST-1 system may reveal how orbital resonances form and evolve, and observations of Io will inform how these worlds react to this extreme tidal forcing.

Heat Release: Heat generated inside Io is transferred to the surface through conduits and fractures to emerge as vast lava flows. These volcanic eruptions release a significant amount of sulfur [11], powering gigantic volcanic plumes that coat the surface in SO_2 frost and creating an atmosphere that changes with day/night and volcanic activity [12]. Much of this material is ejected into the Jovian magnetosphere, producing a torus the scale of Io's orbit. A Na cloud is also present. Exoplanet analogues to the Io plasma torus and Na and K clouds should be detectable in the visible or UV [13].

Io surface is covered with discrete, long-lived volcanic source regions [14]. This, along with tectonic evidence for a thick, cool crust suggests that the dominant style of heat release for Io is through volcanic heat pipes rather than conduction or convection [15, 16]. In this heat loss mode, magma is advected vertically to the surface, where it is deposited in flows that radiate the heat to space (Fig. 2). This efficiently transfers heat out of Io while resurfacing and burying the colder outer layers. This process also affects Io's global tectonics—producing isolated mountain blocks, up-thrust from global crustal shortening [15, 17]. Heat pipe volcanism was likely prevalent on the early Earth, Moon, and other terrestrial planets, and may also be important on tidally heated exoplanets [16].

Some eruptive centers (e.g., Loki) are active on timescales (~480 days) that arise from the Laplace resonance but are longer than the orbital period [18, 19]. Tidally heated exoplanets may also show longer-period modulations to thermal output, observable in the IR.

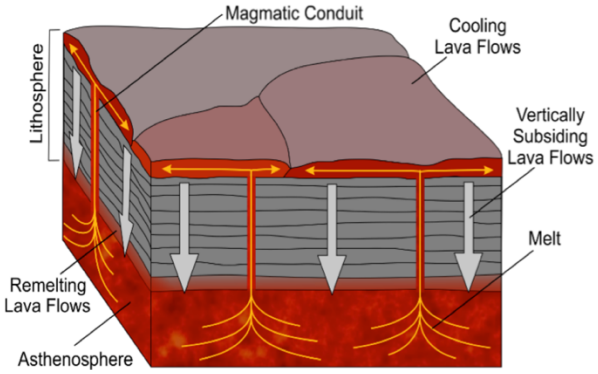

Fig. 2. Heat Pipe mechanism for heat transfer in Io.

Observations of an exoplanetary surface with excess thermal emissions and abundant sulfur and silicate magmatic minerals (e.g., pyroxene and olivine; [20]) might indicate the planetary surface is currently dominated by volcanic processes, similar to Io. Silicate composition can be determined by NIR and transit spectroscopy, and temperatures can be measured by multispectral IR observations [14, 21]. Observations of heterogeneous or distributed heat sources, potentially detectable with observations of secondary eclipses, phase curves or planet-planet occultations [22, 23], may reveal extreme amounts of internal heating.

Io's Magma Ocean: Galileo magnetometer observations revealed that Io contains a significant conductive layer responding to Jupiter's magnetic field. Given the high heat output and Io's bulk composition, this is best explained by a global magma ocean [24]. Magma oceans are likely a ubiquitous stage of terrestrial planet formation. The best example is the Moon, as evidenced by the plagioclase-rich lunar highland crust, formed by flotation in a global magma surface layer. While magma oceans may have been common in the past, Io is the only solar system world that may have an active interior silicate magma ocean. The nature of this ocean, its depth and fraction of solids [24], is still under discussion.

Magma Ocean Worlds: As many exoplanets orbit extremely close to their parent stars, their equilibrium temperatures are high enough to prevent rocky material from cooling. Even without dynamical interactions, these bodies have magma oceans on their surfaces. One example is Kepler-78b: a 1.7 Earth-mass, 1.2 Earth-radius planet orbiting its sun-like star at 2 stellar radii, every 8 hours [25]. Its size and mass led to the prediction that it is rocky and probably iron-rich [26]. It is so close to the star that the surface is expected to be 2000–2800°C, exceeding the melting temperature of mafic silicates (1100–1400°C or less, depending on volatile content). Since Kepler-78b is likely tidally locked, the near-side could be dominated by a magma ocean (Fig. 3) [27]. Similar "exo-Ios" may be common in the cosmos, and observations of these worlds have the potential to address fundamental questions in the evolution of all terrestrial bodies.

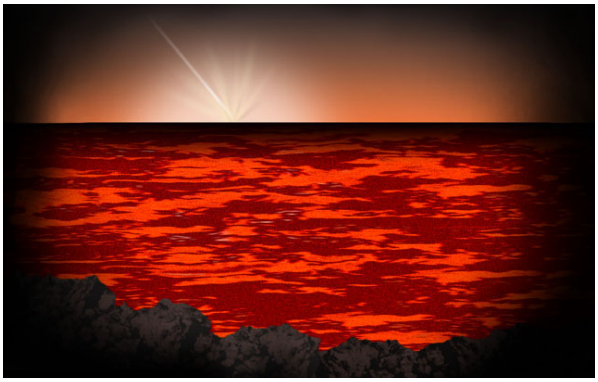

Figure 3. Artist rendition of a magma ocean world.

Exoplanet in our backyard: Io is a promising scientific destination that represents endmember states of many different aspects: tidal heating, orbital resonances, heat generation and output, volcanic activity, plumes, atmosphere-magnetosphere interactions, rapid spatial and temporal changes, a melt-bearing interior and interior structure. All of these characteristics have been observed or postulated for exoplanets, and future observations may be able to address key questions relevant to exoplanets, Io, terrestrial planets, and icy satellites. The proposed Io Volcano Observer (IVO) Discovery mission [28] would address many of the questions around the thermal and orbital evolution of Io, which will better prepare us to explore these other unique objects outside our solar system.

References: [1] Henning et al. (2018). [2] Peale et al. (1979). [3] Steffen & Lissauer (2018). [4] Fabrycky et al. (2014). [5] Trevor (2019). [6] Quinn (2019). [7] Miguel et al. (2019). [8] Luger et al. (2017). [9] MacDonald et al. (2016). [10] Barr et al. (2018). [11] Consolmagno (1979). [12] Geissler et al. (2001). [13] Oza et al. (2019). [14] Veeder et al. (1994). [15] O'Reilly & Davies (1981). [16] Moore (2017). [17] Schenk et al. (2001) JGR. [18] Rathbun et al. (2002). [19] de Kleer et al. (2019). [20] Geissler et al. (1999). [21] Davies et al. (2015). [22] Luger et al. (2018). [23] Demory et al. (2016). [24] Khurana et al. (2011). [25] Pepe et al. (2013). [26] Price & Rogers (2019). [27] Kite et al. (2016). [28] McEwen et al. LPSC (2019).

OPTICAL PROPERTIES OF SULFURIC ACID. Michael J. Radke[1], S. M. Hörst[1], C. He[1], and M. H. Yant[1]
[1] Johns Hopkins University, 3400 N. Charles St., Baltimore, MD 21218, USA (radke@jhu.edu)

Introduction: Aerosols are common in planetary atmospheres, both in our Solar System and beyond [1]. Aerosols have significant effects on the observed transmission and reflection spectra of (exo-)planetary atmospheres. It is not possible to uniquely determine the composition of aerosol from optical spectroscopy. However, thanks to entry probes and landers sent to Venus, we have "ground truth" which we can compare to our remote observations of this cloudy world.

Interpretations of remote sensing observations of Venus' clouds rely heavily on laboratory data to determine properties of the cloud particles. The complex refractive indices—sometimes called the optical properties or optical constants—of aqueous H_2SO_4 have been measured over a wide range of concentrations and temperatures [2]–[12]. While the *real* refractive indices of H_2SO_4 are reported over a wide wavelength range, spanning from ultraviolet to mid-infrared there is only one measurement of the *imaginary* refractive indices at wavelengths below 1.4 μm [4].

Remote sensing of the surface and lower atmosphere of Venus must account for the effects of the overlying clouds [13]. Given that most of these observations are made in visible and near-infrared wavelengths, it is important to verify the only existing data set of the optical properties of H_2SO_4 at these short wavelengths.

Previous measurements of the imaginary refractive index (k) have large discrepancies in the near-infrared (3 to 4 orders of magnitude). These discrepancies are so large that if they were to continue into the blue-ultraviolet, then sulfuric acid itself could be the unknown absorber! Measurements of the real refractive index (n) also show some differences, albeit smaller (only ~5%), in the mid-infrared. Nevertheless, this small difference in n could result in a ~20 wt% difference in the derived concentration of H_2SO_4. Furthermore, for many of the data sets, experimental uncertainties are often unrealistically small or are sometimes not even reported, leaving it unclear as to which data sets might be the most reliable under specific temperature-concentration-wavelength conditions.

Methods: We have determined the complex refractive index of aqueous H_2SO_4 (50–96 wt%) at room temperature (294 K) using a combination of transmission and reflection spectroscopy techniques. We are capable of measuring complex refractive indices 0.2 to 25 μm, reproducing the experiments of [4].

Results: Here we report the imaginary refractive index spectra $k(\lambda)$ of concentrated sulfuric acid solutions in the Venus near-infrared spectral windows. We also provide parameterizations of the refractive indices as a function of acid concentration, in the NIR spectral windows, that can be used to easily derive properties such as cloud opacity and cloud acid concentration.

So far, we have only measured the optical properties of H_2SO_4 at room temperature. However, we plan on repeating these measurements at temperatures as low as 180 K, representative of temperatures in Venus' upper clouds or Earth's stratosphere. We also plan to measure the optical properties of other proposed Venus cloud species in the future (e.g. H_3PO_4, HCl, oxidized sulfur species, and transition metal salts) which may be relevant to the identity of the Venus ultraviolet-blue absorber.

References:

[1] H. R. Wakeford and D. K. Sing, "Transmission spectral properties of clouds for hot Jupiter exoplanets," *A&A*, vol. 573, p. A122, Jan. 2015. [2] M. R. Querry et al., J. Opt. Soc. Am., vol. 64, no. 1, pp. 39–46, Jan. 1974. [3] E. E. Remsberg, D. Lavery, and B. Crawford, "Optical constants for sulfuric and nitric acids," J. Chem. Eng. Data, vol. 19, no. 3, pp. 263–265, Jul. 1974. [4] K. F. Palmer and D. Williams, "Optical constants of sulfuric acid: Application to the clouds of Venus?," Appl. Opt., AO, vol. 14, no. 1, pp. 208–219, Jan. 1975. [5] L. W. Pinkley and D. Williams, "The infrared optical constants of sulfuric acid at 250 K," J. Opt. Soc. Am., JOSA, vol. 66, no. 2, pp. 122–124, Feb. 1976. [6] K. D. Beyer, A. R. Ravishankara, and E. R. Lovejoy, JGR: Atmospheres, vol. 101, no. D9, pp. 14519–14524, 1996. [7] S. F. Gosse, M. Wang, D. Labrie, and P. Chylek, Applied optics, vol. 36, no. 16, pp. 3622–3634, 1997. [8] R. T. Tisdale, D. L. Glandorf, M. A. Tolbert, and O. B. Toon, JGR: Atmospheres, vol. 103, no. D19, pp. 25353–25370, 1998. [9] R. F. Niedziela, M. L. Norman, C. L. DeForest, R. E. Miller, and D. R. Worsnop, J. Phys. Chem. A, vol. 103, no. 40, pp. 8030–8040, Oct. 1999. [10] U. M. Biermann, B. P. Luo, and Th. Peter, J. Phys. Chem. A, vol. 104, no. 4, pp. 783–793, Feb. 2000. [11] U. K. Krieger, J. C. Mössinger, B. Luo, U. Weers, and T. Peter, Appl. Opt., vol. 39, no. 21, pp. 3691–3703, 2000. [12] C. E. Lund Myhre, D. H. Christensen, F. M. Nicolaisen, and C. J. Nielsen, J. Phys. Chem. A, vol. 107, no. 12, pp. 1979–1991, Mar. 2003. [13] G. Arnold, R. Haus, D. Kappel, P. Drossart, and G. Piccioni, JGR, vol. 113, Oct. 2008.

DO INTRINSIC MAGNETIC FIELDS PROTECT PLANETARY ATMOSPHERES FROM STELLAR WINDS? LESSONS FROM MEASUREMENTS IN THE SOLAR SYSTEM. Robin Ramstad[1] and Stas Barabash[2], [1]University of Colorado Boulder, Laboratory for Atmospheric and Space Physics, [2]Swedish Institute of Space Physics, Kiruna, Sweden

Introduction: A long-standing paradigm has held that intrinsic magnetic fields protect the atmospheres of planets with strong internal dynamos by creating magnetic pressure that stand off stellar winds at large distances. The stellar winds are thus not able to interact as closely with the planets' ionospheres, hypothetically leading to less efficient transfer of energy and momentum from the upstream fast flowing plasma. Intuitively, this makes a lot of sense and has formed the basis for much thought on how planetary atmospheres and habitability evolve over time. Over the last couple of decades this hypothesis has been tested by direct measurements of ion escape from the terrestrial planets in the solar system. When compared, Venus, Earth and Mars together provide a laboratory for studying the influence of gravity and magnetism on solar/stellar wind driven atmospheric escape, as illustrated in Figure 1.

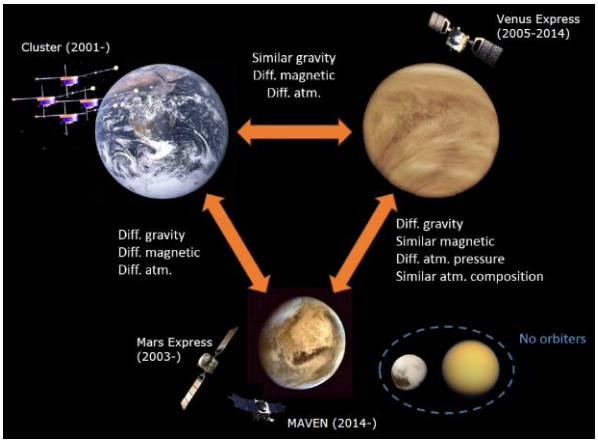

Figure 1: Venus, Earth, and Mars feature both mutually similar and mutually distinct properties, such as surface gravity, atmospheric mass/composition, and magnetism. Orbiters at all three planets measure the rate of atmospheric ion escape and the driving influence of upstream solar wind and solar photoionizing radiation.

Recent results: The interaction of the solar wind with any conductive obstacle, magnetized or not, induces electric and magnetic fields. The induced electromagnetic fields can accelerate charged atmospheric particles (ions), allowing the solar wind to drive a non-thermal atmospheric ion escape process. Recent studies of ion flux measurements from Venus by the Venus Express orbiter, from Mars by the Mars Express and MAVEN orbiters, and from Earth most recently by the Cluster mission have focused on the influence of the solar wind and solar extreme ultraviolet (EUV) radiation as drivers. The results show mutually different heavy ion escape trends for all the three objects, which may be related to their gravity, the average upstream conditions experienced due to the different heliocentric distance of the three planets, and the sizes of the obstacles, which in the case of Earth is increased by the presence of the geomagnetic field, as shown in Figure 2.

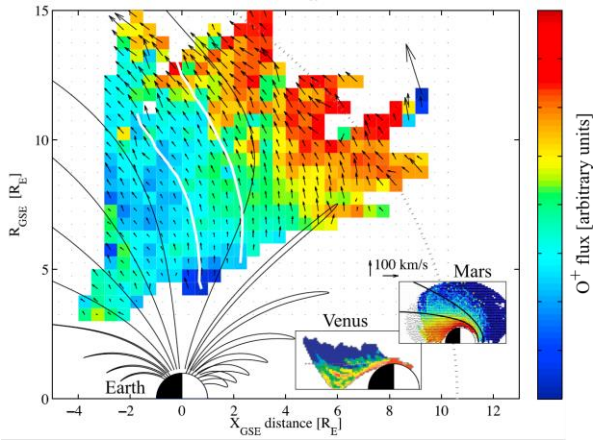

Figure 2: Maps of O^+ ion escape from Earth, Venus, and Mars shown at the same spatial scale in cylindrical coordinate systems. The solar wind is incident from the right in all panels. The influence of the Earth's geomagnetic field drastically changes the interaction area with the solar wind and the area of ionospheric outflow, compared to the non-magnetized planets. Blue colors show low fluxes and red colors show high fluxes in all panels. Adapted from Nilsson et al. 2012, Fedorov et al., 2011, and Ramstad et al. 2017.

In particular, the measurements show that Mars and Venus are not sensitive to the energy (dynamic pressure) of the solar wind [4,5,6], and have strong but diverging dependence on solar EUV [5,7,8]. In contrast, O^+ escape from the Earth is not sensitive to EUV but is rather extremely sensitive to high solar wind dynamic pressures.[9]

A generalized understanding of ion escape: To explain the divergent trends, we suggest that the trends of the three planets results result from different regimes of state that limit the respective ion escape rates. This implies that heavy ion escape from Venus and Earth are energy-limited processes, while ion escape from Mars

is a supply-limited process. In addition, with this nuanced picture of ion escape follows that the Earth's geomagnetic field increases energy transfer from the solar wind in comparison to the induced magnetospheres of Venus and Mars, which appear to efficiently screen the ionospheres of the two planets from the upstream solar wind. The limitation states provide a framework for understanding the roles of gravity, magnetism and upstream conditions in a manner that is potentially consistent across all planets. We show how long-term measurements of ion escape at Venus, Earth, Mars, and potentially other planetary bodies in the future, can be used to move towards the creation of a general model for atmospheric ion escape. This would lead to a highly useful tool for understanding the evolution of planets both inside and outside of the solar system.

References:

[1] Nilsson H. et al. (2012) *JGR*, *117*, A11201.

[2] Fedorov et al. (2011) *PSS*, *56*, 812-817.

[3] Ramstad R. (2017) *Doctoral thesis*.

[4] Ramstad R. et al. (2015) *JGR*, *120*, 1298–1309.

[5] Ramstad R. et al. (2018) *JGR*, *123*, 3051–3060.

[6] Masunaga K. et al. (2019) *Icarus*, *321*, 379-387.

[7] Kollmann P. et al. (2016) *Icarus*, *274*, 73-82.

[8] Dong Y. et al. (2017) *JGR*, *122*, 4009-4022.

[9] Schillings A. et al. (2019) *EPP*, *71*(70).

EPISTEMIC CONSTRAINS REGARDING THE STUDY OF EXOPLANETS. R. Reyes[1*] and D.Tovar,[1,2]. 1) Grupo de Ciencias Planetarias y Astrobiología, Departamento de Biología, Departamento de Geociencias, Universidad Nacional de Colombia. Carrera 45 # 26 – 85 Edificio Uriel Gutiérrez, Bogotá D.C., Colombia. 2) Licenciatura en Ciencias Naturales, Facultad de Educación, Universidad de La Sabana. Km 7 vía Bogotá, Puente del Común, Chía, Colombia.

*rareyesq@unal.edu.co

Introduction: The epistemic validity of knowledge about life in cosmos is associated to discoveries in this area and the conceptual heritage. All this built by the astro-scientific community, about transformation modes of matter and energy in the universe. Particularly the location, size and composition of exoplanets, a transdisciplinary evaluation of the process related to categorization of habitable areas and delimitation of potential planetary analogs to Earth is required [2].

Knowledge acquired in this area operates under the principle of homogeneity of nature, which dictates that "…the same physical phenomena given the same circumstances run the same way. In other words, what the laws of nature as described by physics, chemistry, biology, and other sciences admit necessarily happens, under favourable conditions"[3].

This principle raised due to the discovery of "imperfections in the sky" (carefully described for first time by Galileo Galilei), constituted an epistemological break that imposed the need for a new frame of reference for the study of natural phenomena in the cosmic context.

However, according to NASA, exoplanet archive Exoplanet Science Institute, around 4000 exoplanets have been found in the last 3 decades [1]. These findings have boosted astrobiology, its development and consolidation as a scientific discipline, whose study object requires the articulation of a variety of study fields.

The number of exoplanets detected is the best evidence that astronomers comunity contirbutes the most to solving the famous Drake equation (in its classical approach). However, when it is intended to clarify the number to replace in the second variable of the equation (fp), the promising figure drops to a value close to 10% from original, or even less base on NASA Exoplanet Science Institute (NExScl).

This steep decline is due to the fact that certainty about values to be replaced in the second and third term of Drake's equation is based on data coming from bodies located light-years away; therefore, there are scarce and difficult to obtain. Additionally, they demand multiple tests to effectively determine the fraction of stars with planets orbiting around them, which have the potential to host life in their star system (fp), as well as the third variable in equation (ne) (number of planets with ecological conditions regarding to the origin and evolution of life) [6].

Historically, the study of the molecular rotation spectra in the gas phase with radio astronomy, by high-resolution measurement in visible wavelength from the earth's surface, was the precursor process to the development of remote detection by space telescope spectroscopy. The latter technique is used for the method of radial velocities (RV) and transit spectroscopy from the near-UV (~ 200 nm wavelength) to the near-IR (1,800 nm), the RV measures the radial component of the velocity of the star, ie, the component along the line of sight which allows estimating a minimum value for the mass of the exoplanet [1].

Transit spectroscopy is useful in determining the atmospheric composition when comparing with the light emitted by the star when the planet is behind the star and high contrast measurements are obtained [5].

Both spectroscopic methodologies have biases inherent in the nature of the variables they measure, in the case of VR the planet's mass is estimated, but its real value is not determined. And in the case of transit, a privileged position is required from which sufficient observations can be accumulated to discern the sources of alterations in the luminosity of the star and isolate the behavior corresponding to the planet of interest, in order to approximate the value of its orbital distance.

However, when interpreting the data obtained by these remote sensing techniques for the solution of (fp) and (ne) the methodological bias meets the conceptual limitations, since there is no universal habitable zone applicable to all exoplanets [5]. Different authors postulate that the commissioning of equipment with greater sensitivity such as the James Web and HabEx will enrich the current databases, with information with greater fidelity (Figure 1). Nonetheless, postulate an explanatory framework that allows the correct statistical interpretation of this información is necesary.

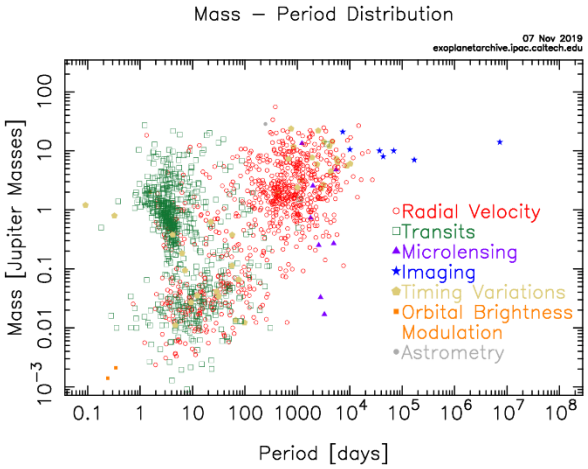

Fig 1. Known exoplanets as of November 2019. Modified from NASA exoplanets archive.

Complementing the evidence of size and composition that with the possible atmospheric dynamics that contribute to determine the location, or not, of the exoplanet in the habitability zone and the characterization of earth like exoplanets in analogous evolutionary stages according to 2015 NASA's roadmap.

References:

[1] Cenadelli, D., & Bernagozzi, A. (2018). The Discovery of the First Exoplanets. Handbook of Exoplanets, 3–20. https://doi.org/10.1007/978-3-319-55333-7_134

[2] Chon-Torres, O. A. (2018). Disciplinary nature of astrobiology and astrobioethic's epistemic foundations. International Journal of Astrobiology, (August). https://doi.org/10.1017/S147355041800023X

[3] Dunér, D., Erik, P., & Gustav, H. (Eds.). (2013). The History and Philosophy of Astrobiology: Perspectives on Extraterrestrial Life and the Human Mind. Cambridge Scholars.

[4] Gillett, A. J. (2018). Invention through bricolage: epistemic engineering in scientific communities. RT. A Journal on Research Policy and Evaluation, 6(1). https://doi.org/10.13130/2282-5398/9113

[5] Seager, S. (2013). Exoplanets Habitability. Science, 340, 577. DOI: 10.1126/science.1232226.

[6] Ćirković, M. Vukotić, B. (2013). Astrobiological landscape: A platform for the neo-Copernican synthesis? International Journal of Astrobiology. vol: 12 (1) pp: 87-93

Solar System Ice Giants versus Exoplanet Ice Giants. A. M. Rymer[1], M. Hofstadter[2], A. Simon[3], K. Mandt[1], K. M. Sayanagi[4], I. de Pater[5]
[1]Johns Hopkins Applied Physics Laboratory, Laurel, MD, USA (Abigail.Rymer@jhuapl.edu) [2]Jet Propulsion Laboratory, California Institute of Technology, [3]NASA Goddard, [4]Hampton University, Hampton, VA [5]UC Berkeley, CA

Introduction: Major revelations of the structure and mechanics of the interiors of Jupiter and Saturn from Juno and the Cassini Grand Finale, respectively, are a stark contrast to our ignorance of ice giant interiors (e.g., Masters et al., 2014; Turrini et al., 2014; Hofstadter et al., 2017; Dougherty et al., 2018; Galanti et al., 2019; Moore et al., 2018; Guillot et al., 2018). The composition and interior of Neptune is poorly constrained. It is of particular importance to determine the global ice-to-rock-ratio, the noble gas abundances, and the isotopic ratios of H, C, N, and O which are key to understanding how the giant planets formed and evolved (e.g., Mousis et al., 2018).

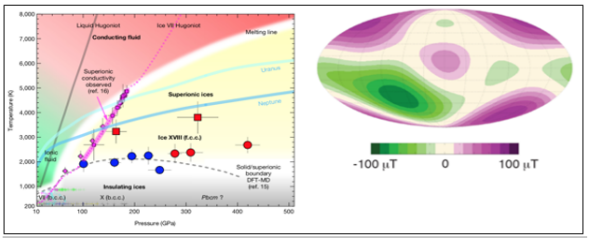

Figure 1. Left: Phase diagram of water showing hypothesized interior conditions for the ice giants (Millot et al. 2019); magnetic fields are likely generated in the shallow ionic fluid region. Right: Radial magnetic field at the 1 bar pressure level as measured by Voyager 2, including the dipole, quadrupole, and octupole components (Holme & Bloxham, 1996). Color represents field intensity with purple (green) denoting outward (inward) directed fields.

The Kepler Mission discovery of vast numbers of 2-4 Earth radii exoplanets, often called "mini-Neptunes", give additional impetus to understanding the structure and composition of Neptune. The last several years of exoplanets detection and characterization have taught us that planets with the sizes of Neptune are very common in our galaxy and therefore a better understanding of this planetary class is desirable. The formation of the ice giants is still an open question in the fields of planetary science and astrophysics (e.g., Pollack et al., 1996, Dodson-Robinson & Bodenheimer, 2010, Helled & Bodenheimer, 2014). Neptune emits the largest amount of internal heat relative to insolation of all giant planets, and especially compared to Uranus' which emits the lowest amount. What is responsible for this inter-ice giant dichotomy and how is it rectified against their similar magnetic fields and zonal flows?

Opportunities to Study the Exoplanets in our Backyard From an Interstellar Probe. A. M. Rymer[1], K. Stevenson[1], K. Mandt[1], R. McNutt[1], P. Brandt[1], N. Izenberg[1], A. Cocoros[1], C. Beichman[2]
[1]Johns Hopkins Applied Physics Laboratory, Laurel, MD, USA (Abigail.Rymer@jhuapl.edu)
[2]JPL, Pasadena, CA, USA.

The *Interstellar Probe* would be a robotic one-way mission into the local interstellar medium with the science objective of understanding our heliosphere as a habitable astrosphere. As the Interstellar Probe travels through and beyond the orbit of the solar system planets it will have the opportunity to look back at our own planets as we currently view exoplanets. This unprecedented opportunity would be available no matter what trajectory the probe takes into interstellar space and would provide the chance to consider high-level questions relating to exoplanetary research such as: What does our solar system look like to our nearest neighbors? Would ETs be capable of detecting life on Earth and, if so, what methods would they most likely use? What insights can we gain about exoplanetary systems by observing our own system at up to 1000 AU?

Here we discuss the opportunity and elucidate on the measurement techniques and other considerations that would be needed to make exoplanetary relevant measurements from the Interstellar Probe.

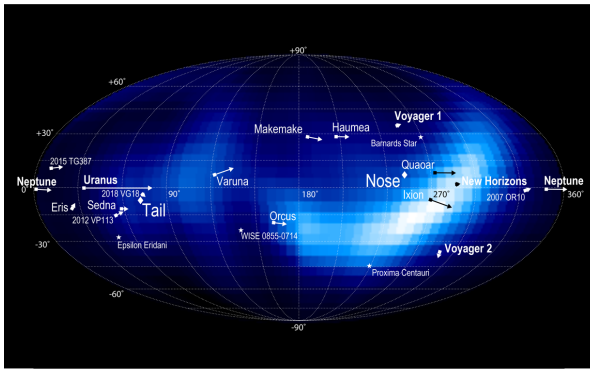

Figure 1. Figure showing the 'ribbon' feature on the edge of our heliosphere (by the IBEX mission) along with the locations of several key object locations, such as the 'Nose' and 'Tail' of the heliosphere, the current locations of the Voyage spacecraft and the locations of planets and KBOs during the likely Interstellar Probe epoch.

Planetary Atmospheric Dynamics Regimes: Lessons to be Learned from Planets in Our Solar System and Elsewhere. Kunio M. Sayanagi[1] and Adam P. Showman[2], Jonathan L. Mitchell[3,4], [1]Atmospheric and Planetary Sciences Department, Hampton University (kunio.sayanagi@hamptonu.edu), [2]Lunar and Planetary Laboratory, University of Arizona, (showman@lpl.arizona.edu), [3]Earth, Planetary and Space Sciences Department, University of California Los Angeles, [4]Atmospheric and Oceanic Sciences, University of California Los Angeles (jonmitch@ucla.edu)

Introduction: The ever-growing catalog of exoplanets presents us with an opportunity to answer many outstanding questions in planetary atmospheric dynamics. The growing number of observable targets with diverse planetary properties will likely fill gaps between the atmospheric circulation regimes that are known today. At the same time, future exploration of solar system planets will also improve our understanding of a myriad of processes that operate in these atmospheres. We anticipate that future progress in planetary atmospheric dynamics will be made through gaining more detailed understanding of the processes in atmospheres we can access in our solar system, as well as learning about the diverse outcomes, shaped by those same processes, manifested in exoplanets.

Known Atmospheric Dynamics Regimes: The basic circulation regime can be categorized using the prevailing zonal wind speed as a function of latitude. Regimes of the zonal winds that have been identified through observation are the following:

(1) Super-Rotation (e.g. Venus, Titan, Hot Jupiters): Atmospheric super-rotation is characterized by an atmosphere which has a higher angular momentum per mass than the underlying planet.

(2) Earth-like (e.g. Earth, Mars): Earth-like circulation has a small number of mid-latitude jets that blows prograde (i.e. in the direction of the planetary rotation). In the meridional dimension, the Hadley circulation transports the heat from tropical latitudes to mid latitudes, and the peak of the subtropical jet corresponds to be downwelling branch of the circulation.

(3) Jupiter-like (e.g., Jupiter, Saturn): In a Jupiter-like circulation regime, a broad, fast, equatorial jet blows in the prograde direction, surrounded by numerous mid-latitude jets. The width and number of the mid-latitude jets is believed to be controlled by how fast the rotation rate is (Jupiter and Saturn have rotation rate of ~10 hours).

(4) Ice Giant-like (e.g., Uranus, Neptune): The Ice Giants regime has a retrograde (direction opposite of the planetary rotation) equatorial flow, and a single prograde peak in each of the hemispheres.

Processes that Control Dynamical Regimes: Fundamental properties of planets and their atmospheres that affect the dynamical regimes include:

- Planetary Radius
- Rotation Rate
- Obliquity
- Solar Insolation / Energy Balance
- Presence and Types of Condensible Species
- Surface Pressure

Review and Outlook: In the coming years and decades, we anticipate that new discoveries in exoplanets will fill the gaps between atmospheric dynamics regimes known today. Ultimately, with enough observations and theoretical work, we expect that these distinct regimes will fit together as part of a large continuum. We also hope that future exploration of solar system planets will bring new breakthroughs; in particular, we anticipate that orbital survey of each of the planets with significant atmospheres will reveal how various atmospheric processes operate under different conditions. The planets that have been examined by orbital missions so far are Venus, Earth, Mars, Jupiter and Saturn; the next targets to be explored are Uranus and Neptune.

In our presentation, we will first review the known atmospheric regimes, and present our current understanding of how various processes contribute in shaping the observed dynamical regimes. Second, we will discuss how these processes may work in shaping cases that fall between the known regimes. Through these discussions, our overall objective will be to review fundamental open questions about the processes that shape and maintain these atmospheric dynamics regimes, and to identify future investigations that are needed to make progress.

Bibliography:

Mitchell, J. L., & Vallis, G. K. (2010). The transition to superrotation in terrestrial atmospheres. *Journal of Geophysical Research: Planets*, *115*(E12).

Read, P. L., et al. 2018. Comparative terrestrial atmospheric circulation regimes in simplified global circulation models. Part II: Energy budgets and spectral transfers. Quarterly Journal of the Royal Meteorological Society, vol. 144, issue 717, pp. 2558-2576

Sayanagi, K.M., Baines, K.H., Dyudina, U.A., Fletcher, L.N., Sanchez-Lavega, A., West, R.A., 2018, *Saturn's Polar Atmosphere*. in: Saturn in the 21st Century, p.337-376. Cambridge Univ. Press.

Showman, A.P., et al. 2013. *Atmospheric circulation of terrestrial exoplanets.* In: Comparative Climatology of Terrestrial Planets (S.J. Mackwell et al., Eds.), Univ. Arizona Press. pp. 277-326.

Showman, A.P., et al. 2019. *The global atmospheric circulation of Saturn.* In: Saturn in the 21st Century (K.H. Baines, F.M. Flasar, N. Krupp, and T.S. Stallard, Eds), Cambridge University Press

Wang, Y., et al. 2018. *Comparative terrestrial atmospheric circulation regimes in simplified global circulation models. Part I: From cyclostrophic superrotation to geostrophic turbulence.* Quarterly Journal of the Royal Meteorological Society, vol. 144, issue 717, pp. 2537-2557

Vasavada, A.R. and A.P. Showman 2005. *Jovian atmospheric dynamics: an update after Galileo and Cassini.* Reports on Progress in Physics 68, 1935-1996.

Incorporating Saturation Behavior of Magnetosphere-Ionosphere Interaction in Radio Emission Estimates for Extrasolar Planets. A. M. Sciola[1], F. R. Toffoletto[1], D. Alexander[1], and A. O. Farrish[1], [1]Rice University Department of Physics and Astronomy, 6100 Main St., Houston, Texas 77005; Anthony.M.Sciola@rice.edu.

Introduction: Coherent radio emission is observed at each magnetized solar system planet, suggesting that it is a fundamental product of interaction between a magnetized planet and the stellar wind of its host star and therefore should also be produced by magnetized exoplanets. The dominant emission mechanism is the Electron Cyclotron Maser Instability (ECMI) whose frequency is that of the local electron gyrofrequency, meaning that detection of ECMI emission from an exoplanet would provide information on the magnitude of the exoplanetary magnetic field. Such information is valuable in estimating parameters such as ionospheric escape rates and helps constrain planetary formation and dynamo models.

It has been found that the power of the radio emission produced at each magnetized solar system planet is linearly proportional to the incident solar wind power for average solar wind conditions, which is known as the Radiometric Bode's Law (RBL) [1-4]. It has been proposed that Hot Jupiters, Jupiter-like exoplanets which closely orbit their host star, are likely to experience an incident stellar wind power orders of magnitude greater than that seen at Jupiter and therefore should produce radio emission orders of magnitude greater than Jupiter's, which should be detectable by current radio telescopes in extreme cases. Despite this prediction, to date no such exoplanetary radio emission has been observed.

The linear relationship of the RBL suggests that the processes which convert stellar wind energy into emission energy in the planet's ionosphere all scale linearly with the stellar wind. On the contrary, it is found at Earth that the ionospheric potential, the magnitude of which is determined in part by the motional electric field of the solar wind, saturates for large values of the magnetic field carried by the solar wind. *Kivelson and Ridley (2008)* (KR08 hereafter) suggested that Alfvén wave reflection due to the mismatch between the solar wind Alfvén conductance and ionospheric Pedersen conductance explains this saturation behavior [5].

Method: We adopt the wave reflection formalism of KR08 to quantify the limiting of energy which is transferred from the solar wind to the planetary ionosphere, where we then assume an efficiency factor at which a proportion of the transmitted energy is converted to ECMI emission. While similar in form to RBL, this approach more readily accounts for the extreme conditions that a majority of the known closely-orbiting exoplanets are expected to experience, as it is estimated that these exoplanets would exist well within the saturation regime.

Results: For the unsaturated regime that solar system planets generally reside within, we find good agreement between our model and the powers predicted by RBL. For select exoplanetary systems where the planet is expected to experience saturation, our model predicts a radio emission of one to several orders of magnitude less than that predicted by RBL, with a strong dependence on the magnitude of the ionospheric conductance. Additionally we find that while the energy transmission becomes more proportionally limited for closer orbital distances, the total emission power that our model predicts still increases with decreasing orbital distance.

References: [1] Desch M. D. and Kaiser M. L. (1984) *Nature, 310*, 755-757. [2] Zarka P. (1992) *ASR, 12*, 99-115. [3] Zarka P. (1998) *JGR: Planets, 103*, 20159-20194. [4] Zarka P. et al. (2001) *Astrophysics and Space Science, 277*, 293-300. [5] Kivelson M. G. and Ridley A. J. (2008) *J Geophys. Res., 113*, A05214.

Planetary models contribute to studies of exoplanet habitability in an uncertain and statistical way J. Seales* and A. Lenardic, Rice University, Department of Earth, Environmental and Planetary Science, Houston, TX 77005, jds16@rice.edu

Introduction: It is thought that all but one terrestrial planet within our solar system has had water at its surface. Some suggest that Venus was potentially habitable for billions of years before an outpouring of CO2 drove the atmosphere towards its present state [1,2]. Mars, too, potentially had water at its surface prior to losing a large proportion with the rest being locked up in ice at present. Earth, on the other hand, has retained its surface water for billions of years, during which life has evolved and diversified. Each of these three planets were capable of sustaining life at some point in time; however, two did not retain their water because their evolutionary path did not allow it while Earth's path did.

The exact path a planet has taken is difficult to determine, but important for assessing life potential. We can use available constraints to assess the statistical range of evolutionary paths a planet could have taken. This then allows for the construction of probability distributions of planetary evolution. For example, using Earth data, the most rich data set we have, we can constrain model potentiality space consistent with observational data. Two constraints are of particular importance: surface and interior temperatures. The Earth system modulated surface temperatures between the freezing and boiling point of water for billions of years [3]. Earth's interior has cooled by hundreds of degrees over the previous three billion years [4]. Both data sets can be used to distinguish successful from unsuccessful Earth system models and to determine the probability distribution for Earth evolution models.

There is a lack of certainty on which particular Earth models to use – model selection uncertainty. In addition there are other layers of model uncertainty that need to be considered in a full analysis. For the Earth system, we can consider, at a minimum, the solar evolution, climactic evolution and interior evolution. Here we will use the solar modal of [5], a climate model that takes elements from both [6] and [7] and a range of interior models that allows us to test multiple hypotheses regarding how plate tectonics is thought to work on Earth [8-11]. After coupling these models together as our model Earth system, we also need to account for uncertainty in initial conditions, model input values, structural uncertainty, and the way uncertainty is accounted for. Doing so produces a distribution of possible surface and interior temperatures as a function of time. Comparing these resultant distributions to our observational data constraints provides the probability distribution for successful Earth models, subject to model and data uncertainties.

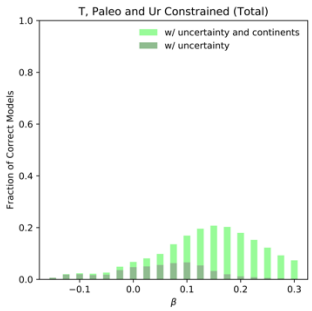

Figure 1: Fractional probability of successful models

Results: We initially considered this framework to constrain interior evolution models that allow for a range of assumptions regarding the physics of Earth cooling. The models rely on a parameterization between planetary heat loss and the vigor of convection within a terrestrial planets rocky interior. This is expressed through a Nusselt-Rayleigh number scaling, $Nu \sim Ra^{\beta}$, where Nu represents heat loss, Ra represents convective vigor, and the exponent β captures different physical assumptions. Generally, a higher value of β means convection is resisted by mantle viscosity. Decreasing β suggest that tectonic plate strength contributes to convective resistance. Decreasing β to zero assumes that heat flow remains fixed over time. When β takes on negative values, this assumes that thicker lithosphere is formed at higher temperatures and thus lower heat flows occur at higher temperatures. We compared a range of potential plate tectonic model predictions, subject layered uncertainty, to paleo and present day data constraints [e.g., 4, 12, 13]. Figure 1 shows the probability of success for each set of physical assumptions. We see that taking into account all of the data constraints and uncertainties, there is a range of models that have a higher probability of matching data constraints. However, we must not forget that though one model may be more probable than another, each model is consistent with Earth observations subject to model and data uncertainty. Therefore, what we actually have is the subset of permissible model evolution paths. This is insightful in that though the Earth has only been governed by one unique combination of physical/chemical conditions,

model and data uncertainty do not allow us to constrain these uniquely, i.e., we must accept a level of model ambiguity (multiple models, based on different physical assumptions, are permissible).

Discussion: As a next step, we can couple permissible paths from the interior model to a climactic model (again accounting for layered model uncertainties). The resultant output will be the set of possible climactic evolutionary paths that the Earth may have taken. Whether these paths are viable will be determined by comparing them to the surface temperature constraint. Delineating successful from failing models allows us to: 1) refine the set of hypothetical models that may have governed Earth's evolution, 2) refine the probability distribution for permissible Earth model evolutions, and 3) map out the range of potential paths that Earth-like planets may have taken.

Thus far we have restricted our analysis to Earth, but there are other potential applications of this workflow. For instance, one may vary the length of the window needed for maintaining liquid water at the surface and when this window is needed to occur during the planet's evolution to allow for life in order to assess the range of permissible interior dynamics. Furthermore, this workflow is not limited to a single tectonic regime. We could also apply it to of a single plate planet, Mars for instance. Though the Martian data is not as abundant Earth's, we do have some constraints on the interior evolution [14,15] as well as potentially when water was present. For Venus, however, we have even fewer data, particularly on the internal evolution, but we can take variable hypotheses about tectonic transitions and their timing to assess which are feasible. In total, each of these applications have a certain utility to help us understand the probability that life may be around some other star and highlight the need to think about this type of problem from an evolutionary rather than point perspective.

References:

[1] Ernst R.E. & Desnoyers D.W. (2004), *PEPI*, 146, 195.
[2] Way and Del Genio (2019), EPSC, Abstract #1846.
[3] Mojzsis et al. (2001), *Nature*, 407, 179-181.
[4] Ganne and Feng (2017), *Geochem Geophys Geosy*, 18, 872-888.
[5] Rushby et al. (2013), *Astrobiology,* 13, 833-849.
[6] Foley (2015), *Astrophys J*, 812, 36**.**
[7] Mello and Friaça (2019), *Int J Astrobiol*, 1-18.
[8] Korenaga (2003), *GRL*, 30, 47-63.
[9] Christensen (1985), *JGR*, 90, 2995-3007.
[10] Conrad and Hager (1999), *GRL*, 26, 3041-3044.
[11] Schubert et al. (1979), *Icarus*, 38, 192-211.
[12] Jaupart et al. (2007), Temperatures, Heat and Energy inthe Mantle of the Earth, volume 7. Elsevier B.V.,
[13] Herzberg and Asimow (2008), *Geochem Geophys Geosy*, 9, Q09001.
[14] Filiberto and Dasgupta (2015), *JGR*, 120, 109-122.
[15] Ruiz et al. (2011), *Icarus*, 215, 508-517.

Investigating the Interactions between Saturn's Upper Atmosphere and Rings from Cassini INMS Measurements. J. Serigano[1], S.M. Hörst[1], C. He[1], T. Gautier[2], R.V. Yelle[3], T. Koskinen[3], [1]Johns Hopkins University, Baltimore, MD, USA, [2]CNRS, Sorbonne Université, Guyancourt, France, [3]University of Arizona, Tucson, AZ, USA.

Cassini's Grand Finale: In September 2017, the Cassini-Huygens mission to the Saturn system came to an end as the spacecraft intentionally entered the planet's atmosphere. Prior to entry, the spacecraft executed a series of 22 highly inclined orbits, the Grand Finale orbits (26 April 2017 to 15 September 2017), through the previously unexplored region between Saturn and its extensive ring system, yielding the first ever direct sampling of the planet's upper atmosphere.

During these proximal orbits, the spacecraft obtained measurements near the equatorial ring plane at various heights above the planet's 1-bar pressure level. The final five of these orbits directly sampled Saturn's upper thermosphere. The spacecraft's last encounter, known as the final plunge, represents the deepest sampling of Saturn's atmosphere and provided measurements down to approximately 1370 km above the 1-bar pressure level before losing contact with Earth.

INMS Observations: The Ion and Neutral Mass Spectrometer (INMS) aboard Cassini returned a surprisingly complex mass spectrum from the planet's upper atmosphere. These first ever direct measurements enable the investigation of the chemical composition of the upper atmosphere, the thermal structure and energetics of the upper atmosphere, and the transfer of material from the rings to the atmosphere. The measurements were taken with the Closed Source Neutral (CSN) mode of INMS, which measures neutral species by ionizing the sampled molecules in order to detect the signature of the fragmented species. INMS has a mass range of 1 to 99 amu with a resolution of 1 amu.

Modeling: INMS measurements are complicated by the fact that multiple species contribute to the signal of individual mass channels, creating a complex combination of mass peaks associated with a mix of the fragmentation patterns of the species detected by the instrument. An accurate determination of the molecules present in the atmosphere must begin by first decomposing the spectrum in order to determine the relative contribution of each species to their respective mass channels. Due to a lack of proper calibration data for certain molecules, we decompose the mass spectrum using a mass spectral deconvolution algorithm that uses a Monte-Carlo approach to handle the uncertainty in fragmentation peak intensities of the molecules.

Results: INMS measurements of Saturn's upper atmosphere revealed a much more chemically complex region than previously believed (see Figure 1) with evidence of many molecules having an external origin into the atmosphere, most likely from Saturn's rings [1, 2, 3]. Recent work has also suggested that the mass influx of this neutral ring material entering the atmosphere is unsustainably large, approximately 10^4 kg/s. An influx of such magnitude would deplete the entire ring system in less than 10^6 years, leading to the speculation that the observed influx is time-dependent [2, 3].

We report here ongoing work to understand this mass spectrum and constrain the relative abundances of species present within the spectrum. Density profiles of major and minor constituents suggest that multiple species (along with CH_4) exhibit behavior indicative of an external source, and that Saturn's upper atmospheric composition is heavily influenced by infalling ring material.

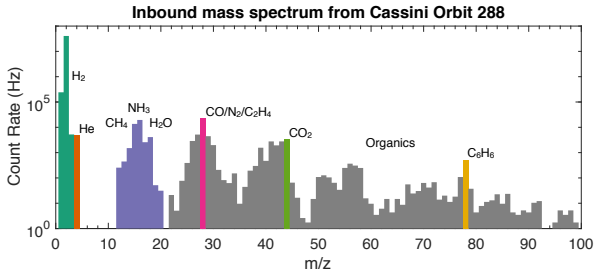

Figure 1: This mass spectrum of Saturn's upper atmosphere contains complex organic molecules that were not predicted prior to Cassini's proximal orbits.

References:

[1] Yelle, R. V., et al.: "Thermal Structure and Composition of Saturn's Upper Atmosphere From Cassini/Ion Neutral Mass Spectrometer Measurements." *Geophysical Research Letters*, 45.20, 10-951, 2018.

[2] Waite, J. H., et al.: "Chemical Interactions between Saturn's Atmosphere and its Rings." *Science*, 362.6410, eaat2382, 2018.

[3] Perry, M. E., et al: "Material Flux from the Rings of Saturn into its Atmosphere." *Geophysical Research Letters*, 45.19, 10-093, 2018.

Experimental Observations on Water-Rock Interaction at High Pressures and their Implications for the Interiors of Uranus and Neptune. S.-H. Shim[1], C. Nisr[1], T. Kim[2], Y. Lee[2], H. Chen[1], K. Leinenweber[1], A. V. G. Chizmeshya[1], S. Speziale[3], V. B. Prakapenka[4], C. Prescher[4], S.Tkachev[4], Y. Meng[5], and Z. Liu[6], [1]Arizona State University, Tempe, Arizona, USA (shdshim@asu.edu), [2]Yonsei University, Seoul, Korea. [3]Helmholtz-Zentrum Potsdam, Germany, [4]University of Chicago, Chicago, IL, USA, [5]rgonne National Lab, IL, USA, [6]George Washington University, Washington, DC, USA.

Introduction: Uranus and Neptune have a thick ice layer above the rocky core. Recent studies have suggested that the ice layer may contain significant amounts of heavier elements and possibly develop a compositional gradient [1, 2]. Although studies have used simple mechanical mixtures of H_2O and silicates, the state of materials remains uncertain in such H_2O rich conditions. Understanding water-rock interaction at high pressure-temperature is also important for water-rich exoplanetary bodies, such as waterworlds and sub-Neptunes which are common in our galaxy [3].

Recent high-pressure experiments have discovered oxides and silicates which can contain a few wt% of H_2O in their crystal structures [4]. However, these experiments are designed mostly for simulating H_2O undersaturated conditions of Earth's interior. In order to understand the water-rock interaction at high pressure and temperature conditions of the water-rich planets, we have conducted a series of experiments in laser-heated diamond-anvil cell combined with synchrotron X-ray diffraction and electron microscopy. In this abstract, we present experimental observations for H_2O-SiO_2. Our MgO-FeO-H_2O experiments are reported in T. Kim et al. in this meeting. We also discuss implications of these experimental results for the internal structure and dynamics of water-rich planets.

Experimental Methods: We loaded pure silica together with H_2O in diamond-anvil cells. Experiments were conducted at 7-110 GPa and 700-2000 K in laser-heated diamond-anvil cell. We have measured X-ray diffraction patterns during high-pressure experiments at the GSECARS sector of Advanced Photon Source. We measured infrared spectra and chemical compositions for the recovered samples. We also have conducted density functional theory calculations (DFT).

Results: Our data support large solubility of H_2O in the crystal structures of dense polymorphs of SiO_2 at high pressure and high temperature. (1) The recovered samples show anomalously expanded volumes (up to 4%) at 1 bar. Our DFT calculations indicate that such large volume expansion is consistent with H_2O incorporation up to $x = 0.2$ in $(Si_{1-x}H_{4x})O_2$. (2) The infrared measurements of the recovered samples found strong OH vibrational modes.

We also found that H_2O alters the phase behavior of SiO_2. For example, $CaCl_2$-type structure (distorted stishovite) appears at much lower pressures ~20 GPa in hydrous system. At pressures above 60 GPa, H_2O stabilizes a NiAs-type structure in hydrous system, which is not thermodynamically stable in dry SiO_2.

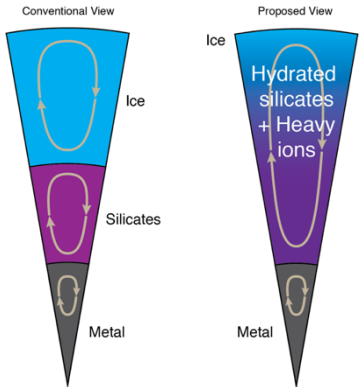

Figure 1: The internal structure of the water-rich planets. (Left) Conventional view. (Right) Proposed structure based on inter-solubility of rock and ice.

Discussion and Implications: Our experimental observations provide a possible explanation for the compositional gradient in the outer layer of water-rich planets. At shallower depths, because of low mutual solubility, nearly pure H_2O would be dominant. Because pressure would enhance the mutual solubility, hydrous silica may become dominant at greater depths, instead of separate layers of ice and rock (Fig. 1). Our experiments on (Mg,Fe)O + H_2O found a large solubility of Mg^{++} in H_2O at high pressure-temperature. Such an effect would also contribute to the compositional gradient proposed for Uranus and Neptune.

Because H_2O incorporation increases the compressibility of silica, the solubility of H_2O in silica could alter the mass-radius relations of water-world planets. Our initial result suggests that the conventional mass-radius relation based on separate ice and rock layers could underestimate the amount of H_2O, while the uncertainties in the current astrophysical measurements are too large to distinguish such an effect.

The large solubility of Mg^{++} in H_2O suggests that the deep rocky layer in the water-rich planet would

have silica-rich composition because of preferential leaching of Mg to the H_2O-rich layer.

It has been believed that the phase changes in H_2O play an important role for the observed magnetic field of Uranus and Neptune [5]. If significant amounts of rock components are dissolved in the H_2O layer as shown in our experiments, the properties of the ice layer can be altered. If the solubility of H_2O in SiO_2 and Mg^{++} solubility in H_2O gradually increases with pressure, materials transported by convection would undergo mixing and de-mixing in the interiors of water-world planets, affecting the geochemical cycle.

Acknowledgements: The work has been supported by NASA (80NSSC18K0353) and NSF (EAR1338810). The results reported herein benefit from NASA's Nexus for Exoplanet System Science (NExSS) research coordination network. S.-H.S. and H.C were supported by the Keck foundation. The synchrotron experiments were conducted at GSECARS, Advanced Photon Source (APS) (NSF, EAR-1128799) and (DOE, DE-FG02-94ER14466).

References: [1] Nettelmann N. et al. (2016) *Icarus* 275, 107-116. [2] Vazan A. and Helled R. (2019) arXiv:1908.10682. [3] Howard A. W. (2013) *Science* 340, 572-576. [4] Nishi M. et al. (2014) *Nature Geoscience* 7, 224-227. [5] Redmer R. et al. (2011) *Icarus*, 211, 798-803.

THE MATRIX OF LIFE FOR EXOPLANETS. G. P. Słowik[1] and P. Dąbrowski[2], [1]Department of Anatomy and Histology, Collegium Medicum, University of Zielona Gora, Zyty 28, 65-046 Zielona Gora, Poland, (grzegslowik@o2.pl), [2]Division of Normal Anatomy, Department of Human Morphology and Embryology, Wroclaw Medical University, Chalubinskiego 6a, 56-368, Wroclaw, Poland, (pawel.dabrowski@umed.wroc.pl)

Introduction: In order to determine the universal biomarkers of microbiological life in exoplanet biotopes, it is essential from the theoretical and empirical perspective to construct the so-called multi-division matrix of life (ML), containing quantified data on variability of environmental conditions. The ML is to inform about the peripheral adaptation possibilities of unicellular organisms known from terrestrial ecosystems, such as extremophilic bacteria and / or archaea - microorganisms discovered in 1977 [1] by molecular biologists Carl Woese and George Fox [2] and constituting an ingredient of the so-called third domain of life on Earth. Archeons differ from both prokaryotic and eukaryotic organisms. They live in the vicinity of hot hydrothermal chimneys located in the ocean rift zone at the depth of nearly 4000 m, hot volcanic springs on the Earth's surface, highly saline places, as well as the coldest Earth's polar zones. Because of their adaptability and survival skills in extremely adverse environments, they constitute a group of archetypal (model) organisms, which are theoretically capable of surviving on exoplanets. Until recently, extraterrestrial research focused on the detection of water as a universal solvent that is involved in all metabolic processes. Currently, the role of methane is emphasized (next to oxygen, which is one of the "canonical" biomarkers [3] on modern Earth) as an indicator of life, available not only as a result of geological processes (e.g. serpentineisation). Methane can be produced on a global scale by anaerobic microorganisms (methanogenic organisms), which include representatives of, for example, Methanosarcina genus, that has several species producing methane by three different metabolic pathways [4]. Therefore, objective assessment of survival skills, manifested in metabolic capacity, and the ability to transfer genetic information of microorganisms that are analogues of terrestrial unicellular forms requires the definition of variable chemical and biological parameters in the ML. The ML is a theoretical model of survival conditions correlated with forms of microorganisms that can theoretically show adaptive abilities in selected ecosystems of both researched exoplanets and their natural satellites.

The matrix of life and Scale of life: Below are selected elements of the ML, taking into account a group of local astrophysico-chemical, environmental (including climatic and hydrological) and geological factors characterizing a given exoplanet:

1. Astrophysical:
- distance from the mother star
- existence of a magnetosphere
- type of orbit
- speed of the exoplanet rotation around its axis
- presence of a planetary system
- diameter and mass of the exoplanet
- temperature (of the surface, water reservoirs and atmosphere)
- pressure (both in water reservoirs and atmosphere)
- presence of condensation centers in the atmosphere of the exoplanet
- presence of free electric current carriers in the atmosphere

2. Chemical:
- composition of gases forming the exoplanet atmosphere (the presence of CO_2, CO, O_2, O, CH_4, N_2)
- degree of acidity of the atmosphere and / or soil (pH value)
- salinity
- presence of Fe, S, P

3. Environmental (including climatic and hydrological):
- presence of water on the exoplanet (in different states of matter: solid, liquid or gas)
- glaciation
- geysers

4. Geological:
- type of the exoplanet surface
- geological activity of the planet's interior
- plate tectonics and rock-forming phenomena
- volcanism

Each element of the a_{nm} matrix of the life is assigned a statistical weight w_{nm}, which reflects the contribution of this element to the whole of the considered features of this matrix. The ML is important information about the astrobiological condition of a given exoplanet, and its reflection is a calculated value of the matrix of life determinant (so-called "determinant of life" - DL) (for each correlation of ML variables). The values of these determinants will in a stochastic and at the same time objective manner determine the possibilities of the emergence, proliferation and survival of life in the environment of a given exoplanet or its moon. As a result of grouping the values of determinants specified for each of the ML, one can obtain their natural gradient, which is a universal scale of life (SL).

Transferring life and potential terrestrial analogues of extraterrestrial life:

In consideration of the development of life on exoplanets and their natural satellites, attention should be paid to the possibility of "transferring" microbiological life between them. This possibility is provided by food chain substrates available in meteorites. A candidate among terrestrial analogues of extraterrestrial life, especially life in the clouds of Venus, able to survive on this type of cosmic objects, seems to be a microorganism whose terrestrial counterpart is the extremophilic bacterium - Acidithiobacillus ferrooxidans [5, 6]. The proposed mathematical models for the assessment of conditions for extraterrestrial life in the form of ML and SL will allow for better assessment and selection of future goals in the search for traces of life in the Universe.

References:

[1] Woese C.R. and Fox G.E. (1977), Proceedings of the National Academy of Sciences of the United States of America (Evolution), 74 (11), 5088-5090. [2] Woese C.R. et al. (1990), Proceedings of the National Academy of Sciences of the United States of America (Evolution), 87, 4576-4579. [3] Arney G.N. (2019), The Astrophysical Journal, 873:L7. [4] Holmes, D.E., Smith, J.A. (2016), Advances in Applied Microbiology, 97, 1-61. [5] [González-Toril E. et al. (2005) Astrobiology, 5 (3), 406-414. [6] Limaye S. et. al. (2018) Astrobiology 18 (9), 1181-1198.

Probing the Bulk Composition of Exoplanets with Engulfment Events.

M. Soares-Furtado[1], M. Cantiello[1,2], and M. MacLeod[3]
[1]Princeton University, [2]Flatiron Computational Center for Astrophysics, and [3]Harvard Center for Astrophysics

Introduction: As a star evolves away from the main sequence and expands in size, close-orbiting substellar companions are engulfed. While this process is common, the short tidal inspiral timescale makes it challenging to directly observe a planetary engulfment event. In my most recent work, , I explore the strength and survival time of the 7Li enrichment signature in the convective envelopes of cannibal stars. I demonstrate that engulfment signatures are observable at 5-sigma confidence levels up to one billion years after the engulfment event. I describe how we can refine our understanding of planet formation using these stellar cannibals.

TRANSMISSION AND EMISSION COLOR RATIOS FOR EXOPLANET CHARACTERIZATION. K.S. Sotzen[1,2], N.R. Izenberg[1], C.M. Lisse[1], K.B. Stevenson[1], J.J. Linden[1], S.M. Hörst[2,3], N.K. Lewis[4], K.E. Mandt[1]. [1]Johns Hopkins University Applied Physics Laboratory, Laurel, MD, USA, [2]Johns Hopkins University, Baltimore, MD, USA, [3]Space Telescope Science Institute, Baltimore, MD, USA, USA, [4]Cornell University, Ithaca, NY, USA. (11100 Johns Hopkins Rd, 200-E530, Laurel, MD 20723, USA, kristin.sotzen@jhuapl.edu)

The majority of exoplanets found to date have been discovered via the transit method, and transmission and emission spectra represent the primary method of studying these distant worlds. Current methods of characterizing transiting exoplanets entail the use of spectrographs on large telescopes, requiring significant observation time to study each planet. However, Crow et al (2011) showed that color-color reflectance ratios can be used to broadly categorize solar system bodies, and Sing et al (2016) and Stevenson (2016) showed trends in hot Jupiter water abundances as a function of blue-optical vs NIR/MIR altitude differences and temperature/gravity respectively. Building on these concepts, we are investigating the use of transmission and emission color-color ratios for coarse categorization of exoplanets (e.g., hot Jupiter, Jovian, ice giant, or Earth-like) as well as assessing the nature and habitability of these worlds. We will present our results to date, including spectrum modeling methods, model comparison frameworks, and waveband selection criteria.

This method could allow for broad characterization of a large number of planets much more efficiently than current methods permit. For example, a TESS follow-on mission could observe multiple band transits to identify exoplanets by category and to break degeneracies between planet size and density (e.g., rocky vs icy). Additionally, data collected via this method could inform follow-up observing time of large telescopes for more detailed study of worlds of interest.

Finally, these data could be used to study planetary system structure for different types and ages of stars, with potentially significant impact to our understanding of planetary system formation and evolution. This information would provide context for our solar system's formation and dynamical history as well as our commonality with potentially-habitable worlds and systems.

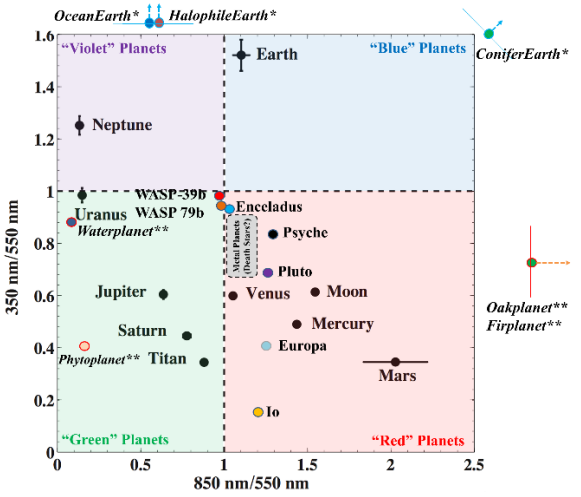

Figure 1 [4]. Color-color ratios expanded from [1]. The three bands that comprise the two color ratios are each 100 nm broad filters centered on the noted wavelength. The 350 nm/550 nm ratio can also be referred to as "UV/Vis", and the 850 nm/550 nm ratio is "IR/Vis." *Italicized are* model planets. (*)Model planets with Earthlike atmosphere from the Virtual Planetary Laboratory (VPL) [7,8]. OceanEarth is a water-covered planet. HalophileEarth is an organism-covered planet. ConiferEarth is a tree-covered planet. (**)Model planets with no atmosphere from [9-15]. Phytoplanet, Oakplanet, and Firplanet , are airless worlds covered by different organisms.

References:

[1] Crow *et al*., (2011) *Astrophys. J.* 729:130. [2] Stevenson, K.B., (2016). *Astrophys. J. Letters*. 817:2, L16. [3] Sing et al., (2015). *Nature*. 529. [4] Stickle et al., (2019). LPSC 50, # 2871. [5] Traub (2003), *ESA SP-539*. [6] Krissansen-Totton *et al*., (2016) *Astron J.* 817:31. [7] Meadows *et al*., (2001) *Bull. AAS* 33, 1114. [8] depts.washington.edu/naivpl/content/welcome-virtual-planetary-laboratory. [9] waspplanets.net/2018/03/02/comprehensive-spectrum-of-wasp-39b. [10] Bell *et al*., (1979). [11] Spencer *et al*., (1996) *Annu. Rev. Earth Planet. Sci.* 24: 125–190. [12] Verbiscer *et al*. (2005). [13] Kolaly *et al*., (1998) *JPL Publication 97-21*. [14] speclab.cr.usgs.gov/spectral.lib06/. [15] Schwieterman *et al*., (2018) *Astrobiology*18-6.

CANDIDATE DETECTION OF A HOT JUPITER AROUND A DISKED STAR. Asa G. Stahl[1] and Christopher M. Johns-Krull[1], [1]Department of Physics and Astronomy, Rice University, MS-108, 6100 Main St, Houston, TX 77005, USA

Motivation: Although the formation and evolutionary history of hot Jupiters (giant planets with P < 10 days) has profound implications for all planets, including terrestrial planets and potentially habitable worlds [1], it remains unclear how these enigmatic objects form [2]. It is unknown whether the population of hot Jupiters currently observed around main sequence stars is primordial or comprises the remnants of a much larger initial population destroyed by subsequent migration or tidal disruption [3]. Depending on how frequent hot Jupiter formation is as well as how and when they arrive at their current locations, forming hot Jupiters could destroy or disrupt the first generation of planets formed. Determining how hot Jupiters form is also thought to be our best means of investigating the orbital migration of planets via disk interactions [2], a process which represents a significant unknown in planet evolution despite its potentially transformative effects [4].

Observations of hot Jupiters around young stars, particularly those that still retain their protoplanetary disks, are important for investigating such issues because they directly probe systems during or soon after the epoch of planet formation and migration. However, there are major challenges to detecting planets around young stars. Pre-main sequence stars within the mass range of the Sun (T-Tauri stars) are highly active, and their spotted surfaces and variable accretion can easily drown out - or even mimic - planetary signals [5]. The first planet around a T-Tauri star young enough to still host its disk was confirmed this year [6]. More are needed to place sufficient constraints on the formation pathway(s) of hot Jupiters.

Observations: E204 is an M4.5 star surrounded by a primordial circumstellar disk and is part of the 4-12 Myr old [7] Upper Scorpius association [8,9]. E204's notable photometric dipping behavior was first discovered using K2 Campaign 2 photometry [10]. In analyzing more recent K2 Campaign 15 data, we find it exhibits dipping consistent in period and phase with that observed in Campaign 2 (Figure 1), implying that the structure obscuring its starlight is fairly stable on a timescale of at least ~2.5 years and hundreds of periods. Compared to common explanations for dipping phenomena (e.g. accretion and starspots), this is remarkably stable [11]. Instead, we postulate an inner disk warp stably maintained by a companion [12] best describes the observations.

In order to search for evidence of such a companion, we used the PHOENIX spectrograph on Gemini South to obtain K band radial velocity (RV) measurements of E204. We detected significant RV fluctuations suggestive of a planetary companion (Figure 2). The best fit to the RV data indicates a semiamplitude of 1537±290 m s^{-1} with a period of 2.589±0.089 days (consistent with the 2.645 day period of the photometric variations) and an eccentricity of 0.734±0.09.

Discussion: While stellar activity can often lead to RV false positives in surveys of T-Tauri stars, the amplitude and eccentricity indicated by our best fit are incompatible with a simple spot-induced signal. A semiamplitude of 1537 m s^{-1} is much larger than can easily be induced by a spot in the IR. SOAP 2.0 [13] spot simulations suggest that at the wavelength of our PHOENIX observations, a large spot (e.g. 20% the size of the visible stellar hemisphere) with a temperature difference from the photosphere of 500 K is expected to produce a semiamplitude of only ~65 m s^{-1}, over 20 times less than what is observed. Furthermore, spot-induced RV signals produce primarily symmetric variations, with changes of spot latitude and system inclination only altering the width or symmetrical skew of the RV curve. Spots are thus unlikely to produce the asymmetric RV variations of such an eccentric planet. We therefore consider the presence of an orbiting companion interacting with the circumstellar disk to be the best explanation for the current observations.

Summary: We have detected a candidate 2.2 M_{Jup} planet around a disk-hosting star in Upper Scorpius, which, if confirmed, would offer a powerful window into how hot Jupiters form and present an exceptional case study for theories of migration. If confirmed, this would be the second robust detection of a planet embedded in a disk, the first detection of a young hot Jupiter with e > 0.6, and the second potential detection of a hot Jupiter undergoing destructive migration. Such a discovery would provide major insight into the origin and early evolution of planetary systems and constrain the timescale of planet formation and migration.

References:

[1] R. Helled et al. (2014) *Protostars and Planets*

VI, 643-665. [2] R. Dawson and J. Johnson (2018) *Annual Review of Astronomy and Astrophysics*, 175-221. [3] J. Donati et al. (2016) *Nature*, 534, 662-666. [4] S. Paardekooper and A. Johansen (2018), *Space Science Reviews*, 214, 1. [5] C. Crockett et al. (2012) *ApJ*, 761, 164. [6] L. Flagg et al. (2019) *ApJ Letters*, 878, L37. [7] Fang et al. (2017) *ApJ*, 842, 123. [8] Ardila et al. (2000) *AJ*, 120, 479-487. [9] Rebull et al. (2018) *AJ*, 155, 196. [10] Ansdell et al. (2016) *ApJ*, 816, 69. [11] Cody et al. (2014) *AJ*, 147, 82. [12] Nealon et al. (2018) *MNRAS*, 481, 20-35. [13] Dumusque et al. (2014) *ApJ*, 796, 132.

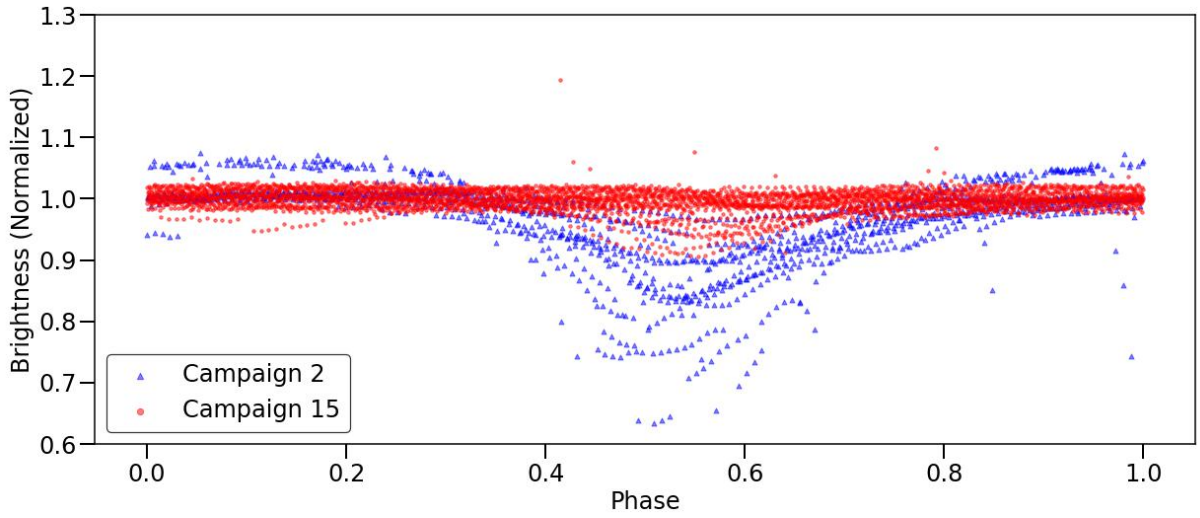

Figure 1: Phase-folded K2 lightcurve for E204. The latter half of of the Campaign 15 data is omitted for visual clarity, as the dips present are too shallow to be easily visible in a figure of this size.

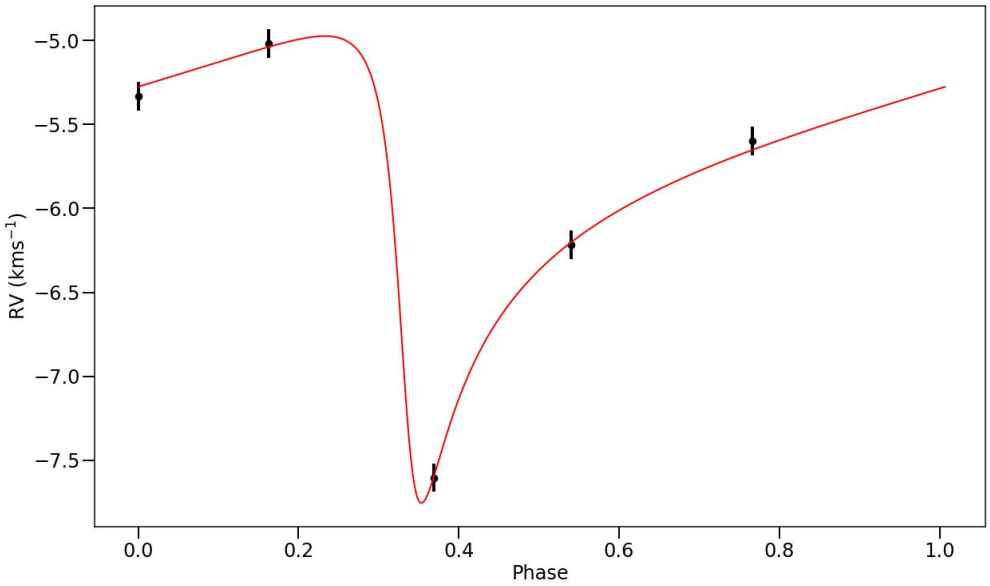

Figure 2: RV data for E204 with best fit.

EXO-OCEANS IN OUR BACKYARD: OUR SOLAR SYSTEM'S OCEAN WORLDS AS ANALOGUE HABITABLE ICE-COVERED EXOPLANETS. S. D. Vance[1], R. K. Barnes[2], and B. Journaux[3]. [1]Jet Propulsion Laboratory, California Institute of Technology (svance@jpl.caltech.edu), Pasadena, CA, 91109. [2]Astronomy Department, University of Washington, Seattle, WA 98195. [3]Dept. of Earth and Space Sciences, University of Washington, Seattle, WA 98195.

The Solar System's host of planetary bodies includes many ice-covered ocean worlds: Europa, Ganymede, and Callisto at Jupiter; and Enceladus, Dione, and Titan at Saturn being the best studied of these. The emerging study of these ocean worlds promises to reveal geodynamic and chemical processes that do not occur on Earth, but which may be common in moons and planets around other stars. Laboratory investigations, coupled with improved computational capabilities, are advancing the ability to predict the properties of these ocean worlds in a self-consistent way. These forward models can serve the science planning for exploration mission concepts (e.g., NASA's Europa Clipper and Dragonfly, and ESA's JUpiter ICy moon Explorer), which are set to reveal the nature of their surface geologic features, the dynamics of their icy lithospheres, and transport processes in their oceans.

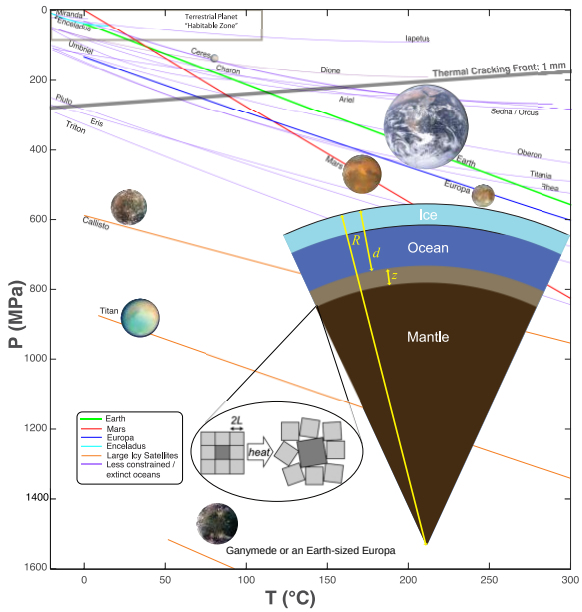

Figure 1. Pressure and temperature constrain the chemical and geodynamic properties of ocean worlds and of potential habitable ice-covered exoplanets (HICEPs). The different curves shown here employ models comprising a hydrosphere layer and an underlying solid layer. Geotherms begin at the seafloor. The fracture front for thermal cracking based on thermal expansion anisotropy is shown for olivine grain sizes of 1 mm. The inset depicts the resulting depth of fluid infiltration *z*. Modified from [2].

We will describe recent work modeling the extent of fluid-rock interactions in icy ocean worlds [1,2]. Figure 1 illustrates how the pressure and temperature regimes for ocean worlds in our solar system, and beyond, relate to basic constraints on water-rock interactions and other phenomena. Experimental efforts are improving our knowledge of the physical chemistry of solids and fluids in planetary hydrospheres [3,4] (e.g., Figure 2), and these data are being used in radial structure models seeking to constrain our knowledge of the thicknesses and compositions of the different layers within these worlds [5]. These efforts will help to distinguish among properties linked to planetary formation, evolution, and habitability, such as internal heat and redox state [5,6].

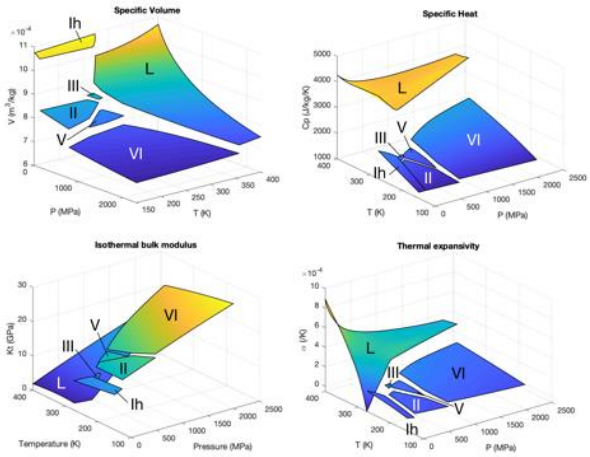

Figure 2. New experimental results are revising the body of fundamental data relevant to ocean worlds in the solar system and beyond, enabling detailed chemical and physical modeling. Contours show self-consistent thermodynamic properties—specific volume, specific heat, isothermal bulk modulus, and thermal expansivity—of solid (Ih, II, III, V, VI) and liquid water (L) from 150-400K and to 2000 MPa. From [4].

The icy worlds of our Solar System may also represent analogues to habitable ice-covered-exoplanets (HICEPS). With water the third most abundant molecule in the Milky Way and the Solar System as an example, we should expect that

numerous Earth-sized and larger planets exist beyond the classic habitable zone (HZ) that possess large inventories of water. These worlds will likely support large internal heat sources that sustain a subsurface liquid water layer. Moreover, their surface gravities are large enough to retain an atmosphere that includes molecules created in the water layer. Spectroscopy with next generation space telescopes thus offers a window into their interiors and the possibility of confirming the existence of a habitable layer. For the case of reflection spectroscopy, ice-covered worlds have higher surface albedo than planets with surface water oceans and hence spectral lines may be easier to detect, even if ice-covered exoplanets tend to be more distant from their host star.

In Figure 3 we show where "super-Europas," i.e. planets beyond the HZ that may be significantly tidally heated, can exist. TRAPPIST-1 h, orbiting a 0.09 solar mass star at 0.06 AU [7], may be a HICEP. In Figure 4 we show that *Kepler* may have discovered HICEPs. The sensitivity of the transit technique to HICEPs suggests that the application of experiments and modeling of the icy worlds in our Solar System will provide critical insight into the diversity of habitable environments in the universe.

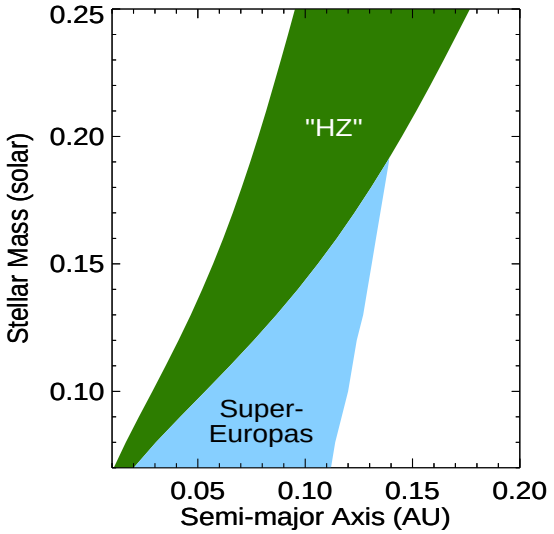

Figure 3: Comparison of the radiative HZ [8] to the plausible realm of super-Europas. For the latter, we assumed a 1 Earth-mass, 1 Earth-radius planet and the tidal heating model from [9], with a tidal Q of 100 and k_2 of 0.3. The light blue region is where planets beyond the HZ with eccentricities up to 0.5 will have surface energy fluxes due to tidal heating in excess of 0.1 W/m_2, which is the surface energy flux on Europa, scaled from Io [10].

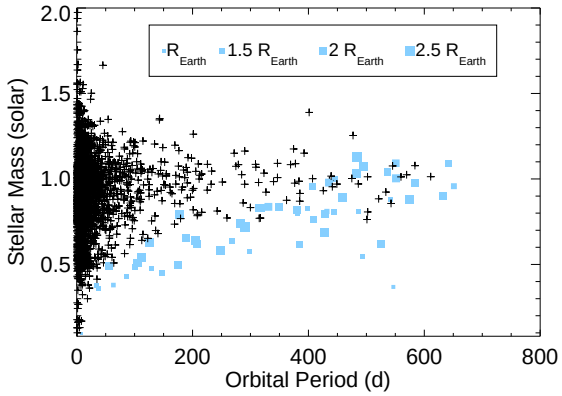

Figure 4: Potential HICEPs detected by the *Kepler* mission. We use the best-fit values for the candidates and planets and define a HICEP (light blue squares) to be any planet that receive less than 90% Earth's insolation. Plus symbols correspond to hotter planets/candidates.

References: [1] Vance et al. (2007) *Astrobiology*, 7(6):987–1005. [2] Vance et al. (2016) *GRL*, 10.1002/2016GL068547. [3] Bollengier et al. (2019) J. Chem. Phys. 151, 054501. [4] Journaux et al. (2019) ArXiv 1907.09598 (under review in JGR Planets) [5] Vance S. et al. (2018) *JGR-Planets*, 180-205. [6] Journaux et al. (2017). *Earth and Planetary Science Letters*, 463:36–47. [7] Luger, R. et al. *Nature Astronomy*, 1:129. [8] Kopparapu, R. *et al.*, (2013) *ApJ*, 765:131. [9] Barnes, R. (2019) *PASP*, in press. [10] O'Brien, D.P. et al. (2002), *Icarus*, 156: 152-161.

Surf, Sand, and Sun: Testing the Cosmic Shoreline using Ensemble Albedos

Monica Vidaurri (monica.r.vidaurri@nasa.gov)

The cosmic shoreline represents the dividing distance from a host star where gravitational escape velocity (v) is high, and insolation (or the bombardment of the star's rays, I) is low. This dividing line is defined as $I \propto v_{esc}^4$, and by applying this power law to the planets in a system, the cosmic shoreline can be visualized. Planets that exist on the side of the shoreline closest to the star can be said to lack volatiles, and exist within a zone that does not allow an atmosphere. Conversely, it can be assumed that planets existing on the side of the shoreline furthest from the star may have an atmosphere. To test the known power law that defines the cosmic shoreline, data from the Kepler confirmed planets list is split into two bins: Terrans and Neptunes. Sub-bins are then created to separate those with atmospheres and those without, utilizing the cosmic shoreline power law. Ensemble albedo is generated from this data, and placed against the cosmic shoreline plots of these bins. The ongoing study is utilizing the Python program *phasma* in order to generate ensemble phase curves, and serves as a model for a new program that will generate ensemble albedos. While a confident mass-radius relationship can be used to define a Terran ensemble, the program *forecaster* is used to determine the constitution of the Neptunes ensemble, as opposed to historically ambiguous mass-radius relationships with Neptunes. Re-creating this data with TESS confirmed Terrans + Neptunes will be the next step in validating the results gained from the initial Kepler ensemble albedos.

Possible climate histories of Venus type worlds. M. J. Way[1] and A. D. Del Genio[1], [1]NASA Goddard Institute for Space Studies, 2880 Broadway, New York, New York, USA (michael.j.way@nasa.gov)

Introduction: There are two well-known scenarios for Venus' climate evolution. In one Venus had a long-lived magma ocean phase in its first 100Myr with a steam and CO_2 dominated atmosphere [1]. The faint young sun with its high XUV flux would cause photodissociation of the steam atmosphere and hydrodynamic escape would cause most of the hydrogen to escape and the left over oxygen would be absorbed by the magma ocean. Hence Venus would have started out hot and dry and the high D/H ratio measured by Pioneer Venus [2] would be from this period of water loss. The other scenario is that Venus' magma ocean lifetime would have been roughly the same length of time as Earth's (~1Myr) and water would have condensed on its surface in its early history. As long as Venus remained in the slowly rotating climate dynamics regime [3,4] its cloud albedo feedback would have kept it temperate for possibly billions of years. The only way to confirm which one of these scenarios occurred for Venus is to visit it and make the necessary measurements of noble and volatile gases [5]. But exoplanet observations of young exo-Venus type worlds around young F,G,K dwarf stars may constrain whether both scenarios are equally probable for a population of such planets. We present a vision of Venus' climate history that places it and its exo-Venus cousins in an 'Optimistic Venus Zone' within the conventionally named 'Venus Zone' [6] and hence encourage the exoplanet community to seek out these worlds as possible habitable environments.

Methods: We use ROCKE-3D, a three-dimensional general circulation model [7] to model 4 different types of topographies & water inventories (see Figure 1):

1.) Arid-Venus: Modern Venus topography with 20 cm of water stored in the soil at model start. One can think of this as a Dune type world.
2.) 10m-Venus: Modern Venus topography with 10m water equivalent layer placed in the lowest lying topographic regions at model start. See top image in Figure 1.
3.) 310m-Venus: Modern Venus topography with 310m water equivalent layer placed in the lowest lying topographic regions at model start. See middle image in Figure 1.
4.) 310m-Earth: Modern Earth type topography and land sea mask with a 310 meter deep bathtub ocean. See bottom image in Figure 1.

These water inventories fit within the error estimates of the Pioneer Venus D/H ratio measurements [2]. We then model several different atmospheres at different time-slices. 10Bar CO_2 dominated at 4.2Ga, 1 Bar CO_2 dominated at 4.2Ga, 1Bar N_2 dominated (modern Earth like composition) at 2.9Ga, 0.25Bar N_2 dominated at 2.9Ga, 1Bar N_2 dominated at 0.715Ga, Present day, and several Gigayear into the future (Figure 2). We use present day rotation rate & obliquity for all simulations in Figure 2.

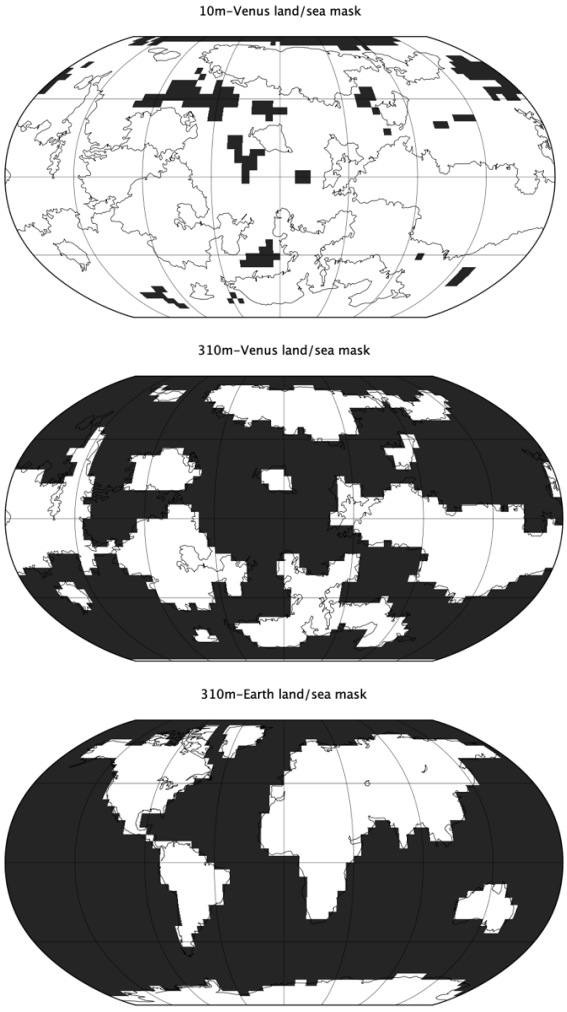

Figure 1: Black = ocean/lakes, white = land.

Results: Figure 2 shows a sketch of our final results. Each error bar contains the mean surface temperature of the four different topographies mentioned in the Methods section. The 10bar atmosphere at 4.2Ga has surface temperatures over 120C, but the higher pressure means that surface liquid water can still condense on the surface. The 1bar CO_2 atmospheres at 4.2Ga are warm, but none are over 90C. We then assume that a carbonate-

silicate cycle begins to work (as it did in early Earth's history) and N_2 dominated atmospheres (akin to that of modern Earth) take over sometime between 4.2 and 2.9Ga. We also include 1 set of simulations at 2.9Ga with 0.25Bar atmospheric density. This is inspired by atmospheric proxies in Earth's Archean epoch [8,9]. As one can see these cases are much cooler and there are grid cells with subzero temperatures. Going forward in time it is clear that the mean surface temperatures remain moderate even with insolations more than double that received by modern day Earth. This implies that it is not the increase of solar insolation through time that may have changed Venus' climate from temperate to its current hothouse state. We speculate that it was a series of simultaneous Large Igneous Provinces (i.e. The Deccan or Siberian traps on Earth) that would have loaded the atmosphere with large amounts of CO_2, This would have increased surface temperatures and boiled off any shallow ocean, shutting down subductive plate tectonics and associated weathering processes. CO_2 would eventually become the main outgassing component as described in [10]. This scenario also fits in nicely with recent work by [11] that shows the timescale for a transition from a mobile to a stagnant lid plate tectonics would take ~1Gyr. This may imply a connection with the age of 80% Venus' surface being ~750Myr old.

Exoplanet Connection: We would like to emphasize that if this "optimistic" scenario for Venus is correct then we should be cautious about concluding that extrasolar planets in the 'Venus Zone' outside the conventional 'Habitable Zone' are uninhabitable [6]. Hence we stress the need to search for young Venus type worlds around F, G and K dwarf stars (it is difficult to make the necessary observations of young exo-Venus' around M-dwarfs due to their activity) to see if they indeed retain a steam atmosphere for ~100Myr. If not, and they are slow rotators (sidereal day lengths of 64 Earth days or longer) they may indeed host clement conditions despite residing well inside the traditional habitable zone.

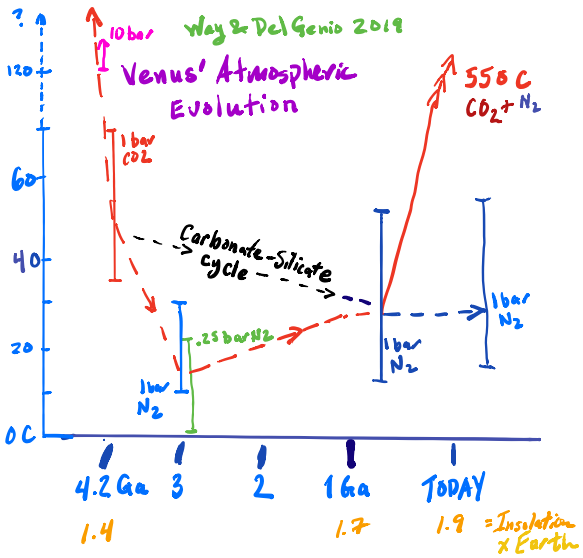

Figure 2: Possible climate evolution of Venus. Each error bar contains the mean surface temperatures for each topography mentioned in the Methods section.

References:

[1] Hamano et al. (2013) Nature 497 607.
[2] Donahue et al. (1982) Science, 216 , 630.
[3] Yang et al. (2014) ApJL, 787 L2.
[4] Way et al. (2018) ApJS, 239, 24.
[5] Baines et al. (2013) CCTP2, 137. 10.2458/azu_uapress_9780816530595-ch006
[6] Kane et al. (2014) ApJL, 794, L5.
[7] Way et al. (2017) ApJS, 231, 12
[8] Som, et al. (2012) Nature, 484 , 359
[9] Som et al. (2016) Nat.Geo., 9 , 448
[10] Gaillard & Scaillet (2014) EPSL 403, 307
[11] Weller & Kiefer (2019) JGRP 10.1029/2019JE005960

ENVISION : EUROPE'S PROPOSED MISSION TO VENUS. T. Widemann[1], R. C. Ghail[2], C. F. Wilson[3], D. V. Titov[4] and the EnVision Team, [1]Paris Observatory, Meudon, France, [2]Royal Holloway, University of London, United Kingdom, [3]Univ Oxford, Oxford, United Kingdom, [4]ESA- ESTEC, Noordwijk, Netherlands.

Introduction: EnVision [1,2] is a Venus orbiter mission that will determine the nature and current state of geological activity on Venus, and its relationship with the atmosphere, to understand how and why Venus and Earth evolved so differently. EnVision is one of three ESA M5 missions in Phase A study with a final down-selection expected in June 2021. The EnVision mission is studied in collaboration with NASA, with the potential sharing of responsibilities currently under science, technical and programmatic assessment.

If selected, the proposed mission will launch in late November 2032 on Ariane 62. Following orbit insertion and periapsis walk-down, orbit circularisation will be achieved by aerobraking over a period of several months, followed by a nominal science phase lasting at least 4 Venus days (2.7 Earth years).

EnVision will use a number of different techniques to search for active geological processes, measure changes in surface temperature associated with active volcanism, characterise regional and local geological features, determine crustal support mechanisms and constrain mantle and core properties :

The **Synthetic Aperture Radar, VenSAR**, will:

- Obtain images at a range of spatial resolutions from regional coverage to images of targeted localities;
- Measure topography from stereo and InSAR observation;
- Characterize volcanic and tectonic activity, estimate rates of weathering and surface alteration; and
- Characterize surface mechanical properties and weathering through multi-polarisation radar, and emissivity mapping.

The **Subsurface Sounder, SRS,** will:

- Characterize the vertical structure and stratigraphy of geological units including volcanic flows; and
- Determine the depths of weathering and aeolian deposits.

The **Venus Spectrometer suite, VenSpec,** will:

- Obtain global maps of surface emissivity in five wavelength bands in the near-infrared to constrain surface composition and inform evolution scenarios [3]; and
- Measure variations of SO2, SO and chemically-related gaseous species in the mesosphere and nightside troposphere, in order to link these variations to atmospheric dynamics, chemistry and volcanism.

The **Radio Science & Geodesy** investigation will:

- Constrain crustal & lithospheric structure at finer spatial scale than Magellan; and
- Measure spin rate and spin axis variations to constrain interior structure.

EnVision will produce a huge dataset of geophysical data of a quality similar to that available for Earth and Mars, and will permit investigation across a large range of disciplines. Lab-based and modelling work will also be required to interpret results from the mission. We therefore invite scientists from across planetary, exoplanetary and earth science disciplines to participate in the analysis of the data.

References:

[1] Ghail R. C, Wilson, C., Widemann, T., Bruzzone, L., Dumoulin, C., Helbert, J., Herrick, R., Marcq, E., Mason, P., Rosenblatt, P., Vandaele, A. C., Burtz, L. J. (2016) EnVision M5 proposal, https://arxiv.org/abs/1703.09010

[2] www.envisionvenus.eu

[3] Helbert, J., Dyar, D., Widemann**, T**., Marcq, E., Walter, I., Guignan, G., Wendler, D., Mueller, N., Kappel, D., Arnold, G., D'Amore, M., Maturilli, A., Ferrari, S., Tsang, C., Boerner, A., Jaenchen, J., Smrekar, S. (2018), The Venus Emissivity Mapper (VEM) – obtaining global mineralogy of Venus from orbit, *SPIE Proc., Infrared Remote Sensing and Instrumentation* XXVI, San Diego, CA (2018).

Measurements of the Ultraviolet Spectral Characteristics of Low-mass Exoplanetary Systems (Mega- MUSCLES).

David J. Wilson[1] and the Mega-MUSCLES Collaboration, [1]Mcdonald Observatory, University of Texas at Austin, djwilson394@gmail.com.

M dwarf stars have emerged as ideal targets for exoplanet observations. Their small radii aids planetary discovery, their close-in habitable zones allow short observing campaigns, and their red spectra provide opportunities for transit spectroscopy with JWST. The potential of M dwarfs has been underlined by the discovery of remarkable systems such as the seven Earth-sized planets orbiting TRAPPIST-1 and the habitable-zone planet around the closest star to the Sun.

However, to accurately assess the conditions in these systems requires a firm understanding of how M dwarfs differ from the Sun, beyond just their smaller size and mass. Of particular importance are the time-variable, high-energy ultraviolet and x-ray regions of the M dwarf spectral energy distribution (SED), which can influence the chemistry and lifetime of exoplanet atmospheres, as well as their surface radiation environments. Ideally, ultraviolet and x-ray observations should be obtained for any star with exoplanets of interest. Unfortunately this is impractical as those wavebands are extremely faint for most M dwarfs, requiring too large an investment of telescope time to obtain data at most stars.

The Measurements of the Ultraviolet Spectral Characteristics of Low-mass Exoplanetary Systems (Mega-MUSCLES) Treasury project, together with the precursor MUSCLES project, aims to produce full SEDs of a representative sample of M dwarfs, covering a wide range of stellar mass, age, and planetary system architecture. We have obtained x-ray and ultraviolet data for 12 stars using the Hubble, Chandra and XMM space telescopes, along with ground-based data in the optical and state-of-the-art DEM modelling to fill in the unobservable extreme ultraviolet regions. Our completed SEDs will be available as a community resource, with the aim that a close MUSCLES analogue should exist for most M dwarfs of interest.

In this presentation I will overview the Mega-MUSCLES project, describing our choice of targets, observation strategy and SED production methodology. I will also discuss notable targets such as the TRAPPIST-1 host star, comparing our observations with previous data and model predictions. Finally, I will present an exciting by-product of the Mega-MUSCLES project: time-resolved ultraviolet spectroscopy of stellar flares at multiple targets, spanning a range of stellar types, ages and flare energies.

Abiotic Oxygen on Venus-Like Exoplanets Around M-Dwarfs

Michael L. Wong[1,2], Victoria S. Meadows[1,2], Peter Gao[2,3], Carver J. Bierson[4], Xi Zhang[4]
[1]Department of Astronomy & Astrobiology Program, University of Washington, Seattle, WA
[2]Virtual Planetary Laboratory, Seattle, WA
[3]Department of Astronomy, UC Berkeley, Berkeley, CA
[4]Department of Earth & Planetary Sciences, UC Santa Cruz, Santa Cruz, CA

Introduction: Terrestrial exoplanets in the habitable zones of nearby M dwarfs represent the first targets for the search for life outside of the Solar System. Atmospheric oxygen (O_2) is considered to be a canonical biosignature based on the high O_2 content (~21% by volume) of Earth's present-day atmosphere, the overwhelming majority of which comes from oxygenic photosynthesis: $CO_2 + H_2O + \text{light} \rightarrow CH_2O + O_2$. Thus, it has been long thought that one of the most obvious biosignatures on alien worlds would be the spectroscopic detection of O_2 (or its photochemical product O_3) created by a global biosphere of photosynthetic life forms (Meadows et al., 2018). However, recent studies have shown that large amounts of O_2 can be created abiotically—especially on terrestrial planets around M dwarfs. In particular, Gao et al. (2015) showed that desiccated worlds with CO_2-rich atmospheres can build up ~15% O_2 via CO_2 photolysis.

Terrestrial planets with CO_2-rich atmospheres may be common in M-dwarf systems. During an M-dwarf's prolonged pre–main sequence phase, its planets receive far greater instellations than they will during the star's main-sequence lifetime. Thus, many terrestrial planets within an M dwarf's main-sequence habitable zone might have been driven into runaway greenhouses early on, evolving into hot, Venus-like states (Luger & Barnes, 2015). These thick, CO_2-rich atmospheres have the potential to create large amounts of O_2 via photochemistry alone.

Venus, however, has little atmospheric O_2, despite ongoing CO_2 photolysis. This has been attributed to catalytic cycles involving ClO_x and SO_x that regenerate CO_2 from CO and O (Mills et al., 2007; Yung & DeMore, 1999). We seek to ascertain how these cycles behave on Venus-like planets with different outgassing rates around different types of stars.

Model: We have constructed a 1-D photochemical model based on Zhang et al. (2012) to study the atmospheric chemistry of Venus-like extrasolar planets. The model simulates 464 chemical reactions between 68 chemical species composed of H, C, O, N, S, and Cl. The atmosphere is primarily composed of CO_2 (~90 bars) and N_2 (~3 bars) with trace amounts of H_2O, SO_2, OCS, HCl, and other constituents. These trace species contribute the HO_x, ClO_x, SO_x, and NO_x catalysts that can recombine photochemically generated CO and O into CO_2. We assume that the surface mixing ratios of trace atmospheric species are controlled by surface mineralogical buffers relevant to Venus (Zolotov 2018). We compare the effect of G- and M-dwarf spectral energy distributions on Venus-like worlds, placing the planets at orbital distances with the same total incident flux as Venus.

Preliminary results: Different spectral energy distributions result in different O_2 buildup. FUV photons drive CO_2 photolysis, while NUV photons drive catalyst production. The high FUV/NUV ratio of TRAPPIST-1 can cause a Venus-like planet to contain several percent O_2 in the upper atmosphere. However, around a Sun-like star, where the NUV flux outweighs the FUV flux by orders of magnitude, the column density of O_2 is limited to < 1 ppb.

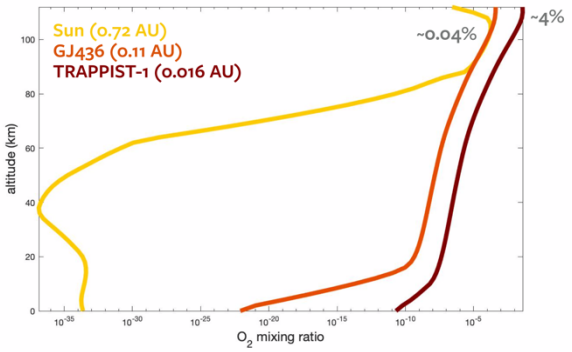

Figure: O_2 profiles of a Venus-like world around the Sun (G2V; yellow), GJ 436 (M2.5V; orange), and TRAPPIST-1 (M8V; maroon).

References: Gao, P. et al. (2015) *ApJ* 806:249. Luger, R. & Barnes, R. (2015) *Astrobiology* 15(2) 119–143. Meadows, V.S. et al. (2018) *Astrobiology* 18(6) 630–662. Mills, F. P. et al. (2007) *AGU* 73–100. Yung, Y. L. & DeMore, W. B. (1999) Oxford University Press. Zhang, X. et al. (2012) *Icarus* 217(2) 714–739. Zolotov, M. Y. (2018) *Rev. Mineral. Geochem.* 84 351–392.

WATER-CO_2-BASALT INTERACTIONS ON TERRESTRIAL PLANETS AND EXOPLANETS. M. Yu. Zolotov, School of Earth and Space Exploration, Arizona State University, Tempe, AZ 85287-1404. E-mail: zolotov@asu.edu.

Introduction: Basalts are the most abundant surface rocks on terrestrial planets, and H_2O and CO_2 are the main products of volcanic degassing on Earth. In the Earth's history, water-CO_2-rock reactions affected speciation of atmospheric gases and surface waters, mineralogy of altered rocks and chemical sediments, and surface temperature [1, 2]. On Earth and Mars, masses and compositions of crustal carbonates provide constraints on past CO_2-bearing aqueous environments. On Mars, carbonates in weathering profiles [3] and some climate models [4] imply an early dense CO_2 atmosphere. Venus' current CO_2-rich atmosphere could reveal thermal decomposition of ancient water-deposited carbonates. CO_2-bearing habitable zone (HZ) exoplanets have been discussed as well [1, 2, 5-10]. The outstanding question is what atmospheric CO_2 can tell us about a HZ planet? Here we further evaluate chemistry and mineralogy of CO_2-bearing environments.

Models: We explore how water/CO_2/rock ratios, CO_2 fugacity (f < 0.5 MPa), temperature (T < 200 °C) and pressure (P < 500 MPa) affect compositions of solid, aqueous and gas phases through calculations of chemical equilibria in the water-CO_2-basalt system. Open system calculations are performed at fixed $f$$CO_2$. The rock is presented by Archaean magnesian basalt [11] in which all Fe is in ferrous (Fe^{2+}) form. Formation of hydrocarbons is suppressed because their low-P formation is inhibited at T < 200 °C. Amounts of water and rock are referred to masses of surface water bodies and permeable rocks. The runs are performed with the *GEOCHEQ* code used elsewhere [e.g. 12].

Results: Secondary mineralogy and composition of aqueous and gas phases are non-linearly affected by water/CO_2/rock ratios and $f$$CO_2$ (Fig. 1). Systems with variable CO_2 content ($x$$CO_2$) and open systems with variable $f$$CO_2$ reveal roughly similar results. Increasing of $x$$CO_2$ or $f$$CO_2$ leads to sequential formation of carbonates (calcite, dolomite, siderite and sometimes magnesite). The increase in the carbonate content corresponds to formation of more Si/Al-rich solids. Sparse calcite coexists with Fe/Mg-rich smectites (saponite) and zeolites, while abundant Ca-Mg, Fe and Mg carbonates form with Si/Al-rich phyllosilicates and silica minerals (talc, beidellite, montmorillonite, kaolinite, amorphous silica). Formation of abundant silica at elevated $x(f)$ CO_2 corresponds to a maximum amount of carbonates (Fig. 1a). Further increase in $x(f)$ CO_2 does not cause formation of carbonates and favors dissolution of Fe and Mg carbonates in increasingly more acidic solution. In CO_2-poor systems, the rock strongly

Fig. 1. Chemical equilibrium speciation of the water-CO_2-basalt system as a function of $f$$CO_2$ at the water/rock mass ratio of 3, 25 °C and 1 bar total pressure. a, Mineralogy; b, aqueous solution, c, pH; d, gas phase. Dol, dolomite; sid, siderite; ms, magnesite; am. SiO_2, amorphous silica; CO_2,aq, dissolved CO_2^0.

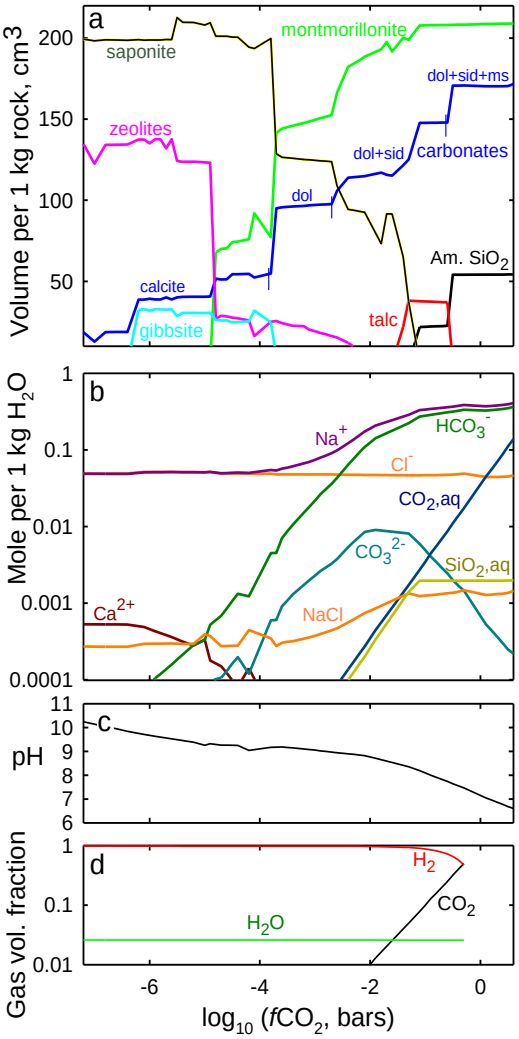

affects composition and acidity (pH) of aqueous solution in which Na^+ and Cl^- ions dominate. At elevated $x(f)$ CO_2 values, Na^+, HCO_3^- and CO_2,aq dominate in solution and the pH is strongly affected by dissolved CO_2. The CO_2,aq/(HCO_3^- + CO_3^{2-}) ratio increases as solution becomes more acidic (Fig. 1b,c). The gas phase consists of H_2, H_2O, and CO_2. CO_2 gas is abundant in equilibrium with low-pH solution and Si/Al-rich solids formed via an advanced alteration of basalt.

Deeper surface water reservoirs (higher water/rock ratios and pressures) accumulate more inorganic C and favor formation of Al/Si-rich phases at the water-rock interface. An increase in the water/rock mass ratio (e.g. beyond ~10^4 at 25 ^{o}C) causes sequential dissolution of carbonates and Si/Al-rich phases (talc, silica, montmorillonite, beidellite, kaolinite and then gibbsite/diaspore) in increasingly lower-*pH* solution (due to lesser concentrations of cations at a fixed fCO_2).

Could CO_2-rich atmospheres be common on HZ planets? The models suggest that atmospheres of terrestrial planets (early Venus, Earth and Mars) and HZ exoplanets with surface water may contain dense CO_2 atmospheres only if (1) a significant surface area is covered by a thick layer of minerals that are sparingly soluble in acidic solutions (silica, Al-rich clay minerals, Al hydroxide/oxyhydroxide), (2) the layer is impermeable and (3) a significant CO_2 mass is supplied. Although all three conditions may not be reached on a majority of terrestrial HZ planets, variations in occurrence, thickness and permeability of weathering crusts, and in CO_2 supply should affect atmospheric fCO_2.

Dense CO_2 atmospheres may not form if CO_2 is supplied by magma only. CO_2 is a low-solubility gas in silicate melts [13] and erupting basalts contain more than enough cations to trap all degassed CO_2 to carbonates. Though, CO_2 could be supplied by metamorphic decarbonatization (e.g. during a runaway greenhouse heating of past Venus' crust) and cometary ices.

Dense CO_2 atmospheres may not exist on terrestrial HZ planets with abundant surface water and active resurfacing by erosion, impacts and/or volcanism. A rapid aqueous deposition of carbonates in weathering crusts, lakes etc. could have prevented any prolonged existence of such atmospheres on early Earth, Mars and Venus. Such atmospheres may not exist on HZ planets with thin permeable layers of surface Si/Al-rich phases because carbonates could precipitate in middle parts of weathering profiles from neutralized solutions on land [3, 12] and below water reservoirs [8]. Subduction, burial or other submergence [e.g. 1, 2, 9] of carbonate-bearing rocks isolate CO_2 in temporal crustal reservoirs that compose a majority of planetary CO_2 abundance.

Common HZ planets with deep water oceans may not have dense CO_2 atmospheres as well. A significant amount of CO_2 could be dissolved in cold pressurized waters [7, 10, this work], especially in alkaline Na-rich solutions formed through water-rock interaction ('soda oceans'). Elevated pressures beneath ocean floors suppress silicate melting and degassing of magmas, if they form. Huge masses of cometary CO_2 are needed to acidify deep oceans and form Si/Al-rich minerals at the ocean floors. CO_2 hydrates could form at the bottom of low-*pH* oceans [10]. Though, high pressure and a limited volcanic/erosional/impact resurfacing at deep oceanic floors favor formation of low-permeability layers that limit water-rock interaction and trapping of inorganic carbon species in carbonates.

Desert HZ planets with sparse surface water bodies, rare rains and a rapid CO_2 supply could have CO_2-rich atmospheres. As on today's Venus, high-pressure CO_2-rich atmospheres could indicate kinetically suppressed trapping of degassed CO_2 without liquid water.

Elevated temperature decreases CO_2 solubility in water but favors precipitation of carbonates (by both thermodynamic and kinetic reasons) that stabilizes the greenhouse temperature [e.g. 1, 2]. Overall, dense CO_2 atmospheres could be less likely on planets with warm oceans.

Mineralogy could reveal CO_2-rich environments: A presence of silica and/or Si/Al-rich minerals in aqueously-deposited geological formations may indicate elevated CO_2/(rock + water) ratios and fCO_2 at the time of precipitation. In the solar system, possible examples are Archean SiO_2-rich banded iron formations [14], upper parts of Noachian weathering profiles on Mars [12, 15] and a subsurface water ocean on Enceladus that emits icy grains with Na carbonates and silica [16, 17]. A detection of Si/Al-rich chemical sediments on Venus' tessera terrains could be indicative of past CO_2-rich aqueous environments, and a detection of Na-rich salt deposits or flows (e.g. in channels [18]) may inform about past seas [19]. Likewise, a direct or indirect detection of abundant Si/Al-rich minerals and carbonates on Venus-like exoplanets could be interpreted in terms of past CO_2-rich aqueous processes.

References: [1] Kasting J. F. and Catling D. (2003) *Annu. Rev. Astron. Astrophys*., *41*, 429–463. [2] Kasting J. F. et al. (1993) *Icarus*, *101*, 108–128. [3] Bulter B. et al. (2019) *JGR-P*, *124*, 989–1007. [4] Wordsworth R. D. (2016) *Annu. Rev. Earth Planet. Sci*., *44*, 381–408. [5] Abbot D. S. et al. (2012) *Astrophys. J*., *756*, 178–191. [6] Kitzmann D. et al. (2015) *MNRAS*, *452*, 3752–3758. [7] Levi A. et al. (2016) *Astrophys. J*., *838*, 24. [8] Krissansen-Totton J. et al. (2018) *PNAS*, *115*, 4105–4110. [9] Foley B. J. and Smye A. J. (2018) *Astrobiology*, *18*, 873–896. [10] Marounina N. and Rogers L. A. (2019) arXiv:1904.10458. [11] BVTP Project (1981) Lunar and Planetary Institute. page 16, #1. [12] Zolotov M. Yu. and Mironenko M. V. (2016) *Icarus*, *275*, 203–220. [13] Lowenstern J. B. (1999) *Mineralium Deposita*, *36*, 490–502. [14] Bekker A. et al. (2014) *Treatise on Geochemistry*, 2nd ed., vol. 9, 561–628. [15] Carter J. et al. (2015) *Icarus*, *248*, 373–382. [16] Postberg F. et al. (2011) *Nature*, *474*, 620–622. [17] Hsu H-W. et al., *Nature*, *519*, 207–210. [18] Baker V. R. et al. (1997) In: *Venus II*, 757–793. University of Arizona Press. [19] Zolotov M. Yu. (2019) In: *Oxford Research Encyclopedia of Planetary Science*. Doi:10.1093/acrefore/9780190647926.013.14